

UNCLASSIFIED

AD NUMBER

ADB001826

LIMITATION CHANGES

TO:

Approved for public release; distribution is unlimited.

FROM:

Distribution authorized to U.S. Gov't. agencies only; Administrative/Operational Use; 01 JAN 1970. Other requests shall be referred to Army Missile Command, Redstone Arsenal, AL.

AUTHORITY

AMSMI ltr 24 Jun 1975

THIS PAGE IS UNCLASSIFIED

THIS REPORT HAS BEEN DELIMITED  
AND CLEARED FOR PUBLIC RELEASE  
UNDER DOD DIRECTIVE 5200.20 AND  
NO RESTRICTIONS ARE IMPOSED UPON  
ITS USE AND DISCLOSURE.

DISTRIBUTION STATEMENT A

APPROVED FOR PUBLIC RELEASE;  
DISTRIBUTION UNLIMITED.

REPORT RF 2376--FR-2 (U)

AD \_\_\_\_\_

AD B001826

THE LAND COMBAT MODEL (DYNCOM)

Research Completed by December, 1969

FINAL REPORT

by

Gordon M. Clark

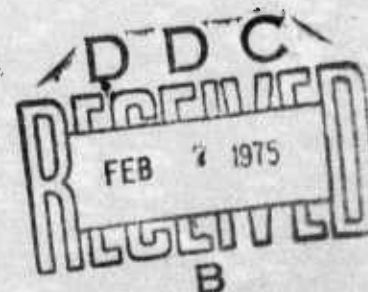
January 1, 1970

Distribution limited to U.S. Gov't. agencies only;  
Contractor Performance Evaluation: *JAN. 1970*  
Other requests for this document must be referred to

~~This document is subject to Special Export Controls and each transmittal to foreign governments or foreign nationals may be made only with prior approval of Headquarters, U. S. Army Missile Command, Attn: AMSMI-C, Redstone Arsenal, Alabama~~

U. S. ARMY MISSILE COMMAND  
Systems Analysis Division  
Systems Analysis Office  
Redstone Arsenal, Alabama 35809

SYSTEMS RESEARCH GROUP  
Department of Industrial and Systems Engineering  
The Ohio State University  
Columbus, Ohio 43210



Unclassified

SECURITY CLASSIFICATION OF THIS PAGE (When Data Entered)

REPORT DOCUMENTATION PAGE		READ INSTRUCTIONS BEFORE COMPLETING FORM
1. REPORT NUMBER	2. GOVT ACCESSION NO.	3. RECIPIENT'S CATALOG NUMBER
4. TITLE (and Subtitle) THE LAND COMBAT MODEL (DYNCOM) Research Completed by December, 1969		5. TYPE OF REPORT & PERIOD COVERED Final - November 1968 through December 1969
7. AUTHOR(s)  Gordon M. Clark		6. PERFORMING ORG. REPORT NUMBER RF 2376--FR-2 (U)
9. PERFORMING ORGANIZATION NAME AND ADDRESS SYSTEMS RESEARCH GROUP Dept. of Industrial and Systems Engineering The Ohio State University, Columbus, Ohio 43210		8. CONTRACT OR GRANT NUMBER(s)  DAAH 01-67-C-1240
11. CONTROLLING OFFICE NAME AND ADDRESS The Ohio State University Research Foundation 1314 Kinnear Road Columbus, Ohio 43202		10. PROGRAM ELEMENT, PROJECT, TASK AREA & WORK UNIT NUMBERS
14. MONITORING AGENCY NAME & ADDRESS (if different from Controlling Office) U. S. Army Missile Command AMSMI-CS Redstone Arsenal, Alabama 35809		12. REPORT DATE January 1, 1970
		13. NUMBER OF PAGES ix plus 238
		15. SECURITY CLASS. (of this report)  Unclassified
		15a. DECLASSIFICATION/DOWNGRADING SCHEDULE
16. DISTRIBUTION STATEMENT (of this Report) This document is subject to Special Export Controls and each transmittal to a foreign government or foreign nationals may be made only with prior approval of Headquarters, U. S. Army Missile Command, Attn: AMSMI-CS, Redstone Arsenal, Alabama 35809		
17. DISTRIBUTION STATEMENT (of the abstract entered in Block 20, if different from Report)		
18. SUPPLEMENTARY NOTES		
19. KEY WORDS (Continue on reverse side if necessary and identify by block number) Armor, Missiles, Crew-Served Weapons, Combat Simulation, Computer Simulation, Communication, Route Selection, Detection, Pinpoint, Mobility, Attrition Firepower, Combat Effectiveness, Estimation, Mathematical Statistics, Land Combat, Field Experiment, Feed-Back Control Model, Beam-Rider Missile, Human tracker		
20. ABSTRACT (Continue on reverse side if necessary and identify by block number) This report presents the results of research, completed by December 1969, to design principal submodels for the DYNCOM combat simulation. Dyncom is a high-resolution simulation of battalion-sized combat units having armor, crew-served anti-tank, helicopter, and artillery weapons. These weapons can be equipped with missiles, and the model was developed to predict the effect of missile performance characteristics on the effectiveness of tactical units in engagements with enemy forces. The principal research areas described in this report are: 1) Analysis of communication experimental		



Unclassified

SECURITY CLASSIFICATION OF THIS PAGE(When Data Entered)

results to provide inputs to the DYNCOM Communications Model, 2) Design of a Crew-Served Weapon Movement Model for dismounted crew-served weapons to select fire positions, routes, and represent movement, 3) Extensions to the Beam-Rider Missile Model to represent continuous flight traces, estimate parameters from flight data, and represent the effects of tracker performance on missile performance, 4) Development of a method for prediction of detection times under conditions of limited visibility, and 5) Development of a model and experimental plan for prediction of detection (pinpoint) times of the signatures of concealed firing weapons.

Unclassified

SECURITY CLASSIFICATION OF THIS PAGE(When Data Entered)

## FOREWORD

Research conducted by the Systems Research Group of The Ohio State University under contract number DAAH 01-67-C-1240 is described in this report. This volume is the second volume of a five volume report presenting the DYNCOM Land Combat Model. The first volume, Volume 1, introduces the DYNCOM model and presents the design of principal submodels completed by October 1968. This volume describes basic submodels completed by December 1969. Volume 3 presents the Aerial Platform Combat Operations Modules, and Volume 5 is the classified annex to this report. Volume 4 contains documentation for the DYNCOM computer program consisting mainly of common descriptions, subroutine descriptions, and flow charts.

Both complete descriptions of research results for unclassified work and unclassified summaries of unclassified results appear in this volume, i. e., Volume 2. Chapter 1 summarizes the principal characteristics of the DYNCOM model and introduces the research areas described in this volume. The principal research areas that are described in their entirety in this volume are:

1. Analysis of communication experimental results (Chapter 3),
2. Crew-Served Weapon Movement Model (Chapter 5),
3. Extensions to the Beam-Rider Missile Models (Chapter 6),
4. Prediction of detection (pinpoint) times of the signatures of concealed firing weapons (Chapter 9).

The summaries of classified research outline research to develop models of:

1. Indirect-fire electro-optical guided missile systems (Chapter 2),
2. DRAGON missile system (Chapter 4), and
3. Electronic countermeasures (Chapter 7).

Although this is a final report for the Land Combat Model (DYNCOM) contract, comments, suggestions, and criticisms addressed to the authors of the report are welcome since our group maintains a continuing interest in and participation in military operations research.

Conclusions drawn in this report represent the current views of the Systems Research Group, Department of Industrial and Systems Engineering, The Ohio State University, and should not be considered as having official USAMICOM or Department of Army approval, either expressed or implied, until reviewed and evaluated by those agencies and subsequently endorsed.

The cooperation received from MICOM personnel in the conduct of this research has been extremely helpful. In particular, we wish to acknowledge the advice and assistance provided by Mr. Ernest Petty.

In addition, we wish to acknowledge the important contributions of the programmers who have performed a tremendous effort to make the DYNCOM computer program possible. In particular, Messrs. Leslie Moss and Charles Harget have been instrumental in seeing that the DYNCOM program has been implemented successfully.

Moreover, we must acknowledge the contributions of the secretarial staff who made this report possible. Mrs. Gordon Graber patiently typed the rough drafts and final text.

## TABLE OF CONTENTS

	Page
FOREWORD . . . . .	iii
LIST OF FIGURES . . . . .	vii
LIST OF TABLES . . . . .	ix
CHAPTER	
1      EXTENSIONS TO THE LAND COMBAT MODEL (DYNCOM) . . . . .	1
2      INDIRECT-FIRE, ELECTRO-OPTICAL GUIDED MISSILE SYSTEM. . . . .	17
3      COMMUNICATION EXPERIMENT RESULTS. . . . .	21
4      DRAGON MISSILE MODEL . . . . .	61
5      CREW-SERVED WEAPON MOVEMENT MODEL . . . . .	63
6      EXTENSION TO DYNCOM BEAM-RIDER MISSILE MODELS . . . . .	109
7      ELECTRONIC COUNTERMEASURES . . . . .	135
8      NIGHT DETECTION MODEL . . . . .	137
9      WEAPON SIGNATURE (PINPOINT) MODEL . . . . .	153
APPENDIXES . . . . .	171
A      ARMORED CAVALRY RADIO NET STRUCTURE . . . . .	173
B      A SAMPLE TRANSCRIPTION OF NET TRAFFIC . . . . .	174
C      FORMATTED MILIRARY COMMUNICATIONS . . . . .	176
D      SUMMARY OF FORT ORD DATA . . . . .	181
E      COVERAGE OF TAPE RECORDINGS . . . . .	182

APPENDIXES		Page
F	HISTOGRAMS OF COMMUNICATION DATA . . . . .	184
G	CHARACTERISTICS OF THE TWO-PARAMETER GAMMA DISTRIBUTION . . . . .	190
H	MAXIMUM LIKELIHOOD ESTIMATORS FOR THE GAMMA DISTRIBUTION PARAMETERS . . . . .	191
I	GOODNESS-OF-FIT TESTS . . . . .	193
J	THEORETICAL DISTRIBUTIONS WITH PARAMETERS AND GRAPHS . . . . .	195
K	SIMULATION FLOWCHARTS . . . . .	207
L	SOLUTION FOR MISSILE DISPLACEMENT IN THE CONTINUOUS FLIGHT TRACE MODEL . . . . .	218
M	ESTIMATORS FOR PARAMETERS IN THE CON- TINUOUS FLIGHT-TRACE MODEL. . . . .	221
N	COMPUTATION OF STOCHASTIC ACCELERATION ERROR VARIANCES. . . . .	227
O	DETERMINATION OF DEMAND RATES . . . . .	235
P	GENERATION OF GAMMA DISTRIBUTED RANDOM TIMES . . . . .	238

# LIST OF FIGURES

Figure		Page
1.1	Selection of the Next Current Event . . . . .	8
1.2	DYNCOM Schematic . . . . .	10
3.1	Simplified Net Structure . . . . .	22
3.2	Study B Results . . . . .	45
3.3	Study C Results . . . . .	49
5.1	Threat Locations Attack Mode . . . . .	68
5.2	Threat Locations Defense Mode . . . . .	69
5.3	Logic Flow Diagram of the Extended Crew-Served Weapon Models . . . . .	70
6.1	Beam-Rider Missile Deviation from Tracker Line of Sight . . . . .	110
6.2	Monte Carlo Procedure-Discontinuous Flight Trace Model. . . . .	112
6.3	Continuous Flight Trace Model Block Diagram . . . . .	115
6.4	Typical Result from Continuous Flight Trace Model . . . . .	117
6.5	Missile Constant Flight Bias . . . . .	119
6.6	Former Flight Path Representation with Cones Repre- sented FOV Limitations Emanating to Launcher . . . . .	120
6.7	Missile Body Axis Coinciding with Flight Path . . . . .	122
6.8	Direction Cosines of Missile-Launcher Vector . . . . .	122
6.9	Illustration of FOVLIM . . . . .	124
6.10	Compensatory and Pursuit Tracking . . . . .	125
6.11	General Model of Pursuit Tracking System . . . . .	126



Figure		Page
6.12	Simple Tracking Task with Illustration of Response and Reaction Periods . . . . .	128
8.1	Contrast Threshold as a Function of $\alpha$ and $\beta'_b$ (foot-lamberts) for $\beta = 0^0$ . . . . .	142
8.2	Probability of Fixating on the Target as a Function of the Number of Confusing Forms for Various Search Times . .	147
9.1	Matrix of Transition Probabilities for Markov Chain . . .	165
9.2	Matrix of Observed Transitions of Detection States . . .	166
9.3	A Set of Hypothetical Data for One Observer when $m = 5$ . .	168
N.1	Stochastic Input Function $x(t)$ . . . . .	229
P.1	Cumulative Distribution Function . . . . .	238

# LIST OF TABLES

Table		Page
3.1	Fort Carson Demand Rates . . . . .	43
3.2	Fort Carson Conversation Duration Distributions . . . . .	43
3.3	Performance of Simulated Fort Carson Communication System . . . . .	46
3.4	Study B Results . . . . .	46
3.5	Study C Variations . . . . .	48
3.6	Study C Results . . . . .	48
3.7	Single-Relayer Demand Rates . . . . .	51
3.8	Study D Results . . . . .	51
3.9	Study E Results . . . . .	53
3.10	Summary of Stepwise Regression . . . . .	55
3.11	Summary of Simulation Results . . . . .	57-58
8.1	Values of Regression Coefficients $A_i(B_b')$ , for Computing $C_{.50}(\alpha, B_b'   \beta = 0^0)$ . . . . .	143
J.1	Gamma Distribution Parameters . . . . .	206
O.1	Origins of Conversations . . . . .	235

## CHAPTER 1

### EXTENSIONS TO THE LAND COMBAT MODEL (DYNCOM)

by  
G. M. Clark

#### Introduction

New missile or modifications to existing missile systems are being proposed to increase the combat effectiveness of the army at reduced cost. These systems involve changes in accuracy, lethality, flight trajectory, effective range, firing rate, guidance method, target acquisition capability, launcher mobility, and use of indirect fire in place of direct fire. The effectiveness of these changes interacts strongly with unit tactics, unit organization, capabilities of other organic weapons, and battlefield environment. To evaluate the cost-effectiveness of these changes, the U. S. Army Missile Command (MICOM) has contracted for the development of DYNCOM, a high-resolution simulation of mobile combat between battalion-sized armored forces. This report describes the results of research completed by November 1969 to extend the capability of DYNCOM.

This volume is the second volume of a five volume final report, and research, other than work on the aerial platform module, completed between October 1968 and November 1969 is described in this report. The principal research areas are:

1. analysis of communication experimental results (Chapter 3),
2. Crew-Served Weapon Movement Model (Chapter 5),
3. extensions to the Beam-Rider Missile Models (Chapter 6),
4. prediction of detection times under conditions of limited visibility (Chapter 8), and
5. prediction of detection (pinpoint) times of the signatures of concealed firing weapons (Chapter 9).

In addition, summaries are presented of research completed between October

1968 and November 1969, but described in detail in the classified annex, Volume 5, of this final report. These summaries describe completed research in the areas of:

1. indirect-fire electro-optical guided missile systems,
2. DRAGON missile system, and
3. countermeasures.

Volume 1 of this report presents the basic structure of DYNCOM and a description of research to develop DYNCOM completed before October 1968. Volume 3 presents the Aerial Platform Module. Classified results are described in Volume 5, and Volume 4 is the programmer's manual containing program input data formats and flowcharts.

The reader of this volume, Volume 2, is referred to Chapter 1 of Volume 1 for an introduction to DYNCOM. However, a brief overview of the principal characteristics of DYNCOM is presented in this chapter to serve as point of reference for the research described in this volume.

#### Overview of DYNCOM

The principal characteristics of DYNCOM are:

1. High resolution
2. Dynamic tactics
3. Flexibility in use

The original design objectives established for DYNCOM emphasized the above characteristics because of MICOM's needs in the analysis of missile systems. These characteristics are discussed below.

The prime characteristic of DYNCOM has been a high-resolution representation of individual weapon firepower, mobility, protection, and detection capabilities and their interactions with the terrain. For example, this high-resolution representation permits the simulation of different missile flight trajectories such as a beam-rider missile as it interacts with the terrain-profile, and these missile flight trajectories can be compared with the parabolic trajectory of a conventional tank main gun. Fundamental concepts are emphasized such as cover, concealment, fields of fire, and terrain mobility characteristics. Moreover, this representation is achieved in the context of a dynamic combat situation where both forces can be mobile at the same time. Because of this detailed representation of individual weapon performance as it interacts with

terrain, DYNCOM is a high-resolution simulation.

Dynamic tactics are represented by DYNCOM since the high-resolution representation of individual weapon performance requires situation-dependent movement and firing tactics to represent weapon performance in a valid manner. Combat is represented in DYNCOM as an adaptive process where each unit is constantly evaluating the battle situation in order to pick the tactic most appropriate for the tactical doctrine expressed by the input data. Assault routes, tactical formations, firing assignments, and the timing of withdrawal and advance movements are situation-dependent and generated internal to the simulation. The simulation event-sequencing procedure has been designed to emphasize flexibility and avoid prescheduling a battle. If the battle situation merits a new tactic at any point of the battle, changes are generated to a unit's route, formation, or firing assignments.

Because of the detailed nature of DYNCOM, flexibility in use is an important characteristic. Alternative designs, tactics, unit organization, and battlefield environment are frequently derived during the course of a study that were not initially apparent. DYNCOM has been purposely designed to be flexible so that different combat situations and environments could be represented without changing the simulation program and with a minimal amount of change in input data required. This flexibility is achieved because of the fundamental nature of the input data permitting maximum use of available data sources. For example, the digital terrain elevations used to construct a terrain surface are obtained directly from the Army Topographic Command and only require processing by a computer program to prepare inputs for DYNCOM. Another advantage derived from the basic nature of the input data is that alteration of input conditions can be performed in a localized manner with a minimal number of parameters affected. The input data are partitioned into independent data sets organized to describe weapon physical characteristics, terrain, unit organization, and tactical decision criteria. The interactions among these input data sets are computed by DYNCOM and are not specified by input data.

In order to represent a wide range of different tactical situations and scenarios without requiring program changes, basic concepts for representing the organization and tactical role of individual combatants and combat units have been established for DYNCOM and are described in the following section.

#### Tactical Organization

DYNCOM has sufficient flexibility to represent combat engagements ranging in size from a single weapon to an armored battalion. Attacking, supporting fire, and delaying maneuver units are described. A coordinated attack against a sequence of objectives conducted by several teams moving

within separate axes of advance can be represented. Phase lines are used to control the speed of advance of adjacent units. As the attacking teams advance, the supporting fire maneuver units move forward to fire support positions. Moreover, the delaying force can have several maneuver units that are assigned a sequence of delay and outpost positions. Movement of each maneuver unit is represented during the attack, advance to fire support positions, and withdrawal from delay and outpost positions. Thus, DYNCOM represents a dynamic combat situation where both forces can move simultaneously.

In order to provide flexibility for representing diverse weapons and combat situations ranging in size from a single weapon to a battalion engagement, tactical organizations are constructed in DYNCOM by forming maneuver units composed of elements with different capabilities. An element is the smallest combat entity provided a point location in DYNCOM. An element could be a tank, an armored personnel carrier that can launch indirect-fire missiles, or an anti-tank crew-served weapon. The capabilities possessed by an element are stipulated by input data specifying its mobility and weapon type codes and its initial ammunition supply. The weapon type specifies uniquely a set of firepower characteristics; i. e., weapons, projectile types, and protection characteristics (silhouette and vulnerability with respect to enemy projectiles).

These firepower and mobility capabilities are retained until the ammunition supply is consumed or the element suffers a firepower or mobility kill. Loss of firepower capability does not imply loss of mobility, and the element can continue moving. Similarly, loss of mobility does not imply loss of firepower. The input data are organized so that the mobility characteristics are described in detail for each mobility type code. For example, mobility type one might be a main battle tank and type two might be an armored personnel carrier. Similarly, the firepower and protection characteristics are described for each weapon type code. Weapon type one might be a main battle tank with a beam-rider missile, type two a main battle tank with a conventional main gun, type three an armored personnel carrier with indirect-fire missiles, and type four an armored personnel carrier with a rapid-fire weapon. In addition, a weapon type may employ up to six different projectiles or weapons with unique accuracy and lethality characteristics. The initial ammunition supply by projectile type must be specified by input data for each element, which is stored in common area LAMMO (see page B-120 of Volume 4A). Also, the mobility types for each element are specified by input data stored in common area LMOBT (page B-138 of Volume 4A).

The movement activities of individual elements in DYNCOM are controlled by maneuver units. While moving, each element guides on his maneuver unit leader who designates routes and formations. If the maneuver unit is occupying a stationary position, the decision to initiate movement is made by the maneuver unit leader.



A maneuver unit can vary in size from one to seven platoons, and a maneuver unit composed of more than one platoon is a team maneuver unit. Platoons can have up to two sections, and they can be as small as a single element. Sections vary in size from one to four elements.

The organization of each maneuver unit affects the flow of intelligence information concerning the location of enemy weapons. Each platoon is provided a communication net known as the platoon tactical net. The platoon leaders and other elements, designated by input data, are on a net called the company tactical net. Fire-request nets are provided for communication of requests for supporting fire by forward observers. The elements on each net are established by input data, and the net organization is altered when casualties occur. A firepower kill is assumed to imply loss of communication capability.

Designated elements in a maneuver unit serve as artillery forward observers by initiating requests for fire against targets of opportunity and on-call fire missions. These fire requests are acted upon by artillery units where each unit consists of a fire direction center and a firing battery. Up to twelve elements can be simultaneously identified as forward observers, and four artillery units can be represented. When a forward observer becomes a casualty (either firepower or mobility kill), it is replaced by another undamaged element in its maneuver unit.

Similarly, designated elements in each maneuver unit have the capability to launch indirect-fire missiles (called missile launchers) and other elements can be missile forward observers that request indirect missile fire and illuminate targets. Common area LFUNC stores input data specifying whether an element is a missile launcher or a forward observer. For the MISTIC system, it is assumed that any element having MISTIC missiles in its ammunition supply can also fire in the direct-fire mode.

### Sequence of Events

DYNCOM simulates a battle by specifying a sequence of combat activities for each element for the duration of the engagement. The interactions among the combat activities of each element are resolved by defining fundamental events with respect to its actions. An event is a commitment to action during which a combat element will not alter its activities regardless of the actions of other elements. Examples are provided by movement for a short time interval, firing one main gun round, or a single burst from a rapid-fire weapon.

Combat elements have events which are determined by their movement and firing activities. Artillery forward observer elements, however, can have

two types of events occurring simultaneously, that is, an event performed by the weapon carrying the forward observer and an event performed by the forward observer to request artillery fires. Typical forward observer events are selection, data preparation, communication of a fire request, waiting for a fire mission to be executed, and communication of a fire adjustment. Artillery units have events which are defined by activity performed to execute a fire mission. A fire direction center has plot and stand-by events, and the firing battery has firing and stand-by events.

The nature of each event implies a time to perform the event which can be specified deterministically or stochastically. Times for artillery events, such as data preparation, communication, plotting fire missions, and executing fire missions, are determined by Monte-Carlo sampling from the pertinent distributions. Artillery forward-observer target selection events are of constant duration, and they are repeated until the forward observer identifies or loses a target.

A different system is used for indirect-fire missile launchers and forward observers. Events for missile forward observers are determined by the combat actions of the vehicle carrying the forward observer; thus, the data preparation and communication activities are not represented by separate events. However, data preparation, communication, and illumination time delays and requirements are explicitly determined during the simulation of a forward observer combat element event. On the other hand, the time delays for a launcher to launch a missile and communicate with the forward observer are determined as events for the launcher in the same manner as a normal firing event. Once an indirect-fire missile has been launched, a missile element is created by DYNCOM and simulated along with the other combatant elements. By creating new missile elements, the launchers of semi-active missiles can assume new combat activities without waiting for the missile to arrive at the target area and yet the outcome of a missile flight can be related to the current activities for the illuminating forward observer and target. On the other hand, launchers for electro-optical missiles must acquire the target, and forward observers are free to search for new targets after missile launch. Missile flight events are repeated until the missile arrives at the target at which time the missile element is destroyed.

The procedure for determining the event time for a ground combatant element varies depending on what actions are represented. Four cases are considered, and are noted below together with the symbols used to identify each case:

1. firing while stationary ( $\overline{MF}$ ),
2. moving and not firing ( $M\overline{F}$ ),

3. neither moving nor firing ( $\overline{MF}$ ), and
4. moving and firing simultaneously (MF).

The calculation of the time for firing without moving event,  $\overline{MF}$ , depends on the manner in which the weapon is fired. An event for a weapon that is fired by adjusting the aiming point after each round includes loading, laying, and flight times. A tank main gun or an anti-tank weapon, including beam-rider missiles, would be fired in this manner. The event commences once the decision to fire is made and terminates when the projectile impacts. It should be noted that the loading activity may be occurring simultaneously with laying or projectile flight. The firing time  $t_f$  is determined by adding the result of a Monte Carlo sampling from the pertinent firing-time distribution to a range dependent flight time. For rapid-fire weapons, the firing occurs for a specified time interval  $t_{rf}$ ; e.g., ten seconds. The number of rounds fired then becomes a variable dependent on the weapon's rate of fire.

The length of a movement event without firing activity; i.e.,  $\overline{MF}$ , is defined by a fixed time interval and the distance traveled becomes a function of the movement time  $t_m$ . When obstacles or terrain seriously reduce an element's mobility, allowing a change in the direction of movement at the end of a time period gives the element more flexibility than forcing it to travel an arbitrarily prescribed distance.

Event times for the remaining cases are specified by applying two rules:

1. For an MF event, set the event time equivalent to the firing time  $t_f$ .
2. For an  $\overline{MF}$  event, set the event time equivalent to the movement time  $t_m$ .

The processing sequence for these events is ordered in time by using "clocks" which are set for the time that each element will complete its present event. While the simulation is processing a given event, this event is called the "current event," and the element performing the event is called the "current element." Once a current element has been processed, its clock is updated by the current event time; then, the next current element to be processed can be determined by searching each clock to find the clock with lowest time. Figure 1.1 illustrates the selection of the next current event from a set of element clocks, and the beginning and end of each event are noted in the figure by vertical tick marks.

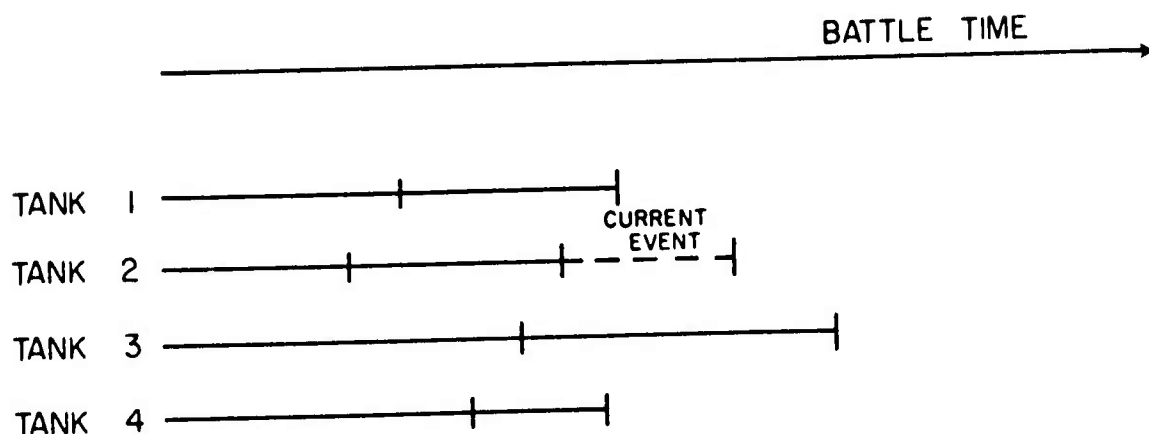


Figure 1.1. --Selection of the Next Current Event

The entire battle is represented by a repetitive cycle of selecting a current element, determining its actions during the current event, and then selecting another current element. The battle is started by putting small random numbers in each clock, and then searching for the clock showing the minimum time. The battle is ended when one of the three conditions noted below is met:

1. The attacking force has seized all of its objectives,
2. The attack has been aborted, and the attacking force has been forced to assume defensive positions, or
3. One of the opposing forces has been annihilated.

#### Processing a Combatant Element

The event structure employed by DYNCOM is instrumental in providing flexibility and permitting the simulation to represent a dynamic battle. The beginning of each event provides an opportunity for tactics to be reviewed and altered in response to changes in the battle situation occurring in previous events. Accordingly, the simulation program is designed to evaluate the battle situation at the onset of each event before an element is committed to action in its current event.

The overall computational sequence for a ground combatant element is illustrated in Figure 1.2 by the loop starting with the Sequence Controller and labeled "Armor". The first step in processing a ground combatant element is to transmit messages on the nets which it is monitoring to give it the benefit of intelligence provided by other friendly elements. After messages have been received, the intelligence acquired by visual search during the current element's previous event is determined. Also, intelligence lost by the current element due to loss of intervisibility or to its becoming neutralized is assessed. If the current element is a maneuver unit leader, it can evaluate its intelligence and the battle situation, and then change its unit's movement plan if required. Each element evaluates its firing activities prior to executing the current event. The final steps in computation procedure determine the outcome of movement and firing activities performed by the current element in the current event. Processing of an aerial platform combat element is performed with a similar structure and is described in Volume 3 of this final report.

### Program Modules

The simulation program that describes the outcome of each event has a modular structure that corresponds to the steps in the processing sequence. Most of these modules are shown in the DYNCOM schematic shown in Figure 1.2. These modules simplify the understanding of the program organization. Moreover, these program modules correspond to functions performed by an element, and they are the result of a model designed to represent this function. Although these modules represent separate identifiable parts of the program, their functioning is inter-related in that information is passed from one module to another. The models and corresponding program modules can be revised to represent different combat situations or weapon capabilities, and various combinations of these modules can be assembled as required. Research described in this volume has the objective of extending the capabilities of the Communications, Intelligence, Beam-Rider Missile, Indirect-Fire Semi-Active Missile, and Crew-Served Weapon Unit Controller Modules.

The functions performed by each program module are described below.

Communications. --In order to assess communication time delays, the Communications Module represents communication traffic on platoon tactical nets, company tactical nets, and fire-request nets. Messages reporting newly detected enemy weapons and requesting supporting fire are explicitly described. When messages are originated for transmission and the nets are busy, queues are formed so that these messages can be transmitted at a later time. In order to disseminate information throughout this tactical organization, the Communications Module will originate messages on the company net after they have been sent on a platoon net, and vice versa.

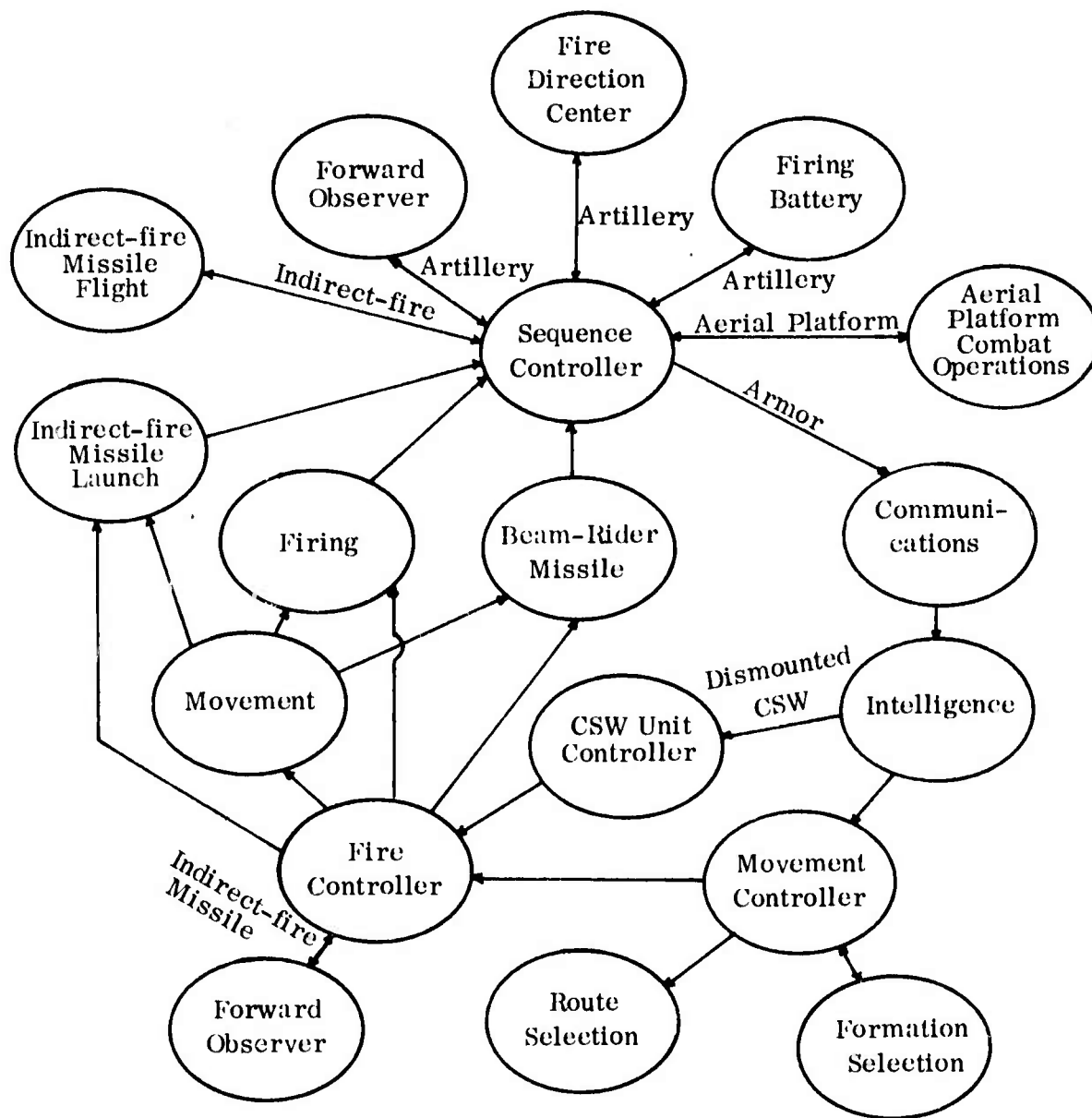


Figure 1.2. --DYNCOM Schematic



Intelligence. --An intelligence list is maintained by the Intelligence Module for each element giving the enemy weapons that he has approximately located, visually detected, or pinpointed, and this list is updated each event as intelligence is gained or lost. Approximate knowledge is possessed when the enemy element was reported on a communication net or when the enemy element was previously detected but is no longer intervisible. A visual-detection model is used in determining detection times. This model considers variables which affect the detectability of a weapon such as range, concealment, crossing velocity, and scene complexity. Also, both the neutralization status of the observer and the firing activities of undetected enemy weapons are considered in applying this visual detection model. Concealed firing enemy weapons may be pinpointed as opposed to being visually detected by placing an observer's sights upon the firing weapon signature.

Crew-Served Weapon Unit Controller. --The Crew-Served Weapon Unit Controller Module controls the activities of dismounted crew-served weapon units by selecting an attack or defense mode of deployment, selecting desired firing positions, selecting routes, and representing movement between the crew-served weapon carrier and desired firing positions in the dismounted mode.

Movement Controller. --The Movement Controller module represents the selection of routes, formations, and desired unit speeds by maneuver unit leaders. The timing of withdrawal and advance movements by delaying outposts, and supporting fire units is specified by the Movement Controller. Threat criteria based on unit leader intelligence and other factors are used to initiate the withdrawal of outposts and delay units. Phase lines are used to coordinate the speed of advance of attacking units and to trigger the advance of supporting fire units. Extensive use is made of the route-selection and formation-selection submodels. Assault routes are computed in the vicinity of the axis of advance in order to determine routes that have desirable trafficability, cover, and fields of fire, and the commander's intelligence concerning enemy weapons, strong points, and terrain condition is considered. Using the locations of detected enemy weapons, the principal direction of threat is identified in order to determine formations and desired speeds for mobile maneuver units. If the unit is in a minefield, the decision to breach the minefield, traverse the minefield, or perform a retrograde movement out of the minefield is made by the Movement Controller.

Fire Controller. --As enemy elements are detected, the Fire Controller makes the decision to engage a target, determines the highest priority target, monitors the length of the fire mission, determines whether the target is to be engaged while the firer is moving, directs the firer to a fire position, selects a projectile, maintains the ammunition supply records, determines when for-

ward observers request indirect missile fire, and assigns indirect-fire targets to missile launchers. In selecting targets, the Fire Controller considers such factors as:

1. target range,
2. target weapon type,
3. target cover,
4. projectile effective ranges,
5. firer's sector of responsibility,
6. whether the target is firing,
7. whether the target is firing at the firer,
8. whether other friendly weapons are engaging the target, and
9. unit integrity.

Also, targets can be transferred to other firing units in order to represent fire and movement tactics.

Movement. --The Movement Module represents movement by ground vehicles and does not describe movement of dismounted crew-served weapons. Using the unit formation and route designated by the Movement Controller, the Movement Module computes the current element's desired position at the end of his current event. This desired position is determined relative to the position and speed of the unit leader so that the unit maintains formation integrity. The element is placed at its desired position if it is capable of traveling the desired distance. Otherwise, the new element position is computed as the farthest point it can achieve along its route. The calculation of vehicle mobility capability considers the vehicle's physical characteristics and the mobility environment along its movement path. If the vehicle enters a minefield, the Movement Module determines whether a mine is detonated and damage occurs.

Firing. --Using the uncovered target profile, target range, projectile dispersion, and target vulnerability characteristics, the accuracy and lethality of ballistic trajectory direct-fire weapons is assessed by the Firing Module. Given a hit, the target is placed in a neutralized status.

Beam-Rider Missile. --Using a feedback control model, gunner tracking performance of a target is represented, and the resulting flight trace of a beam-rider missile is determined. Based on this flight trace, the model determines whether the missile avoids impact with the intervening terrain and hits the target. Given a hit, missile lethality is assessed.

Indirect-Fire Missile Module. --This module is also referred to as the MISTIC Module, and it represents both semi-active and electro-optical systems. For both systems, a forward observer, either a helicopter or a ground combatant, detects and requests hard-point fire. Once this request is received by a launcher, time delays to verify the fire request and launch a missile are determined. Also, the launcher may be either a helicopter or a ground vehicle. The flight trace of a missile searching for the target is used to determine when the target enters the missile field of view. For semi-active systems, the ability of a forward observer to illuminate the target is assessed and used to determine if and when the target is acquired by the missile. Electro-optical systems require target acquisition by the launcher and time delays to achieve this acquisition are represented. If acquisition occurs, the tracking performance of the missile is assessed and used in determining whether the missile hits and inflicts damage upon the target. Although this module was primarily designed to represent indirect-fire where target acquisition is performed by the forward observer, direct fire by the launcher can also be represented.

Aerial Platform Combat Operations. -- The Aerial Platform Combat Operations Module (TAPCOM) was designed for DYNCOM to represent three tactics for indirect-fire semi-active missiles (MISTIC). These tactics are: 1) airborne launcher, airborne illumination; 2) airborne launcher, ground illumination; and 3) ground launcher, airborne illumination. TAPCOM continuously represents the combat activities of aerial vehicles with resolution comparable to the ground Armor Module; moreover, TAPCOM has a modular structure similar to the Armor Module. The aerial platform in DYNCOM acquires its own intelligence and communicates with ground units. In addition, flight paths are dynamically determined by TAPCOM, and the aerial vehicles are moved along these flight paths.

Artillery. --The Artillery Module consists of three submodels; i. e., forward observer, fire direction center, and the firing battery models. Targets of opportunity are dynamically constructed by the forward observer, and on-call missions are requested when required. Time delays to request and deliver artillery fires are represented. Also, scheduled fires are executed by the firing batteries. Target neutralization and terminal effects for each artillery volley are determined.

Terrain and Environment. --The Terrain and Environmental Module specifies environmental conditions at each element position and intervisibility relationships between observer-enemy weapon pairs. This module performs its calculations for arbitrarily selected battlefield positions and is not dependent on a prescheduled route or movement path. In addition, this module is used by both ground and aerial units. The principal models which specify environmental conditions are listed below:

1. A line-of-sight algorithm is used to compute the fraction of a weapon's height that is covered,
2. A concealment model determines the fraction of a weapon's height that is concealed,
3. A macro-terrain model determines the terrain gradient along a movement path, and
4. A micro-environment model specifies the environmental conditions at specified points of the battlefield.

Moreover, cover and concealment models determine the cover and concealment provided by the micro-environment at fire positions designated by the Fire Controller, crew-served weapon unit controller, or TAPCOM.

A schematic of the simulation program is shown in Figure 1.2, which presents the sequence in which the program modules are employed. The Sequence Controller updates the element's clocks and determines the following current element. Flowcharts of the DYNCOM main program, implementing this schematic, and of subroutine SEQCNT which performs the function of the Sequence Controller, are shown on pages E-3 of Volume 4A and F-867 of Volume 4B, respectively. Note that a loop is formed by the Communications, Intelligence, Movement Controller, CSW Unit Controller, Fire Controller, Movement, and Firing Modules. This loop is called the Armor Module, and it is used to represent an event for a ground combatant element. Aerial platform elements are represented by The Aerial Platform Combat Operations Module (TAPCOM) which has a similar structure to the Armor Module (see Volume 3). The Beam-Rider Missile Module may be implemented as part of the Armor Module (or as part of TAPCOM). Indirect-fire missile targets can be acquired and requested by a missile forward observer module implemented by both the Armor and TAPCOM Modules. Indirect-fire missile targets are also represented by the Armor and TAPCOM Modules, and the Launch Module is used to represent the time delays necessary to launch a missile and create a new missile element. Events for this new missile element are represented by the Indirect-Fire Missile Flight Module. Fire Direction Center, Forward Observer, and Firing Battery Modules are part of the Artillery Module.

## Research Results Presented in This Volume

The overview of DYNCOM described in the preceeding section provides a background and context for understanding the research results presented and summarized in this volume. The models presented in this volume are summarized below.

### Analysis of Communication Experimental Results (Chapter 3)

The primary objectives of the communication experimental analysis reported in Chapter 3 were to estimate the distribution of message duration times, to estimate the rates that certain messages are generated, and to verify certain assumptions inherent in the DYNCOM Communication Model presented in Chapter 4 of Volume 1. Available communication data were analyzed, and communication traffic recorded during a field experiment involved two troops of an armored cavalry squadron were analyzed to satisfy the above objectives.

In addition, research is reported in this chapter to analyze the structure of tactical nets for the purpose of improving communication performance. Alternate net structures are recommended.

### Crew-Served Weapon Movement Model (Chapter 5)

The crew-served weapon models described in Chapter 9 of Volume 1 were extended to improve the representation of crew-served weapon movement while dismounted from their carrier vehicles. DYNCOM represents the deployment of crew-served weapons from their carrier vehicles to assume firing positions in either an attack or defensive mode. The models presented in Chapter 5 determines the location of these firing positions, selects routes to the firing positions, and moves the crew-served weapons along the selected routes.

### Extensions to the Beam-Rider Missile Models (Chapter 6)

The original Beam-Rider Missile Model described in Chapter 8 of Volume 1 was extended to improve the representation of beam-rider missiles that continuously apply in-flight corrections to fly along a path designated by a tracker. These extensions are:

1. development of a missile flight model that is continuous,
2. derivation of parameter estimation procedures for the continuous flight trace model,
3. representation of the effects of a restricted field of view on missile flight, and

4. formulation of a model describing the role of the human tracker in beam-rider missile performance.

#### Prediction of Detection Times Under Conditions of Limited Visibility (Chapter 8)

Methodology is presented in Chapter 8 for predicting the time required by an observer to detect military targets under conditions of night illumination and reduced visibility associated with haze, fog, and other weather conditions. This methodology is based upon theoretical relationships developed during laboratory experiments for predicting the probability of an observer detecting an object during specified time intervals. In addition, procedures for estimating model input parameter values from detection-time data collected during field experiments are presented.

#### Prediction of Detection (Pinpoint) Times of the Firing Signatures of Concealed Firing Weapons (Chapter 9)

Concealed or camouflaged firing weapons are pinpointed by an observer laying his weapon's sights upon the firing weapon's signature as evidenced by smoke, dust, flash, or vapor trail. In Chapter 9, a model for predicting the distribution of pinpoint times of concealed firing weapons is presented. In addition, an outline of experimental-design procedures for estimating the parameters of the model are presented. Estimators for model parameters using pinpoint data are specified.

#### Summaries of Other Models

In addition to research presented in this volume, unclassified summaries of research results described in detail in the classified annex for this final report are presented. Completed research to develop models for the systems listed below is summarized in this volume.

1. Indirect-fire electro-optical guided missile systems (Chapter 2),
2. DRAGON missile system (Chapter 4), and
3. Countermeasures (Chapter 7).



CHAPTER 2  
INDIRECT-FIRE, ELECTRO-OPTICAL  
GUIDED MISSILE SYSTEM

Unclassified Summary  
by  
R. J. Wilhelm

Introduction

Methodology has been developed and is reported in Chapter 2 of Volume 5 to describe the flight characteristics of the electro-optical missile systems and to relate their performance to combat unit effectiveness.

The electro-optical guided missile characteristically includes a missile equipped with a television camera and transmitter which transmit an image of a segment of the terrain below the missile's flight path to a control center. The E-O system serves as indirect-fire support in response to requests from forward observers. The primary difference between the electro-optical guided missile system and the indirect-fire, semi-active system, described in Chapter 1 of Volume 5 and summarized in Chapter 3, Volume 1, is the method by which the missile is guided to the target. The system depends upon a human operator, viewing the television image, to detect and lock onto the target. Following lock-on, the guidance system can direct the missile to the target with no further human intervention.

The role of the forward observer is determined by the guidance system being employed (i. e., semi-active or electro-optical (E-O) guidance). In both systems the forward observer provides information to the launcher regarding approximate location and description of the target. After providing this information, the forward observer plays no further part in the missile system operation if E-O guidance is being employed. The E-O system would appear to provide two possible advantages over the semi-active system regarding the forward observer role:

1. The forward observer is able to communicate more target positions to the launch site in a given time period because he is not required to continuously observe the target during missile flight; and

2. The forward observer is less susceptible to being detected by the enemy because of his passive role in the system.

Because several phases of the E-O system operation are identical to the semi-active system described in Chapter 1 of Volume 5, the basic models used to represent both systems are the same. Substantial differences between the two systems related to target acquisition and lock-on are confined to the flight of the missile from pitch-over to lock-on or fly-by. The E-O system requires a human operator to detect the target image and lock the missile tracker onto the target based on information from this image.

In order to describe the detection performance of an observer searching for a designated target on a television screen, a detection rate function relating the observer's detection capabilities to various battlefield parameters is required. Results from studies performed by North American Rockwell [1] and Martin Marietta Corporation [2] were analyzed to determine data requirements for the detection rate function. Because existing television display target detection data were deemed inadequate, experimental requirements and a proposed design for a field experiment were established. The data resulting from the field experiment would be utilized to obtain parameter estimates for the detection rate function in DYNCOM. To date, however, the field experiment has not been conducted. Therefore, the additional DYNCOM models developed to represent the detection capabilities of the human component of the E-O system utilize an approximate model with parameter estimates obtained from unaided visual ground detection experimentation as reported in reference [3].

These interim routines portray the target location on the television screen, the search procedure utilized by the observer over the screen, and a Monte Carlo determination of whether or not the target is detected. The routines can be modified as required when experimental data become available.

A complete description of the indirect-fire, electro-optical guided missile system appears in the classified annex, i. e., Chapter 2 of Volume 5.

#### REFERENCES

1. North American Rockwell, Target Acquisition Study for an Indirect-Fire Point Optical Contrast Guidance System, NR 68H706 (CONFIDENTIAL) September 1968.
2. Martin Marietta Corporation, Target Acquisition Studies: Fixed Television Fields of View, OR 9656, October 1968.
3. Clark, G. M. , and Howland, D. , (eds.) The Tank Weapon System, Annual Report, RF 573 AR 66-2 (U), Systems Research Group, The Ohio State University, AD 815023, December 1966.

# CHAPTER 3

## COMMUNICATION EXPERIMENT RESULTS

by

N. B. Wilson

Any system which involves coordinated activities of more than one individual must include some means of communication among these elements. A modern military force is such a system and is one in which the ability to communicate is especially critical. Poor battlefield communications can easily result in irreparable damage and defeat. Although military communication systems serve many purposes, the functions involving combat forces during a military engagement are discussed in this chapter. In an earlier plan of the communication experiment (Chapter 5 of Volume 1), the following objectives were identified:

1. determine probability density functions of message transmission times,
2. determine message classifications,
3. determine message priorities,
4. determine the nature of message reevaluation at transmission,
5. determine the nature of message relaying,
6. determine the dependence of duration on activity,
7. determine the effect of message repetition,
8. investigate the effect of equipment reliability, and
9. investigate the correspondence between the experimental and combat situations.

Some of these objectives were accomplished and others could not be achieved. The following conclusions were drawn from the experiment reported in this chapter (corresponding to the nine objectives listed above):

1. The duration of message transmission times has a Gamma probability distribution and the parameter values were estimated using the experimental data.
2. Message classification was not possible.
3. Message priorities are not applicable for battalion-sized activities. Priority messages were too infrequent for analysis.

4. A very short (not measurable) wait time is allotted for reevaluation of message.
5. No message relaying was analyzed.
6. No dependence of duration on activity could be identified.
7. Message repetition is included in the Gamma probability density functions given in 1 above.
8. Equipment reliability is an insignificant consideration because of the short duration of the combat actions represented by DYNCOM.
9. Correspondence of experimental conditions to those of combat was felt to be good.

A military communication network is a complex collection of communication channels which directly or indirectly connect the individuals and organizations participating in a military action. Although the communication channels may represent any of several physical information transmitting techniques, voice-transmitting radios are most frequently used in modern systems and are represented in the DYNCOM Communications Model. The network is composed of several groups of individuals and organizations, each assigned to one or more specific radio frequencies. These groups are said to be members of a net and can monitor or transmit on the net frequency. Generally, two types of information traverse a net: that which is of interest only to the members of the net, and that which would be of interest to members of other nets. Standard procedure designates at least one member of a net to be a leader, or information relayer. It is the duty of these individuals to evaluate the information which traverses the net and to determine and relay that information which is of interest to individuals or organizations on other nets. This relay is accomplished by passing the information on to another net. To do this, the leaders and relayers must have access to more than one net. A simplified net structure is depicted in Figure 3.1. If a net member at the bottom level, say unit A, wishes to send

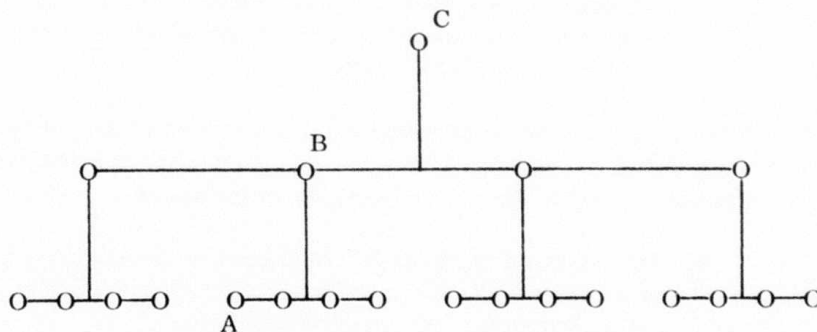


Figure 3.1.--Simplified Net Structure

any information to unit C at the top of the figure, he must relay it through the net leader, unit B, at the center level of the figure.

The net structures employed currently by the U. S. Army are generally more complex than the one in Figure 3.1. An example of a military net structure for an armored cavalry troop is shown in Appendix A. The Communications Model describes the operation of two levels of the complex military net structure. These two levels are the lowest two in the organization of a military communication system on the battlefield. They are the platoon and company tactical nets of a combat company. Furthermore, the model does not include those portions of the company communication system devoted to administration and logistics. Although these functions are of great importance to the long-range success of a military action, their efficiency is not as critical as that of the tactical nets.

The tactical nets provide communication among the fighting elements on the battlefield and make possible the coordination of the activities of these elements. The information traversing these nets includes reports of activities of both enemy and friendly forces, commands, requests for information, requests for assistance, etc. These types of information are of critical importance to the success of the action. The failure of the communication system can easily result in defeat of the forces involved. A communication system can fail to provide communication among elements if humans or equipment do not perform properly. It can also fail to fulfill its purpose even when all equipment is operating perfectly and all humans are performing correctly. This type of failure can occur as a result of poor system design.

DYNCOM is a complex computer program with component parts which model the many activities of elements engaged in combat. The operating characteristics of the simulated fighting elements are provided as inputs to the program. These inputs are based on performance data for existing weapon systems, and on expected or analytically derived data for proposed weapon systems. By including both existing and proposed weapon systems in a simulated battle, the military planner can economically predict, to some degree, the combat performance of proposed weapons without building and testing expensive prototypes.

Among the battlefield activities which are explicitly simulated in DYNCOM is communication. Two types of communication are explicitly represented in the Communications Model. These are reports of enemy locations and requests for indirect fire support from artillery or missiles. All other types of communication are collectively simulated as a group called "tactical" communications. This group includes all of the many other types of communication which occur on the battlefield. The two explicitly simulated types of communication are generated in response to specific events which occur in the simulation. Intelligence communications are generated when the intelligence model of DYNCOM determines that a friendly element has detected a previously unknown enemy element. The simulated communication served to inform other battlefield elements of the location



of the enemy and, consequently, makes it easier for them to detect it. The requests for indirect-fire support are generated when the firing model of DYNCOM recognizes a situation in which such support would be requested on the battlefield. The requests, when received by missile launchers or artillery, trigger a chain of events directed toward the delivery of the requested fire support.

The importance of the Communication Model lies in its incorporation of the delays which result when the communication nets become busy. At such times, queues of waiting users form, and their communications are delayed. Such delays cause consequent delays in the delivery times of supporting fires and in the times at which other elements can detect the enemy. The "tactical" communications are generated randomly at a rate hypothesized by the model designer, and serve to maintain the net traffic at a realistic level.

As study proceeded, it became apparent that the area of communication is in need of much research. Since it is of great importance to the success of military actions, it would seem that extensive analyses would have been performed. This is not, however, the case. Research results and data are difficult to find in the available literature. In particular, no empirical data were available to describe the times required to transmit information of the types simulated in the Communication Model or to describe the rates of generation of the "tactical" communications.

The goals of the research described in this chapter are motivated by the lack of meaningful prior research. Specifically, these goals are:

1. to develop data describing the time characteristics of military communication,
2. to modify the Communications Model to incorporate the results of the study in DYNCOM,
3. to define a measure of effectiveness, by means of which various communication systems can be compared, and
4. to simulate real and hypothetical communication systems and compare their performance.

The following sections of this chapter will be addressed to these problems and their solutions.

The model of communication systems which has been developed is sufficiently general to apply to several variations of the basic military communication system. An immediate product of the research lies in the numerical values describing the time characteristics of communication on the battlefield. These results will be used immediately in DYNCOM, and will be available for use in other simulations of military communications. All extensive mathematical discussions, tables, and computer programs appear in appendices.

### Model of the Communication System<sup>1</sup>

The basic communication system consists of elements connected by communication channels. An element may be a single human being or it may be a group of human beings. Such a group may be the crew of a tank, the staff at a command post, or any other such combat organization. Regardless of the nature of an element, it is treated as a single entity in the Communications Model. The group concept should be remembered if the capability of a single human to perform some of the tasks called for by the assumptions of the model is doubtful.

Each of the elements in the communication system has access to one or more nets. A net may connect any number of elements (at least two) and physically represents the common access of these elements to a specific single communication channel.

There will be two specific types of elements in the communication system. The first type will have access to only one net and will send and receive all information on this net, regardless of the nature of the information. The other types of element will have access to more than one net and will relay portions of the traffic from each net to the other nets as necessary. This second type of element is characterized by the platoon leader of a combat platoon. It is his responsibility to maintain contact with the members of his platoon and with his commanding officer. When he learns of an important event on his platoon net, he relays the information to his commanding officer. Similarly, when information affecting his platoon is received on the company net, he relays it to the members of the platoon.

The structure discussed above points out the existence of two distinct types of conversations which may occur on any net. They are those which are of interest only to the elements on the net on which they occurred and those which are of interest to elements on other nets. These two types will be referred to as "internal" and "external" conversations, respectively, and is the only distinction that will be made among the several possible types of conversations which occur in actuality.

---

<sup>1</sup>This section is a discussion of a communications model that is separate from DYNCOM. The model developed in this section is used to study the relationships among certain communication system variables.



To facilitate discussion of the traffic which traverses a net, clear distinction must be made between messages and conversations, defined as follows:

Message - An uninterrupted verbalization by one element, generally directed to one other element.

Conversation - A continuous exchange of message between two elements, concerning a single subject. If a continuous exchange of messages includes discussion of more than one subject, it will be broken into more than one component conversation for analysis purposes.

Examples of messages and conversations appear in Appendix B. The exchanges transcribed occurred during a zone reconnaissance action of an armored cavalry troop (company) consisting of two platoons. The conversations were monitored on one of the platoon nets. Reviewing these conversations, it is clear that messages and conversations can be readily recognized.

Prior to any military activity, the exact needs for communication cannot be anticipated. If the events that were to occur could be predicted, there would be no need for any communication. Since the events cannot be predicted, they can be handled mathematically only as random events. Further, since the random events of the battle determine the volume and nature of the demands on the communication system, these demands must be treated as random variables in any analysis of the system. Although the characteristics of the communication needs might well depend upon the general type of activity, they do remain random with their distributions and parameters depending upon the activity.

The occurrence of demands on the system is assumed random with Poisson distributions. The basis for this assumption and determination of the parameters is discussed in Appendix O. Just as the times of occurrence of demands on this communication system are random, the length of time required to meet the demands are random. That is, the duration of a conversation cannot be predicted exactly. On the basis of the data discussed in a later section, distributions describing the durations of the conversation types in varying situations will be developed. These conversation durations are sensitive to both the durations of messages within a conversation and to the number of messages composing a conversation.

Analysis of the combat situation reveals many variables in a military communication system besides occurrence and duration of conversations that are of consequence and that could be explicitly considered as random factors. These include forgetting of information by elements, attrition of battlefield forces, reliability of equipment and humans, and information content of conversations. For the analyses of this chapter, these factors must be rejected as potential control variables since no data are available to adequately describe their effects. They are, however, real parts of any military communication

system, and as such they are implicitly included since the data collected were subject to their effects. It is important to understand, then, that the conclusions of this research are relevant only in the context in which the data were collected. Most military communication systems using two-way radio at the company level can be described by the model developed herein, but any generalization should be made with caution.

The situation in which the data were collected will be discussed in detail in a later section. While the collected data will be used as a basis for development of an initial model, the model itself can later be used to study the effects of hypothesized or currently available changes in the various parameters and in the structure of the system. Thus, while the initial model will be an attempt to capture a specific real-world situation, the resulting model will be a tool for analysis of general communication systems. The results of studies performed with the general model will be discussed in a later section.

Several attempts have been made to model military communication systems. An extensive model has been developed by Philco Corporation for the U. S. Army Combat Development Command Communications Electronics Agency (CDCCEA, 1966). The model is in the form of a simulation, "Ground Combat Communications System" (GCCS). This simulation not only simulates the activities of a communication system, but also simulates a division-size military action to generate demands on the communication system. The combat simulation is extremely detailed and can be manipulated through literally thousands of variables which describe the individual characteristics of the elements on the simulated battlefield. While the structure of GCCS is similar to that of DYNCOM, the primary objective of GCCS is to evaluate communication systems, while DYNCOM evaluates weapon systems by predicting their performance. Within the simulation, GCCS, the demands on the communication system are deterministic in that the simulation recognizes specific situations in which communication should occur and generates the appropriate communications. Thus, although the demands on the communication system can still not be predicted before a battle is simulated, the interactions which result from the effects of communication can be evaluated and observed. For example, the communicated knowledge about an enemy element can result in the eventual destruction of that enemy element, thus reducing both the number of elements on enemy communication nets and reducing the number of potential objects for friendly communications. While it is an impressive and effective tool for analysis of large military systems, GCCS is too expensive and not sufficiently detailed for the communication analyses of this paper.

Murphy (1962) developed a model of the general military command and control system to investigate the flow of information through it. He applies queueing theory to seek optimal policies for operation of these systems. His model is similar to the one to be developed in this chapter, but his goals were different. He sought to optimize the performance of specific existing communication

systems in terms of information flow, while this chapter seeks to improve the system in general by locating its points of weakness and by analyzing alternative structures. Bennet (1957) also seeks to improve the system, but limits his efforts to the implementation of overlapping nets into the existing system.

Although some related research has been performed, no data have been found to describe the basic characteristics of military communication. Without an accurate description of the system, analyses of the system are subject to question. For this reason, data describing the system accurately are needed before any analysis is begun.

#### Available Communication Data

The search for data which describes the performance and demands of a communication system similar to the one being studied revealed very few efforts to collect any such data. All but one report found failed to provide relevant data. Lennahan (1960) describes an experiment conducted at Fort Stewart, Ga., in which the battalion command nets of two medium tank battalions were monitored during three exercises. The information presented in the report does not satisfy any of the data needs of this study, since the goals of the experiment were analyses of the frequencies of occurrence of the various types of communications that occur on the command nets. No conversation duration data were presented in the report, but the message classifications have been helpful in some stages of the analysis for this study.

Brown (1967) describes an experiment conducted at Fort Benning, Ga., in which observers collected communication data on seven Ranger patrols. The primary goal was, again, the classification of messages. The specific interest was in the number of distinct types of communication, and not in the durations of conversations. The eventual goal of the research was the development of an actual communication system for person-to-person communication on the battlefield. Again, while the research was enlightening and worthwhile in its own right, it did not provide any numerical data for use in this study.

One unpublished report did contain data that were relevant to the problems addressed herein. The data were obtained from the U. S. Army Combat Developments Command, Experimentation Command (CDCEC, 1968). This report presents data collected during an experiment at Fort Ord, California. The general scenario of the experimental situation is as follows. Aggressor forces have invaded the United States, landing amphibious forces in the vicinity of San Francisco and Los Angeles. An Aggressor Airborne brigade has made a successful para-drop in the vicinity of the Los Padres Forest. They are attempting to strike east and cut Highway 101. The data collected were generated by the MOMAR (Mobile Modern Army) 1st Medium Company as they attacked the aggressor in a wooded area and under a nuclear environment.

The report of the Fort Ord exercise (conducted 9 November 1960) includes an analysis only of data collected within the scenario described above, although recordings were made during several other scenarios. The data include a verbatim transcription of the messages for the entire period, times for each conversation, and the length of time that elapsed between each successive conversation that occurred. While the messages that constituted the conversations were not explicitly timed, they are of the same types found in a later experiment conducted at Fort Carson, Colorado, (to be discussed in a later section) and their durations can be estimated. The information of real value which can be gained from the Fort Ord experiment is a distribution of conversation durations and distributions of the numbers of the various message types that are included in conversations. While these distributions are not presented in the report, they can be easily computed from the data that are given. The data are summarized in Appendix D. These data will be used in conjunction with the data developed in a later section to fill the data requirements of this study.

After reviewing the transcribed messages and groups of messages, it is evident that certain of them are not typical of a true battlefield atmosphere since they include conversations with experimental controllers and "discussions" of the activities of these controllers. The final analysis of these data does not consider these unrealistic conversations and, as can be seen in the data summary of Appendix F, alters the general appearance of the data histograms. Although the situation in which the data were collected was somewhat artificial at times, a great amount of useful information has been extracted from the report.

The conversations analyzed in the CDCEC report were generated on a MOMAR Medium Command net, and thus do not include the communications of the platoon nets. This is not, however, completely undesirable since a command or company net is a part of the general model developed herein. These data can, therefore, be used both in the analyses of the general military communication system and to validate the data discussed in the next section. Tape recordings of platoon-net traffic were also prepared during the Fort Ord experiment, but these have not yet been analyzed by CDCEC. If they are at some later date processed, the data could be used to validate and strengthen the data base employed in the analyses discussed in the final section of this chapter.

While the related literature has provided insights and some data for the analyses to be performed in this thesis, the need remained for a large amount of detailed data describing the time characteristics of military platoon net traffic.

## Communication Data Experiment

When a search for data failed to provide a description of the types of military communication germane to this study, it became apparent that an experiment would be necessary. An extensive data-collection effort was undertaken. The results obtained are directly applicable to the situations simulated in DYNCOM and are currently being used for that purpose. The data can also serve as a data base for further studies and other simulations of military communication. The planning, design, and conduct of the experiment are discussed in this section, along with data-processing techniques and results.

### Planning the Experiment<sup>1</sup>

The first problem confronted in planning the experiment was the location of a suitable site. After lengthy consideration, a list of characteristics was compiled describing the ideal site. This list includes the following: (see Chapter 2, Volume 1)

1. exercises at the company level or higher must be available for observation,
2. the individuals involved in the exercises should be trained Army personnel, not new trainees,
3. several types of military action should be performed within a period of two or three days to allow collection of a wide range of data,
4. enough radio traffic must be available to allow collection of a large data set,
5. the terrain should be sufficiently irregular to permit an approximate evaluation of the effects of line-of-sight on communication, and
6. the exercises observed should not be "canned" ones which the participants have performed many times before.

The initial candidate location was Fort Knox, Kentucky, the location of the U. S. Army Armor Agency. A visit to this location and discussion with military personnel revealed that the majority of the exercises performed at Fort Knox were for basic training. These exercises would not satisfy the needs of the experiment because the situations would be artificial and the communications would not approximate actual battlefield communications.

---

<sup>1</sup>This subsection is a summary of the experimental plan presented in Chapter 5 of Volume 1.

The next candidate site, and the eventual choice, was Fort Carson, Colorado. This site proved to be ideal, satisfying most of the conditions stated above. During a preliminary trip to Fort Carson, arrangements were made to observe and collect data during exercises of two troops of an armored cavalry squadron. The constituent elements of this organization can be seen in Appendix A. The size of such a troop is comparable to that of a standard Army company, thus satisfying requirement (1). The personnel of the troops were generally well trained, many being recent returnees from Viet Nam. The purpose of an armored cavalry troop is stated in U. S. Army field manual FM17-36:

The armored cavalry troop is designed to perform reconnaissance, provide security, and engage in offensive, defensive, and delaying action as an economy of force unit. It is employed on missions that complement the squadron mission or the mission of the unit to which it is attached.

The typical activities of the armored cavalry include zone reconnaissance, road reconnaissance, and delaying actions. All of these were scheduled for the proposed observation period. The exercise described in this section does not actually fit the normal definition of an experiment since no efforts were made to control the activities of the observed personnel. In fact, efforts were made to make the observers as inconspicuous as possible in hopes that the realism of the recorded communications would not be impaired. Fortunately, the scheduled exercises were to be conducted within a vast military reservation in the foothills of the Rocky Mountains, meaning that the participants would be in terrain unfamiliar to them and would not be operating in areas with the undesirable characteristics of a training field. Such characteristics were observed at Fort Knox in the form of easily visible tank trails and other effects of repeated use.

#### Conduct of the Experiment

The squadron to be observed was incomplete because one of its original three troops had been sent to Viet Nam. The remaining two troops would, however, provide a sufficiently wide range of activities and types of communication to satisfy the needs of this study and the data requirements of DYNCOM. The primary interest was in the troop and platoon nets, but two other areas of communication were recorded for general interest and possible later analysis. These were the S2 and S3 areas in which the squadron command, control, intelligence, and fire support coordination took place.

Of the two troops to be observed, one was incomplete in that it consisted of only two platoons instead of the normal three. This was the result of equipment and manpower shortages. For the exercises scheduled, this deficiency did



not seriously affect the volume of communication traffic. The traffic on the two platoon nets was not affected by the deficiency. The traffic density on the troop net was, as would be expected, lower than would be observed with three platoons, but this density does not affect the conversation durations of interest.

The communication traffic of nine nets was recorded. These were:

1. Bravo troop - Troop net
2. Bravo troop - Platoon 1
3. Bravo troop - Platoon 2
4. Charley troop - Troop net
5. Charley troop - Platoon 1
6. Charley troop - Platoon 2
7. Charley troop - Platoon 3
8. S2 command and control area
9. S3 enemy intelligence area.

All recordings of net traffic were made with portable cassette-type tape recorders. The use of small portables allowed great flexibility in the placement of personnel. The original intention was to place one observer in the vehicles of each of the troop commanders to monitor and record the troop nets. One other observer was to travel with each of the troops in a separate vehicle to observe the action from a distance and to record at least one of the platoon nets. The latter proved impossible due to a shortage of vehicles. Consequently, only two observers were able to travel with the troops, one with each of the commanders. The other nets were monitored and recorded from stationary radio receivers in the area of the command post.

The data-collection effort required seven men for three days. The first day was spent traveling to Fort Carson, Colorado, and training the observers for the data collection of the following days. The first day was also needed for coordination with the military personnel involved, to guarantee that the observers would have access to the required vehicles, transportation and radios. Although arrangements had been made in advance, some of the equipment that had been promised was not available, requiring improvisation. The officers of the 4th Squadron, 12th Cavalry made great efforts and the success of the experiment is largely a result of their full cooperation.

During the second and third days of the data-collection exercise, the net traffic of the troops was recorded during most periods of activity. A summary of the periods and the coverage of the recordings is given in Appendix E. The mid-day lull of the 18th was the result of a period of time set aside for maintenance, lunch, and classes. There was no radio traffic during this time. The night action of the 18th was a limited infiltration exercise, with extensive radio traffic. The recording on the 19th was curtailed when the troops stopped for lunch and classes and to allow time for the research team to travel back to Columbus, Ohio, that night.

A review of the recorded net traffic reveals that the portable tape recorders provided an excellent record of the conversations. The traffic is as comprehensible as it was when heard directly on the monitoring radio receivers. Only minor problems developed during the taping of the traffic when tapes jammed in the recorders. This problem occurred only four times and was easily remedied by the observers affected. Such jams resulted in only momentary losses of coverage. In general, the information recorded is easily sufficient to permit thorough analysis of the traffic which occurred during the exercises.

### Data Processing

The reduction of the data on the recording tapes required two phases of processing: the measurement of message and conversation durations, and a statistical analysis of these durations. The goal of the processing was a set of general probability distributions and parameters describing the company and platoon level communications of a military communication system.

The first phase of the processing of the tapes was accomplished by the time-consuming use of a stopwatch to record the durations of messages and conversations. Time limitations dictated that only selected portions of the tapes be processed. These portions were selected to provide what was felt to be a characteristic sample of the types of communication which occurred during the exercises observed. They were also selected from the segments having the highest densities of traffic flow, since such periods represent the most critical phases of operation of the military nets in terms of mission success.

The message and conversation durations were keypunched onto computer cards for processing and evaluation. The first step in the analysis of the data was preparation of histograms. This was done to provide a visual representation of the data to assist in the selection of candidate probability distributions to describe the random process involved. A computer program was designed to prepare these histograms and compute certain characteristics of the data. The histograms themselves are collected in Appendix F. The set of histograms includes those prepared from the Fort Ord data discussed earlier as well as the Fort Carson data.

### Results of Experiment

The histograms of the data representing conversation durations indicate a characteristic shape for all data sets. The general form of the histograms is a unimodal distribution which is distinctly skewed to the right with a lower bound very near zero. While several standard probability distributions can assume this general form, the two-parameter gamma distribution, beginning at the origin, appeared to fit well and filled the needs of this analysis. It also provided sufficient flexibility to permit later manipulation of its form for purposes of



sensitivity analysis. The assumption of a gamma distribution appears to be justifiable when it is noted that the sum of several similarly scaled gamma distributed variables is again gamma distributed. The characteristics of the two-parameter gamma distribution are reviewed in Appendix G. The fact that the sum of several gamma distributed variables is gamma distributed would support the hypothesis that a conversation is composed of several component parts, each part having a duration that is gamma distributed. Analysis of message and space durations indicate that this assumption is reasonable.

After accepting the two-parameter gamma distribution as a descriptor for conversation durations, the next problem was estimation of parameters from the collected data. Several techniques for the estimation of the parameters of a gamma distribution were reviewed, including those of Wilk, et al. (1962), Sarndal (1964), and Stacy and Mihram (1965). Finally selected as the most effective and convenient technique was the one described by Greenwood and Durand (1960). They develop the maximum likelihood estimators for the parameters of the two-parameter gamma distribution and provide polynomial estimators for these maximum-likelihood estimates. The polynomial approximations are well suited for use when a computer is available. The development of the maximum-likelihood estimators is summarized in Appendix II, along with the polynomial approximations.

The problem of parameter estimation does not end with the use of the polynomial approximators. Any set of data could be subjected to the estimation procedures described in Appendix II and yield parameters of a particular gamma distribution. This does not, however, guarantee that the resulting distribution effectively approximates the data. Some criterion to measure the "goodness-of-fit" of the approximating distributions must be applied. The standard test for goodness-of-fit is the chi-square test, in which the data are grouped, and the probability points of the groups are compared to the corresponding points of the hypothesized distribution. The major objection to the use of this test in the situation of this study is the grouping requirement. Since there is no hard and fast rule for grouping data for the chi-square test, it is, to a large degree, arbitrary. The results of the test can depend greatly upon the way in which the data are grouped. The effect of interval size and definition in data grouping is illustrated by the two histograms prepared from the Fort Ord - Situation 6 - data in Appendix F. It is obvious that interval size can drastically affect the appearance of the distribution. A further objection to the chi-square test for these data is the required treatment of a continuous measurement as a discrete variable. Time (duration) is a continuous variable which can assume any real value within a specified range, while the assumptions of the chi-square test imply that the variables tested are discrete.

The test selected as most applicable and most effective for this study is the Kolmogorov-Smirnov test for goodness-of-fit. This test rejects or fails to reject the hypothesized distribution on the basis of the maximum deviation between the theoretical and actual cumulative probability function. The characteristics and examples of both the chi-square and Kolmogorov-Smirnov tests are presented in Appendix I. A program was prepared for the computer in which the approximating polynomials described earlier are used to approximate the gamma parameters for a data set and the Kolmogorov-Smirnov test applied to the resulting hypothesized distribution. Both the hypothesized and the actual probability distribution are plotted on the same graph in the form of their cumulative probability functions to permit visual analysis of the fit. The outputs of the analyses of the Fort Carson and Fort Ord data are collected in Appendix J.

The results of the data analyses and the goodness-of-fit testing indicate that the assumption of a gamma distribution was a reasonable approximation for the data. On the basis of these findings, the gamma assumption will be carried through the remainder of this chapter. A compilation of the parameters of the distributions of interest for this paper can be found at the end of Appendix J. These parameters will be used in analyses of a later section and for inputs to DYNCOM.

#### Communication Model Simulation

Once a physical process such as communication has been modeled mathematically, it is desirable to test the model and to apply it. One approach which is especially applicable for complex systems is the development of a simulation. The development of such a simulation of a communication system is discussed in this section.

The simulation developed in this chapter is significantly less complex than DYNCOM and GCCS. While the communication segments of both of these simulations depend upon a combat simulator to generate demands on the communication system, the simulation discussed in this section randomly generates demands and does not include any interaction between battlefield activity of elements and their communication activity.

The principal motivation for a simulation in the context of this study is to provide a tool to permit the analysis of the relative effectiveness of various operating procedures and design characteristics applied to the basic military communication system. The analyses performed is discussed in the next section. This section explains the assumptions of the simulation and the general structure of the computer program used to simulate the system.

The basic component of the simulation is the individual battlefield element defined earlier. These elements are connected by nets with the net configuration being determined by inputs to the computer program. The behavior of the elements is determined by the individual characteristics of each element, the state of the simulated system, and the activities of the other elements. The interactions between the elements are, however, limited to competition for access to radio nets.

Three distinct types of elements are considered. These are called (1) platoon elements, (2) platoon leaders, and (3) company commander. Platoon elements have access to only one radio net, and must generally depend upon the platoon leader to relay critical communications to the company commander. The platoon leaders have access to two nets and have the responsibility of relaying communications between the two nets. Although, in actuality, there is only one platoon leader in standard military platoons, there is usually a platoon sergeant who also has access to both nets. The platoon sergeant is also called a platoon leader for purposes of simulation, giving him access to both nets and allowing him to relay communications between the nets. The company commander is the only element of the company net who is not a platoon leader. The company commander behaves on the company net much as the platoon elements does on the platoon nets.

As mentioned earlier, only two basic classifications of communications will be considered in this study. These two types have been labeled internal and external. In the military context, this means communications that are of interest only to members of the sender's net and those that are of interest to members of other nets, respectively. The demands for each of these types of communications are generated randomly for each element, according to a probability distribution determined by input parameters. The platoon leaders generate both types of demands on both of the nets to which they have access. Although the external communications generated by the platoon leaders do not have to be relayed, they will compete with the relayed communications for net time and are considered of equal importance for purposes of analysis.

With the designated structure of the communication system, the types of communication which can occur are:

1. internal communications on the platoon net,
2. internal communications on the company net,
3. communications relayed from the company net to the platoon net,
4. communications relayed from the platoon net to the company net,
5. external communications from the platoon elements to the platoon leaders for relay to the company net, and
6. external communications from the company commander to platoon leaders for relay to platoon nets.

Because no criterion has been developed to determine relationships among battle-field elements, external communications from the company commander are randomly passed to one of the platoon leaders for relay. This assumes that all platoons are equally likely to receive communications from the company commander and divide them equally among the platoons. If this assumption were unsatisfactory for a specific study, specified platoons could easily be weighted to receive any specified portion of these communications.

Within the computer simulation, queues are being maintained for each net with communications waiting to be relayed. Two queues are needed for each platoon net because communications are relayed both to the company and the platoon net by the platoon leaders of each platoon net. No queues are needed for the company net since higher levels of the military net structure are not being considered in the model of this study. Within the queues, a first-come-first-served priority system applies. That is, when a platoon leader gains access to a net, he sends communications from the queue of that net and his own communications for that net in the order in which they occurred, subject to the priority system discussed in the following paragraph.

A priority system for platoon leaders was established to fit the military procedure as well as possible. When a platoon leader is able to gain access to both his platoon net and the company net simultaneously, the following rules determine which of the nets he will use:

1. If there are any external communications to be relayed or sent on the company net, use the company net.
2. Otherwise, if there are any external communications to be relayed or sent on the platoon net, use the platoon net.
3. Otherwise, if there are any internal communications to be sent on the company net, use the company net.
4. Otherwise, if there are any internal communications to be sent on the platoon net, use the platoon net.

If none of the above cases hold, there are no demands on either net which the platoon leader can satisfy. These rules are subject to variation for the analyses of the next section. When a platoon leader can gain access to only one of the nets because the other is busy, those three priorities applying to that net are used. Similarly, when a platoon element or the company commander gains access to the net, external communications have priority over internal communications.

When an element gains access to a net and begins to send, that element maintains control of the net as long as it has an uninterrupted sequence of communications, both internal and external. An example might well illustrate both the access rule and the priority system. Consider a platoon element with the following unfilled demands with the indicated durations. The following sequence of events would occur in the simulation.

<u>Internal Demands</u>			<u>External Demands</u>		
	Time	Duration		Time	Duration
I <sub>1</sub>	14.2	.7	E <sub>1</sub>	14.1	.6
I <sub>2</sub>	14.6	.3	E <sub>2</sub>	15.9	.4
I <sub>3</sub>	17.0	.5	E <sub>3</sub>	18.3	.6

1. Assume that the net became available to the element at time 14.5, then of the two demands in existence at that time, I<sub>1</sub> and E<sub>1</sub>, the demand E<sub>1</sub> would have priority and be sent. The net would then be busy until time 15.1.
2. Of the two demands available at time 15.1, I<sub>1</sub> and I<sub>2</sub>, the earliest, I<sub>1</sub>, would have priority and be sent. The net would then be busy until time 15.8.
3. Only one demand, I<sub>2</sub>, is in existence at time 15.8, and it would be sent. The net would then be busy until time 16.1.
4. Only one demand, E<sub>2</sub>, is in existence at time 16.1, and it would be sent. The net would then be busy until time 16.5.
5. No demands are in existence at time 16.5. Although future demands will exist, the net is relinquished at time 16.5 since a continuous flow of communication can no longer be maintained.

The rules controlling the behavior of the platoon leaders are very similar to those controlling the other elements. The only added complexity with platoon leaders lies in the procedure described earlier for selecting a net. The logic controlling the simulation is best analyzed by reviewing the flow charts of Appendix K. An abbreviated flow chart of the entire simulation precedes the detailed flow charts.

The structure of the simulation implies certain characteristics of the simulated system. It is assumed that a sending element cannot be interrupted by another element. Further, a communication being sent by an element cannot be interrupted by another communication of the same element. From the data describing military communications, these assumptions appear to be reasonable. These same characteristics should apply to most existing communication systems but, if not, minor adaptations can be made to introduce a preemptive priority system.

Within the simulation, access to newly freed nets is determined randomly. This procedure is meant to simulate the typical situation in which, regardless of how long a potential user has waited, he must compete with all other potential

senders for access to the net. A telephone network has the same characteristic. This procedure is effected in the computer program by randomly selecting one of the potential users of a net when it becomes free. If a net is free and no element has need of it, the time of availability is successively advanced by a small time increment until an element needs it. In this way, the simulation moves through time, filling the demands of the elements.

As mentioned earlier, the times between demands on the nets and the durations of the communications are determined randomly. Each element is assigned parameters describing a probability distribution of times between demands for each type of demand the element may generate and for the durations of each type of communication. Thus, the platoon elements and the company commander each have two space-between-demands probability distributions and two conversation duration probability distributions. Platoon leaders, being on two nets, have a similar set of parameters for each net.

In order to generate random times, the inverse of the cumulative probability function of each of the probability distributions is needed. Using the fact that the cumulative probability distribution of any probability distribution can be generated by transforming a  $U(0,1)$  random variable by the inverse of the desired cumulative density function (Hogg and Craig, 1966), random numbers approximating a population from any probability distribution can be generated using a uniform random number generator (on the interval zero to one) and the inverse of the cumulative probability function.

The procedure is discussed briefly in Appendix P. Because a closed form expression for the inverse of the gamma distribution is unavailable, a special procedure was applied to approximate the cumulative probability function. After reviewing the data describing communication durations for the military communication system, it was obvious that only a small group of the infinite family of gamma distributions would be needed to approximate those times. By using numerical integration, points on the cumulative probability distributions of several members of the gamma distribution in the region of interest were generated. These points were then subjected to multiple regression techniques to find an approximation which would provide a time as a function of a random number drawn from the uniform distribution, and of the parameters of the distribution for which a random time is needed. The procedure used to obtain this estimating function is described in Appendix P.

The simulation developed and discussed in this chapter will be used for the analyses of the next section. The inputs to the simulation will be based on the data discussed in previous sections. Also, hypothetical inputs are tried, searching for a better system and for the parameters to which the existing system is most sensitive.



The performance of the simulated communication system is measured according to criteria developed in the next section and the performances of the various real and hypothetical systems will be compared. The measurements of the criteria will be performed by the computer program itself and the results of each simulated system will be a part of the output of the simulation program. These results and criteria will be discussed in detail in the next section.

### Communication Model Performance

In this section, the models, data, and insights developed in the preceding sections are combined to perform an analysis of the general communication system which has been the subject of this study. The simulation of the previous section is used to predict the performance of several communication systems. The data and insights gained through the experiment and the literature search provide a data base and familiarity with the system to support experimentation through variation of the simulation structure and parameters. With these tools, systems can be analyzed which are quite different from that observed during the experiment at Fort Carson.

The first study of this section analyzes a system which resembles the one observed during the experiment at Fort Carson as closely as possible. During that experiment, no method was available to accurately determine demand rates for the elements involved. From the tape recordings, one can determine only which element has control of a net. There is no way to tell which elements are waiting for access to a net. Demand rates could be approximated only from overall usage of the nets, as discussed in Appendix O. The approximated demand rates do, however, produce net traffic in the simulation that is very similar to the observed traffic, implying that they are reasonable approximations. The similarity was noted especially in the time distribution of spaces between communications on nets, and in particular in the frequency of occurrence of spaces with zero duration. Using the estimated demand rates and the observed communication-duration distributions, the Fort Carson armored-cavalry communication system is simulated. From the simulation output, interactions can be observed, waiting times calculated, and the overall operation of the network studied.

With the simulation as a tool, variations of the Fort Carson type communication system have been analyzed. Although the U. S. Army has been developing communication systems for many years, it seemed that there was still some room for improvement. In this section, some proposed improvements are simulated and their performance compared with that of the simulated Fort Carson system. These improvements maintain the basic identity of the observed system; i.e., the concept of the platoon and the use of radios will not be altered, but modifications in the net configuration and in various parameters of the system are made. Some variations of the Fort Carson system are simulated simply to determine the response of the system to various parameter changes.



If we wish to evaluate and compare communication systems, some measure is needed which will indicate how well a system is performing. The best type of measure appears to be one by which the Army personnel using the system would judge it, specifically, the amount of time one must wait when he needs access to a net. The measure that is applied to the analyzed systems, therefore, is a long-run average of waiting times over the simulation of a specific parameter set and system configuration. The waiting time for a single communication is defined as the length of time between the generation of a demand and the beginning of transmission of the communication.

The remainder of this chapter consists of analyses of several variations of the general communication system. These studies are separated according to the specific parameters which are varied. The results of the studies are then pooled to provide an overall sensitivity analysis of the system and to provide an estimator of waiting time for proposed systems.

A set of ten variables that describe the configuration of a simulated communication system, including the parameters, have been formulated. These variables are used to describe changes in the basic system for the studies that follow. These same variables are submitted to statistical analysis by pooling all simulation results to determine an estimator of waiting time. The variables are defined as follows:

1.  $d_{pi}$  total demand rate on a platoon net for internal-type communications,
2.  $d_{pe}$  total demand rate on a platoon net for external-type communications,
3.  $d_{ci}$  total demand rate on the company net for internal-type communications,
4.  $d_{ce}$  total demand rate on the company net for external-type communications,
5.  $\mu_i$  mean of duration distribution for internal communications,
6.  $\mu_e$  mean of duration distribution for external communications,
7.  $\sigma_i^2$  variance of duration distribution for internal communications,
8.  $\sigma_e^2$  variance of duration distribution for external communications,
9.  $R$  number of relay elements in the system, and
10.  $d_R$  demand rate describing the total load of a relay element, including both his own communications and those to be relayed.

The results of simulation runs are presented in a tabular form in this chapter for the various studies. Because there is some random variation in the results, more than one replication of each configuration was performed.

The results presented are:

1. W      average waiting time for one simulation replication,
2. M      mean of all W values for a system configuration,
3.  $S^2$     sample variance of all W values for a system configuration,
4. n      average number of communications per minute over all replications of a system configuration,
5. rcpl    number of replications simulated for a system configuration.

#### Study A

This study contains the results of simulation replications of a system that resembles the one observed at Fort Carson. The data collected during the experiment described in an earlier section and those found during the literature search are used in this study. These data are fully discussed in Appendices J and O. The simulation structure is as developed in the preceding section.

Forty-five minutes of net activity is simulated for each replication. After reviewing simulation results, this amount of time appeared sufficient for fluctuations in the variable, W, to become small from minute to minute of simulated system activity. Further, this is the amount of time recorded on each of the tapes during the Fort Carson experiment. Comparison of numbers of communications is of interest for possible later research.

The mathematical characteristics of the system are summarized in Tables 3.1 and 3.2. The derivations of these data are discussed in Appendices J and O.

The results of the Fort Carson simulation replications are summarized in Table 3.3. The results of this study will be referred to as A-1.

All simulation replications in this and subsequent studies are initialized with no communications in the relay queues. Thus, the activity simulated would resemble the type that would occur when a combat company makes initial contact with the enemy. The time of occurrence of the first of each demand type for each element is determined by randomly drawing a time from an exponential distribution with its parameter equal to the demand rate for the particular demand type.

#### Study B

This study seeks to determine the effects of changes in demand rates on communication system performance. For this study, several variations on the basic Fort Carson system are simulated. The values of the variables were arbitrarily selected to investigate the effects of the variables. These variations are numbered and discussed as follows:

Table 3.1  
Fort Carson Demand Rates

Element	Platoon Net (com. /min.)		Company Net (com. /min.)	
	Internal	External	Internal	External
Platoon Leader	.250	.130	.025	.040
Platoon Sergeant	.250	.130	.025	.040
Platoon Elements	.010	.010	--	--
Company Commander	--	--	.060	.150*

\*Note that the external communications from the company commander are randomly divided among the platoons for relay, each platoon having equal probability of receiving a communication.

Table 3.2  
Fort Carson Conversation Duration Distributions

Conversation Type	Gamma Distribution Parameters	
	shape (a)	scale (b)
Internal	1.70	19.45 sec.
External	1.83	20.84 sec.

- B-1 Double the external demand rate for all non-relayer elements on the platoon nets. All other demand rates and the duration distributions remain at the Fort Carson values.
- B-2 Change the external demand rate of the company commander from .15 to .27. All other parameters remain at the Fort Carson values.
- B-3 Change the platoon net internal demand rate of the relay elements from .25 to .30. All other parameters remain at the Fort Carson values.
- B-4 Change the company net internal demand rate of the relay elements from .025 to .15. All other parameters remain at the Fort Carson values.
- B-5 Change all demand rates to a level 1% above the Fort Carson values. Other parameters remain at the Fort Carson values.
- B-6 Change all demand rates to a level 2% above the Fort Carson values. Other parameters remain at the Fort Carson values.
- B-7 Change all demand rates to a level 4% above the Fort Carson values. Other parameters remain at the Fort Carson values.
- B-8 Change all demand rates to a level 10% above the Fort Carson values. Other parameters remain at the Fort Carson values.
- B-9 Change all demand rates to a level 20% above the Fort Carson values. Other parameters remain at the Fort Carson values.

The first four variations are investigated primarily for qualitative comparisons in this study. They also provide useful quantitative information for the overall analysis at the end of the chapter. The last five variations of this study provide useful information about the response of the Fort Carson system to demand variations. The simulation results of this study are tabulated in Table 3.4.

The simulation results of variations B-5 through B-9 are presented graphically in Figure 3.2. A regression line representing the best least-squares fit is also plotted on the graph. The results of variations B-5 through B-9 indicate that the existing Fort Carson system would react to homogeneous demand rate increases with an approximately linear increase in  $W$ . The regression equation for the data is  $W = .47106 + .00327 x$ , where  $x$  is the percentage increase in demand rates over the Fort Carson values. The standard error of the equation is .098 and the  $F$  ratio is 1.307. While the  $F$  ratio would indicate that the effect is not significant at the .05 level, it is felt that further simulation runs would follow the same trend and produce significant results. On the basis of the indications of this study, the communication system designer can predict the effect of such increases in demand rates and can weigh them against any value to be gained from such increases.

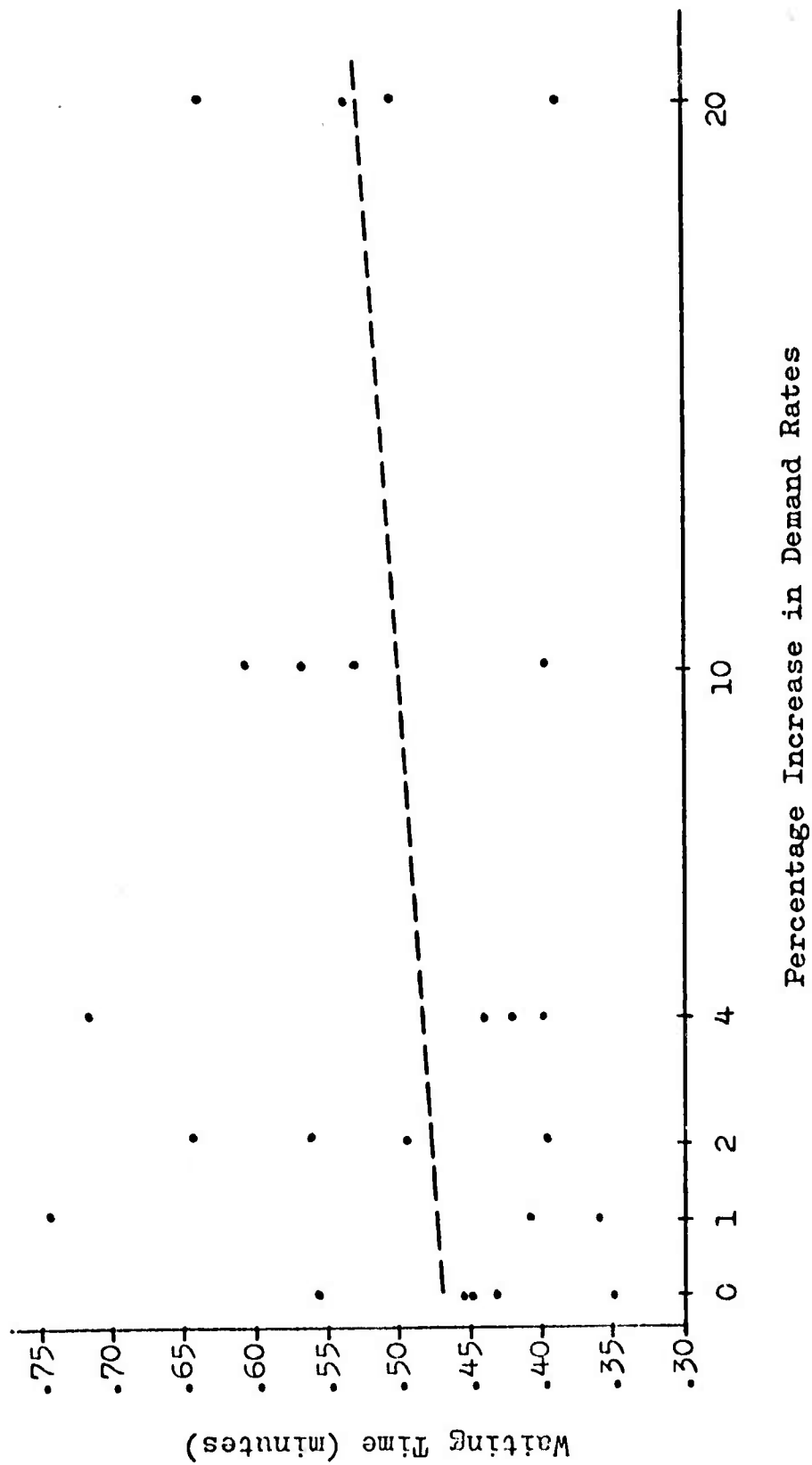


Figure 3.2. --Study B Results

Table 3.3

Performance of Simulated Fort Carson  
Communication System

Configuration	M	S <sup>2</sup>	n	rep
A-1	.448 min.	.006 min <sup>2</sup>	3.8 com./min.	5

Table 3.4

## Study B Results

Configuration	M	S <sup>2</sup>	n	rep
B-1	.475 min.	.025 min <sup>2</sup>	3.6 com./min.	4
B-2	.472 min.	.035 min <sup>2</sup>	3.6 com./min.	4
B-3	.440 min.	.009 min <sup>2</sup>	3.5 com./min.	4
B-4	1.010 min.	.101 min <sup>2</sup>	4.2 com./min.	4
B-5	.510 min.	.027 min <sup>2</sup>	3.5 com./min.	3
B-6	.522 min.	.009 min <sup>2</sup>	3.4 com./min.	4
B-7	.495 min.	.017 min <sup>2</sup>	3.7 com./min.	4
B-8	.529 min.	.003 min <sup>2</sup>	4.0 com./min.	4
B-9	.521 min.	.005 min <sup>2</sup>	3.9 com./min.	4

### Study C

This study seeks to determine the effects of changes in conversation duration distribution parameters on communication system performance. For this study, several variations of the basic Fort Carson system are simulated. These variations involve changes only in the conversation duration distribution parameters for the internal and external communications. All other parameters retain the Fort Carson values as discussed in Study A. The affected parameters are listed in Table 3.5, along with identification numbers. For each configuration, only the values of the gamma distribution shape parameter,  $a$ , and the scale parameter,  $b$ , are listed for the two distributions concerned.

The variations selected represent a range of parameter values which this author feels are reasonable predictions of future communication capabilities. The relative values of internal and external communication distribution parameters reflect the fact that external communications are generally of longer duration than internal ones. Formatted reports occurring on company nets (see Appendix C) are, to a large extent, responsible for this difference.

Because no single parameter was obviously sufficient to describe the combinations of internal and external communication duration distributions, the effects of the means of the two distributions will be investigated separately. The mean of the gamma distribution is equal to the product of the two parameters ( $\text{mean} = ab$ ). In Figure 3.3,  $W$  values of several replications are plotted against both of the means on the same graph. The excessive number of points at the internal mean of .64 minutes and at the external mean of .55 minutes represent the inclusion of replications of configuration A-1 in the data.

Regression analysis reveals no statistically significant effect for either of the distribution means. The  $F$  ratios are .91 and .47 for the internal and external means, respectively. These values fall far below the critical values for the  $F$  test at the .05 significance level. These results might be of special interest to the communication system designer who is seeking to shorten the communication duration distribution means. This study indicates that, within the range of parameters analyzed, little or no reduction in  $W$  can be expected by shortening communications. Several more replications would be desirable to further investigate these variables. Also, statistical analysis of other functions of the conversation duration distributions would be of interest for later research.

The results of the simulation replications of this study are tabulated in Table 3.6.



Table 3.5  
Study C Variations

Configuration	Internal		External	
	a	b	a	b
C-1	1.50	18.00 sec.	1.60	19.00 sec.
C-2	1.60	18.00 sec.	1.70	19.00 sec.
C-3	1.60	19.00 sec.	1.70	20.00 sec.
C-4	1.60	20.00 sec.	1.70	20.00 sec.
C-5	1.60	20.00 sec.	1.70	21.00 sec.
C-6	1.70	18.00 sec.	1.83	19.00 sec.

Table 3.6  
Study C Results

Configuration	M	S <sup>2</sup>	n	rep
C-1	.490 min.	.001 min. <sup>2</sup>	3.5 com./min.	2
C-2	.395 min.	.002 min. <sup>2</sup>	3.6 com./min.	2
C-3	.375 min.	.001 min. <sup>2</sup>	3.6 com./min.	2
C-4	.465 min.	.002 min. <sup>2</sup>	3.5 com./min.	2
C-5	.380 min.	.001 min. <sup>2</sup>	3.3 com./min.	2
C-6	.445 min.	.002 min. <sup>2</sup>	3.7 com./min.	2

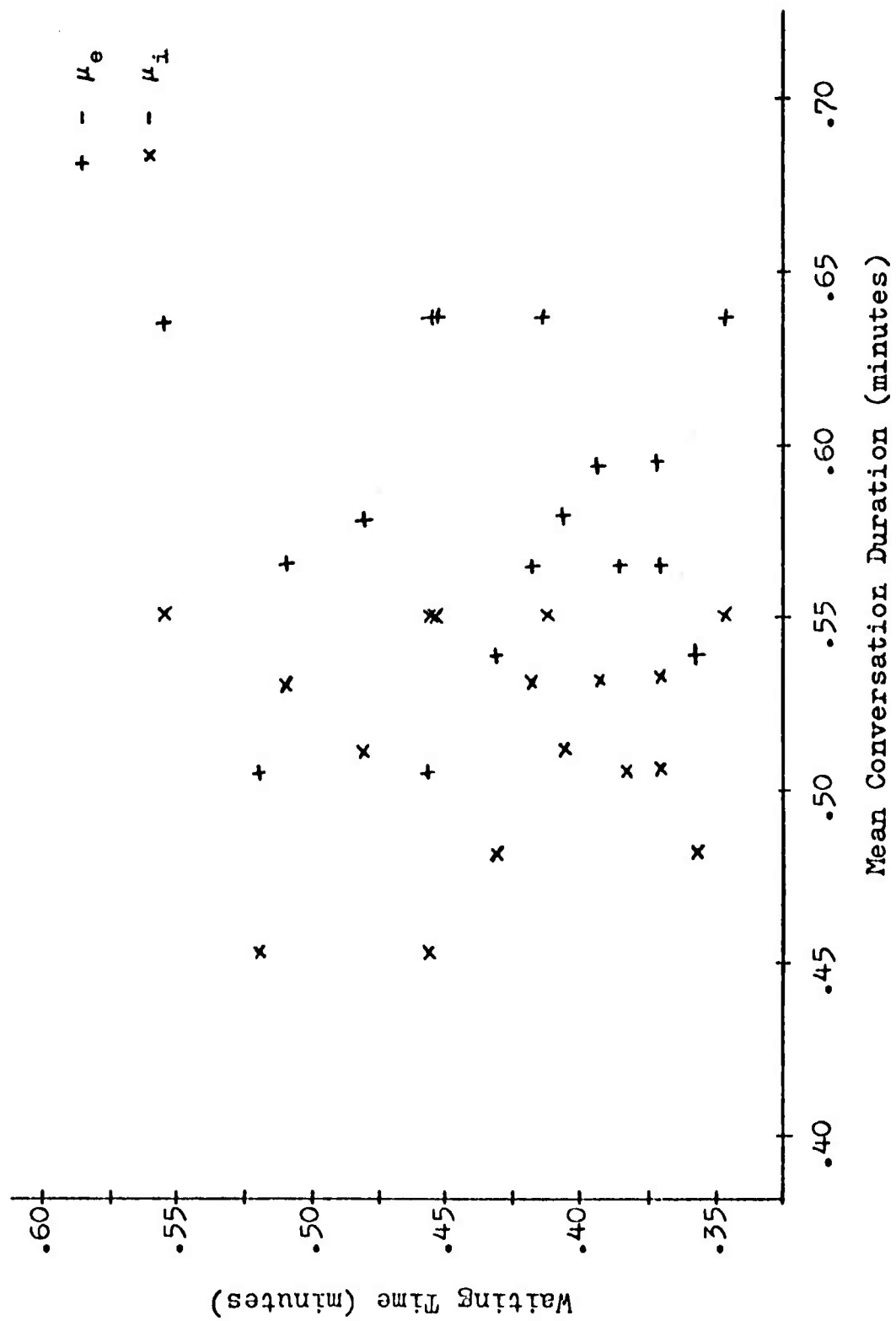


Figure 3.3. --Study C Results

### Study D

This study investigates the effect of a minor alteration in the structure of the communication system. For this study, each platoon has only one relay element. The platoon sergeant is reduced to a regular platoon element, having the same demand rates as platoon elements and being unable to relay communications. The platoon leader's demand rates are doubled and full relay responsibility rests on him. The mathematical characteristics of this single-relayer system are summarized in Table 3.7. The conversation duration distribution parameters are maintained at the level of case A-1, the Fort Carson simulation.

The variations investigated are parallel to the variations B-1 through B-4. This similarity permits comparison and evaluation of the results of this study. The variations are listed and numbered below.

- D-1      Use the single-relayer demand rates of Table 3.7 and the conversation duration distribution parameters of case A-1. (This case is comparable to A-1.)
- D-2      Double the external demand rate for all non-relayers (platoon leaders) on the platoon nets. All other parameters maintain the values of case D-1. (This case is comparable to B-1.)
- D-3      Change the external demand rate of the company commander from .15 to .27. All other parameters maintain the values of case D-1. (This case is comparable to B-2.)
- D-4      Change the platoon net internal demand rate of the relay elements from .50 to .60. All other parameters maintain the values of case D-1. (This case is comparable to B-3.)
- D-5      Change the company net internal demand rate of the relay elements from .05 to .30. All other parameters maintain the values of case D-1. (This case is comparable to B-4.)

The results of this study are tabulated in Table 3.8. The comparable results of cases A-1 and B-1 through B-4 are repeated to provide a basis for comparison. No statistical analysis of these results was performed. It was felt that the poor performance was, indeed, obvious.

The results of this study indicate that the elimination of the platoon sergeant from the present organization would lead to greatly deteriorated communication system performance. Any benefit gained in terms of tighter control or reduced manpower requirements would probably be far overshadowed by the poor performance of the system.

Table 3.7  
Single-relayer Demand Rates

Element	Platoon Net (com. /min.)		Company Net (com. /min.)	
	Internal	External	Internal	External
Platoon Leader	.500	.260	.050	.080
Platoon Sergeant	.010	.010	--	--
Platoon Elements	.010	.010	--	--
Company Commander	--	--	.100	.150

Table 3.8  
Study D Results

Configuration	M	S <sup>2</sup>	n	rep
D-1	.780 min.	--	2.9 com. /min.	1
A-1	.448 min.	.006 min. <sup>2</sup>	3.8 com. /min.	5
D-2	.570 min.	--	3.4 com. /min.	1
B-1	.475 min.	.025 min. <sup>2</sup>	3.6 com. /min.	4
D-3	.740 min.	--	3.6 com. /min.	1
B-2	.472 min.	.035 min. <sup>2</sup>	3.6 com. /min.	4
D-4	.550 min.	--	3.6 com. /min.	1
B-3	.440 min.	.009 min. <sup>2</sup>	3.5 com. /min.	4
D-5	1.250 min.	--	3.9 com. /min.	1
B-4	1.010 min.	.101 min. <sup>2</sup>	4.2 com. /min.	4

### Study E

This study offers what this author feels to be an improvement to the present military communication system. The prior studies and review of detailed simulation outputs indicate that the relay elements, with their won high demand rates, are the main contributors to high waiting time averages. The platoon leaders and sergeants must spend a great amount of time communicating, when they could be concentrating on their leadership requirements. The system analyzed in this study eliminates the need for relay of communications by any element.

The system proposed places the full burden of communication evaluation on the company commander element. It must be remembered that this element can be composed of more than one individual. To implement the proposed scheme, at least one radio man must travel with the company commander. The system requires that the company commander element monitor all platoon nets at all times. This guarantees that any information on the platoon nets of interest to the company commander will reach him. Similarly, when the company commander has a communication critical to all elements of a platoon, he can transmit it on the appropriate platoon net. Matters that do not need to be considered by all elements of a platoon net can still be discussed on the company net. The platoon leaders and sergeants will still share the company net with the company commander.

While the demand rates for all elements will remain the same as case A-1, the actual load on the system will be reduced under the proposed system. The reduction results from the elimination of relays, which resulted in two conversations each under the Fort Carson system. Of special importance is the reduction in lead on the platoon leader and sergeant.

Simulation replications of the proposed system were made only with the basic Fort Carson parameters as used in case A-1. Because the system itself represents a significant deviation from the original system, variations on this proposed system do not seem to be in order at this time. The results of simulation replications are listed in Table 3.9. Comparing this result with the result of case A-1 reveals a significant improvement over the Fort Carson configuration and parameters.

### Analysis of Pooled Results

This final section of the chapter treats the results of the preceding studies as outcomes of an experiment. The ten variables described at the beginning of this chapter are treated as independent variables with the waiting time,  $W$ , being the dependent variable.

Table 3.9  
Study E Results

Configuration	M	$S^2$	n	rep
E-1	.240 min.	.018 min. <sup>2</sup>	3.0 com./min.	4

The results of the replications of studies A through D were pooled and punched on computer cards along with those values of the ten variables describing the system configuration during each replication. The results of Study E were not included in this analysis because it represents a major change in system design rather than simple parameter changes or minor design alterations. Some additional configurations were simulated beyond those of the preceding studies in order to provide better coverage of the ranges of certain variables. These additional replications are identified by the prefix X in their identification numbers. All of the data points are collected in Table 3.11 at the end of this section.

The goal of the analysis of this section was to discover which dependent variables most profoundly affect system performance. To evaluate the effects of the variables, the results of the replications were submitted to stepwise regression analysis. In this regression, each of the ten variables and the squares of each of the ten variables were treated as independent variables. At each step of the regression, one variable is added to the regression equation. The variable added is the one which makes the greatest reduction in the error sum of squares of the regression. The results of the analysis reveal a definite dominance of certain variables. The effect of these variables can best be indicated by summarizing the steps of the regression. The values of interest are the multiple  $\bar{R}$  (a measure of correlation) and S.E.E., the standard error of estimate (standard deviation about the regression surface). The results are summarized in Table 3.10.

After reviewing the summary of Table 3.10, it is obvious that beyond the third or fourth step of the regression procedure, little improvement is made in the multiple  $\bar{R}$ . It is also noteworthy that the standard error of estimate begins to increase after the fourth step. In light of these facts, the regression equation containing only the first four variables entered is offered as an approximation for  $W$ . This estimation applies only in systems comparable to that described in the preceding sections and within the ranges of variables considered in this section. The estimate is:

$$W^* = 0.5631 d_{ci}^2 - 0.1129 d_{ce}^2 + 0.7993 \mu_c^2 - 0.0545 \bar{R}$$

where  $d_{ce}$ ,  $d_{ci}$ , and  $\mu_c$  are measured in minutes.

At first evaluation, the negative coefficient of the  $d_{ce}^2$  term appears contradictory to the observed increasing behavior of  $W$  as a function of demand rates. If, however, one combines the first two terms of the approximating polynomial as the product

$$(\sqrt{.5631} d_{ci} + \sqrt{.1129} d_{ce})(\sqrt{.5631} d_{ci} - \sqrt{.1129} d_{ce})$$



Table 3. 10

## Summary of Stepwise Regression

Step	Variable Entered	Multiple $\bar{R}$	S. E. E.
1	$d_{ci}^2$	.645	.176
2	$\bar{R}$	.683	.170
3	$\mu_e^2$	.697	.168
4	$d_{ce}^2$	.699	.169
5	$d_{ce}$	.700	.170
6	$\mu_i^2$	.701	.172
7	$\sigma_e^2$	.701	.173
8	$\mu_e$	.705	.174
9	$\sigma_i^2$	.706	.175
10	$\mu_i$	.709	.176
11	$d_{pi}$	.710	.177
12	$d_{pe}$	.711	.179
13	$d_{pe}$	.713	.180
14	$d_{pi}$	.719	.180
15	$d_{\bar{R}}^2$	.720	.182
16	$d_{ci}$	.720	.184
17	$\bar{R}^2$	.721	.186
18	$d_{\bar{R}}$	.721	.188
19	$(\sigma_i^2)^2$	.721	.188
20	$(\sigma_e^2)^2$	.721	.188

a different interpretation might be applied. One could consider  $W$  to be a function of the sum,  $d_{ci} + d_{ce}$ , and of the difference,  $d_{ci} - d_{ce}$ , along with the  $\mu_e^2$  and  $\bar{R}$  terms. While this idea has not been thoroughly investigated, it does provide a more intuitively attractive alternative interpretation of the data.

The regression analysis provided other information than an estimate of waiting time. Reviewing the relative weights applied to the different variables one can predict, to some degree, whether specific system changes will have a significant effect. Study B revealed that the demand rates could have significant effects on the Fort Carson system (at certain significance levels within reason), while Study C found no significant effect of conversation duration distribution parameters. These results are reasonable when one looks at the ranges of the variables under investigation in each of these studies. The small range of  $\mu_e$  in Study C (.45 to .55) is not adequate for the variables to have a major effect of  $W$ .

In conclusion, while a great amount of random variation makes an absolute prediction of  $W$  impossible in the field or in the simulation, the underlying effects of the variables describing a communication system have been evaluated. Results have shown the relay elements to be major sources of delay in the system and a valid alternative to ease the problem has been offered. While the foregoing research does not cover all alternative communication system parameter values and configurations, the basis for later research has been developed. It is hoped that the information contained in this study will be of value both as a descriptor of communication system performance and as motivation for further research.

Table 3.11. --Summary of Simulation Results

	W	$d_{p1}$	$d_{pe}$	$d_{ci}$	$d_{ce}$	$\mu_i$	$\mu_e$	$\sigma_i^2$	$\sigma_e^2$	R	$d_R$
A-1	0.35	.570	.380	.250	.600	.550	.640	.178	.222	6.0	.505
A-1	0.43	.570	.380	.250	.600	.550	.640	.178	.222	6.0	.505
A-1	0.56	.570	.380	.250	.600	.550	.640	.178	.222	6.0	.505
A-1	0.45	.570	.380	.250	.600	.550	.640	.178	.222	6.0	.505
A-1	0.45	.570	.380	.250	.600	.550	.640	.178	.222	6.0	.505
B-1	0.38	.570	.450	.250	.810	.550	.640	.178	.222	6.0	.540
B-1	0.32	.570	.450	.250	.810	.550	.640	.178	.222	6.0	.540
B-1	0.73	.570	.450	.250	.810	.550	.640	.178	.222	6.0	.540
B-1	0.47	.570	.450	.250	.810	.550	.640	.178	.222	6.0	.540
B-2	0.35	.570	.420	.250	.720	.550	.640	.178	.222	6.0	.525
B-2	0.28	.570	.420	.250	.720	.550	.640	.178	.222	6.0	.525
B-2	0.48	.570	.420	.250	.720	.550	.640	.178	.222	6.0	.525
B-2	0.78	.570	.420	.250	.720	.550	.640	.178	.222	6.0	.525
B-3	0.38	.670	.380	.250	.600	.550	.640	.178	.222	6.0	.555
B-3	0.34	.670	.380	.250	.600	.550	.640	.178	.222	6.0	.555
B-3	0.60	.670	.380	.250	.600	.550	.640	.178	.222	6.0	.555
B-3	0.44	.670	.380	.250	.600	.550	.640	.178	.222	6.0	.555
B-4	0.85	.570	.380	1.00	.600	.550	.640	.178	.222	6.0	.630
B-4	0.65	.570	.380	1.00	.600	.550	.640	.178	.222	6.0	.630
B-4	0.95	.570	.380	1.00	.600	.550	.640	.178	.222	6.0	.630
B-4	1.59	.570	.380	1.00	.600	.550	.640	.178	.222	6.0	.630
B-5	0.42	.578	.384	.253	.606	.550	.640	.178	.222	6.0	.510
B-5	0.37	.578	.384	.253	.606	.550	.640	.178	.222	6.0	.510
B-5	0.74	.578	.384	.253	.606	.550	.640	.178	.222	6.0	.510
B-6	0.49	.582	.388	.255	.612	.550	.640	.178	.222	6.0	.515
B-6	0.64	.582	.388	.255	.612	.550	.640	.178	.222	6.0	.515
B-6	0.57	.582	.388	.255	.612	.550	.640	.178	.222	6.0	.515
B-6	0.39	.582	.388	.255	.612	.550	.640	.178	.222	6.0	.515
B-7	0.44	.592	.395	.260	.622	.550	.640	.178	.222	6.0	.525
B-7	0.40	.592	.395	.260	.622	.550	.640	.178	.222	6.0	.525
B-7	0.42	.592	.395	.260	.622	.550	.640	.178	.222	6.0	.525
B-7	0.72	.592	.395	.260	.622	.550	.640	.178	.222	6.0	.525
B-8	0.61	.628	.419	.275	.660	.550	.640	.178	.222	6.0	.556
B-8	0.53	.628	.419	.275	.660	.550	.640	.178	.222	6.0	.556
B-8	0.40	.628	.419	.275	.660	.550	.640	.178	.222	6.0	.556
B-8	0.57	.628	.419	.275	.660	.550	.640	.178	.222	6.0	.556
B-9	0.54	.683	.456	.300	.720	.550	.640	.178	.222	6.0	.607
B-9	0.39	.683	.456	.300	.720	.550	.640	.178	.222	6.0	.607
B-9	0.64	.683	.456	.300	.720	.550	.640	.178	.222	6.0	.607
B-9	0.51	.683	.456	.300	.720	.550	.640	.178	.222	6.0	.607

Table 3.11 (Continued)

	W	d <sub>pi</sub>	d <sub>pe</sub>	d <sub>ci</sub>	d <sub>ce</sub>	$\mu_i$	$\mu_e$	$\sigma_i^2$	$\sigma_e^2$	R	d <sub>R</sub>
C-1	0.46	.570	.390	.250	.600	.450	.506	.135	.160	6.0	.505
C-1	0.52	.570	.380	.250	.600	.450	.506	.135	.160	6.0	.505
C-2	0.36	.570	.380	.250	.600	.480	.538	.144	.170	6.0	.505
C-2	0.43	.570	.380	.250	.600	.480	.538	.144	.170	6.0	.505
C-3	0.37	.570	.380	.250	.600	.506	.567	.160	.189	6.0	.505
C-3	0.38	.570	.380	.250	.600	.506	.567	.160	.189	6.0	.505
C-4	0.51	.570	.380	.250	.600	.533	.567	.178	.189	6.0	.505
C-4	0.51	.570	.380	.250	.600	.533	.567	.178	.189	6.0	.505
C-5	0.39	.570	.380	.250	.600	.533	.595	.178	.208	6.0	.505
C-5	0.37	.570	.380	.250	.600	.533	.595	.178	.208	6.0	.505
C-6	0.41	.570	.380	.250	.600	.510	.580	.153	.184	6.0	.505
C-6	0.48	.570	.380	.250	.600	.510	.580	.153	.184	6.0	.505
D-1	0.78	.580	.390	.250	.630	.550	.640	.178	.222	3.0	1.02
D-2	0.57	.580	.470	.250	.870	.550	.640	.178	.222	3.0	1.10
D-3	0.74	.580	.430	.250	.750	.550	.640	.178	.222	3.0	1.06
D-4	0.55	.680	.390	.250	.630	.550	.640	.178	.222	3.0	1.12
D-5	1.25	.580	.390	1.00	.630	.550	.640	.178	.222	3.0	1.27
X-1	0.44	.570	.380	.250	.600	.580	.670	.197	.246	6.0	.505
X-1	0.34	.570	.380	.250	.600	.580	.670	.197	.246	6.0	.505
X-1	0.42	.570	.380	.250	.600	.580	.670	.197	.246	6.0	.505
X-1	0.67	.570	.380	.250	.600	.580	.670	.197	.246	6.0	.505
X-2	0.47	.570	.380	.250	.600	.610	.700	.218	.268	6.0	.505
X-2	0.58	.570	.380	.250	.600	.610	.700	.218	.268	6.0	.505
X-2	0.46	.570	.380	.250	.600	.610	.700	.218	.268	6.0	.505
X-2	0.92	.570	.380	.250	.600	.610	.700	.218	.268	6.0	.505
X-3	0.63	.570	.450	.250	.810	.610	.700	.218	.268	6.0	.540
X-3	0.48	.570	.450	.250	.810	.610	.700	.218	.268	6.0	.540
X-3	0.56	.570	.450	.250	.810	.610	.700	.218	.268	6.0	.540
X-3	0.43	.570	.450	.250	.810	.610	.700	.218	.268	6.0	.540
X-4	0.68	.570	.380	.250	.600	.455	.640	.148	.222	6.0	.505
X-4	0.39	.570	.380	.250	.600	.455	.640	.148	.222	6.0	.505
X-4	0.28	.570	.380	.250	.600	.455	.640	.148	.222	6.0	.505
X-4	0.45	.570	.380	.250	.600	.455	.640	.148	.222	6.0	.505
X-5	0.60	.580	.390	.250	.630	.580	.670	.197	.246	3.0	1.02
X-6	0.64	.580	.470	.250	.870	.610	.700	.218	.268	3.0	1.02

## REFERENCES

- Bennet, W. S., Overlapping Communication Nets: An Application of Moe's Principle and a User Distribution, Report No. ORO-SP-26, Operations Research Office, Johns Hopkins University, August 1957.
- Bishop, A. B. and Stollmack, S. (eds.) The Tank Weapon System, RF 573, AR 68-1 (U), Systems Research Group, The Ohio State University, Columbus, Ohio, September 1968. AD 850367.
- Brown, R. L., A Content Analysis of Communication Within Army Small-Unit Patrolling Operations, Technical Report 67-7, AD 817795, HumRRO, George Washington University, June 1967.
- CDCCEA, Ground Combat-Communications Simulation System, Report No. 0192(S)-R, Final Report Volume I, Philco Corporation, June 1966.
- CDCEC, Preliminary Data - IRUS, U. S. Army Combat Developments Command, Experimentation Command, Project Team V, Fort Ord, California, July 1968.
- Clark, G. M., "Intelligence" (in) The Tank Weapon System, edited by A. B. Bishop and G. M. Clark, RF 573, AR 69-2A (U), Systems Research Group, The Ohio State University, Columbus, Ohio, October 1969. AD 864919.
- FM17-36, Divisional Armored and Air Cavalry Units, Headquarters, Department of the Army, October 1965.
- Greenwood, J. A. and Durand, D., "Aids for Fitting the Gamma Distribution by Maximum Likelihood," Technometrics, Vol. 2, No. 1, February 1960, pp. 55-65.
- Hastings, C., et al., Approximations for Digital Computers, Princeton University Press, Princeton, New Jersey, 1955.
- Hogg, R. V. and Craig, A. T., Introduction to Mathematical Statistics, (2nd Edition), The Macmillan Company, New York, 1966.
- Lennahan, C. B., Communication Data for Tank Battalions: Fort Stewart, Ga., Report No. ORO-TP-13, Operations Research Office, Johns Hopkins University, December 1960.
- Lloyd, D. K. and Lipow, M., Reliability: Management Methods, and Mathematical Mathematics, Englewood Cliffs, New Jersey: Prentice-Hall, Inc. 1962.

- Murphy, A. D., "A Queueing Model of Information Flow in a Command and Control System," Master's Thesis, U. S. Navy Postgraduate School, Monterey, California, 1962. AD 483012.
- Sarndal, C., "Estimation of the Parameters of the Gamma Distribution by Sample Quantiles," Technometrics, Vol. 6, No. 4, November 1964, pp. 405-414.
- Stacy, E. W. and Mihram, G. A., "Parameter Estimation for a Generalized Gamma Distribution," Technometrics, Vol. 7, No. 3, August 1965, pp. 349-358.
- Stollmack, S. and Bishop, A. B., (eds.) Appendix E (in) The Tank Weapon System, RF 573, AR 68-1 (U), Systems Research Group, The Ohio State University, Columbus, Ohio, September 1968. AD 850367.
- Whitney, D. R., Elements of Mathematical Statistics, Henry Holt and Company, New York, 1959.
- Wilk, M. B., et al., "Probability Plots for the Gamma Distribution," Technometrics, Vol. 4, No. 1, February 1962.

## CHAPTER 4

### DRAGON MISSILE MODEL

#### Unclassified Summary

by

J. J. Rheinfrank

The DRAGON surface attack guided missile system is being developed for the infantryman as a medium anti-tank/assault weapon. It can be carried anywhere a soldier can pack a rifle, set up rapidly, and fired on any terrain. It is the Army's first guided missile system light enough to be carried by one man (shoulder fired) that has a warhead big enough to kill most armor and other hard targets encountered on the battlefield.

The DRAGON weapon system employs a command-to-line-of-sight guidance system and consists of a Tracker and a Round. The Round contains a recoilless launcher and a missile. The Tracker, which includes a telescope for the gunner to sight the target, a sensor device, and an electronics package, is reusable and is attached to the Round for each firing. The launcher is a smooth bore fiberglass tube. The aft end is enlarged to accommodate a propellant container and breech. Pre-packaged within the launcher, the missile is never seen by the gunner until it is fired. The expended Round is then discarded.

The propulsion system is unique. The missile contains several pairs of small rocket motors mounted in rows around the missile body. The gunner sights the target through the telescopic sight, then launches the missile. While he holds his sight on the target, the tracker senses missile position relative to the gunner's line of sight and sends command signals over a wire link to the missile. This causes the rocket motors, or side thrusters, to fire. As commands are sent continuously to the missile, the side thrusters apply corrective control forces. The thrusters are fired at appropriate roll angles so that the missile is automatically guided throughout its flight.

Because of its light weight, the DRAGON is particularly desirable in airborne and airmobile operations. In terrain that is difficult for wheeled and tracked vehicles to negotiate, such as in assault river crossing operations or in heavily wooded or mountainous areas, the DRAGON is particularly effective.



Deployed at the platoon level, the DRAGON as a defensive weapon will cover armor approaches into the platoon area; offensively, it may be used against either hard or soft targets.<sup>1</sup>

A detailed discussion of the DRAGON missile system and the DYNCOM DRAGON simulation module is given in Chapter 3 of the classified volume, i. e., Volume 5.

---

<sup>1</sup>This unclassified summary is adapted from a Private Communication with Mr. Ernest Petty, January 15, 1969.

## CHAPTER 5

### CREW-SERVED WEAPON MOVEMENT MODEL

by

S. Parry

#### Dismounted Crew-Served Weapon Unit Operations

Armor operations involve employment of combined arms forces at brigade, task force, and team level. The primary mission of crew-served weapons is to provide the unit commander with organic assault and antitank capabilities. Weapons generally classed as "crew-served" include antitank rockets, machine guns, mortars, recoilless rifles, and the ENTAC, TOW, MAW, and LAW missile systems.

A crew-served weapon (CSW) unit is considered to be composed of one weapon, and the personnel and equipment required for the operation of that weapon. A CSW unit performs functions similar to those of other battlefield units in that they may fire and be fired upon, detect and be detected, communicate intelligence, and serve as forward observers or illuminators for indirect-fire missiles. There are, however, differences between the basic characteristics of the dismounted CSW unit and the armored vehicle as follows:

1. The dismounted CSW unit is more susceptible to enemy fire because of its lack of protection and limited movement speed;
2. Because crew-served weapons are generally man-portable, they are more difficult to detect because of their greater ability to attain and maintain concealment than an armored vehicle;
3. Dismounted CSW units may be placed in strategic locations unattainable by armored vehicles due to the CSW unit's ability to avoid detection and to move over terrain that is untrafficable for armored vehicles.

As a result of previous research performed for MICOM, reported in Chapter 9 of Volume 1, the following aspects of CSW unit employment were modeled:

1. the process by which crews dismount from personnel carriers, establish defensive positions at the point of dismount, and re-mount when appropriate;
2. the detection of dismounted crew-served weapon units; and
3. the level of damage inflicted upon crew-served weapon targets.

In addition, modifications were made to existing simulation models such as the Communications, Movement Controller, Fire Controller, and Firing Models in order to represent crew-served weapon units.

To more effectively evaluate the combat performance of crew-served weapons in armored-unit engagements, research was conducted to extend these previously developed crew-served weapon models. The models resulting from this research, as described in the remainder of this chapter, are outlined below.

1. Methodology for determining optimal firing positions for dismounted CSW units operating in either attack or defense modes was developed.
2. The capability to represent either single or multiple CSW units dismounting from a personnel carrier, and their subsequent operations, was developed.
3. Given a desired firing position for a dismounted CSW unit, a dynamic route selection model was developed to choose the optimal route of advance from the dismount point to the desired firing position in accordance with specified tactical doctrine.
4. A movement model was developed to move dismounted CSW units along their selected routes to their respective firing positions.

#### Deployment Modes for Dismounted Crew-Served Weapon Units

The basic mission of crew-served weapon units in an armor operation as currently represented in DYNCOM is to provide organic fire support against hard-point targets when required. Because of the vulnerability of dismounted crew-served weapon units to enemy fire, the units will generally remain mounted on armored personnel carriers until their employment in a dismounted role is required as determined by the battlefield situation and specified tactical doctrine. The models, however, provide the capability to specify an initial dismounted mode for any or all crew-served weapon units in the battle.

The purpose of the extended crew-served weapon models developed for DYNCOM and reported in this chapter is to describe the operations of crew-served weapon units after dismounting from their respective armored personnel carriers. A crew-served weapon unit in DYNCOM is defined to be made up of one crew-served weapon, along with the manpower and ammunition required for dismounted employment of the weapon. A dismounted CSW unit is represented in the simulation as a rectangular solid on the battlefield, its size determined by the number of men in the unit. Each crew-served weapon unit represented in DYNCOM is assigned a CSW unit identification number, NCR, in addition to its normal DYNCOM element number. The variable, LCSWFN(CE), contains the identification number, NCR, for element CE if CE is a crew-served weapon unit, and zero otherwise.

Each CSW unit is assigned to a particular personnel carrier, with each carrier capable of transporting up to four units. The variable LAPCCW(I, LAPC), which is specified by input, defines the organizational structure of CSW units in DYNCOM, where

LAPCCW(I, LAPC) = the CSW unit identification number,  
NCR, of the I<sup>th</sup> unit mounted on  
personnel carrier, LAPC.

Since the activities of crew-served weapons are simulated by the DYNCOM armor module, CSW units are assigned weapon codes, target profiles, priority ratings, ammunition availabilities, etc., which are specified by input data. A complete description of variables used to describe crew-served weapon units is given in later sections.

When it is determined by DYNCOM that a specified APC is to dismount its crew-served weapon units, the mode of deployment for the dismounted units (attack or defense) must be determined. These two modes of deployment utilized in the extended crew-served weapon models are defined as follows:

1. The attack mode implies that each CSW unit mounted on the APC dismounts, selects a desired firing position in advance of the APC based on its assigned sector of responsibility and location of the threat, and moves to that desired position along the optimal route as determined by the Route Selection Model for CSW units.
2. The defense mode implies that each CSW unit mounted on the APC dismount, selects a defensive firing position along a line through the APC perpendicular to the location of the threat, and deploys directly to that position.

The following assumptions concerning the offensive and defensive tactical deployment of CSW units are currently made in DYNCOM.

1. All CSW units mounted on a specified personnel carrier, LAPC, dismount when either:
  - a. the maneuver unit leader stops,
  - b. LAPC reaches a specified distance, DSDMT(LAPC), from a full objective, or
  - c. the personnel carrier becomes a mobility kill.
2. The attack mode is employed by dismounted CSW units when its maneuver unit is an attacking unit and has not reached a full objective.
3. The defense mode is employed by dismounted CSW units when its maneuver unit is a delaying or defending unit, or when an attacking maneuver unit reaches a full objective.

If it has been determined that a specified personnel carrier, noted by LAPC, is to dismount its CSW units, and they are to deploy in the attack mode, each crew will select a firing position in its sector of responsibility relative to the enemy threat location.

In the current version of DYNCOM, a personnel carrier on which CSW units are mounted is represented as a section. The location of the threat position, (XT, YT), of a specified personnel carrier, LAPC, operating in an attacking maneuver unit, is determined as follows:

1. If carrier LAPC has a single enemy target assigned to it, the coordinates of the target's location is taken to be the threat position, (XT, YT).
2. If LAPC has multiple enemy targets assigned to it, (XT, YT) is taken to be the coordinates of the centroid of those targets' current positions.
3. If LAPC reaches a distance, DSDMT(LAPC), from a full objective, the personnel carrier stops and dismounts its CSW units. The threat position (XT, YT) is taken to be the location of the full objective. The tactical doctrine of whether to

dismount CSW units at a specified distance from a full objective is specified by input data as follows:

$$\text{DSDMT(LAPC)} = \begin{cases} D \sim \text{CSW units will dismount from} \\ \quad \text{LAPC at a distance, } D, \text{ from} \\ \quad \text{a full objective; and} \\ 0 \sim \text{otherwise.} \end{cases}$$

Assume that the personnel carrier, LAPC, has an assigned sector of responsibility of angle  $\text{ANGSEC(LAPC)}$  and that there are  $\text{NCTOT}$  CSW units mounted on LAPC. Furthermore, assume that  $\text{SECMID}$  is the angle from the dismount point bisecting the assigned sector of responsibility, measured in the X-Y battlefield coordinate system. The distance of the threat position from the dismount point is noted by  $\text{DTHRT}$ . An example of the sector of responsibility for a personnel carrier is given in Figure 5.1 for  $\text{NCTOT} = 4$  CSW units. The coordinates of the dismount point are noted in Figure 5.1 by  $(X_C, Y_C)$ . Each CSW unit is assigned equal-sized sectors of responsibility denoted by the angle,  $\text{SECTOR}$ , in the figure. The coordinates of the assumed threat location for each unit are determined as a function of  $\text{DTHRT}$  and the unit's sector of responsibility. The assumed threat locations for each CSW unit are noted by  $(X_{T1}, Y_{T1}), \dots, (X_{T4}, Y_{T4})$  for each of the four units in Figure 5.1 and are used to determine the optimal firing position for each CSW unit. The selection of primary and alternate desired firing positions is discussed in a subsequent section.

If the dismounted CSW units are to deploy in the defense mode, each crew selects a firing position along a line through the personnel carrier, LAPC, perpendicular to the specified direction of the threat as shown in Figure 5.2. The length of the line along which the dismounted CSW units are deployed, noted by  $\text{RLIMIT(LAPC)}$  is specified by input data. The threat position,  $(X_T, Y_T)$ , is taken to be the centroid of enemy target locations assigned to LAPC.

### Crew-Served Weapon Unit Controller

The basic structure of the extended crew-served weapon models in DYNCOM, illustrated in Figure 5.3, is given in the following discussion. When it is determined in the simulation that the current element is either a personnel carrier which is to dismount CSW units in the current event or a dismounted CSW unit, subroutine  $\text{CSWCON}$ , which controls the computations for crew-served weapon units, is called. If the element is a personnel carrier, primary

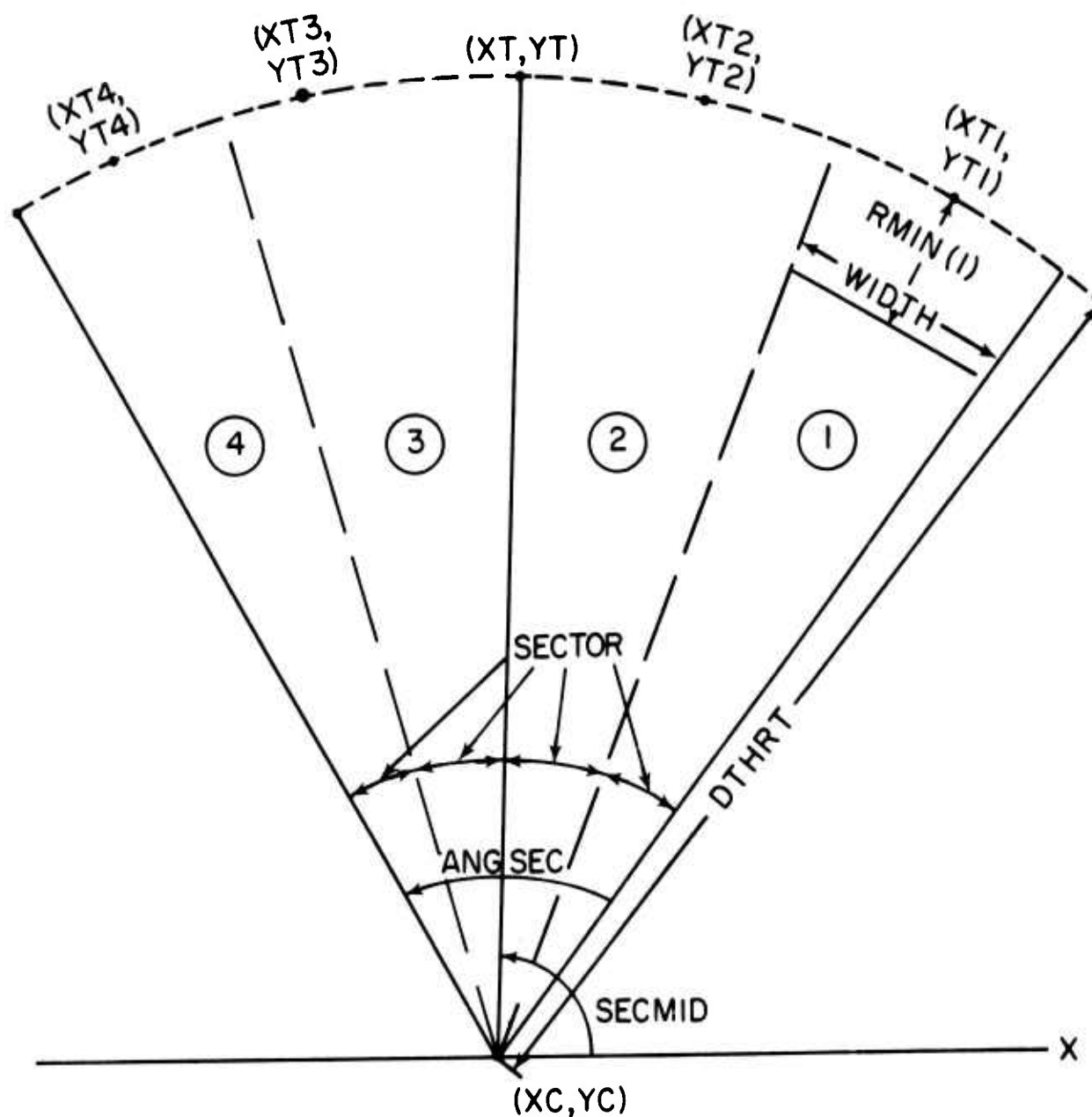


Figure 5. 1. --Threat Locations Attack Mode



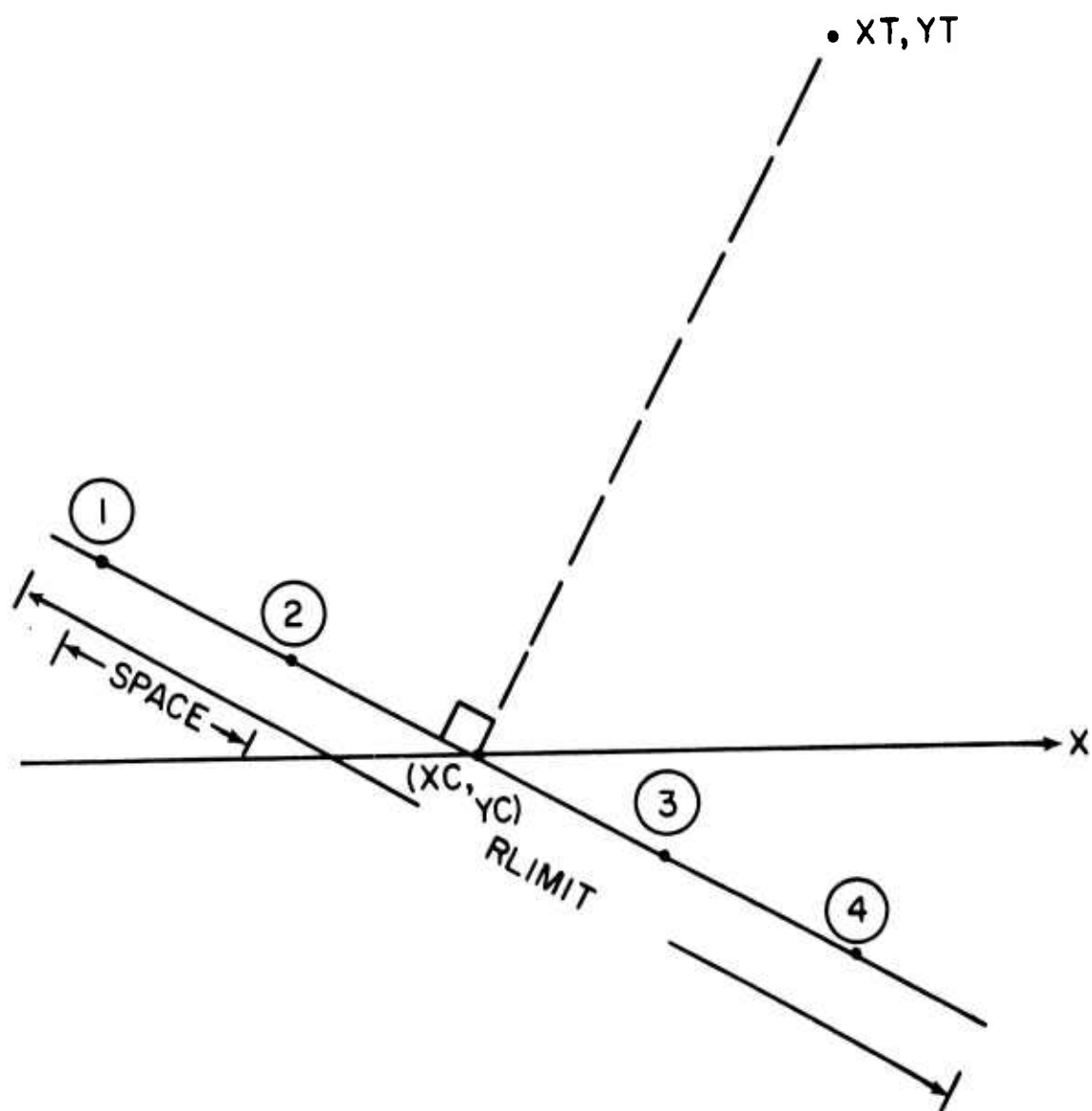


Figure 5. 2. --Threat Locations Defense Mode

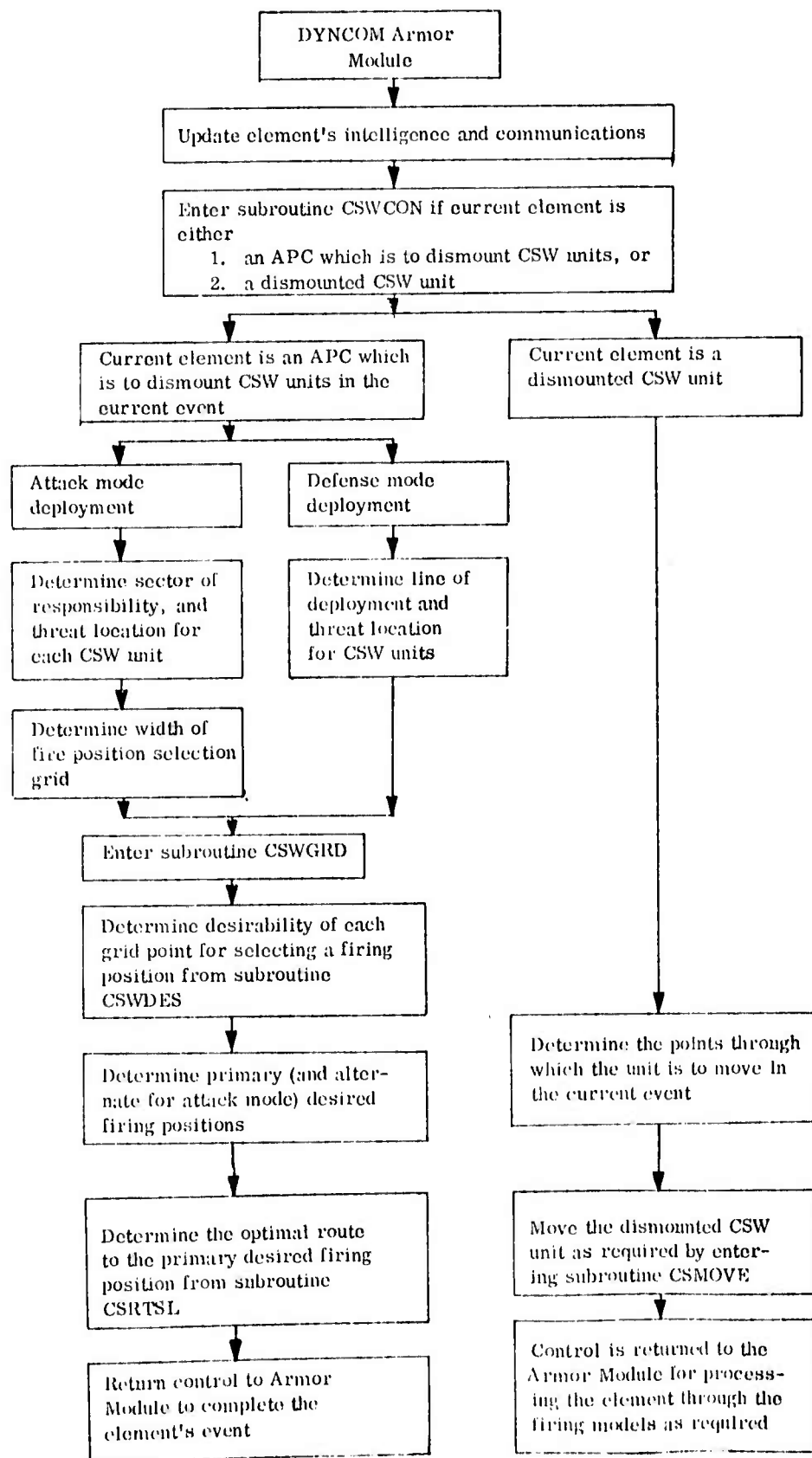


Figure 5.3. --Logic Flow Diagram of the Extended Crew-Served Weapon Models

and alternate desired firing positions, as well as the optimal route to the primary firing position, are determined as a function of the deployment mode for each CSW unit on the personnel carrier. If the element is a dismounted CSW unit, the movement path for the event is determined, and the element is moved as required. Control is then returned to the basic armor module to process the unit through the firing models.

The computational procedure of subroutine CSWCON is given below. The logic and computational procedures employed to determine desired firing positions and optimal routes, and to move dismounted CSW units, are presented in later sections. A complete list of all variable definitions for the extended crew-served weapon models is given at the end of the chapter.

1. If the current element, ICE, is not an APC, go to step 20. Otherwise, go to step 2.
2. If all crews on the APC (element number LAPC) seek firing positions in the attack mode; i.e., CSDSMT = 1; go to step 3. Otherwise, go to step 15.
3. Determine NCTOT, the number of crews mounted on LAPC.
4. Compute the sector of responsibility, SECTOR, for each crew; i.e.,

$$\text{SECTOR} = \frac{\text{ANGSEC}(\text{LAPC})}{\text{NCTOT}} .$$

5. Set NCR equal to the CSW unit number of the first crew mounted on LAPC.
6. Compute the angle, ANGAL, of the line through the center of the crew's sector of responsibility; i.e.,

$$\text{ANGAL} = \text{SECMID} - \frac{(\text{ANGSEC}(\text{LAPC}) + \text{SECTOR})}{2} .$$

7. Compute coordinates, (XTI, YTI), of the position relative to which crew NCR will select its firing position; i.e.,

$$\begin{cases} \text{XTI} &= \text{XC} + (\text{DTHRT}) \cdot \cos(\text{ANGAL}) \\ \text{YTI} &= \text{YC} + (\text{DTHRT}) \cdot \sin(\text{ANGAL}) \\ \text{DIWC} &= \text{DTHRT} - \text{RMIN}(\text{NCR}) \text{ (see Figure 1).} \end{cases}$$

8. Compute coordinates, (XXR1, YYR1) and (XXR2, YYR2) of the boundary points for determining the width of the fire position selection grid; i.e.,

$$\begin{cases} \text{XXR1} &= \text{XC} + (\text{DIWC}) \cdot \cos(\text{ANGAL} - \text{SECTOR}/2) \\ \text{YYR1} &= \text{YC} + (\text{DIWC}) \cdot \sin(\text{ANGAL} - \text{SECTOR}/2) \\ \text{XXR2} &= \text{XC} + (\text{DIWC}) \cdot \cos(\text{ANGAL} + \text{SECTOR}/2) \\ \text{YYR2} &= \text{YC} + (\text{DIWC}) \cdot \sin(\text{ANGAL} + \text{SECTOR}/2). \end{cases}$$

9. Compute WIDTH, the width of the fire position selection grid; i.e.,

$$\text{WIDTH} = \sqrt{(\text{XXR1} - \text{XXR2})^2 + (\text{YYR1} - \text{YYR2})^2}.$$

10. Determine the primary desired firing position, (XDF, YDF); the alternate desired firing position, (XDFA, YDFA); and the optimal route, [CSXRT(I, NCR), CSYRT(I, NCR)] for crew-served weapon unit NCR by a call to subroutine CSWGRD.

$$11. \text{ Set } \begin{cases} \text{CXCUR}(\text{NCR}) &= \text{XC} \\ \text{CYCUR}(\text{NCR}) &= \text{YC} \\ \text{CLCPE}(\text{NCR}) &= \text{LAST} - 1 \\ \text{CSMAKE}(\text{NCR}) &= 1 \\ \text{CCLOCK}(\text{NCR}) &= \text{ECLOCK}(\text{LAPC}) + \text{DISMTT}(\text{NKWEP}). \end{cases}$$

12. If all crews mounted on LAPC have been considered, go to step 36. Otherwise, go to step 13.

13. Set NCR equal to the CSW unit number of the next crew mounted on LAPC.

14. Increment the sector of responsibility; i.e.,

$$\text{ANGAL} + \text{SECTOR} \rightarrow \text{ANGAL}; \text{ go to step 7.}$$

15. Set NCTOT equal to the number of crew-served weapon units mounted on LAPC.

16. Determine (XT, YT) for the dismounted crews in defensive positions.
17. Set CSDECN(NCR) = 2.
18. Determine the desired firing positions for the crews in defensive positions by a call to subroutine CSWGRD.
19. Set  $\begin{cases} \text{CCLOCK(NCR)} = \text{ECLOCK(LAPC)} + \text{DISMTT(NKWEF)} \\ \text{CSMAKE(NCR)} = 1 \end{cases}$   
for all crews mounted on LAPC; go to step 36.
20. Set NCR equal to crew-served weapon unit number of ICE.
21. If NCR has a firing position and route; i.e.,  
 $\text{CSMAKE(NCR)} \neq 0$  or  $\text{CSALT(NCR)} \neq 0$ ;  
go to step 27. Otherwise, go to step 22.
22. If NCR is being employed in the attack mode; i.e.,  
 $\text{CSDECN(NCR)} = 1$ ; go to step 24. Otherwise, go to step 23.
23. Set NCTOT = 1.
24. Set  $\begin{cases} \text{XC} &= \text{CXCUR(NCR)} \\ \text{YC} &= \text{CYCUR(NCR)} \\ \text{CSMAKE(NCR)} &= 1 \\ \text{CSALT(NCR)} &= 1. \end{cases}$
25. Determine (XT, YT), the coordinates of the position of the threat for crew NCR.
26. Determine the primary desired firing position,  $[\text{XDF(NCR)}, \text{YDF(NCR)}]$ ; the alternate desired firing position,  $[\text{XDFA(NCR)}, \text{YDFA(NCR)}]$ ; and the optimal route  $[\text{CSXRT(I, NCR)}, \text{CSYRT(I, NCR)}]$  by a call to subroutine CSWGRD.
27. If NCR is to move in this event; i.e.,  $\text{CSMAKE(NCR)} = 1$  or  $\text{CSALT(NCR)} = 1$ ; go to step 28. Otherwise, go to step 30.
28. Set CTIME equal to the allotted event time.

29. Move CSW unit NCR as required by a call to subroutine CSMOVE;  
go to step 36.
30. If CSW unit NCR is to remain at its current firing position; i.e.,  
 $CSMVT(NCR) = 0$ ; go to step 36. Otherwise, go to step 31.
31. If CSW unit NCR has fired its specified number of rounds,  
 $RNDCNT(NCR)$ , at its current firing position; i.e., if  
 $RNDCNT(NCR) \geq CSMVT(NCR)$ , go to step 32. Otherwise, go  
to step 36.
32. If CSW unit NCR is currently positioned at its primary desired  
firing position  $[XDF(NCR), YDF(NCR)]$ , go to step 33. Otherwise,  
go to step 34.
33. Set  $\left\{ \begin{array}{ll} CSA LT(NCR) & = 1 \\ CSXRT(1, NCR) & = XDFA(NCR) \\ CSYRT(1, NCR) & = YDFA(NCR) \\ CSXRT(2, NCR) & = XDF(NCR) \\ CSYRT(2, NCR) & = YDF(NCR) \\ CLCPE(NCR) & = 1; \text{ go to step 35.} \end{array} \right.$
34. Set  $\left\{ \begin{array}{ll} CSMAKE(NCR) & = 1 \\ CSXRT(1, NCR) & = XDF(NCR) \\ CSYRT(1, NCR) & = YDF(NCR) \\ CSXRT(2, NCR) & = XDFA(NCR) \\ CSYRT(2, NCR) & = YDFA(NCR) \\ CLCPE(NCR) & = 1. \end{array} \right.$
35. Move CSW unit NCR as required by a call to subroutine CSMOVE.
36. The computations are complete.

The selection of firing positions for dismounted CSW units deployed in either the attack or defense mode is discussed in the following section.

#### Selection of Firing Positions

Three basic factors are considered in the selection of a primary desired firing position for a dismounted crew-served unit as follows:

1. the portion of the threat position covered relative to the candidate firing position, noted by TGCOV;
2. the portion of the candidate firing position covered or concealed relative to the threat position, noted by CSWCO; and
3. the range-firepower index for the CSW unit relative to the candidate firing position, noted by RFI.<sup>1</sup>

#### Attack Mode Deployment

If the CSW units are to deploy in the attack mode after dismounting, a fire-position selection grid is constructed in the sector of responsibility for each dismounted CSW unit. The variables RMIN(NCR) and RMAX(NCR), specified by input data, are used to determine the length and width, respectively, of the fire-position selection grid, where

RMIN(NCR) = the minimum desired firing range for CSW unit NCR; i.e., very little increase in firing effectiveness would be realized from a lesser range, and

RMAX(NCR) = the maximum desired firing range for CSW unit NCR; i.e., the weapon is essentially ineffective at greater ranges.

The width of the fire-position selection grid for a specified CSW unit is computed as the width of the sector at a distance, RMIN(NCR), from the threat position. An illustration of the grid width, noted by WIDTH, is given in Figure 1 for CSW unit 1. The length of the grid is computed as a function of RMAX(NCR) and RMIN(NCR). The number of points in the grid is determined as a function of the grid size and the spacing between points, noted by SPACE, specified by input data.

Each point in the fire position selection grid is evaluated as to its desirability as a firing position, considering the three factors previously

---

<sup>1</sup>RFI is determined from input arrays RXFIRE(K) and RYFIRE(K, NCR), described later in detail, as a number in the interval [0, 1]. RFI may be considered to be the effective hit probability for a specified weapon at various ranges, thus relating weapon effectiveness to a candidate firing position.



described. Tactical doctrine concerning the relative importance of each factor in the selection of a firing position is input by assigning weight to each of the three factors, noted by  $CW(I)$ ;  $I = 1, 2, 3$ ; where

$CW(1)$  = weight of TGCov,

$CW(2)$  = weight of CSWCO,

$CW(3)$  = weight of RFI, and

$$\sum_{I=1}^3 CW(I) = 1.$$

The equation used to compute the desirability, DESIR, of a grid point is given by

$$DESIR = [CW(1)] \cdot [1-TGCov] + [CW(2)] \cdot [CSWCO] + [CW(3)] \cdot [RFI]. \quad (1)$$

It should be noted that the three terms in (1) have values between zero and one, as do the weights. For example,  $RFI = 1$  would be the most desirable range-firepower index and would occur at a range,  $RMIN(NCR)$ , from the threat position. Recall that TGCov is the portion of the threat position covered relative to the firing position, the factor  $(1-TGCov)$ , is used in computing DESIR. A value of  $CSWCO = 1$  is the most desirable since the unit desires to remain covered and/or concealed relative to the threat location.

After the desirability of each grid point has been determined, the resulting candidate list is searched for the grid point with maximum desirability and this point becomes the primary desired firing position for the CSW unit in the attack mode. The selection of the alternate desired firing position for the unit is made as a function of its maximum allowable distance from the primary position, specified by input data. The grid point with the maximum desirability within the allowable distance from the primary position is selected as the alternate desired firing position. The purpose of selecting an alternate firing position is to provide the capability of representing "shoot and scoot" tactics on the part of the CSW unit. The variable,  $CSMVT(NCR)$ , specified by input data for each CSW unit is the number of rounds that CSW unit NCR will fire before moving to its alternate firing position.

The unit will return to its primary position after having fired  $CSMVT(NCR)$  rounds from its alternate position. This process continues until termination of the mission. A discussion of the events resulting in termination of the mission is presented in a later section.

### Defense Mode Deployment

If the CSW units mounted on a specified APC are to deploy in the defensive mode after dismounting, the deployment occurs along a line through the APC perpendicular to the threat position specified for the APC (see Figure 2). The fire-position selection grid for defensive deployment consists of points along the deployment line of length,  $RLIMIT(LAPC)$ , (specified by input data for each personnel carrier,  $LAPC$ ), located a distance,  $SPACE$ , apart. If the length of the deployment line is not sufficient for deploying all CSW units mounted on the APC, the line is extended equal distances on each side of the APC as required. The desirability of each grid point as a firing position is determined as in the attack mode, except that the range-firepower index,  $RFI$ , is not considered, since range to the threat position is approximately constant for all points on the deployment line. The equation used to compute the desirability of a specified grid point for defensive deployment is given by

$$DESIR = [DCW(1)] \cdot [1 - TRCOVR] + [DCW(2)] \cdot [CRWCON] \quad (2)$$

where

$TRCOVR$  = the portion of the threat position covered relative to the candidate firing position;

$CRWCON$  = the portion of the candidate firing position covered or concealed relative to the threat position;

$DCW(1)$  = weight of  $TRCOVR$ ; and

$DCW(2)$  = weight of  $CRWCON$

where

$$DCW(1) + DCW(2) = 1.$$

Each CSW unit mounted on the APC is sequentially assigned a defensive firing position in descending order of grid point desirability. It is important to note that the CSW unit,  $NCR$ , designated by input data as the "first" unit on carrier,  $LAPC$ ; i.e.,  $LAPCCW(1, LAPC) = NCR$  for personnel carrier  $LAPC$ , will receive the most desirable firing position, and so on for the remaining designated units on the APC.

The computational procedures used to determine desired firing positions in both the attack and defense mode are accomplished in subroutine  $CSWGRD$  and are given below.

1. Compute ANGLE, the angle from the crew's dismount point (XC, YC) to the threat point (XT, YT); i.e.,

$$\text{ANGLE} = \tan^{-1} \left[ \frac{YT - YC}{XT - XC} \right] .$$

2. If  $XC < XT$ , go to step 4. Otherwise, go to step 3.

3.  $\text{ANGLE} + \pi \rightarrow \text{ANGLE}$ .

4. Compute 
$$\begin{cases} \text{SINANG} = \sin(\text{ANGLE}) \\ \text{COSANG} = \cos(\text{ANGLE}) \end{cases} .$$

5. If CSW unit NCR is being employed in the defensive mode; i.e., if  $\text{CSDECN}(\text{NCR}) = 2$ ; go to step 40, otherwise, go to step 6.

6. Compute RTCT, the distance from the dismount point to the threat point; i.e.,

$$\text{RTCT} = \sqrt{(XT - XC)^2 + (YT - YC)^2} .$$

7. Compute RDIF, the distance from the maximum effective range of CSW unit NCR to the threat point; i.e.,

$$\text{RDIF} = \text{RTCT} - \text{RMAX}(\text{NCR}) .$$

8. If  $\text{RTCT} \leq \text{RMIN}(\text{NCR})$ , go to step 40, otherwise, go to step 9.

9. If  $\text{RTCT} \leq \text{RMAX}(\text{NCR})$ , go to step 12, otherwise, go to step 10.

10. Compute LENGTH, the length of the fire-position selection grid; i.e.,

$$\text{LENGTH} = \text{RMAX}(\text{NCR}) - \text{RMIN}(\text{NCR}) .$$

11. Set CTEST = 1, go to step 14.

12. Compute LENGTH, the length of the fire-position selection grid; i.e.,

$$\text{LENGTH} = \text{RTCT} - \text{RMIN}(\text{NCR}) .$$

13. Set CTEST = 0.

14. Compute IMAX, the number of rows in the fire-position selection grid; i.e.,

$$\text{IMAX} = \left[ \frac{\text{LENGTH}}{\text{SPACE}} \right], \text{ where}$$

$$[X] = \text{greatest integer} \leq X$$

SPACE = the specified distance between grid points.

15. Determine JMAX, the number of columns in the fire-position selection grid; i.e., set JMAX = WIDTH.

16. If JMAX is odd, go to step 18; otherwise, go to step 17.

17. Set JC =  $\left[ \frac{\text{JMAX}}{2} \right]$ ; go to step 19.

18. Set JC =  $\left[ \frac{\text{JMAX}}{2} \right] + 1$ .

19. Set IC = 1.

20. If CTEST = 0, go to step 22; otherwise, go to step 21.

21. Compute

$$\begin{cases} \text{CDELX} = (\text{RDIF}) \cdot (\text{COSANG}), \\ \text{CDELY} = (\text{RDIF}) \cdot (\text{SINANG}); \text{ go to step 23.} \end{cases}$$

22. Set

$$\begin{cases} \text{CDELX} = 0 \\ \text{CDELY} = 0. \end{cases}$$

23. Set

$$\begin{cases} I = \text{IMAX} \\ J = 1. \end{cases}$$

24. Determine DESIR, the desirability of fire-position selection grid point (I, J), by a call to subroutine CSWDES.<sup>1</sup>

<sup>1</sup>The computational procedures of subroutine CSWDES are given following the computational procedures of CSWGRD.

25. Set  $\text{DESIRE}(I, J) = \text{DESIR}$ .

26. If  $J = J\text{MAX}$ , go to step 28; otherwise, go to step 27.

27.  $J + 1 \rightarrow J$ ; go to step 24.

28. If  $I = 1$ , go to step 30; otherwise, go to step 29.

29. Set

$$\begin{cases} J = 1 ; \text{ go to step 24.} \\ I - 1 \rightarrow I \end{cases}$$

30. Determine  $(IF, JF)$ , the values of  $(I, J)$  corresponding to

$$\begin{matrix} \text{Max} & [\text{DESIRE}(I, J)] \\ (I, J) \end{matrix}$$

31. Compute  $(XDF, YDF)$ , the coordinates of grid points  $(IF, JF)$  by a call to subroutine  $\text{CXYLOC}$ .

32. Determine  $(ITEM, JTEM)$ , the values of  $(I, J)$  corresponding to

$$\begin{matrix} \text{Max} & [\text{DESIRE}(I, J)] \\ (I, J) \neq \text{previous maximums.} \end{matrix}$$

33. Compute  $(XTEM, YTEM)$ , the coordinates of grid point  $(ITEM, JTEM)$  by a call to subroutine  $\text{CXYLOC}$ .

34. Compute  $DTEM$ , the distance from  $(XDF, YDF)$  to  $(XTEM, YTEM)$

$$DTEM = \sqrt{(XDF - XTEM)^2 + (YDF - YTEM)^2}.$$

35. If  $DTEM$  is within the specified allowable distance from the primary desired firing position  $(XDF, YDF)$ ; i.e., if

$$DTEM \leq (\text{CALLOW}) \cdot (\text{SPACE}); \text{ go to step 37, otherwise}$$

go to step 36.

36. If entire  $\text{DESIRE}(I, J)$  array has been considered, go to step 38; otherwise, go to step 32.

37. Determine (XDFA, YDFA), the alternate desired firing position; i.e., set

$$\begin{aligned}XDFA &= XTEM \\YDFA &= YTEM;\end{aligned}$$

go to step 39.

38. Record the alternate desired firing position as the primary desired firing position, i.e., set

$$\begin{aligned}XDFA &= XDF \\YDFA &= YDF.\end{aligned}$$

39. Determine the optimal route from (XC, YC) to (XDF, YDF) by a call to subroutine CSRTSL<sup>1</sup>; go to step 70.

40. <sup>2</sup>If the computations are for multiple crews, i.e., NCTOT > 1, go to step 41; otherwise, go to step 43.

41. Set MULTST = 1.

42. Set NCR equal to the CSW unit number of the first crew mounted on the specified APC, go to step 44.

43. Set MULTST = 0.

44. Compute JMAX, the number of grid points along the defensive deployment line of specified length, RLIMIT; i.e.,

$$JMAX = \left[ \frac{RLIMIT}{SPACE} \right] + 1.$$

45. If JMAX is odd, go to step 47; otherwise, go to step 46.

46. Set JC =  $\left[ \frac{JMAX}{2} \right]$  ; go to step 48.

---

<sup>1</sup>A detailed discussion and computational procedures for route selection by dismounted CSW units is given in a subsequent section.

<sup>2</sup>The computations for employment of CSW units in the defensive mode begin at step 40.

47. Set  $JC = \left[ \frac{JMAX}{2} \right] + 1.$

48. Set

$$\begin{cases} JC = 1 \\ I = 1 \\ CDELX = 0 \\ CDELY = 0. \end{cases}$$

49. Determine (XIJ, YIJ), the coordinates of grid point (I, J) by a call to subroutine CXYLOC.

50. Determine TRCOVR, the percent of the specified threat position (XT, YT) covered relative to (XIJ, YIJ) by a call to subroutine LOSPC.

51. Determine CRWCON, the percent of CSW unit NCR covered and concealed at (XIJ, YIJ) relative to the specified threat position (XT, YT) by a call to subroutine LOSPC.

52. Compute DESIR, the desirability of grid point (I, J); i.e.,

$$DESIR = [DCW(1)] \cdot [1 - TRCOVR] + [DCW(2)] \cdot [CRWCON] .$$

53. Set DESIRE(I, J) = DESIR.

54. If  $J = JMAX$ , go to step 56; otherwise, go to step 55.

55.  $J + 1 \rightarrow J$ ; go to step 49.

56. Determine JF, the value of J corresponding to

$$\text{Max}_J [DESIRE(I, J)] .$$

57. Compute (XDF, YDF), the coordinates of grid point (I, JF), by a call to subroutine CXYLOC.



58. Record (XC, YC), the dismount point, (XDF, YDF), the desired firing position in the defensive mode, and CLCPE(NCR), the next movement control point flag for CSW unit NCR; i.e., set

$$\left\{ \begin{array}{ll} \text{CSXRT}(2, \text{NCR}) & = \text{XC} \\ \text{CSYRT}(2, \text{NCR}) & = \text{YC} \\ \text{CSXRT}(1, \text{NCR}) & = \text{XDF} \\ \text{CSYRT}(1, \text{NCR}) & = \text{YDF} \\ \text{CLCPE}(\text{NCR}) & = 1 \\ \text{CXCUR}(\text{NCR}) & = \text{XC} \\ \text{CYCUR}(\text{NCR}) & = \text{YC} \end{array} \right.$$

59. If the computation is for multiple crews; i.e., MULTST = 1, go to step 60; otherwise, go to step 70.

60. Set J2T = JMAX + 1.

61. If all crews on the specified APC have been assigned firing positions, go to step 70; otherwise, go to step 62.

62. Set DESIRE(JF) = -1.

63. If any firing positions along the defensive deployment line of specified length RLIMIT remain; i.e., if DESIRE(I, J)  $\geq$  0 for any J = 1, ..., JMAX; go to step 64; otherwise, go to step 65.

64. Set NCR equal to next CSW unit number mounted on the specified APC, go to step 56.

65. Set NCR equal to next CSW unit number mounted on the specified APC.

66. Compute (XDF, YDF), the coordinates of grid point (I, J2T), by a call to subroutine CXYLOC.

67. Set

$$\left\{ \begin{array}{ll} \text{CSXRT}(2, \text{NCR}) & = \text{XC} \\ \text{CSYRT}(2, \text{NCR}) & = \text{YC} \\ \text{CSXRT}(1, \text{NCR}) & = \text{XDF} \\ \text{CSYRT}(1, \text{NCR}) & = \text{YDF} \\ \text{CXCUR}(\text{NCR}) & = \text{XC} \\ \text{CYCUR}(\text{NCR}) & = \text{YC} \\ \text{CLCPE}(\text{NCR}) & = 1 \end{array} \right.$$

68. If all crews mounted on the specified APC have been assigned firing positions, go to step 70; otherwise, go to step 69.
69.  $J2T + 1 \rightarrow J2T$ .
70. The computations are complete.

The computations to determine the desirability of a specified fire position selection grid point are accomplished in subroutine CSWDES and are given below.

1. Compute (XIJ, YIJ), the coordinates of grid point (I, J), by a call to subroutine CXYLOC.
2. Compute RTEM, the distance from (XIJ, YIJ) to the threat point (XT, YT):

$$RTEM = \sqrt{(XIJ - XT)^2 + (YIJ - YT)^2}.$$

3. Determine KA for the RXFIRE(K) array such that

$$RXFIRE(KA) \leq RTEM < RXFIRE(KA + 1).$$

4. Compute the interpolation factor, INT; i.e.,

$$INT = \frac{RTEM - RXFIRE(KA)}{RXFIRE(KA+1) - RXFIRE(KA)}.$$

5. Compute RFI, the range-firepower index for CSW unit NCR; i.e.,

$$RFI = RYFIRE(KA, NCR) + [RYFIRE(KA+1, NCR) - RYFIRE(KA, NCR)] \cdot INT.$$

6. If RFI = 0, go to step 7; otherwise, go to step 8.

7. Set DESIR = 0; go to step 11.

8. Compute TGCOV, the percent of the specified threat position (XT, YT) covered relative to (XIJ, YIJ) by a call to subroutine LOSPC.
9. Compute CSWCO, the percent of the crew at (XIJ, YIJ) covered and concealed relative to the specified threat position (XT, YT) by a call to subroutine LOSPC.

10. Compute DESIR, the desirability index, at (XIJ, YIJ); i.e.,

$$\text{DESIR} = [\text{CW}(1)] \cdot [1 - \text{TGCOV}] + [\text{CW}(2)] \cdot [\text{CSWCO}] + [\text{CW}(3)] \cdot [\text{RFI}].$$

11. The computations are complete.

#### Route Selection--Dismounted CSW Units

The criteria used to determine the route along which a dismounted CSW unit will move are based upon factors which can be measured during a simulated battle. The major factors influencing route selection are cover, concealment, and travel time. The Route Selection Model for dismounted CSW units has been adapted from the model for armored units (see Movement Controller, Chapter 5 of reference 2). The major differences between the route selection procedure utilized for dismounted CSW units and armored units are summarized below. It is assumed that the reader is familiar with the armor Route Selection Model referenced above.

1. The axis of advance for a CSW unit is specified by a line from the dismount point to the primary desired firing position and is determined within the simulation for each mission.
2. The number of points in the route selection grid is determined for each mission by the distance from the dismount point to the desired firing position and the distance, SPACE, between grid points specified by input data.
3. The relative difficulty of each grid point due to enemy strong-points and known enemy elements is computed as it is for armored units. Separate input data arrays specifying tactical doctrine, however, are provided for CSW units. Also, the equation for computing total route difficulty differs from that for armored vehicles (see step 9 of the computational procedure of subroutine CSTCDF).
4. The locations of known minefields are not considered in CSW unit route selection, since only antitank mines are currently represented in DYNCOM.
5. The configuration of the CSW unit route selection grid is square, and each grid point has seven neighbor points as opposed to nine used by the armor unit Route Selection Model (see Figure 4).

6. The CSW route selection procedure forces termination of the route at (XDF, YDF), the primary desired firing position for the specified CSW unit.

It should be noted that the dynamic route selection procedure is utilized only when the attack mode is employed. Dismounted CSW units deploying in the defensive mode travel on a straight line path from the dismount point to their respective defensive firing positions.

The computations which determine the primary and alternate desired firing positions and the optimal route to the primary firing position are performed in subroutine CSWGRD previously discussed. Computation of the desirability of a specified fire-position selection grid point is accomplished by subroutine CSWDES also previously discussed. Given the dismount point and the primary desired firing position for a CSW unit deploying in the attack mode, subroutine CSRTSL determines the optimal route to be traversed by the dismounted unit. For a specified route selection grid point, the neighbor points are determined by subroutine CSNBOR. The relative tactical difficulty for each route selection grid point is computed by subroutine CSTCDF, with the estimated travel time being determined by subroutine CETIME.

The computational procedures for each of these subroutines utilized in the route-selection procedure for dismounted CSW units are given below.<sup>1</sup>

#### Subroutine CSRTSL

1. Compute ANGR, the angle from the dismount point (XC, YC) to the primary desired firing position (XDF, YDF); i.e.,

$$\text{ANGR} = \tan^{-1} \left[ \frac{\text{YDF} - \text{YC}}{\text{XDF} - \text{XC}} \right] .$$

2. If  $\text{XC} < \text{XDF}$ , go to step 4; otherwise, go to step 3.
3.  $\text{ANGR} + \pi \rightarrow \text{ANGR}$ .

---

<sup>1</sup>The computational procedure of CETIME is given in a later section after discussion of the movement of dismounted crew-served weapon units.

4. Compute SINAR and COSAR, the sine and cosine of ANGR, respectively; i.e.,

$$\begin{aligned}\text{SINAR} &= \text{sine (ANGR)} \\ \text{COSAR} &= \text{cos (ANGR)}.\end{aligned}$$

5. Compute RGRID, the length of the route-selection grid; i.e.,

$$\text{RGRID} = \sqrt{(\text{XC} - \text{XDF})^2 + (\text{YC} - \text{YDF})^2}.$$

6. Compute IRMAX, the number of rows in the grid; i.e.,

$$\text{IRMAX} = \left[ \frac{\text{RGRID}}{\text{SPACE}} \right] + 1$$

where

$$\begin{aligned}\text{SPACE} &= \text{distance between grid points,} \\ [X] &= \text{greatest integer } \leq X.\end{aligned}$$

7. Determine JRMAX, the number of columns in the grid; i.e.,

$$\text{JRMAX} = \text{JCOLS}.$$

8. If JRMAX is odd, go to step 9; otherwise, go to step 10.

9. Set  $\text{JC} = \left[ \frac{\text{JRMAX}}{2} \right] + 1$ ; go to step 11.

10. Set  $\text{JC} = \left[ \frac{\text{JRMAX}}{2} \right]$ .

11. Set  $\text{IC} = 2$ .

12. Initialize  $\text{EC}(\text{I}, \text{J})$ , the route-selection grid difficulty array; i.e.,

$$\text{EC}(\text{I}, \text{J}) = 0; \text{I} = 1, \dots, \text{IRMAX}; \text{J} = 1, \dots, \text{JRMAX}.$$

13. Set

$$\begin{cases} \text{I} = 1 \\ \text{J} = 1. \end{cases}$$

14. Compute  $(\text{XIJ}, \text{YIJ})$ , the coordinates of grid point  $(\text{I}, \text{J})$  by a call to subroutine CRTLOC.

15. Set  $K = 1$ .

16. If a line of sight exists to enemy strongpoint  $(SC(K), TC(K))$ , go to step 17; otherwise, go to step 21.

17. Compute

$$CDIST = \sqrt{[XIJ - SC(K)]^2 + [YIJ - TC(K)]^2}.$$

18. Determine  $L$ , the enemy weapon code such that

$$TEC(L + 1) < CDIST \leq TEC(L)$$

where

$TEC(L)$  = effective range of enemy weapon code  $L$  against a dismounted CSW unit.

19. If  $L = 0$ , go to step 21; otherwise, go to step 20.

20. Increase  $EC(I, J)$  by the difficulty,  $CSDSP(L)$ , due to enemy strongpoint of weapon code  $L$ ; i.e.,

$$EC(I, J) + CSDSP(L) \rightarrow EC(I, J).$$

21. If all enemy strongpoints have been considered; i.e.,  $K = KSP$ , go to step 23; otherwise, go to step 22.

22.  $K + 1 \rightarrow K$ ; go to step 16.

23. Set  $M = 1$ .

24. If enemy element  $M$  has been detected by the CSW unit; i.e.,  $LDET = 1$ , go to step 25; otherwise, go to step 31.

25. If enemy element  $M$  has suffered a firepower or total kill; i.e.,  $LKILL(M) = 1$ , go to step 31; otherwise, go to step 26.

26. Determine  $KT$ , the weapon code for enemy element  $M$ .

27. Compute

$$CEDIS = \sqrt{[XIJ - UC(M)]^2 + [YIJ - VC(M)]^2}$$

where  $UC(M), VC(M)$  = coordinates of the location of enemy element  $M$ .

28. If grid point (I, J) is within effective range of enemy element; i.e.,  $CEDIS \leq TEC(KT)$ ; go to step 29; otherwise, go to step 31.
29. If a line of sight exists to  $[UC(M), VC(M)]$ , go to step 30; otherwise, go to step 31.
30. Increase  $EC(I, J)$  by the difficulty,  $CSDEE(KT)$ , due to enemy element M; i.e.,  

$$EC(I, J) + CSDEE(KT) \rightarrow EC(I, J).$$
31. If all enemy elements have been considered; i.e.,  $M = MSP$ , go to step 33; otherwise, go to step 32.
32.  $M + 1 \rightarrow M$ ; go to step 24.
33. If all grid rows have been considered; i.e.,  $I = IRMAX$ , go to step 35; otherwise, go to step 34.
34.  $I + 1 \rightarrow I$ ; go to step 14.
35. If all grid columns have been considered; i.e.,  $J = JRMAX$ , go to step 37; otherwise, go to step 36.
36. Set  

$$\begin{cases} I = 1 \\ J + 1 \rightarrow J \end{cases} ; \text{ go to step 14.}$$
37. Set  

$$\begin{cases} I = IC \\ J = JC. \end{cases}$$
38. Determine coordinates (XIJ, YIJ) of grid point (I, J) by a call to subroutine CRTLOC.
39. Set  $K = 1$ .
40. Determine (M, N), the grid point designation for the  $K^{th}$  neighbor point of (I, J), by a call to subroutine CSNBOR.
41. If  $M > IRMAX$ , go to step 45; otherwise, go to step 42.



42. If  $M < 1$ , go to step 45; otherwise, go to step 43.
43. If  $N < J_{RMAX}$ , go to step 45; otherwise, go to step 44.
44. If  $N < 1$ , go to step 45; otherwise, go to step 47.
45. If all neighbor points have been considered; i.e.,  $K = 7$ , go to step 53; otherwise, go to step 46.
46.  $K + 1 \rightarrow K$ ; go to step 40.
47. If there is an entry for grid point  $(M, N)$  in list U, go to step 53; otherwise, go to step 48.
48. Determine  $(X_{MN}, Y_{MN})$ , the coordinates of grid point  $(M, N)$ , by a call to subroutine CRTLOC.
49. Determine DIFF, the difficulty of grid point  $(M, N)$ , by a call to subroutine CSTCDF.
50. <sup>1</sup>If there is an entry,  $(c, d)$ , for grid point  $(m, n)$  in list V, go to step 51; otherwise, go to step 52.
51. If the difficulty to travel to  $(m, n)$ , using the previously determined optimal difficulty,  $a, b d_{i,j}^* + d_{i,j}^{m,n} < c, d_{m,n}$ , go to step 52; otherwise, go to step 53.
52. Set  $i, j d_{m,n} = a, b d_{i,j}^* + d_{i,j}^{m,n}$ , and enter into list V.
53.  $K + 1 \rightarrow K$ .
54. If  $K > 7$ , go to step 55; otherwise, go to step 40.
55. Determine  $a, b d_{s,t}^*$ , the minimum difficulty from list V and record this entry in list U.
56. If the selected grid point  $(s, t)$  is in the last row of the grid; i.e.,  $S = I_{RMAX}$ , go to step 57; otherwise, go to step 58.

---

<sup>1</sup>Grid point notation of capital and lower case letters will be used interchangeably in the remaining steps. See tabulation of variable definitions at the end of the chapter and in Movement Controller, Chapter 5 of reference 2.

57. If the selected grid point (s, t) is in the JC column; i.e.,  $t = JC$ , go to step 59; otherwise, go to step 58.

58. Set

$$\begin{cases} I = s \\ J = t \end{cases} ; \text{ go to step 38.}$$

59. Compute CSXRT(I, NCR), CSYRT(I, NCR),  $I = 1, 2, \dots, \text{LAST}$ , the coordinates of the complete minimum difficulty route from (XC, YC) to (XDF, YDF) for CSW unit NCR.

Note:

$$I = \begin{cases} 1 \sim \text{corresponds to coordinates of grid point} \\ \quad (\text{IRMAX}, JC), \text{ noted by } (XDF, YDF) \\ \cdot \\ \cdot \\ \cdot \\ \text{LAST} \sim \text{corresponds to coordinates of grid} \\ \quad \text{point } (IC, JC), \text{ noted as } (XC, YC). \end{cases}$$

60. The computations are complete.

#### Subroutine CSNBOR

1. If  $K = 1$ , set

$$\begin{cases} M = I - 1 \\ N = J - 1 \end{cases}$$

go to step 8; otherwise, go to step 2.

2. If  $K = 2$ , set

$$\begin{cases} M = I - 1 \\ N = J + 1 \end{cases}$$

go to step 8; otherwise, go to step 3.

3. If  $K = 3$ , set

$$\begin{cases} M = I \\ N = J - 1; \text{ go to step 8; otherwise, go to step 4.} \end{cases}$$

4. If  $K = 4$ , set

$$\begin{cases} M = I \\ N = J + 1; \text{ go to step 8; otherwise, go to step 5.} \end{cases}$$

5. If  $K = 5$ , set

$$\begin{cases} M = I + 1 \\ N = J - 1; \text{ go to step 8; otherwise, go to step 6.} \end{cases}$$

6. If  $K = 6$ , set

$$\begin{cases} M = I + 1 \\ N = J; \text{ go to step 8; otherwise, go to step 7.} \end{cases}$$

$$7. \text{ Set } \begin{cases} M = I + 1 \\ N = J + 1. \end{cases}$$

8. The computations are complete.

#### Subroutine CSTCDF

1. Determine  $[CPDPX(I), CPDPY(I)]$ , the coordinates of the plane departure points between  $(XIJ, YIJ)$  and  $(XM, YM)$ , by a call to subroutine PDPSET.
2. Initialize variables, i.e., set

$$\begin{aligned} I &= 1 \\ CTIME &= -1 \\ TOTTIM &= 0 \\ XC1 &= CPDPX(I) \\ YC1 &= CPDPY(I) \\ XC2 &= CPDPX(I + 1) \\ YC2 &= CPDPY(I + 1). \end{aligned}$$

3. Compute the estimated travel time, TRTIME, from (XC1, YC1) to (XC2, YC2) by a call to subroutine CSTIME.

4. Increase TOTTIM, the total estimated travel time; i.e.,

$$\text{TOTTIM} + \text{TRTIME} \rightarrow \text{TOTTIM}.$$

5. If all plane departure points have been utilized; i.e.,  $I \geq N - 1$ , go to step 7; otherwise, go to step 6.

6.  $I + 1 \rightarrow I$ ; go to step 3.

7. If more plane departure points are required; i.e.,

$$\begin{cases} \text{XC2} \neq \text{XM} \\ \text{YC2} \neq \text{YM} ; \end{cases}$$

go to step 8; otherwise, go to step 9.

8. Determine additional plane departure points by a call to subroutine PDPSET, go to step 3.

9. Compute DIFF, the difficulty of the route from (XIJ, YIJ) to (XM, YM); i.e.,

$$\text{DIFF} = [\text{DWC}(1) \cdot \text{EC}(M, N)] + [\text{DWC}(2) \cdot \text{TOTTIM}]$$

where

$\text{DWC}(1)$  = weight (relative importance) of the difficulty due to known enemy elements and enemy strongpoints, and

$\text{DWC}(2)$  = weight (relative importance) of the difficulty due to total travel time.

10. The computations are complete.

Determination of the deployment mode, enemy threat location, primary and alternative firing positions, and optimal route to the primary firing position for a dismounted CSW unit has been discussed in this and previous sections. These factors remained unchanged for the duration of the unit's current mission. Models employed to move the dismounted CSW units on the battlefield, and the factors which result in termination of the mission are discussed in the following section.

### Movement of Dismounted CSW Units

Dismounted CSW units move through the sequence of movement control points generated by the Route Selection Model when deploying in the attack mode. The use of movement control points and plane departure points is adapted from their use by armor units in DYNCOM (see Movement, Chapter 7 of reference [1]). Recall that each dismounted CSW unit is represented in DYNCOM as a rectangular solid whose size is specified as a function of the number of men in the unit. The movement speed, CVLIM, for a dismounted CSW unit is determined as a function of the unit's weapon code, NKWEP; and the grade angle of the terrain being traversed. The limiting speed, CVLIM, is calculated using the following input data:

XCSWIN(K) = incremental values of grade angle from which the corresponding CVLIM is computed for a specified CSW unit;  $K = 1, \dots, \text{INCMAX}$ .

YCSWIN  
(K, NKWEP) = the value of CVLIM corresponding to the  $K^{\text{th}}$  incremental grade angle, XCSWIN(K), for a CSW unit with weapon code, NKWEP.

For any particular value of grade angle, THATA, a linear interpolation between the two adjacent increments is performed to determine CVLIM. Thus, CVLIM is a piecewise linear function of the grade angle for a specified weapon code, NKWEP. The level of resolution with which the functional relationship between speed and grade angle is represented in the simulation is controlled by INCMAX, the number of incremental grade angles and corresponding speeds, which are input.

Dismounted CSW units are moved at a constant velocity between two specified plane departure points. The event time for a movement event is specified by input as for an armored unit movement event. If the dismounted CSW units are deploying in the defense mode, each unit is moved along a straight line path from the dismount point to its desired defensive firing position. Once the firing position is attained, the unit will remain in that position until it is determined that the units are to remount the APC (see Crew-Served Weapons, Chapter 9 of Volume 1. The time required for a dismounted CSW unit deployed in the defensive mode to remount on the APC is taken to be the travel time back to the remount point plus the actual remount time, RETIM, specified by input data.

If the dismounted CSW units are deployed in the attack mode, each unit is moved along its route as determined by the Route Selection Model to its

primary desired firing position. Once the primary firing position is attained, the unit commences its firing mission as determined by the firing models. "Shoot and scoot" tactics are performed between the primary and alternate firing positions for the unit as specified by input tactical doctrine previously discussed. Dismounted CSW units deployed in the attack mode will remount on the APC according to the following logic:

1. At some point in the battle after the APC has stopped and dismounted its CSW units, it may resume movement. If the APC becomes a casualty and can no longer move, the dismounted CSW units assigned to that APC remain at their firing positions for the duration of the battle.
2. The distance, DREMNT, from the dismount point to the centroid of firing positions for the dismounted CSW units is computed.
3. When the APC has traveled a distance, DREMNT, after resuming movement, the APC is stopped.
4. The CSW units assigned to the APC are remounted after a specified remount time, RETIM, and the APC proceeds until it is determined that the crews are once again to be dismounted.

The computational procedures for remounting dismounted CSW units in both the attack and defense modes involve minor modifications to subroutine MOUNT described in Crew-Served Weapons, Chapter 9 of Volume 1. Subroutine CSTIME determines either the estimated or actual travel time between two specified points for a dismounted crew-served weapon unit. The computational procedure of subroutine CSTIME follows.

1. Compute HC1 and HC2, the elevations at (XC1, YC1) and (XC2, YC2), respectively, by calls to subroutine ELVATE.
2. Compute HDIF, the difference in elevations HC1 and HC2; i.e.,

$$HDIF = HC2 - HC1.$$

3. Compute XDIF, the X-Y distance from (XC1, YC1) to (XC2, YC2); i.e.,

$$XDIF = \sqrt{(XC1 - XC2)^2 + (YC1 - YC2)^2}.$$

4. Compute THATA, the grade angle from (XC1, YC1, HC1), to (XC2, YC2, HC2); i.e.,

$$THATA = \tan^{-1} \left( \frac{HDIF}{XDIF} \right) .$$

5. Determine KA from the XCSWIN(K) array such that

$$XCSWIN(KA) \leq THATA < XCSWIN(KA + 1) .$$

6. Compute the interpolation factor, KINT; i.e.,

$$KINT = \frac{THATA - XCSWIN(KA)}{XCSWIN(KA+1) - XCSWIN(KA)} .$$

7. Compute CVLIM, the limiting speed for CSW unit weapon code, NKWEP; i.e.,

$$CVLIM = YCSWIN(KA, NKWEP) + [KINT] \cdot [YCSWIN(KA+1, NKWEP) - YCSWIN(KA, NKWEP)] .$$

8. Compute CDISTA, the distance from (XC1, YC1, HC1) to (XC2, YC2, HC2); i.e.,

$$CDISTA = \sqrt{(XC1-XC2)^2 + (YC1-YC2)^2 + (HC1-HC2)^2} .$$

9. If the event time, CTIME, is to be computed; i.e., if  $CTIME < 0$ , go to step 10; otherwise, go to step 12.

10. Compute TRTIME, the travel time from (XC1, YC1, HC1) to (XC2, YC2, HC2); i.e.,

$$TRTIME = \frac{CDISTA}{CVLIM} .$$

11. Set

$$\begin{cases} CXACT &= XC2 \\ CYACT &= YC2 \\ CDIS &= CDISTA \\ CTIME &= TRTIME; \end{cases}$$

go to step 21.



12. Compute CDIS, the distance traveled in the specified event time, CTIME; i.e.,

$$CDIS = (CTIME) \cdot (CVLIM).$$

13. If the CSW unit can make (XC2, YC2) in the allotted event time; i.e.,  $CDIS > CDISTA$ , go to step 10; otherwise, go to step 14.

14. Compute CRATIO, the portion of CDISTA that the unit can travel in the allotted time; i.e.,

$$CRATIO = \frac{CDIS}{CDISTA}.$$

15. Compute CDXY, the X-Y distance which the unit can travel in the allotted time; i.e.,

$$CDXY = (CRATIO) \cdot (XDIF).$$

16. Compute THUTA, the angle in the X-Y plane, from (XC1, YC1) to (XC2, YC2); i.e.,

$$THUTA = \tan^{-1} \left[ \frac{YC2 - YC1}{XC2 - XC1} \right].$$

17. If  $XC1 \geq XC2$ , go to step 18; otherwise, go to step 19.

18.  $THUTA + \pi \rightarrow THUTA$ .

19. Compute (CXACT, CYACT), the coordinates of the point which the CSW unit can attain in the allotted event time; i.e.,

$$\begin{cases} CXACT = XC1 + (CDXY) \cdot \cos (THUTA) \\ CYACT = YC1 + (CDXY) \cdot \sin (THUTA). \end{cases}$$

20. Determine TRTIME, the total travel time; i.e., set

$$TRTIME = CEVTIM.$$

21. The computations are complete.

Subroutine CSMOVE determines the travel time between two specified battlefield points for a dismounted CSW unit. The computational procedure of subroutine CSMOVE follows.

1. Initialize K, the next movement control point designator for CSW unit NCR; and CEVTIM, the specified event time for the move; i.e.,

$$\begin{cases} K = \text{CLCPE}(\text{NCR}) \\ \text{CEVTIM} = \text{CTIME}. \end{cases}$$

2. Determine H1 and H2, the elevations at the current position,  $[\text{CXCUR}(\text{NCR}, \text{CYCUR}(\text{NCR}))]$ , and the next movement control point  $[\text{CSXRT}(\text{K}, \text{NCR}), \text{CSYRT}(\text{K}, \text{NCR})]$ , respectively, by calls to subroutine ELVATE.
3. Compute CDMCP, the distance remaining to the next movement control point, by a call to function RGXYZ.
4. If CDMPC is approximately zero; i.e.,  $\text{CDMPC} < \text{EPDIS}$ , go to step 5; otherwise, go to step 6.

5. Set

$$\begin{cases} \text{CXACT} = \text{CXCUR}(\text{NCR}) \\ \text{CYACT} = \text{CYCUR}(\text{NCR}); \end{cases}$$

go to step 18.

6. If CEVTIM, the remaining event time, is approximately zero; i.e.,  $\text{CEVTIM} < \text{ETIM}$ , go to step 7; otherwise, go to step 8.

7. Set

$$\begin{cases} \text{CXACT} = \text{CXCUR}(\text{NCR}) \\ \text{CYACT} = \text{CYCUR}(\text{NCR}); \end{cases}$$

go to step 27.

8. Determine  $[\text{CPDPX}(\text{I}), \text{CPDPY}(\text{I})]$ , the plane departure points between  $[\text{CXCUR}(\text{NCR}, \text{CYCUR}(\text{NCR}))]$  and  $[\text{CSXRT}(\text{K}, \text{NCR}), \text{CSYRT}(\text{K}, \text{NCR})]$  by a call to subroutine PDPSET.

9. Set  $\text{I} = 1$ .

10. Set

$$\begin{cases} XC1 = CPDPX(I) \\ YC1 = CPDPY(I) \\ XC2 = CPDPX(I + 1) \\ YC2 = CPDPY(I + 1). \end{cases}$$

11. Determine TRTIME, the travel time; CDIS, the actual distance traveled, and (CXACT, CYACT), the actual position attained in moving from (XC1, YC1) to (XC2, YC2) by a call to subroutine CSTIME.

12. Decrease the remaining event time, CEVTIM; i.e.,

$$CEVTIM - TRTIME \rightarrow CEVTIM.$$

13. If no event time remains; i.e.,  $CEVTIM < ETIM$ , go to step 27; otherwise, go to step 14.

14. If CSW unit NCR attained its next movement control point; i.e.,

$$\begin{cases} CXACT = CSXRT(K, NCR) \\ CYACT = CSYRT(K, NCR); \end{cases}$$

go to step 18; otherwise, go to step 15.

15. If more plane departure points are needed; i.e.,  $I = N - 1$ , go to step 16; otherwise, go to step 17.

16. Determine additional plane departure points by a call to subroutine PDPSET, go to step 9.

17.  $I + 1 \rightarrow I$ ; go to step 10.

18. If CSW unit NCR has attained its final desired position; i.e.,  $CLCPE(NCR) = 1$ , go to step 21; otherwise, go to step 19.

19. Set

$$\begin{cases} CXACT \rightarrow CXCUR(NCR) \\ CYACT \rightarrow CYCUR(NCR) \\ CLCPE(NCR) - 1 \rightarrow CLCPE(NCR). \end{cases}$$

20. Set  $K = CLCPE(NCR)$ ; go to step 2.

21. Set

$$\begin{cases} \text{CXCUR}(\text{NCR}) = \text{CXACT} \\ \text{CYCUR}(\text{NCR}) = \text{CYACT}. \end{cases}$$

22. If CSW unit NCR is currently moving to a primary desired firing position; i.e.,  $\text{CSMAKE}(\text{NCR}) = 1$ , go to step 23; otherwise, go to step 24.
23. Record the fact that NCR made its primary desired firing position; i.e., set  $\text{CSMAKE}(\text{NCR}) = 2$ ; go to step 26.
24. If CSW unit NCR is currently moving to alternate desired firing position; i.e.,  $\text{CSALT}(\text{NCR}) = 1$ ; go to step 25; otherwise, call ERROR.
25. Record the fact that NCR made its alternate desired firing position; i.e., set  $\text{CSALT}(\text{NCR}) = 2$ .
26. Update  $\text{CCLOCK}(\text{NCR})$ , the current clock time for CSW unit NCR; i.e.,  $\text{CCLOCK}(\text{NCR}) + (\text{CTIME} - \text{CEVTIM}) \rightarrow \text{CCLOCK}(\text{NCR})$ ; go to step 29.
27.  $\text{CCLOCK}(\text{NCR}) + \text{CTIME} \rightarrow \text{CCLOCK}(\text{NCR})$ .
28. Set
- $$\begin{cases} \text{CXCUR}(\text{NCR}) = \text{CXACT} \\ \text{CYCUR}(\text{NCR}) = \text{CYACT}. \end{cases}$$
29. The computations are complete.

### Summary and Conclusions

Crew-served weapon units may have important effects upon the outcome of a combat engagement because of their ability to attain cover and concealment relative to the enemy when operating in a dismounted mode. The purpose of the extended crew-served weapon models as developed for DYNCOM is to provide a dynamic representation of the operations of dismounted CSW units which is responsive to input tactical doctrine and battlefield conditions. Because interaction of combat elements with terrain is so important, representations of the selection of firing positions, routes to these firing positions, and movement over these routes as a function of enemy locations, tactical doctrine,

and battle events have been related explicitly to terrain conditions. These models may assist the military planner in answering such questions as:

1. What is the effect on the level of enemy armor casualties of alternate crew-served weapon hardware designs?
2. How does the capabilities of a crew-served weapon system to accomplish a specified mission compare with other weapon systems represented in DYNCOM?
3. How does the effect of crew-served weapons vary with the tactical doctrines employed by both friendly and enemy forces?
4. How is the combat effectiveness of a dismounted CSW unit affected by its decreased exposure to enemy elements due to terrain cover and concealment and by its increased vulnerability to enemy weapons due to lack of defensive armament?

Because dismounted infantry is not currently represented in DYNCOM, dismounted CSW units are employed in support of armored units against hard point targets within the simulation. It is important to note, however, that the structure of the extended crew-served weapon models is flexible to facilitate their incorporation into any dismounted infantry model which may be developed for DYNCOM in the future.

# DEFINITION OF VARIABLES

ANGMID	=	the angle from (XC, YC) through the center of the sector of responsibility defined by ANGSEC for a specified APC dismounting crews in the attack mode.
ANGSEC(LAPC)	=	total angle of sector of responsibility for all CSW units on a specified APC (noted by LAPC) measured from (XC, YC) used to compute firing positions for dismounted crews when attack mode is specified.
CALLOW	=	maximum allowable distance from primary to alternate desired firing position, expressed in units of SPACE.
CCLOCK(NCR)	=	current clock time of CSW unit NCR.
CLCPE(NCR)	=	the location in a list of the next movement control point for CSW unit NCR.
CRWCON	=	percent of crew covered or concealed relative to the threat position in the defensive mode.
CSALT(NCR)	=	alternate desired firing position analog of CSMAKE(NCR).
CSDECN(NCR)	=	$\begin{cases} 2 \sim \text{CSW unit NCR is in defense mode,} \\ 1 \sim \text{CSW unit NCR is in attack mode, and} \\ 0 \sim \text{otherwise.} \end{cases}$
CSDEE(K)	=	increase in tactical difficulty at a route selection grid point due to a known intervisible enemy element at distance CEDIS; where
		$\text{TEC}(K) \geq \text{CEDIS.}$
CSDSMT	=	$\begin{cases} 1 \sim \text{all crews on a specified APC seek attack positions after dismount using ANGSEC, and} \\ 0 \sim \text{all crews seek defensive positions.} \end{cases}$

CSDSP(L) = increase in tactical difficulty at a route-selection grid point due to an intervisible enemy strongpoint at distance CDIST; where

$$TEC(K+1) \leq CDIST \leq TEC(K).$$

CSMAKE(NCR) =  $\begin{cases} 2 \sim \text{CSW unit NCR is currently positioned at its primary desired firing position,} \\ 1 \sim \text{NCR currently moving to primary desired firing position, and} \\ 0 \sim \text{otherwise.} \end{cases}$

CSMVT(NCR) =  $\begin{cases} 0 \sim \text{crew NCR remains at (XDF, YDF) for firing all rounds, and} \\ M \sim \text{crew NCR alternates positions after firing M rounds.} \end{cases}$

CSWCO = percent of crew height covered or concealed relative to (XT, YT) at a specified grid point in the attack mode.

CSXRT(I, NCR)  
CSYRT(I, NCR) = coordinates of the  $I^{\text{th}}$  movement control point specifying the movement path of dismounted CSW unit NCR;  $I = 1, \dots, \text{NPTMAX}$ .

CTIME = event time for a specified CSW unit.

CW(I) = weight (relative importance) assigned to factor I in the attack-fire position selection grid;  
 $I = 1, 2, 3$ ; where

$$I = \begin{cases} 1 \sim \text{weight of TGCOV,} \\ 2 \sim \text{weight of CSWCO, and} \\ 3 \sim \text{weight of RFI.} \end{cases}$$

Note:  $0 \leq CW(I) \leq 1$  and  $\sum_{I=1}^3 CW(I) = 1$ .

CXCUR(NCR)  
CYCUR(NCR) = coordinates of current position for CSW unit NCR.

$d_{i,j}^{m,n}$  = relative tactical difficulty in traveling from (XIJ, YIJ) to (XMN, YMN) in the route-selection grid.



$m, n^{d_{i,j}}$  = total tactical difficulty computed for traveling from the dismount point (XC, YC) to (XI<sub>J</sub>, YI<sub>J</sub>), with grid point (M, N) as an entry point.

$m, n^{d^*_{i,j}}$  = tactical difficulty predicted for the least difficult path to (XI<sub>J</sub>, YI<sub>J</sub>) from (XC, YC), with grid point (M, N) as an entry point.

DCW(I) = weight (relative importance) assigned to factor I in the defense-fire position selection grid; I = 1, 2; where

$$I = \begin{cases} 1 \sim \text{weight of TRCOVR, and} \\ 2 \sim \text{weight of CRWCON.} \end{cases}$$

Note:  $0 \leq \text{DCW}(I) \leq 1$  and  $\sum_{I=1}^2 \text{DCW}(I) = 1$ .

DESIRE(I, J) = desirability of grid point (I, J) in the CSW fire-position selection grid.

DISMTT(NKWE P) = time for a CSW unit of weapon code NKWE P to dismount from the APC.

DTHRT = distance from (XC, YC) that (XT, YT) is assumed to be located for crews selecting firing positions using ANGSEC as sectors of responsibility.

DWC(I) = weight (relative importance) assigned to factor I in the CSW route-selection grid, I = 1, 2; where

$$I = \begin{cases} 1 \sim \text{weight of difficulty} \\ \text{factor, and} \\ 2 \sim \text{weight of total travel time.} \end{cases}$$

Note:  $0 \leq \text{DWC}(I) \leq 1$  and  $\sum_{I=1}^2 \text{DWC}(I) = 1$ .

EC(I, J) = tactical difficulty for grid point (I, J) in the CSW route-selection grid.

HCREW(NKWE P) = height of a dismounted crew of weapon code NKWE P above the terrain.

HTGT	=	height of the threat position (XT, YT) above the terrain.
ICRMAX	=	number of increments used for RXFIRE(K) array.
INCMAX	=	number of increments used for XCSWIN(K) array.
LAPC	=	designator for element number of a specified APC.
LAPCCW(I, LAPC)	=	CSW unit number of the I <sup>th</sup> CSW unit mounted on APC with element number LAPC.
LCSWFN(ICE)	=	$\begin{cases} \text{NCR} \sim \text{element ICE is a crew-served weapon unit with designated number NCR, and} \\ 0 \sim \text{otherwise.} \end{cases}$
LCSWTP(NCR)	=	weapon code for CSW unit NCR (noted by KSWEP).
LENCSW(NKWEP)	=	effective length of CSW unit of weapon code NKWEP used to determine detection status.
MSP	=	number of enemy elements on the battlefield.
NAPCMX	=	maximum number of APC's in the battle.
NCR	=	designator for CSW units; $\text{NCR} = 1, \dots, \text{NCSWMX}$ .
NCSWMX	=	maximum number of CSW units in the battle.
NCTOT	=	number of crews mounted on a specified APC.
NCWMAX	=	maximum number of weapon codes for crew-served weapons in the battle.
NKWEP	=	designator for weapon codes; $\text{NKWEP} = 1, \dots, \text{NCWMAX}$ .
NPTMAX	=	maximum number of movement control points for a specified dismounted CSW unit.
RFI	=	range-firepower index ( $0 \leq \text{RFI} \leq 1$ ).
RLIMIT	=	maximum length of line along which CSW units will select a firing position in the defensive mode.

RMAX(NCR)	=	maximum desirable firing range for a CSW unit of weapon code NKWEP; i.e., maximum effective range of weapon.
RMIN(NCR)	=	minimum desired firing range equivalent of RMAX(NKWEP).
RNDCNT(NCR)	=	number of rounds fired by NCR at its current firing position.
RXFIRE(K)	=	value of the $K^{\text{th}}$ increment of distance from a specified point to (XT, YT) from which RFI is computed for CSW unit NCR. $K = 1, \dots, \text{ICRMAX}$ .

Note: Inputs should be made such that

$$\text{RXFIRE}(1) = \min_{\text{NCR}} [\text{RMIN}(\text{NCR})] \Rightarrow \text{RFI} = 1$$

$$\text{RXFIRE}(\text{ICRMAX}) = \max_{\text{NCR}} [\text{RMAX}(\text{NCR})] \Rightarrow \text{RFI} = 0.$$

SECMID	=	angle from (XC, YC) through the center of ANGSEC measured on the X-Y battlefield coordinate system.
SPACE	=	the distance between grid points in both the fire position selection grid and the route-selection grid for dismounted CSW units.
TEC(L)	=	effective range for enemy weapon of type L against a dismounted CSW unit; where $\text{TEC}(1) \geq \text{TEC}(2) \geq \dots \geq \text{TEC}(N) \geq 0;$ $N = \text{number of enemy weapons}.$
TGCOV	=	attack mode analog of TRCOVR.
TRCOVR	=	percent of the threat position covered relative to a specified grid point in the defensive mode.
XC, YC	=	coordinates of dismount point for crews from a specified APC.

XCSWIN(K)	=	value of grade angle for the K <sup>th</sup> increment from which the corresponding limiting speed for dismounted CSW units will be computed; K = 1, ..., INC MAX.
XDF(NCR), YDF(NCR)	=	primary desired firing position for CSW unit NCR.
XDFA(NCR), YDFA(NCR)	=	alternate desired firing position for CSW unit NCR.
XT, YT	=	coordinates of position relative to which a specified dismounted CSW unit seeks a firing position; referred to as the threat position.

## INPUT VARIABLES REQUIRED

ANGSEC(LAPC)  
CALLOW  
CSDEE(K)  
CSDSP(L)  
CSMVT(NCR)  
CW(I)  
DCW(I)  
DISMTT(NKWE P)  
DWC(I)  
HCREW(NKWE P)  
HTGT  
ICRMAX  
INCMAX  
LAPCCW(I, LAPC)  
LCSWFN(ICE)  
LCSWTP(NCR)  
LENC SW(NKWE P)  
MSP  
NAPCMX  
NCSWMX  
NCWMAX  
RLIMIT  
RMAX(NCR)  
RMIN(NCR)  
RXFIRE(K)  
SPACE  
TEC(L)  
XCSWIN(K)

## REFERENCES

Parry, S. , "Movement Model," Chapter 7 (in) The Tank Weapon System,  
RF 573 AR 69-2B (U), Systems Research Group, The Ohio State Univer-  
sity, Columbus, Ohio, September, 1969.

## CHAPTER 6

### EXTENSION TO DYNCOM BEAM-RIDER MISSILE MODELS

by

G. M. Clark, J. J. Rheinfrank III, and R. M. Lawson

#### Introduction

In research reported in Chapter 8 of Volume 1, a Beam-Rider Missile Model was designed for DYNCOM to represent the performance of beam-rider missiles in combat situations. This Beam-Rider Missile Model was explicitly designed to represent missiles that continuously apply in-flight corrections. Thus, the TOW and Shillelagh missiles can be represented by this model whereas better models can be designed for missiles such as the DRAGON that apply corrections at discrete points in time (see Chapter 3 of Volume 5). The Beam-Rider Missile Model described in this chapter was designed to permit analyses of the relationship among tactical unit effectiveness and specific missile design characteristics such as flight profile, flight velocity, missile agility, tracker performance, and turret turn rate. However, during actual use of this model (reference 1), it became apparent that specific aspects of this model should be extended in order to improve its utility, and research reported to accomplish these extensions is reported in this chapter. To appreciate these extensions, pertinent features of the initial beam-rider missile model are summarized in the following section.

#### Initial Beam-Rider Missile Model

The principal characteristic of beam-rider missiles described by DYNCOM is that their guidance systems are second-order control systems. The deviation of the missile from the tracker's line of sight and the rate of change of this deviation are inputs to this control mechanism as shown in Figure 6.1. This deviation is shown by a dashed line in the figure. It is assumed that the missile imparts an acceleration that is proportional to a linear combination of these guidance system inputs; thus, the missile guidance system creates a force component that is proportional to the missile deviation from the tracker line of sight and the rate that it is closing with respect to the line of sight. Mathematically, this assumption is expressed by the equation

$$h''(t) = -K(h(t) - C - l(t)) - \beta(h'(t) - l'(t)), \quad (6.1)$$

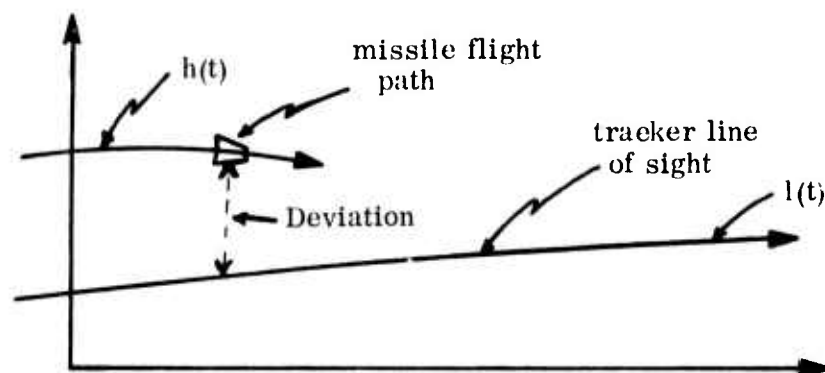


Figure 6.1. --Beam Rider Missile Deviation from Tracker Line of Sight

where

$h(t)$  = missile position at time  $t$  (meters),

$l(t)$  = a position of a point on the tracker line of sight closest to the missile at time  $t$  (meters),

$C$  = a constant flight bias in the missile system (meters), and

$K$  and  $\beta$  are proportionality constants characterizing the missile flight performance.

Note that this model is one dimensional. It is applied by representing missile flight in the pitch and yaw planes independently of each other.

The control equation, 6.1, is implemented within DYNCOM by a recurrence procedure described in Chapter 8 of Volume 1. During small time intervals of length  $TMINC$ , equation 6.1 is applied using the result of the previous time interval as inputs to the current time interval. These inputs are

$h(0)$  = initial missile position (meters)

$h'(0)$  = initial missile velocity (meters/second).

These time intervals are considered to be small enough to represent the tracker's line of sight, i. e.,  $l(t)$ , as a straight line. Note that the tracker in actuality is

continually moving his line of sight so  $l(t)$  is not, in general, linear. Thus, during the time interval,

$$l(t) = Z_0 + Z_1 t,$$

where  $Z_0$  and  $Z_1$  are constants within the time interval TMINC. These tracker constants are recomputed each time interval.

The solution to equation 6.1 is derived in Chapter 8 of Volume 1 and is

$$h(t) = Z_0 + C + Z_1 t + e^{-\frac{\beta}{2}t} \left\{ \left[ h(0) - Z_0 - C \right] \cos \frac{\omega}{2} t + \left[ \beta (h(0) - Z_0 - C) + 2(h'(0) - Z_1) \right] \frac{\sin \frac{\omega}{2} t}{\omega} \right\}. \quad (6.2)$$

where

$$\omega = \sqrt{4K - \beta^2}. \text{ Note that } \beta^2 - 4K \text{ is assumed to be negative because the missile is assumed to be an underdamped system.}$$

The missile is assumed to fly according to equations 6.1 and 6.2, until intervisibility between the missile and the tracker is lost interrupting guidance signals. When this situation occurs, the missile flies along its current velocity vector without any acceleration being applied. Note that the assumption is made that this missile has a  $360^\circ$  field of view and intervisibility is all that is required.

When the Beam-Rider Missile Model was first developed, a model specifically for the tracker was unavailable. However, the logic of a second-order control model, i. e., equation 6.1, appeared reasonable for representing a tracker. When describing a tracker, the variables in equation 6.1 are redefined so that

$h(t)$  = tracker aim angle at time  $t$ , measured in radians,

$l(t)$  = target angle at time  $t$ , measured in radians,

$C$  = tracker constant flight bias, measured in radians.

The assumption was similarly made for the tracker that he attempts to follow the



target by applying an acceleration to his aim angle that is equal to a linear combination of the aim angle's deviation from the target angle and the velocity of the aim angle relative to the target angle. The tracker constant flight bias,  $C$ , is used to represent the tracker's error in perceiving the target position. Analysis of actual flight data shows that  $C$  is a significant variable, but no analyses were made to determine if a better tracker model could be designed than this second-order control model. The tracker model is also one-dimensional and is applied by representing errors in the pitch plane independently of the yaw plane.

In both the tracker and missile application of the control model, equations 6.1 and 6.2 are meant to represent the mean missile and tracker performance. Variations from this mean value solution, equation 6.2, are present because the actual systems are more complex than this model, and many other operational factors occur causing both equipment and human performance variations. These additional variations are represented by random variables applied to the solution of equation 6.2. Accordingly, a typical flight path is shown in Figure 6.2. The distribution of the  $i$ th random error is normal with mean zero and variances  $S_i^2$ . Note that this random variable causes the missile flight path (or tracker aim angle trace) to be discontinuous; moreover, efforts to analyze this procedure have failed to associate this random error with any physical phenomenon capable of interpretation.

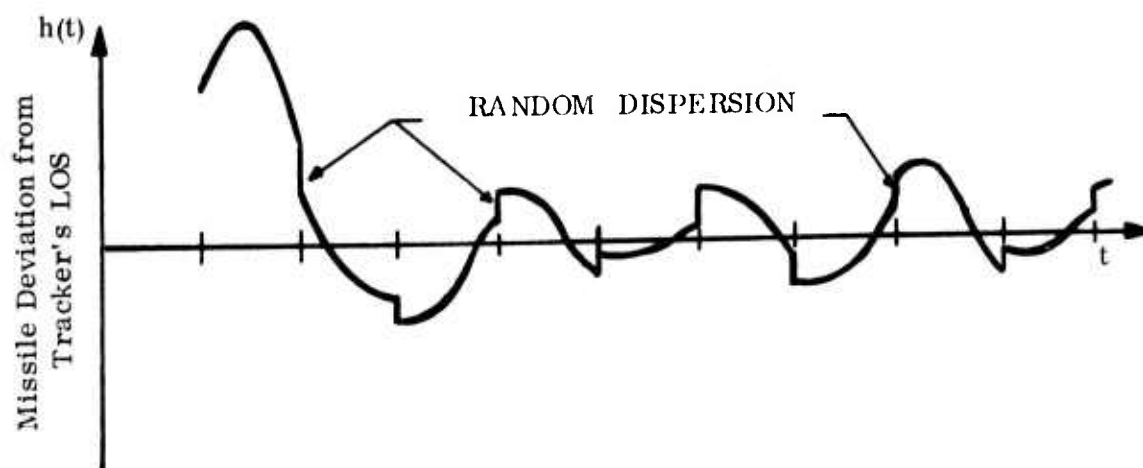


Figure 6.2. --Monte Carlo Procedure-Discontinuous Flight Trace Model

However, procedures are described in Chapter 8 of Volume 1 for selecting values of  $S_i^2$  to give hit probabilities consistent with design capability study results. These design capability studies estimate missile variance as a function of flight range based on the assumption of a fixed tracker line of sight and a smooth terrain profile. Missile variances from these design studies are unequal to the variances, values of  $S_i^2$ , applied in DYNCOM because recursive use of the control model makes the missile position at a given point in time a function of previously sampled random errors. Values of  $S_i^2$  consistent with the design variances are computed by program BRVAR described on page D-3 of Volume 4A.

In addition to values of  $S_i^2$ , procedures have been developed for calculating values for  $\beta$ ,  $\omega$ , and  $C$ , and these values are calculated from data giving the missile and tracker line of sight positions as a function of time. These estimates are calculated by program MBWEST described on page B-12 of Volume 4A.

#### Extensions to Beam-Rider Missile Models

Experience with the model reported in Chapter 8 of Volume 1 and summarized above has indicated that the following four extensions to the model should be investigated:

1. A model representing a flight trajectory which is continuous in time should be derived.
2. A parameter estimation procedure for this continuous flight-trace control model should be developed.
3. The effects of a restricted field of view on guided missile flight should be represented.
4. A model describing the role of the human tracker in beam-rider missile performance should be formulated.

Representation of stochastic variations in missile performance using discontinuous flight traces, like the one depicted in Figure 6.2, was the easiest procedure to implement when the Beam-Rider Missile Model was originally developed. However, real flight traces are continuous, and a more realistic model may give more valid results. The reasons for investigating a continuous flight-trace model are listed below:

1. The stochastic errors are sampled many times during a missile flight and their effects are cumulative.
2. The distribution of stochastic errors is determined by a program BRVAR from input design variances and the assumptions in BRVAR

are based upon the discontinuous flight trace assumption.

3. The estimation of control model parameters  $\beta$ ,  $\omega$ , and  $C$  is also based upon the discontinuous flight trace assumption.

Thus, a model representing continuous flight traces and corresponding parameter estimation procedures may give more valid results.

The extensions to represent a restricted missile field of view and a model of human tracker performance are motivated for reasons similar to those described above. The missile field of view is not represented in the model described in Chapter 8 of Volume 1; thus, representation of the missile field of view will permit description of variations in this design characteristic. Use of the second-order control model to represent human tracker performance was done without consideration of tracker characteristics; thus, the tracker model described in Chapter 8 of Volume 1 should be regarded as preliminary until analyses of tracker performance can be conducted.

Each of the four extensions listed above are investigated in this chapter, and the continuous flight trace model is developed in the following section.

#### Continuous Flight Trace Model

The continuous flight trace model is derived by assuming that stochastic errors in flight are manifested as variations in acceleration. These variations are added to the basic assumption of the Beam-Rider Missile Model, i. e., the missile imparts an acceleration that is proportional to the missile deviation from tracker line of sight and the rate that the missile is closing with the tracker line of sight. That is, the missile guidance system in the continuous flight trace model is assumed to impart an acceleration that is the sum of the three components listed below:

1. a correction for the missile deviation from the tracker line of sight,
2. a correction for the rate that the missile is closing with the tracker line of sight, and
3. a stochastic effect due to other variables.

Thus, equation 6.1 becomes

$$h''(t) = -K(h(t) - C - l(t)) - \beta(h'(t) - l'(t)) + \epsilon(t) \quad (6.3)$$

for the continuous flight trace model. The block diagram for this model is shown in Figure 6.3.

Equation 6.3 is the basic assumption for the continuous flight trace version of the beam-rider missile model. Stochastic effects in this model have physical significance and are manifested as variations in acceleration. These stochastic effects are assumed to be constant during a small time interval of length TMINC which is the length of a basic computational cycle for the beam-rider missile model as implemented by subroutine SHILLY. Thus, the continuous flight trace model consists of computational cycles where a value of  $\epsilon(t)$  is generated by a Monte Carlo procedure, used for a time interval of length TMINC, so that

$$\epsilon(t) = \epsilon(u) \text{ for } t - u \leq \text{TMINC}$$

when  $u$  is the beginning of a computational cycle. Each value of  $\epsilon(u)$  is assumed to be normally distributed, to have a mean of zero, to have a variance of  $\sigma_e^2$ , and to be independent of values in other time intervals. Thus, a simpler notation is used for the values of  $\epsilon(t)$  that more clearly suggests these assumptions. That is,

$\epsilon_i$  = stochastic acceleration effect for the  $i^{\text{th}}$  computational interval.

In fact,  $\epsilon_i$  may be regarded as a constant when just considering a single computational interval.

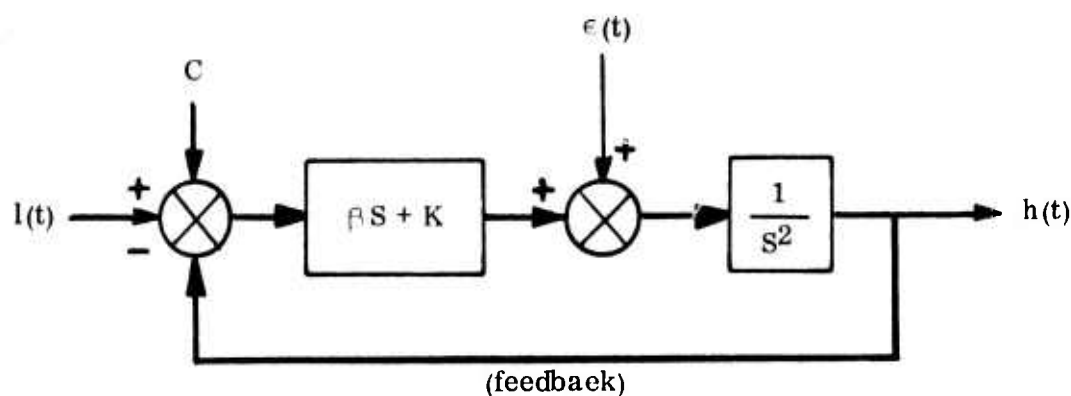


Figure 6.3. --Continuous Flight Trace Model Block Diagram

The solution to equation 6.3 is derived in Appendix L and is

$$\begin{aligned}
 h(t) = & Z_0 + C + 4\epsilon_i/(\beta^2 + \omega^2) + Z_1 t \\
 & + \exp(-\beta t/2) \cdot \left[ (h(0) - Z_0 - C - 4\epsilon_i/(\beta^2 + \omega^2)) \cdot \cos(\omega t/2) \right. \\
 & \left. + (\beta(h(0) - Z_0 - C - 4\epsilon_i/(\beta^2 + \omega^2)) + 2(h'(0) - Z_1)) \cdot \sin(\omega t/2) / \omega \right],
 \end{aligned}
 \tag{L. 4}$$

where

$$\omega = \sqrt{4K - \beta^2}.$$

Equation L. 4 is used to represent missile flight during small time periods of length TMINC in both the pitch and yaw planes. The time parameter or  $t$  has the value of zero at the beginning of each time interval. Besides the model parameters; i. e.,  $K$ ,  $C$ , and  $\omega$  for both pitch and yaw planes, L. 4 requires the following inputs:  $\epsilon_i$ ,  $Z_0$ ,  $Z_1$ ,  $h(0)$ , and  $h'(0)$ .  $\epsilon_i$  is determined by a Monte Carlo procedure generating a normally distributed random variable with a mean of zero and a variance of  $\sigma_c^2$ .  $Z_0$  and  $Z_1$  are determined from the tracker's line-of-sight position during the time interval.  $h(0)$  is the missile displacement from the true tracker-target line at the end of the previous time period given by equation L. 4. An equation for  $h'(t)$  is used to calculate the value of  $h'(t)$  at the end of each time period for use as  $h'(0)$  in the succeeding time interval. The equation for  $h'(t)$  is

$$\begin{aligned}
 h'(t) = & Z_1 - (\beta/2) \cdot \exp(-\beta t/2) \cdot \left[ (h(0) - Z_0 - C - 4\epsilon_i/(\beta^2 + \omega^2)) \cdot \cos(\omega t/2) \right. \\
 & \left. + (\beta(h(0) - Z_0 - C - 4\epsilon_i/(\beta^2 + \omega^2)) + 2(h'(0) - Z_1)) \cdot \sin(\omega t/2)/\omega \right] \\
 & + \exp(-\beta t/2) \cdot \left[ (Z_0 + C + 4\epsilon_i/(\beta^2 + \omega^2) - h(0)) \cdot \sin(\omega t/2) \cdot \omega/2 \right. \\
 & \left. + (\beta(h(0) - Z_0 - C - 4\epsilon_i/(\beta^2 + \omega^2)) + 2(h'(0) - Z_1)) \cdot \cos(\omega t/2)/2 \right].
 \end{aligned}
 \tag{L. 5}$$

A typical result from recursive use of equations L.4 and L.5 is shown in Figure 6.4. This figure should be compared with output from the discontinuous model shown in Figure 6.2.

Subroutine CONEQ calculates missile or tracker displacement values at the end of a single time interval using equations L.4 and L.5 (see page F-111 of Volume 4A for a description of CONEQ). Actually, CONEQ represents either continuous or discontinuous flight traces depending upon input values. The input variable ERR specifies the value of the acceleration error relative to the true tracker-target line of sight for the time interval. If a discontinuous flight trace is to be represented, ERR is set to zero. Subroutine NEWPOS determines whether a continuous or discontinuous flight trace is to be represented prior to calling CONEQ to evaluate the missile and tracker displacements at the end of the time interval. If a discontinuous flight is represented, ERR is set to zero by NEWPOS; however, a value of ERR is determined by a Monte Carlo procedure prior to calling CONEQ in the case of a continuous flight trace. A flag, KCFT, is recorded in common PLEASE to specify which model is to be employed by NEWPOS, where

$$KCFT = \begin{cases} 1 & \text{for continuous flight} \\ 0 & \text{for a discontinuous flight.} \end{cases}$$

See page F-670 of Volume 4B for a description of NEWPOS.

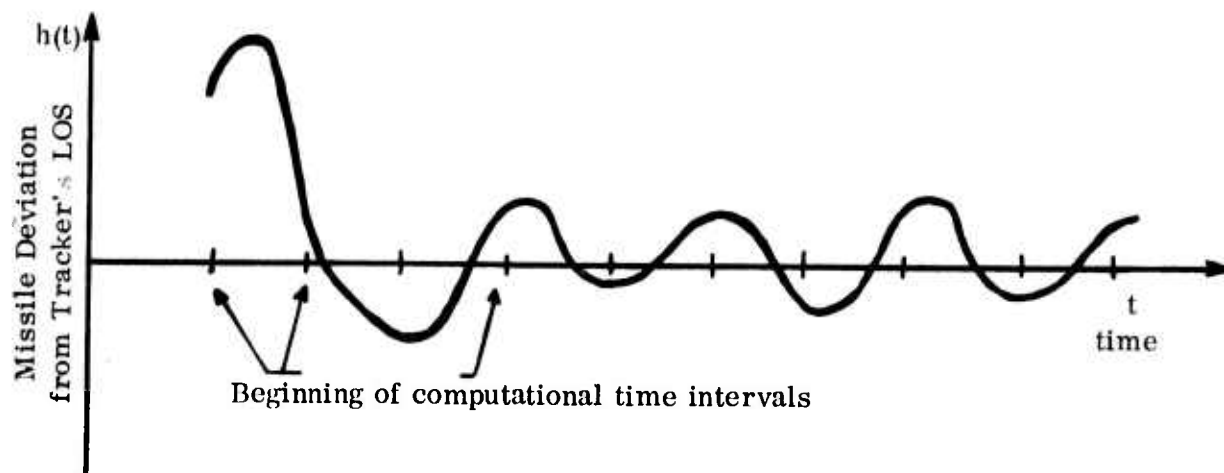


Figure 6.4. --Typical Result from Continuous Flight Trace Model

The DYNCOM user must be concerned with input values to six common areas in order to properly implement the models referred to above, viz., CONEQ and NEWPOS. DYNCOM is currently set up to represent at most two different types of beam-rider missiles, viz., a type one and a type two missile, and either one or both of these missiles may have a continuous flight trace. Common STOR17 gives input values to be placed by subroutine SHIGET into common PLEASE when representing a type-one missile. Similarly, SHIGET loads common PLEASE with values from common STOR18 when representing a type-two missile. The seventh variable in both STOR17 and STOR18 is KCFT and controls whether the two missile types have a continuous flight trace. When designating a continuous flight trace, the variances of the respective missile displacement acceleration errors in pitch and yaw planes must be specified as input. These variances are noted as  $\sigma_c^2$  in the above model description. The variances are recorded as a function of distance from the missile launcher by specifying the variances at a sequence of distance points recorded in common STORE5. STORE7 receives the values of  $\sigma_c^2$  in the pitch plane for a type-one missile, and STORE8 receives the same values for a type-two missile. In the yaw plane, values of  $\sigma_c^2$  are recorded in common STORE9 for a type-one missile, and common STOR10 for a type-two beam-rider missile.

#### Estimators for Parameters of Continuous Flight-Trace Models

To implement equation L.4 giving a continuous flight-trace and more meaningful stochastic error effects, procedures have been developed to estimate the values of the model parameters  $\beta$ ,  $\omega$ , and  $C$  from simulated or actual flight data. Estimators from flight data are required since the model parameters do not correspond exactly to measurable missile component characteristics and/or parameters in the missile design equations. This is true even though the assumptions made in deriving L.4, expressed by equation 6.3, are selected to represent the basic missile performance characteristics. Equation 6.3 was derived to represent basic missile characteristics, but is considerably simpler than the actual missile design relationships. The stochastic acceleration errors,  $\epsilon_i$ , are inserted in the model to correct for these simplifications.

In addition, procedures have been formulated to estimate the values of  $\sigma_c^2$  for input to commons STORE7, STORE8, STORE9, and STOR10. Estimates of  $\sigma_c^2$  are determined from estimates of the overall missile displacement variance as a function of flight range. The reader should note the the variance of missile displacement is not equal to the variance of acceleration errors, i.e.,  $\sigma_c^2$ ; thus, special procedures are required to determine the values of  $\sigma_c^2$  that result in the desired overall missile displacement variance. Estimation of  $\beta$ ,  $\omega$ , and  $C$  is discussed in the following paragraphs before describing methods of estimating  $\sigma_c^2$  because estimates of  $\beta$  and  $\omega$  are required to estimate  $\sigma_c^2$ .



In cases where actual flight data exist, the procedures presented in this section provide estimates for  $\beta$ ,  $\omega$ , and  $C$  values in both the pitch and yaw planes for each flight. In lieu of actual flight data, detailed analogue or digital missile simulation runs can be used to generate input data for the estimation procedure identified in this section. In any case, one set of estimates are generated for each flight trace. The DYNCOM input values for  $\beta$  and  $\omega$  can be estimated by averaging the  $\beta$  and  $\omega$  values over all available individual flight estimates. In DYNCOM, the value of  $C$ , the constant flight bias, is assumed to be constant during a flight but to vary from flight to flight. Visual inspection of actual flight traces have verified this assumption. In Figure 6.5, a typical result is indicated where the presence of a constant flight bias is apparent. Review of a set of these traces has indicated that these constant flight biases vary from flight to flight. The beam-rider missile model assumes that these constant flight biases are normally distributed. Thus, estimates of the means and standard deviations for these constant flight biases are generated from the estimates for individual flights.

In Appendix M, a procedure for generating maximum likelihood estimates of the values for  $\beta$ ,  $\omega$ , and  $C$  is identified given a single flight trace. Proof is given in that appendix that the maximum likelihood estimates for  $\beta$ ,  $\omega$ , and  $C$  are identical for both the continuous and discontinuous flight-trace models; thus, the procedure performed by program MBWEST described in Chapter 8 of Volume 1 and flow charted starting on page D-14 of Volume 4A is used to estimate  $\beta$ ,  $\omega$ , and  $C$  values for both the continuous and discontinuous flight trace models. This result was not anticipated and was surprising.

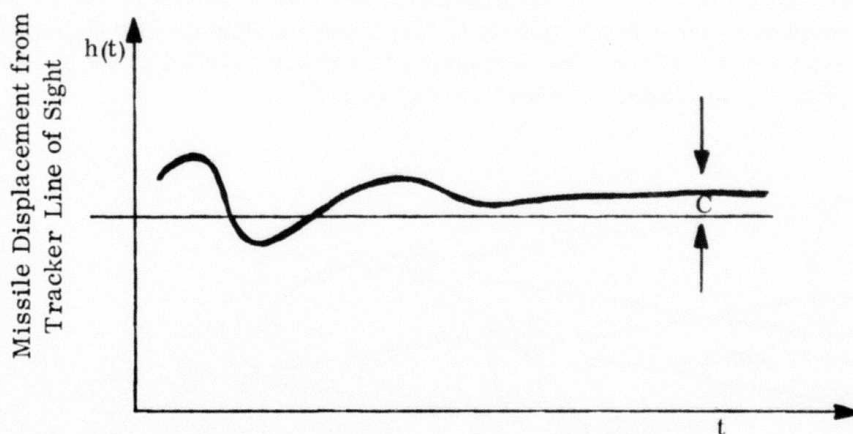


Figure 6.5. --Missile Constant Flight Bias



However, the above result does not necessarily imply that the continuous and discontinuous flight trace models are operationally equivalent. Estimates of the variance  $\sigma_c^2$  are not equal to the sampling variances used in the discontinuous flight trace model. Moreover, the stochastic errors  $\epsilon_i$  applied to the displacement acceleration will give different and more meaningful results.

In Appendix N, procedures are derived for calculating a sequence of values for  $\sigma_c^2$ ; noted as  $\sigma_{ci}^2$ ,  $i = 1, 2, \dots, n$ .  $\sigma_{ci}^2$  is defined to be the variance of  $\epsilon_i$ . These values are to be calculated so that the variance of missile displacements is equivalent to the results calculated from design studies or simulated missile flights. These design studies and simulated missile flights are assumed to be based on a fixed tracker line of sight and no constant flight bias; i. e.,  $C = 0$ . Input values of  $\sigma_{ci}^2$  should be calculated so that the variance of missile impact points simulated in DYNCOM when  $C = 0$  and the tracker line of sight is fixed are equivalent to the variance of missile displacements estimated from design studies for each value of flight range. For a simulated firing event in DYNCOM, random acceleration errors are represented by sampling at periodic intervals during the flight. The recursive use of equations L.4 and L.5 makes the missile position at a given point in time a function of previously sampled errors. See Appendix N for the procedure to calculate values of  $\sigma_{ci}^2$ .

#### Restricted Missile Field of View (FOV)

Signals emanate from the beam-rider missile to the launch point providing tracking data to the control system. The possibility exists that, due to a restricted field of view, this signal may not reach the launch point because the orientation of the missile places the launch point outside this field of view. In the past the missile has been assumed to remain parallel to the ground during all parts of the flight, as shown in Figure 6.6.

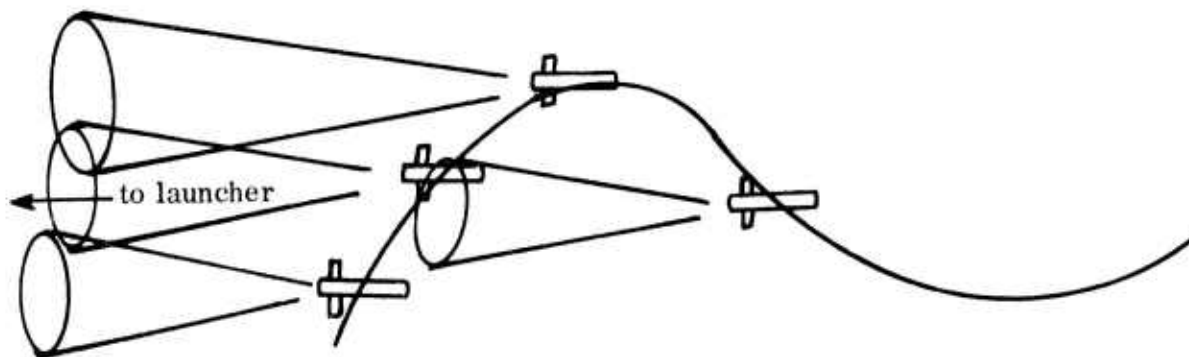


Figure 6.6. -- Former Flight Path Representation with Cones Representing FOV Limitations Emanating to Launcher

As seen in Figure 6.6, cones representing the limitation placed on the field of view will contain the launcher position in all but the most extreme cases. If the assumption is made that the missile body axis coincides with the flight path, a more realistic representation of the field of view limitation results as shown in Figure 6.7.

As shown in Figure 6.7, missile guidance pulses will be missed if the launch point is not included in the cone generated by the field of view. Discussed below is a method for determining whether the launch point is included in the FOV.

#### Field of View Calculations

Let

$P_1 = (X_m, Y_m, Z_m)$  = battlefield coordinates of missile at time  $t$

$P_2 = (X_L, Y_L, Z_L)$  = battlefield coordinates of launcher at time  $t$

and

$D$  = distance between launcher and missile at time  $t$

$$= \sqrt{(X_m - X_L)^2 + (Y_m - Y_L)^2 + (Z_m - Z_L)^2}$$

Using the missile position as reference, the direction cosines of a line joining  $P_1$  and  $P_2$  are shown in Figure 6.8.

The direction cosines are calculated by

$$\begin{aligned} l_c &= \cos \alpha_c = \frac{X_L - X_m}{D} , \\ m_c &= \cos \beta_c = \frac{Y_L - Y_m}{D} , \text{ and} \\ n_c &= \cos \gamma_c = \frac{Z_L - Z_m}{D} . \end{aligned} \tag{6.4}$$

Next, to calculate the direction cosines of the missile heading, the following variables will be used:

$\Delta t$  = interpulse time,

$\dot{x}$  = forward velocity of missile at time  $(t - \Delta t)$ ,

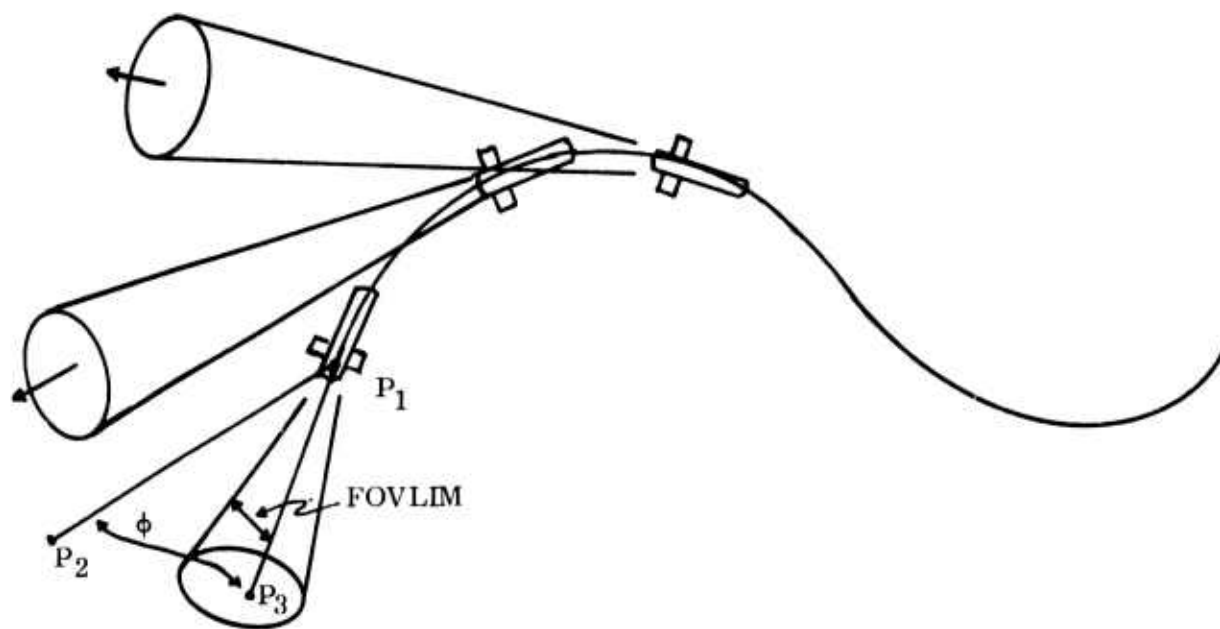


Figure 6.7. --Missile Body Axis Coinciding with Flight Path

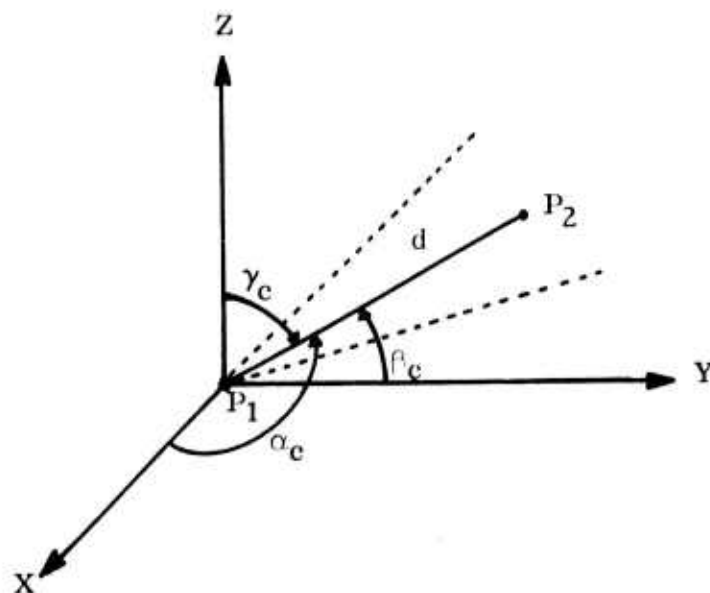


Figure 6.8. --Direction Cosines of Missile-Launcher Vector

$\dot{y}$  = lateral velocity of missile at time  $(t - \Delta t)$ , and

$\dot{z}$  = vertical velocity of missile at time  $(t - \Delta t)$ .

Assuming a constant missile velocity vector during the time interval of length  $\Delta t$ , the distance moved in time  $\Delta t$  is given by

$\dot{x}\Delta t$  = forward direction moved since time  $(t - \Delta t)$ ,

$\dot{y}\Delta t$  = lateral direction moved since time  $(t - \Delta t)$ ,

$\dot{z}\Delta t$  = vertical direction moved since time  $(t - \Delta t)$ ,

and

$$d = \Delta t \sqrt{\dot{x}^2 + \dot{y}^2 + \dot{z}^2}.$$

The direction cosines for the vector of missile heading are given by

$$\begin{aligned} l_m = \cos \alpha_m &= \frac{\dot{x}\Delta t}{d} = \frac{\dot{x}}{\sqrt{\dot{x}^2 + \dot{y}^2 + \dot{z}^2}} \\ m_m = \cos \beta_m &= \frac{\dot{y}\Delta t}{d} = \frac{\dot{y}}{\sqrt{\dot{x}^2 + \dot{y}^2 + \dot{z}^2}} \\ n_m = \cos \gamma_m &= \frac{\dot{z}\Delta t}{d} = \frac{\dot{z}}{\sqrt{\dot{x}^2 + \dot{y}^2 + \dot{z}^2}} \end{aligned} \quad (6.5)$$

In three dimensions, the vector of missile heading is the center line of a cone projecting from the rear of the missile, representing the FOV. Given the half-angle of this field of view, FOVLIM, shown in Figure 6.7, this missile heading vector intersects a plane perpendicular to the heading vector and containing the launcher position. This intersection between the cone and plane forms a circle common to both the plane and cone. The center of this circle is designated as  $P_3$  in Figure 6.7. If the launcher is within this circle, the launcher is within the missile field of view; otherwise, the launcher is outside the missile field of view.

Another equivalent test for determining whether the launcher is within the missile field of view is to compute the size of the angle  $\phi$  shown in Figure 6.9.

If  $\phi$  is larger than FOVLIM, then the launcher is outside the missile field of view. The direction cosines of  $P_1P_2$  and  $P_1P_3$  in Figure 6.9 are given by equations 6.4 and 6.5, respectively. Given these direction cosines, the cosine of the angle  $\phi$  in Figure 6.9 is given by

$$\cos \phi = l_c l_m + m_c m_m + n_c n_m,$$

and  $\phi$  is given by

$$\phi = \cos^{-1} (l_c l_m + m_c m_m + n_c n_m).$$

Thus, the appropriate test whether a pulse was missed in  $(t - \Delta t, t)$  is to determine if  $\phi > \text{FOVLIM}$ . If this is the case, the pulse was missed. The preceding computational procedure has been added to the computational procedure of subroutine SHILLY, the beam-rider missile model, and a flow chart of SHILLY with this FOV restriction appears in Volume 4B. See page F-897 for a flow chart of the FOV computations.

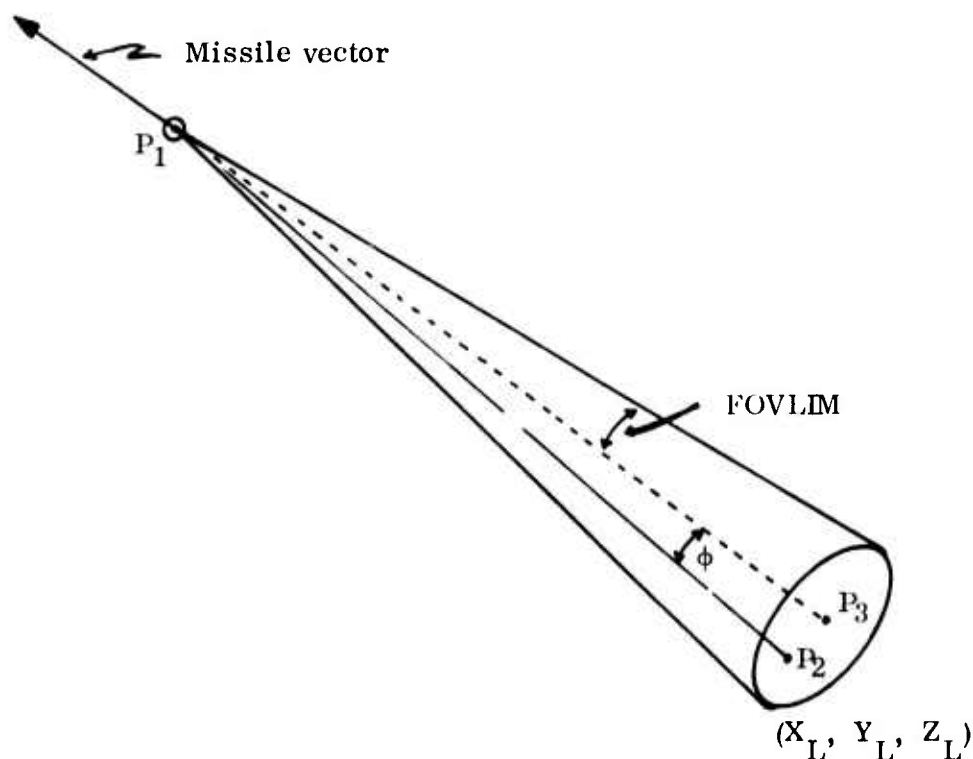


Figure 6.9. --Illustration of FOVLIM

### Human Tracker Model

The human tracking component of the existing DYNCOM missile modules has been simulated by a second order control mechanism (see Chapter 8 of Volume 1 and Chapter 3 of Volume 5), but the use of this second order model has not been supported by analysis of available human tracking results. In this section, the human tracking phenomenon is discussed, available tracking results reviewed, and recommendations are made regarding simulation of the human tracker in the DYNCOM simulation.

#### Compensatory and Pursuit Tracking

There are basically two types of tracking tasks--compensatory and pursuit tracking, as described by McCormick (1). Compensatory tracking is performed on a display with two indications. One is the target and the other is the controlled element (cross hairs), whose position on the display can be changed by the manipulation of some control. The target indication is fixed, and the cross hairs are mobile. The system is considered "on track" when the two indications are superimposed. Any deviation or superposition represents an error, so the goal of the human controller is to minimize error during his function as a tracker by manipulating his controls. In pursuit tracking, both indications are mobile. Therefore, the goal of the tracker is to superimpose the two indications (cross hairs and target) while they are moving. Manipulation of the control mechanism should superimpose the controlled element on the target and keep it there, even though the target is moving. Compensatory and pursuit tracking displays are illustrated in Figure 6.10. Note that the control in the compensatory display is fixed at the center of the display.

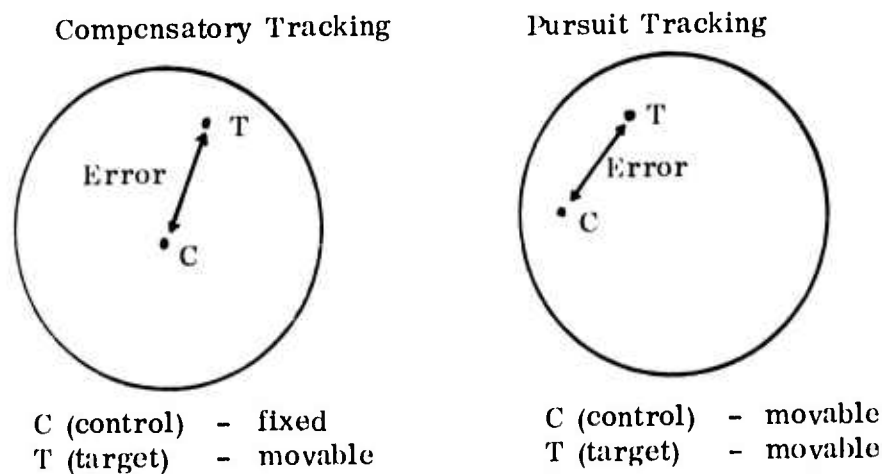


Figure 6.10. --Compensatory and Pursuit Tracking<sup>1</sup>

<sup>1</sup>Adapted from reference 1.

Pursuit tracking is employed in gun-sight tracking of stationary and moving targets and by the beam-rider missiles represented by the model presented in this chapter since the target and tracking elements are both mobile. In pursuit tracking the display contains information regarding the difference in relative positions of the two elements, not an absolute error as in a compensatory tracking display. The tracking task requires that the operator keep the cross hairs of the gun-sight optics trained on the target (either stationary or moving) until the completion of missile flight. To accomplish this, appropriate control in the form of continuous corrections to cross hair position must be performed so that the cross hairs remain superimposed on the aim point. For the beam-rider missile this requires adjustment of the gun tube position using hand controls (Chapter 8 of Volume 1), while for the DRAGON missile the entire round (launch tube and tracker, shoulder mounted) is moved by changing body position (Chapter 3 of Volume 5). Simulation of the pursuit tracking task performed by human operator of a target tracking control mechanism is discussed in the following section.

#### Model of Pursuit Tracking

A general model of the pursuit tracking system is given in Figure 6.11. In systems such as shown in Figure 6.11, a difference exists between desired

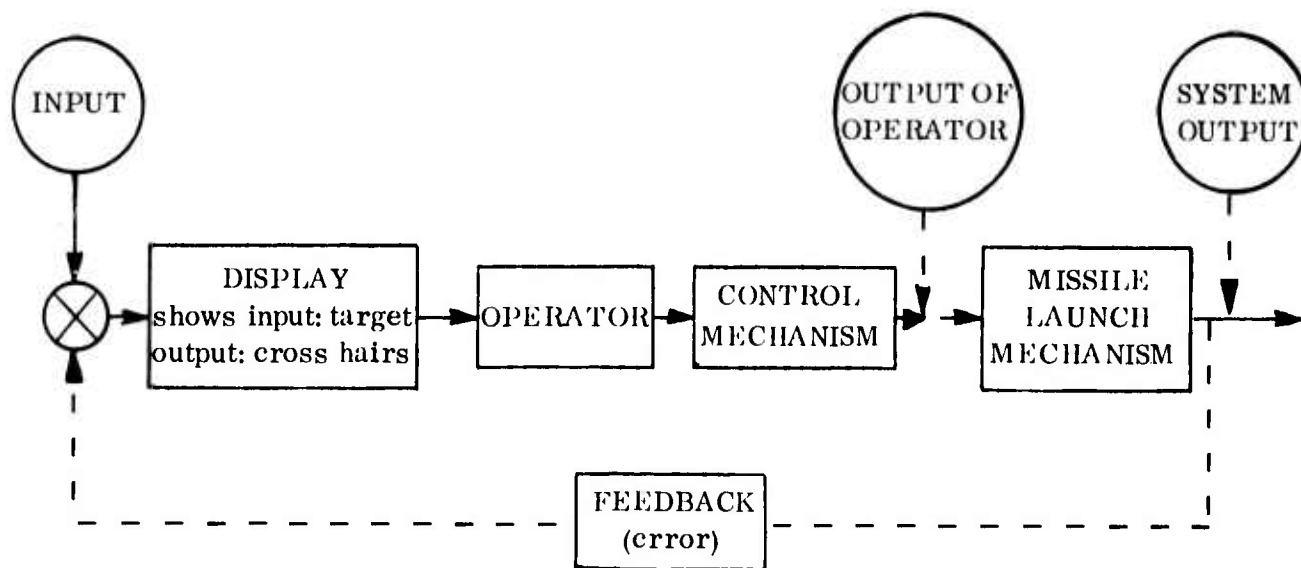


Figure 6.11. --General Model of Pursuit Tracking System<sup>1</sup>

<sup>1</sup>Adapted from reference 1.

output (cross hairs on the aim point) and actual output (actual cross hair position relative to the aim point). This difference or error should be recognized and continuous corrections applied. Regarding the sources of this error, McCormick (in reference 1) states that:

Error is the consequence of a number of contributing factors, relating both to the desired output and to the . . . system involved. If the desired output, for example, is a moving target, its path is characterized by direction (including change of direction), velocity (speed), and acceleration. The output of the system being used, in turn, is the consequence of such variables as its own movement (if it is moving), its own physical dynamics (influenced by its mass, resonant frequency, etc.), and its display and control characteristics, as well as by the performance of the operator. The control device itself has its own dynamics, influenced by its mass, its viscosity (friction that is proportional to speed), its elasticity, and its coulomb friction (friction that is independent of speed).

#### The Human as a Servomechanism

The human component of an engineering system is often characterized as a servomechanism. A closed loop servomechanism is an electromechanical system with components which operate to minimize or eliminate errors between input and output. Emphasizing thus, Craik (in reference 2) makes four basic points describing the human as a component in an engineering system:

1. The human operator behaves as an intermittent correction servo.
2. The corrections are of a ballistic nature.
3. Counteracting processes make corrections appear continuous.
4. Electrical models could fairly exactly simulate the human behavior in tracking.

The term "servo" is important because it links the human with the electromechanical system. The term "servo" is defined by Forster and Ludbrook in reference 4 as "the general type of error actuated, power amplifying, control system in which both input quality and load are subject to random disturbances." In the general pursuit tracking task, characteristics of the human as an electromechanical system bear special mention.

Humans performing a tracking task exhibit a reaction time delay or "intermittent servo response" (reference 2). Craik, explaining the phenomenon, notes that in a servo a follow-up motor is actuated which will run until the misalignment



becomes zero, at which time the input to the motor becomes zero and the motor stops. In the human, at an instant--about 0.3 seconds after the last corrective movement--another movement is initiated which lasts about 0.2 seconds. Mayne in reference 5 notes that this two-part response is characterized by

1. a dead period immediately following the input, and
2. a dynamic portion representing the actual delayed motion of the hand in response to the input.

This phenomenon is illustrated for a simple tracking task in Figure 6.12. In this figure the subject is required to track a moving line which is subjected to a step function at an unknown time zero bringing it to another level. As can be seen from the figure two distinct action periods call the "response" and "reaction" times exist, the total of which are approximately 0.5 seconds. However, simple reaction time such as that illustrated in Figure 6.12 cannot be considered a fundamental component of all responses, since humans can adapt to a tracking task. Craik in reference 3 describes this phenomenon as follows:

The total response time is 0.5 seconds. If the response were, in fact, an intermittent servo response, then a continuous misalignment should produce a response pattern with a periodicity of 0.5 seconds. However, it can be shown that (playing a musical instrument is a good example) complicated patterns of movement can be executed at a rate which would be impossible if they were the resultant of a continuous misalignment--with the time lag. Apparently, they must be individually performed, triggered ballistically, and the sensory feedback must take the form of a delayed modification of the amplitude of subsequent movements. In short, the "internal gear ratio" is altered by the sensory control.

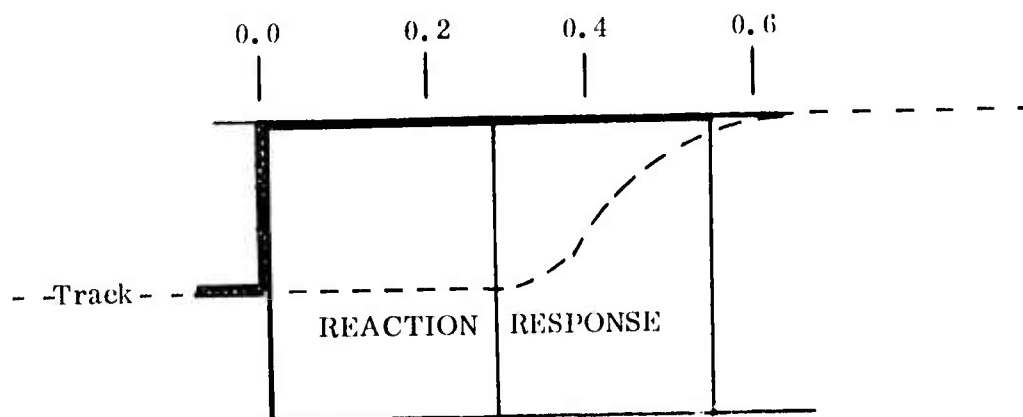


Figure 6.12. --Simple Tracking Task with Illustration of Response and Reaction Periods

Mayne (in reference 5) observes the same type of response mechanism but refers to it in terms of preset or autopilot type of response:

Complex body activity involves a system of many closed loops. Some of the loops have external components such as the eyes, others are totally within the body.

In an autopilot operation, a navigator computes a course, sets the course in the autopilot, and then puts the aircraft on a closed loop control system. Instruments report deviations between preset altitude and direction, and the servo-response will endeavor to reduce the deviation to zero. Changes in conditions may cause the navigator to change the preset course, and the aircraft will then respond to the new program. This will free the navigator from the routine tasks and permit him to perform higher functions. The eyes operate in a manner similar to the navigator. They intervene only at discrete intervals to interrupt the closed-loop controls of the body, but if called upon may operate continuously--as in the case of the navigator--information gathered at discrete intervals by the eyes may be used to alter the internal program (which in this case is a closed-loop control which carries out a habituated motion). An internal space reference is as necessary for humans as the gyroscope is for the aircraft.

Components of engineering systems can be characterized in terms of transfer functions. A transfer function is defined as the ratio of output of a system to its input. Description of the transfer function for humans usually relates a sensual input (visual) to a physical response. Intervening processes such as accuracy, reaction time, perception, sensation are contained in the transfer function of the human. McCormick (in reference 1) suggests that there is no single transfer function for the human being, rather there may be a transfer function for each "class of input-output combinations." Transfer functions for several input-output combinations in typical tracking tasks are given by Fogel in Section 9.3 of reference 6. Kelley (in reference 7), who prefers to call the transfer function the "describing function," lists several others. The transfer function for the human in a gunnery type task is discussed below.

#### Transfer Function Model

Tustin (reference 8) suggests that the human is a nonlinear control system element, and can be represented by two terms, namely a linear transfer function and a "remnant" term. The remnant includes those aspects of control which are nonlinear and some which are random and, therefore, to some degree unpredictable. Fogel (reference 6) characterizes the remnant term as "... noise generated by the man as an input to the controlled system." The nature of the linear transfer function and the remnant term very depending on the input signal and

the nature of the control mechanics. A summary of studies which attempt to isolate the remnant term is given by Fogel in reference 6 for the compensatory tracking task.

The linear portion of the human tracker transfer function widely quoted in the literature is represented by Kelley with the following Laplace expression taken from reference 7:

$$H(s) = \frac{G e^{-\tau s} (1 + T_L s)}{(1 + T_N s) (1 + T_I s)} \quad (6.6)$$

where

$H(s)$  = ratio of the Laplace transform of operator output to that of the input

$G$  = operator gain

$\tau$  = reaction time delay

$T_L$  = lead time constant

$T_N$  = lag constant (neuromuscular)

$T_I$  = lag constant (compensatory)

$s$  = the Laplace operator

The function of the Laplace operator given in equation 6.6 represents the following expression in the time domain, where  $\theta_o$  and  $\theta_i$  are the human trackers output and input, respectively (reference 7):

$$\begin{aligned} \theta_o(t) + (T_N + T_I) \frac{d\theta_o(t)}{dt} + T_N T_I \frac{d^2\theta_o(t)}{dt^2} \\ = G \left[ \theta_i(t - \tau) + T_L \left( \frac{d\theta_i(t - \tau)}{dt} \right) \right] \end{aligned} \quad (6.7)$$

From equation 6.7, the weighted sum of the human tracker's output, output velocity and output acceleration is proportional to a weighted sum of the input plus its rate of change delayed by  $\tau$  seconds. The reader is referred to reference 7 for a complete discussion of the terms  $\tau$ ,  $K$ ,  $T_L$ ,  $T_N$ , and  $T_I$  in the tracker model.

Ornstein (reference 7) assumed a similar standard linear transfer function for the operator in the tracking task (neglecting the remnant terms). The transfer function investigated by Ornstein for the compensatory tracking task is:

$$H(s) = \frac{G e^{-\tau s} (1 + Ws)}{Xs^2 + Vs + Z} \quad (6.8)$$

From equation 6.7,

$$X = T_N T_I,$$

$$Y = T_N + T_P$$

$$W = T_L,$$

$$Z = 1,$$

and  $\tau$  is assumed to be 0.20 seconds. Ornstein used a computer linkup to automatically calculate values of  $X$ ,  $Y$ ,  $W$ , and  $Z$  for operators performing the tracking task. This technique, using rather specialized and complex equipment, was shown to yield reliable and sensitive parameter estimates. Because estimates of the parameters in equation 6.8 require complex equipment and a series of experiments with the tracking equipment and displays used in the missile systems modeled in DYNCOM, an alternate method of estimating the parameters of equation 6.8 is necessary. These parameters must be estimable from existing a priori examples of human tracking data. A simplification of equation 6.8 which permits the use of the estimation procedure presented in Chapter 8 of Volume 1 and discussed in Appendix M is described below.

#### DYNCOM Human Tracker Model

In equation 6.8, dividing the numerator and denominator by  $X$ , the human transfer function becomes:

$$H(s) = \frac{G e^{-\tau s} \left( \frac{1}{X} + \frac{W}{X} s \right)}{s^2 + \frac{Y}{X} s + \frac{1}{X}} \quad (6.9)$$

If the operator gain,  $G$ , is 1, the delay (response) time,  $\tau$ , is zero and  $W = Y$ , equation 6.9 reduces to the transfer function of the simple second order control model presented in Chapter 8 of Volume 1.

$$H(s) = \frac{\beta s + K}{s^2 + \beta s + K} \quad (6.10)$$

Moreover, a normally distributed random error and a constant flight bias can be introduced to the model giving the block diagram shown in Figure 6.3 and a transfer function identical to the continuous flight trace missile model derived in Appendix L. Further research is indicated to investigate the validity of the simplification given in equation 6.10.

A method for estimating system constants  $\beta$ ,  $\omega = \sqrt{4K - \beta^2}$ , and the constant flight bias  $C$  from missile flight data is discussed in Appendix M and on pages 6-10 through 6-12. This same procedure can be used to estimate tracker parameters by using the tracker line-of-sight angular displacement as  $h(t)$  and the true gunner-target line as  $l(t)$ . Estimates of these parameters have shown the significance of the tracker constant flight bias,  $C$ , and have produced seemingly reliable simulated tracker performance.

### Summary and Conclusions

A transfer function model of the human tracker was presented in this section (equation 6.8). However, to estimate parameters of this model, complex equipment must be linked to the operator of the tracking mechanism, while he is performing the tracking task. So that the tracking task can be simulated at the present time in DYNCOM, parameters of the tracker model had to be estimable from a priori recordings of human tracker data. Assumptions about the values of parameters in equation 6.8 were made so that these recordings could be used for estimation. The simplified human tracker model is given by equation 6.10 and by equation 6.3 with  $h(t)$  being the tracker line-of-sight angular displacement and  $l(t)$  being the direction of the true gunner target line. Estimates of the parameters of this model using the method identified in Appendix M are currently being used in the DYNCOM beam-rider missile module.

In conclusion, additional research seems appropriate. Two approaches are meaningful:

1. Investigate the physical significance of the assumptions used to simplify equation 6.8 to indicate the current model's validity.
2. Repeat the estimation procedures employed by Ornstein for the DYNCOM missile systems for more appropriate values of the tracking system parameters.

Both alternatives involve a great amount of effort. The first is an open ended effort since the systems involved (the human being linked with the control

mechanism) are very complex and difficult to describe intuitively. The second requires the acquisition of a significant amount of equipment and an experimental effort beyond the scope of this project. Also it is questionable if such precision is necessary. It is concluded that since the simplified model is consistently producing reasonable results, that further research does not seem to justify the expenditure required.

#### REFERENCES

1. McCormick, Ernest J. Human Factors Engineering, Third Edition, McGraw-Hill Book Company; New York, 1966.
2. Craik, K. J. W., "Theory of the Human Operator in Control Systems I." British Journal of Psychology, Vol. XXXVIII, December 1947.
3. Craik, K. J. W., "Theory of the Human Operator in Control Systems II." British Journal of Psychology, Vol. XXXVIII, March 1948.
4. Forster and Lubdbrook, "Some Industrial Electronic Servo and Regulator Systems," IEE Journal, Proceedings, Vol. 194, Part IIa, 1947, p. 100.
5. Mayne, R., "Some Engineering Aspects of the Mechanism of Body Control," Electrical Engineering, March 1951.
6. Fogel, Lawrence J., Biotechnology: Concepts and Applications, Englewood Cliffs, N. J.: Prentice Hall, 1963.
7. Kelley, Charles R., Manual and Automatic Control, New York: John Wiley & Sons, Inc., 1968.
8. Tustin, A., "The Nature of the Operator Response in Manual Control, and its Implication for Controller Design," IEE Journal, Proceedings, Vol. 94, Part IIa, 1947.
9. Ornstein, G. N., Applications of a Technique for the Automatic Analog Determination of a Human Response Equation Parameters, Columbus, Ohio: North American Aviation Report NAG1H-1, January 1961.

CHAPTER 7  
ELECTRONIC COUNTERMEASURES

Unclassified Summary  
by  
G. M. Clark

DYNCOM has been developed for the purpose of providing a method for evaluating missile system concepts in a simulated combat environment. Several hard-point target missile systems have been represented in DYNCOM; moreover, methodology has been introduced for representing actual flight paths of these missiles and the interaction of their flight paths with the terrain surface and with the combat activities of target and tracking weapons.

The purpose of research described in Chapter 4 of Volume 5 has been to develop methodology for describing those electronic countermeasures (ECM) which are considered most likely to be employed against missile systems currently represented in DYNCOM. The methodology developed can be used to predict the effects of these ECM devices upon the operational effectiveness of each missile system represented.

## CHAPTER 8

### NIGHT DETECTION MODEL

by

R. M. Lawson

In a land combat situation, the performance of a combat unit is affected by weapon system design, tactical doctrine, and battlefield environment. The capability of a combat element to detect an enemy target in a limited visibility environment may differ substantially from that of a clear, daytime environment. Since desirable weapon performance characteristics interact strongly with target acquisition capabilities, a requirement exists for considering target detection capabilities under conditions of limited visibility when planning the development of new weapons and tactical doctrine.

In this chapter, a methodology is presented for predicting the time required by an observer to detect military targets under conditions of night illumination and reduced visibility associated with haze, fog, and other weather conditions.

In reference [6], models were presented for predicting the distributions of time required for observers to detect military targets under daylight illumination conditions and various meteorological conditions.

In addition to the target, terrain, and environmental variables discussed previously in reference [6], the observer's eye adaption luminance level is of significant importance for night illumination levels. Reduced visibility conditions affect the detectability of a target due to the fact that the target's apparent contrast with its background is reduced.

Theoretical relationships between contrast and the detection rate are presented in the following section. For each detection mode (i.e., ground-to-ground, ground-to-air, and air-to-ground) under night illumination levels, the detection probability can be expressed as a function of the following variables:

1. the elapsed search time,
2. the meteorological visibility range,
3. the luminance contrast of the target with its background,



4. the observer's eye adaption luminance level,
5. the cross-sectional area of the target,
6. the range to the target, and
7. a measure of the complexity of the scene.

#### Contrast Threshold and Detection Rate

The inherent target-to-background brightness contrast,  $C$ ; is defined as

$$C' = \frac{B_o' - B_b'}{B_b'} \quad (8.1)$$

where:

- $B_o'$  = luminance (measured at near zero distance) of the target object, and
- $B_b'$  = luminance (measured at near zero distance) of the background of the target.

As the range between the observer and the target increases, the effect of the intervening atmosphere is to reduce (or attenuate) the apparent target-to-background brightness contrast from its value at near zero range. The following two phenomena determine the extent of the contrast attenuation for a target at a given range (reference [7]):

1. Some of the light emanating from the distant target and the background is removed from the line of sight by absorption and scattering due to water vapor, dust, and other matter in the atmosphere.
2. Some light is added along the line of sight due to the scattering effect.

As the range between the observer and the target increases, the target and its background will appear more and more to have the same luminance. Therefore, the apparent contrast of the target with its background will approach zero. The attenuation effect of the intervening atmosphere upon  $C$ , the apparent target-to-background brightness contrast, is described by Koschmieder's Law in reference [7];

$$C = C' \{ e^{-\delta R} \} \quad (8.2)$$

where:

$C$  = the apparent target-to-background brightness contrast at range  $R$  in the particular atmosphere (dimensionless ratio),

$C'$  = the inherent (or intrinsic) target-to-background brightness contrast at near zero range (dimensionless ratio),

$\delta$  = the attenuation coefficient of the atmosphere for the prevailing conditions (units of per length), and

$R$  = the distance between the observer and the target (length).

The effect of atmospheric attenuation on contrast is seldom expressed in terms of  $\delta$ , the attenuation coefficient (reference [6]). Instead, a measure referred to as the meteorological visibility range,  $V$ , is used. The meteorological visibility range,  $V$ , is related to the attenuation coefficient,  $\delta$ , as follows:<sup>1</sup>

$$V = \frac{3.912}{\delta} . \quad (8.3)$$

As noted previously, the detectability of a target is a function of the apparent cross-sectional area of the target and the range to the target. Another investigator, reference [18], has shown that the effect of these two variables can be accurately described in terms of the angle,  $\alpha$ , subtended at the observer's eye by the diameter of a circle having area,  $A$ , equal to the apparent cross-sectional area of the target. The relationship between the range,  $R$ , target cross-sectional area,  $A$ , and  $\alpha$  is as follows:

$$\alpha = \frac{3879.8}{R} \sqrt{A} \quad (8.4)$$

---

<sup>1</sup>The meteorological range,  $V$ , is defined as the horizontal distance through the atmosphere for which the transmittance of the atmosphere is two percent; that is,  $V$  equals the value of  $R$  in equation 2 for which  $C/C'$  is 0.02. Ranges of values of the meteorological range for several atmospheric conditions are given in reference [6].

where  $\alpha$  is measured in minutes of arc and both A and R are of like units of measurement.

The basic detection-time model to be employed for night illumination levels, which has been previously discussed in reference [6], is as follows:

$$P(t_{j-1}, t_j) = 1 - \exp \{ -\mu \cdot g_j \cdot (t_j - t_{j-1}) \} \quad (8.5)$$

where  $P(t_{j-1}, t_j)$  is the conditional probability of detecting the target during the time interval  $(t_{j-1}, t_j)$  (i.e., during the  $j^{\text{th}}$  event) given no detection prior to time  $t_{j-1}$ , and where:

$\mu$  = the fixation rate, which is approximately equal to three per second (reference [17]), and

$g_j$  = the single-fixation detection probability during the  $J^{\text{th}}$  simulation event.

The single-fixation detection probability,  $g$ ,<sup>1</sup> is a function of the target and background parameters C,  $\alpha$ , and  $B_b'$ ; as well as  $\beta$ , the angle between the observer's direction of fixation and the direction of a line-of-sight vector to the target, with  $\beta$  being a random variable. The single-fixation detection probability for a given value of the random variable,  $\beta$ , is denoted by  $g(C, \alpha, B_b' | \beta)$ .<sup>2</sup>

Reference [3] presents data and theoretical arguments to support the claim that the single-fixation detection probability for a given value of  $\beta$ ,  $g(C, \alpha, B_b' | \beta)$ , is described by the normal ogive function with parameters C,  $C_{.50}$ ,<sup>3</sup> and  $\sigma$ ; where  $C_{.50}$  and  $\sigma$  are both functions of  $\alpha$ ,  $B_b'$ , and  $\beta$ . That is, the single-fixation detection probability can be predicted by:

---

<sup>1</sup>In the discussion which follows, the subscript j is omitted.

<sup>2</sup>This notation is employed to denote that the symbols to the left of the vertical line represent measurable parameters of the target and its background and the symbol to the right of the vertical line represents a particular value of a random variable.

<sup>3</sup> $C_{.50}$  is typically referred to in the literature as the contrast threshold.

$$g(C, \alpha, B_b' | \beta) = \Phi \left\{ \frac{C - C_{.50}(\alpha, B_b' | \beta)}{\sigma(\alpha, B_b' | \beta)} \right\}^1 \quad (8.6)$$

where:

$$\Phi \{X\} = \frac{1}{\sqrt{2\pi}} \int_{-\infty}^X e^{-1/2 \mu^2} du. \quad (8.7)$$

In equation 8.6,  $C_{.50}(\alpha, B_b' | \beta)$  is the value of the contrast associated with a 50 percent probability of detection for one fixation.

In reference [4], it is shown that the quantity  $\frac{\sigma(\alpha, B_b' | \beta)}{C_{.50}(\alpha, B_b' | \beta)}$  is approximately constant at a level of 0.39 for all conditions investigated; i.e., for all levels of  $\alpha$ ,  $B_b'$ , and  $\beta$ . Consequently, equation 8.6 can be rewritten as:

$$g(C, \alpha, B_b' | \beta) = \Phi \left\{ \frac{\frac{C}{C_{.50}(\alpha, B_b' | \beta)} - 1}{0.39} \right\}. \quad (8.8)$$

Reference [1] reports an extensive study of the effect of target size and range (in terms of the measure  $\alpha$ ) and eye adaption luminance level on the contrast threshold,  $C_{.50}(\alpha, B_b' | \beta = 0^0)$ , for  $\beta = 0^0$ ; the experimental results are shown in Figure 8.1. As shown in Figure 8.1, for daylight eye adaption luminance levels; i.e., for  $B_b' \geq 40$  foot-lamberts, the contrast threshold does not depend upon the angle,  $\alpha$ , subtended by the target at the observer's eye. However, for nighttime eye adaption luminance levels, the contrast threshold is highly dependent upon the magnitude of  $B_b'$ .

In order to predict the contrast threshold,  $C_{.50}(\alpha, B_b' | \beta = 0^0)$ , for the condition  $\beta = 0^0$ , the smooth curves (represented in Figure 8.1) were fitted to the data using a least squares multiple regression program by Parry in reference [16]. These curves have the following form:

---

<sup>1</sup>It should be emphasized that  $C$  is not to be construed as a random variable in equation 8.6. Rather, the function given in equation 8.6 is an empirical fit expressing  $g$  as a function of the parameters  $C$ ,  $C_{.50}$ , and  $\sigma$ .

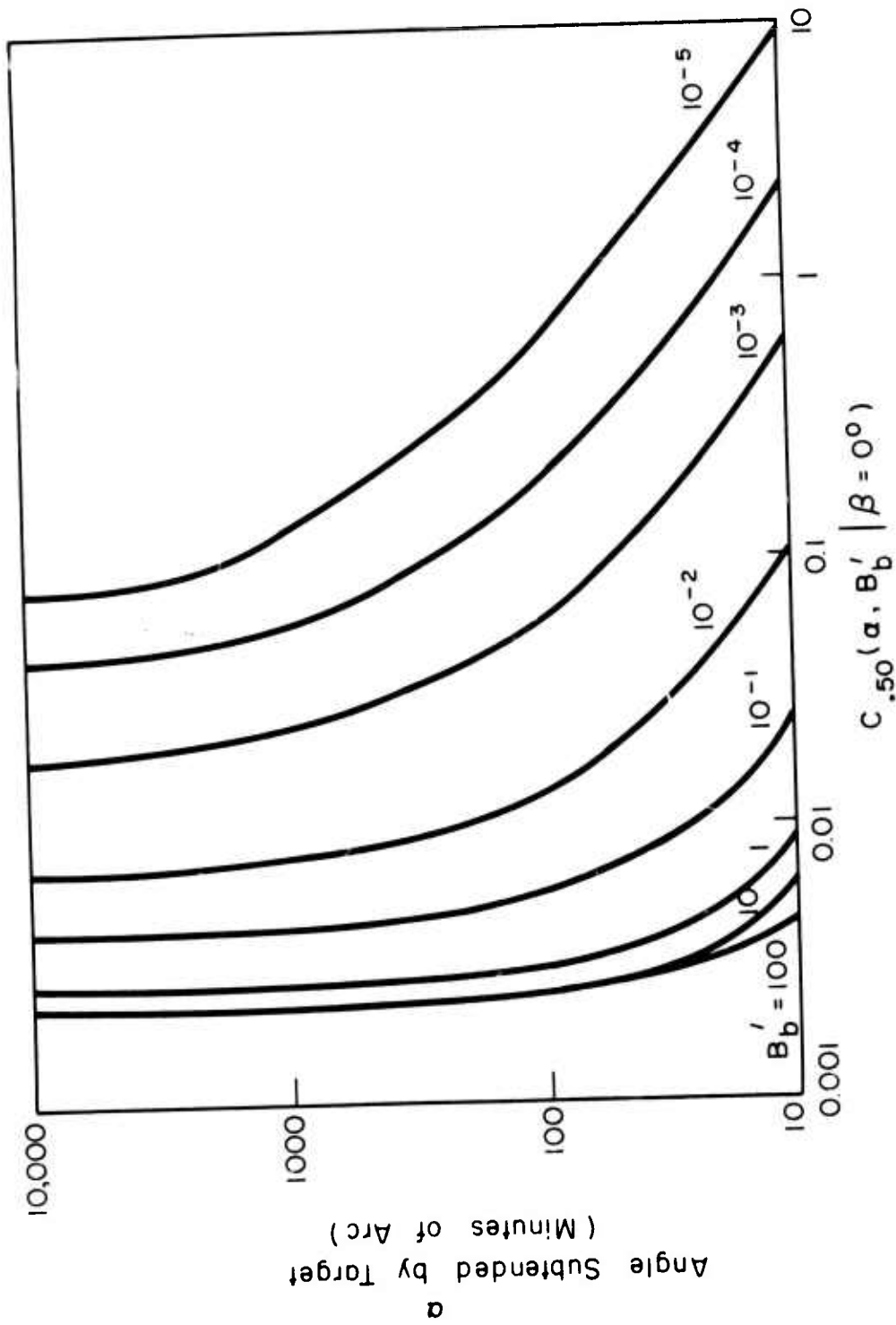


Figure 8.1.1. -- Contrast Threshold as a Function of  $\alpha$  and  $B'_b$  (foot-lamberts) for  $\beta = 0^\circ$

$$\log_{10} \{ C_{.50}(\alpha, B_b' | \beta = 0^0) \} = \sum_{i=0}^4 A_i(B_b') \cdot \{ \log_{10} \alpha \}^i, \quad (8.9)$$

where  $A_i(B_b')$ ,  $i = 0, \dots, 4$ , denotes that for each value of  $B_b'$ , there is a corresponding  $A_i$  coefficient. The various values of  $A_i(B_b')$  for  $B_b' = 10^{-5}, 10^{-4}, \dots, 10^1$  foot-lamberts are tabulated in Table 8.1.

Table 8.1

Values of Regression Coefficients  $A_i(B_b')$ , for Computing  
 $C_{.50}(\alpha, B_b' | \beta = 0^0)$

$B_b'$	$A_0(B_b')$	$A_1(B_b')$	$A_2(B_b')$	$A_3(B_b')$	$A_4(B_b')$
$10^{-5}$	0.62083	-2.8398	1.289900	-0.13208	-0.021927
$10^{-4}$	-0.54717	-2.6520	0.822330	0.15030	-0.074127
$10^{-3}$	-0.40350	-2.4124	0.274350	0.44547	-0.123410
$10^{-2}$	-0.22324	-2.0040	-0.403110	0.77945	-0.177410
$10^{-1}$	0.22523	-2.2196	-0.894170	0.57144	-0.136510
$10^0$	0.86482	-2.2737	-0.078735	0.38690	-0.094006
$10^1$	1.72180	-1.8201	-0.636470	0.63918	-0.120050

Contrast thresholds are normally determined experimentally by oversimplifying the observer's task. That is, subjects in threshold contrast experiments are usually told where and approximately when the target will appear. Several studies have been undertaken to determine the effects of factors such as uncertainty of target location in time and space, and various background properties on the threshold contrast (reference [14]). These

studies have produced a list of "field factors" which relate the contrast threshold, determined for one set of standard conditions measured in a laboratory environment, to nonstandard conditions. Various authors (references [2] and [14]) have suggested using the product of several factors to adjust the laboratory-determined thresholds so that they apply to field conditions. A review of the literature on contrast thresholds indicated that four constants,  $k_i$ ;  $i = 1, 2, 3, 4$ , may be applied to the laboratory-determined thresholds to adjust for actual battlefield conditions. According to these factors, the adjusted threshold,  $C_{.50}(\alpha, B_b' | \beta)$ , is given by:

$$C_{.50}(\alpha, B_b' | \beta) = K \cdot C_{.50}(\alpha, B_b' | \beta) \quad (8.10)$$

where:

$C_{.50}(\alpha, B_b' | \beta)$  = contrast threshold measured under standard laboratory conditions for given values of eye adaption luminance level, target size, etc.

$k_1$  = 1.09; a correction made for lack of knowledge of target size and duration of appearance (reference [2]).

$k_2$  = 1.31; a correction made for uncertain location of target (reference [2]).

$k_3$  = 2.40; a correction made to adjust forced-choice data to yes-no detection data (reference [2]).<sup>1</sup>

$k_4$  = 1.90; a correction made for trained versus naive observers (reference [2]).

$K = \prod_{i=1}^4 k_i = 6.5$ ; the combined field factor for correcting laboratory data-based thresholds to actual field conditions.

In order to apply equation 8.8 to predict detection times, it is necessary to have a representation of the random variable  $\beta$ . Ideally, it would be desirable to have a probability density function (p.d.f.) for  $\beta$ . In the case of an

---

<sup>1</sup>The distinction between these two types of data is discussed in reference [3].

observer searching for a target against a homogeneous background such as the sky, a uniform search distribution has been assumed (reference [15]). However, when searching for targets under night illumination levels, the observer is faced with the task of discriminating the target from many target-like objects such as large rocks, bushes, etc., for ground-to-ground and air-to-ground detection. The number of such discriminations that must be made depends on the density of target-like forms in the background, the size of the area to be searched, and the relative distinctiveness of the target as determined by its location in the scene and its brightness contrast. For example, an extremely bright target might be sensed on the subject's initial scan before he finds it necessary to group stimuli and conduct group-by-group or item-by-item search.<sup>1</sup>

An extensive search of the detection model literature revealed that no one has been successful in relating measures of the density of target-like objects (or confusing) forms in a scene to the observer's distribution of fixation directions in searching that scene. However, Boynton, *et al.* (1958) was able to measure the degradation in the observer's detection performance for various target-to-background brightness contrasts, and various numbers, shapes, and sizes of confusing objects.<sup>2</sup> In these experiments, the target was represented by a polygonal surface of three to twelve sides. The confusing forms or false targets presented with each target were similar in shape and contrast to the real target; their sides being curvilinear rather than linear. The total number of forms presented in the scene was either 16, 64, or 256. The results given in reference [5] include a relationship among the four variables--target-to-background contrast, target size, number of confusing forms, and viewing time for a detection probability of 60%. That is, for the specified conditions and viewing time, the observer percentage of individuals in a group of observers who detected the target was 60%. Using the data of reference [5], an empirical relationship for the detection probability,  $p$ , applicable for all contrasts and target sizes used in the experiment was determined (reference [9]). The sizes and contrasts of the targets in these experiments were such that the probability of detecting the target, given that the observer was fixating upon the target

---

<sup>1</sup>Observers usually conduct search in three phases: first, by quickly scanning the area to find readily evident targets, second, by searching groups of forms which appear to belong together, and third, by conducting an item-by-item search within these groups of stimuli (reference [11]).

<sup>2</sup>The results of the experiments in reference [5] were employed in model development in reference [13].



form, was one.<sup>1</sup> Therefore,  $p$  is taken to be the probability that the observer fixates upon the target form during the time over which search is conducted. The empirical fit given in reference [9] is:

$$p = \frac{1}{1 + \left[ \frac{n}{29(T) \cdot 93} \right]^{1.29}} \quad (8.11)$$

where:

$n$  = the effective number or confusing forms in the scene, and

$T$  = the viewing time (seconds).

The above relationship is shown graphically in Figure 8.2 for three viewing times: 3 seconds, 1 second, and 1/2 second.<sup>2</sup>

If  $T$  is taken to be 1/3 second, equation 8.11 becomes

$$p = \frac{1}{1 + \left[ \frac{n}{10.44} \right]^{1.29}} \quad (8.12)$$

Using the model of reference [9] for predicting the probability that an observer fixates on the target in one fixation as a function of the number of confusing forms,  $n$ , the single-fixation detection probability,  $g$ , can be predicted as follows:

$$g = p \cdot g(C, \alpha, B_b' \mid \beta = 0^0). \quad (8.13)$$

---

<sup>1</sup>Whether this was by design or by chance could not be determined from reference [5]. However, it seems probable that it was by design since the authors were primarily interested in the effect of the number of confusing forms in the scenes upon the detectability of targets and not upon other variables such as size and contrast.

<sup>2</sup>Although the minimum viewing time for the experiment of reference [5] was three seconds, it was assumed in reference [9] that equation 8.11 would hold for a viewing time of 1/2 seconds, the approximate single-fixation time, and later extrapolated the data to 1/3 of a second (reference [10]).

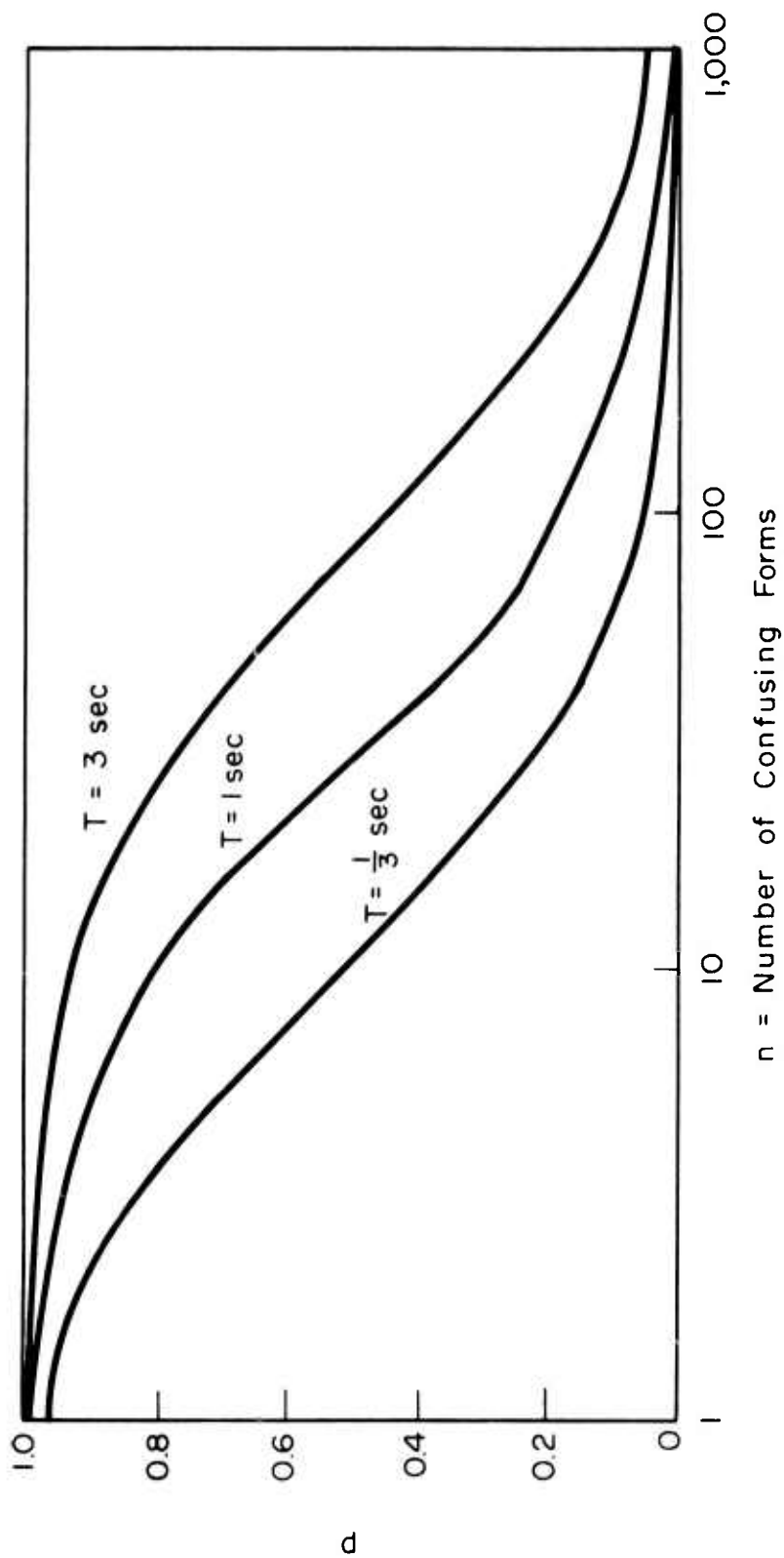


Figure 8.2. --Probability of Fixating on the Target as a Function of the Number of Confusing Forms for Various Search Times

Equation 8.13 follows since  $p$  represents the probability that  $\beta = 0^\circ$  and  $g(C, \alpha, B_b' | \beta = 0^\circ)$  represents the conditional single-fixation detection probability, given  $\beta = 0^\circ$ ; or the probability that the observer is fixating on the target.

In order to predict the probability,  $p$ , of an observer fixating on the target in a given fixation, it is necessary to have an estimate of the effective number of confusing forms,  $n$ , in the scene being searched. A procedure for estimating  $n$  from detection-time data is discussed in the following section.

#### Estimation of the Effective Number of Confusing Forms

It has been shown that for short search time duration (2-3 minutes for ground-to-ground search), the single-fixation detection probability,  $g$ , remains relatively constant (reference [12]). This single-fixation detection probability can be estimated from field detection-time data. The procedure for estimating  $g$  from detection-time data is described in detail in reference [8].<sup>1</sup> The resulting estimate of  $g$  is denoted by  $\hat{g}$ .

Equating  $\hat{g}$  and  $p \cdot g(C, \alpha, B_b' | \beta = 0^\circ)$  we have, from equations 8.8 and 8.13:

$$p = \frac{\hat{g}}{\left\{ \frac{\frac{C}{K \cdot C.50(\alpha, B_b' | \beta = 0^\circ)} - 1}{.390} \right\}} \quad (8.14)$$

where  $K = 6.5$  and  $C.50(\alpha, B_b' | \beta = 0^\circ)$  is estimated using equation 8.9. Substituting equation 8.12 into equation 8.14 and solving explicitly for  $n$ , an estimate of the effective number of confusing forms in the scene, denoted by  $\hat{n}$ , is given by:

$$\hat{n} = 10.44 \left[ \frac{\left\{ \frac{\frac{C}{6.5 C.50(\alpha, B_b' | \beta = 0^\circ)} - 1}{.390} \right\}}{\hat{g}} \right]^{0.775} \quad (8.15)$$

<sup>1</sup>Actually, a procedure for estimating the parameter  $\lambda = 3g$  is described. Thus, in order to predict  $g$  using their method, it is necessary to divide their estimate of  $\lambda$  by 3.

A value of  $\hat{n}$  computed from equation 8.15 should be interpreted as an estimate of the effective number of confusing forms appearing in the scene being searched. An extensive amount of experimentation would be required before  $\hat{n}$  confusing forms could be inferred by counting distinguishable forms in a terrain scene.

Suppose that confusing forms are uniformly distributed over an area so that an observer searching for a target in the area will encounter an average density of  $d$  forms per unit angular measure. That is, an average of  $d$  confusing forms for search sectors of one unit of angular measure would be expected when fixation directions are chosen at random in the scene being searched.<sup>1</sup> Using the concept of density described above, it can be shown that for a randomly chosen observation direction, the probability,  $P(n; \Delta\theta)$ , of finding  $n$  or less confusing forms in a sector of size  $\Delta\theta$  is given by the Poisson distribution function:

$$P(n; \Delta\theta) = \sum_{k=0}^n \frac{e^{-d\Delta\theta} (d\Delta\theta)^k}{k!} . \quad (8.16)$$

Assume that detection-time data have been obtained for observers searching for a specified type of target in a given type of scene under a fixed illumination level. Therefore, knowing the estimate,  $\hat{g}$ , for each target-scene-illumination combination, values of  $\hat{n}_i$ ,  $i = 1, 2, \dots, m$  for each target-scene-illumination combination may be computed using equation 8.15. It is assumed that these values of  $\hat{n}_i$  represent random samples from a Poisson distribution with parameter  $d\Delta\theta$ . Then, the maximum-likelihood estimate,  $\widehat{d\Delta\theta}$ , of  $d\Delta\theta$  is:

$$\widehat{d\Delta\theta} = \frac{\sum_{i=1}^m \hat{n}_i}{m} . \quad (8.17)$$

---

the case of search where the target is known to be located along the horizon, density would be measured in units of per degree. For the case of a two-dimensional search area, a suitable unit be the steradian.

### Applications and Conclusions

The following procedure is recommended for use in DYNCOM for determining  $\hat{g}$  for night illumination levels:

1. Compute  $\alpha$  using the equation

$$\alpha = \frac{3879.8 \sqrt{A}}{R}$$

where both  $\sqrt{A}$  and  $R$  are of like dimensions and  $A$  is the apparent cross-sectional area of the target and  $R$  is the range to the target.

2. Use this value of  $\alpha$  in equation 8.7 with the appropriate value of  $B_b'$  to compute the value of  $C_{.50}(\alpha, B_b' | \beta = 0^\circ)$ .
3. Determine  $g(C, \alpha, B_b' | \beta = 0^\circ)$ , the theoretical single-fixation detection probability for an observer fixating directly upon the target, using the equation

$$= \Phi \left\{ \frac{\frac{C}{K C_{.50}(\alpha, B_b' | \beta = 0)} - 1}{.390} \right\}$$

with  $K = 6.5$  and  $C_{.50}(\alpha, B_b' | \beta = 0^\circ)$  is predicted using equation 8.7.

4. Monte Carlo for a value of  $n$  using equation 8.16 with

$$d = \frac{d\Delta\theta}{\Delta\theta}$$

(for the particular target-scene-illumination combination and the desired value of  $\Delta\theta$ ).

5. Substitute the computed value of  $n$  into equation 8.11 to determine  $p$ , and  $\lambda = \mu p g$ .

The above procedure for determining  $g$  allows the user to select the size of the sector,  $\Delta\theta$ , which may be appropriate. Small sector sizes might be desirable to simulate the effect of prior knowledge of target location on the observer's search pattern. Larger search sectors would be specified when the

observer possessed no specific knowledge of the target's location. For example, in the case which the observer has no knowledge of the target's location (related in DYNCOM by a detection code of zero), for one-dimensional search situation, the appropriate value of  $\Delta\theta$  may be  $360^\circ$ . The values of  $\Delta\theta$  for each of the possible DYNCOM detection codes is input to the simulation for each detection mode (ground-to-ground, ground-to-air, and air-to-ground).

#### REFERENCES

1. Blackwell, H. R., "Contrast Thresholds of the Human Eye," Journal of the Optical Society of America, Vol. 36, November 1946, pp. 624-643.
2. Blackwell, H. R., The Effects of Certain Psychological Variables upon Target Detectability, Engineering Research Institute Report No. 2455-12-F, University of Michigan, June 1958.
3. Blackwell, H. R., "Neural Theories of Simple Visual Discriminations," Journal of the Optical Society of America, Vol. 53, No. 1, January 1963, pp. 129-160.
4. Blackwell, H. R. and McCready, D. W., Jr. Foveal Contrast Thresholds for Various Durations of Single Pulses, Vision Research Laboratories, The Ohio State University, June 1958.
5. Boynton, R. M., Elsworth, C., and Palmer, R. M., Laboratory Studies Pertaining to Visual Air Reconnaissance, WADC Technical Report 55-304, Part III, April 1958.
6. Lawson, R. M., "Air-to-Ground and Ground-to-Air Visual Detection Models," Chapter 13 (in) The Land Combat Model (DYNCOM), edited by A. B. Bishop and G. M. Clark, RF 2376, FR-1 (U), Systems Research Group, The Ohio State University, Columbus, Ohio, June 1969. AD 909540.
7. Middleton, W. E., Vision Through the Atmosphere, University of Toronto Press, Toronto, 1958.
8. Rheinfank, J., and Stollmack, S., "Analysis of Detection Time Data," Chapter 5 (in) The Tank Weapon System, edited by A. Bishop and S. Stollmack, RF 573, AR 68-1 (U), Systems Research Group, The Ohio State University, September 1968. AD 850367.

9. Ryll, E., Aerial Observer Effectiveness and Nap-of-the-Earth, (Project Trace), AD 468570, Cornell Aeronautical Laboratories, Inc., Buffalo, New York, February 1962.
10. Stathacopoulos, A. D., Bivans, E. W., Brennand, J. R., Gilmore, H. F., Jago, W. H., and Rowen, J. W., Surveillance Systems Study (Real-Time Night Reconnaissance/Strike) (U), AD 383920, Defense Research Corporation, Santa Barbara, California, February 1967, (SECRET).
11. Stollmack, S., Analytic Procedures for Determining the Time Required to Detect a Stationary Target, Unpublished Master's Thesis, The Ohio State University, 1965.
12. Stollmack, S., and Brown, P. J., "Detection Time Data Analysis," Chapter 1.3 (in) The Tank Weapon System, edited by D. Howland and G. Clark, RF 573, AR 66-2 (U), Systems Research Group, The Ohio State University, Columbus, Ohio, December 1966. AD 815023.
13. Stollmack, S., and Lawson, R. M., "Contrast Dependent Detection Probability for Stationary Target," Chapter 3 (in) The Tank Weapon System, edited by A. B. Bishop and S. Stollmack, RF 573, AR 68-1 (U), Systems Research Group, The Ohio State University, September 1968. AD 850367.
14. Taylor, J. H., "Use of Visual Performance Data in Visibility Prediction," Applied Optics, Vol. 3, No. 5, May 1964, pp. 562-568.
15. Lawson, R. M., The Distribution of Time Required by Ground-Based Observers to Detect Aerial Targets Against Sky Backgrounds, Unpublished Master's Thesis, The Ohio State University, 1969.
16. Parry, S. "Limited Visibility Environment," Chapter 7 (in) The Land Combat Model (DYNCOM), edited by A. B. Bishop and G. M. Clark, RF 2376 FR-1 (U), Systems Research Group, The Ohio State University, Columbus, Ohio, June 1969. AD 909540
17. White, C. T., and Ford, A., "Ocular Activity in Visual Search," (in) Visual Search Techniques, edited by A. Morris and E. Horne, Publication 712, Armed Forces - NRC Committee on Vision, Washington, D. C., 1960, pp. 124-132.
18. Linge, A., Detection from Aircraft, Report No. ERR-50-150, AD 270630, General Dynamics/Convair, San Diego, California, December 1961.

## CHAPTER 9

### WEAPON SIGNATURE (PINPOINT) MODEL

by

R. M. Lawson

#### Introduction

In combat, crew-served weapon systems (such as the LAW, MAW, TOW, DRAGON, BAT rifle, towed gun, etc.) are typically concealed or camouflaged prior to the initiation of firing against an enemy target (such as an armored tank, APC, or helicopter). For this reason, crew-served weapons will normally be visually acquired only after their firing signatures (flash, smoke, dust, audible report, vapor trail, etc.) have been detected.

Another researcher in the field of target signature detection analysis, in reference [1], has made the statement that

Both experience and Monte-Carlo gaming techniques have indicated that in combat, target acquisition probabilities most probably play a more important role in determining survival probabilities than do hit probabilities, as measured against clearly visible targets.

Thus, it seems reasonable to assume that the ability of observers to acquire concealed or camouflaged crew-served weapon systems on the basis of their firing signatures would be a major consideration in the design and selection of such weapons.

This could mean, for example, that in designing a weapon for "maximum combat effectiveness" (subject to usual constraints on time, material, money, etc.) it would possibly be more profitable to seek methods of reducing the chances of being detected as a target than it would be to seek increases in the accuracy of firing.

The process of laying the sights of a weapon on the point in the terrain from which it is thought that the firing signature of the target emanated has been referred to as "pinpointing" by other investigators, e.g., in reference [4]. The term "pinpointing" was coined in a report, reference [4], of an Operations Research Office (ORO) field experiment. In the ORO experiment, a subject was said to have pinpointed a target if his lay error was within some specified limits. The limits were chosen so that they would (arbitrarily)



include 80% of the data. It seems that it would be more appropriate to define these limits on the lay error in terms of the resulting hit probabilities since such a definition would be a more objective criteria for the pinpoint phenomena.

In this paper, the term pinpoint is defined to be the process of laying the sights on the firing signature of the concealed or camouflaged crew-served weapon system such that the hit probability for the weapon employed is within some specified limits.

The purpose of the research reported in this paper is to develop a model for predicting the probability distribution of detection time and assessing the subsequent accuracy of laying weapon sights upon the firing signatures of concealed or camouflaged crew-served weapons. In addition, an outline of experimental-design procedures for estimating the parameters of the model are presented. In order to establish a basis for such a model, a literature search was conducted to investigate currently existing methodology and models.

One important aspect of the combat effectiveness of a crew-served weapon is its susceptibility to enemy fire. Since in this discussion it is assumed that the enemy weapon system being sought is completely concealed from all potential observers, the susceptibility of the weapon being sought is due entirely to its firing signature (flash, dust, smoke, audible report, etc.). Obviously, as the component of the firing signature of the weapon increase in intensity and duration, the likelihood of an observer detecting and bringing effective fire upon its position increases.

An important measure of the performance of any weapon system usable against crew-served weapon systems is its ability to acquire and bring about effective fire against concealed crew-served weapons. Evaluation of the effectiveness of weapon systems such as crew-served weapons, tanks, and helicopters must include a consideration of position-disclosure characteristics and target acquisition capabilities, as well as other characteristics such as rates of fire, armor protection, etc.

Data concerning hit probabilities, rates of fire, armor protection, etc., are normally available to the military analyst. Before a tank or helicopter crew can initiate effective fire against a concealed or camouflaged target, however, it must locate the target with sufficient precision to lay its weapon sights on or near the center of mass of the target. Thus, it is desirable to have experimentally-determined measurements of the ability of a combat element to detect the signature of a concealed, firing crew-served weapon and bring effective fire to bear against that element.

Several field experiments have been performed to acquire data concerning the acquisition of concealed targets by crews of observers on the basis of firing signatures.

A brief review of these experiments and their results is presented in the following section.

### Literature Review

The purpose of Project PINPOINT, described in reference [ 4 ], was to determine the effect of various factors (firing weapon type, range, number of rounds fired, etc.) on the following:

1. the probability that an observing tank crew (consisting of a tank commander and a gunner) employed in an overwatch mode will locate (detect the signature and lay sights upon) a concealed AT weapon after it has opened fire;<sup>1</sup>
2. the time required, given detection, to locate the concealed weapon after it had opened fire; and
3. the accuracy, given detection, with which the concealed weapon can be located by the observing crew.

In the Project PINPOINT experiments, the observers were considered to be crews, consisting of a tank commander and a gunner, located in tanks and subjected to indirect firing by various antitank (AT) weapons.<sup>2</sup> These AT weapons included the battalion antitank (BAT) rifle, the M48 90-mm. tank gun, and the 76-mm. towed gun. The following independent variables (or treatments) were considered:

---

<sup>1</sup>Here, the term detect is taken to mean the act of sensing the presence of one or more components of the concealed, firing crew-served weapon systems signature.

<sup>2</sup>In Project PINPOINT, the term indirect firing was used to denote that the firing elements were firing at positions other than those occupied by the observing elements.

1. range to the target;
2. bearing of the target with respect to the observer's position and a specified primary observation direction;
3. number of rounds fired by the AT (target) weapon; and
4. the type of AT weapon firing.

The following dependent (or response) variables were measured:

1. the time required by the tank crew to locate the AT weapon after firing its first round;
2. the accuracy with which the AT weapon was located; and
3. the probability of achieving a pinpoint.

In the study, pinpointing was defined as the act of locating an AT weapon's position by a tank crew to within  $\pm 25$  yards horizontal error. The time required for pinpointing was defined as the elapsed time from the moment the first round was fired by the AT weapon until the observing crew initiated the laying of its weapon sights--as denoted by the command "Gunner . . ." given by the tank commander, or the command "Target . . ." given by the gunner.

AT weapons were located at various positions along the edge (tree line) of a wooded area and fired in the approximate direction of the observing tanks located in a clearing facing the tree line. During each phase of the experiment, each of the eight AT weapons fired a sequence of one, two, or three rounds, and five tank crews attempted to pinpoint the AT weapon's position. The relative ranges and angular positions of the AT weapons were varied during the experiment. Eight range intervals, from 470 yards to 1480 yards, and two angular position intervals<sup>1</sup> were used.

After an analysis of the field data resulting from the experiment, the following conclusions were made:

---

<sup>1</sup> The angle made by the intersection of the longitudinal axis of the observing vehicle and a line connecting the respective centers of the tank and the AT weapon was referred to as "head-on" (H) if it was between 0° and 45° and "quartered" (Q) if it was between 45° and 70°.

1. Given that a weapon is pinpointed, the accuracy with which the weapon is located--the lay error (yards)--is not affected by the range to the weapon position, the angular location of the weapon position relative to the observer's tank, the type of AT target weapon, or the number of rounds fired by the AT weapon.
2. The median time required for detection of the firing signature, measured from the time at which the round detected was fired, was approximately five seconds, regardless of which round in the firing sequence was detected. In addition, it was found that if the AT weapon was pinpointed, the time required to detect the firing signature (for the round upon which pinpointing occurred) was not affected by the range to the weapon position, the angular position of the AT weapon relative to the observer's position and principal observation direction, or the type of AT weapon used.
3. The probability that an AT weapon will be detected is dependent on the type of AT weapon used. The BAT rifle and the M48 tank gun were significantly easier to detect than the towed gun (at the 5% level of significance).
4. The probability of pinpointing an AT weapon depends upon the number of rounds fired by the AT weapon.
5. For target ranges of 400 to 1500 yards, the range to the target did not affect the pinpoint probability, regardless of the type of AT weapon used.
6. There is a significant decrease in pinpoint probability as the angle to the target's position (measured from the observer's principal observation direction) increases, i.e., the susceptibility of an AT weapon to pinpointing is less when fired from a flanking position.

It should be noted that each of the above conclusions were based upon analysis of variance techniques employed at the 5% significance level.

Stollmack, reference[ 3 ], reanalyzed the data acquired in the Project PINPOINT experiment in accordance with a different definition of the act of pinpointing. Stollmack defined pinpointing as follows:

True Pinpoint - A pinpoint made such that the associated laying error (yards) can be described by a normal distribution with mean  $\mu = 0$  and variance  $\sigma^2$ .

False Pinpoint - A pinpoint made such that the associated laying error can be described by a uniform distribution with a mean of zero.

In his report, Stollmack noted that in the statistical analysis reported in reference [4], it was stated that the  $\pm 25$  yard lay-error limitation on pinpointing included 80% of the field data. The remaining 20% of the data points were excluded from the Project PINPOINT analysis on the basis that they were non-representative of pinpoint lays, i.e., they were treated as outliers. He also noted that no other justification was given to substantiate the exclusion of this data from the analysis.

Utilizing the definition of the pinpointing process stated above, Stollmack was able to include all of the data, with the possible exclusion of a few extreme outliers, in the analysis of the Project PINPOINT data to determine the distribution of pinpoint lay errors and the resulting distribution of his probabilities.

Stollmack concluded from remarks made in the Project PINPOINT report concerning the short-time duration of visible firing clues (flash, smoke, etc.) that at least two different bases for attaining a pinpoint existed:

1. "Crews who were sufficiently alert could lay their gun sights on the center of the dust and smoke generated by AT weapon before they disappeared . . ."
2. ". . . Crews who were slower would have to pick a likely target position near the suspected origin of the gun flash."

Consequently, Stollmack hypothesized that the laying error data included cases in which crews layed their sights on terrain features which appeared to be likely target positions in the vicinity of the observed flash.

In his subsequent analysis, Stollmack assumed that:

1. Laying errors associated with the "alert crews" of case 1 above are normally distributed with mean at the center of the target.
2. Since AT targets were located in an essentially continuous (uninterrupted) tree line, terrain features which appeared to be likely locations were uniformly distributed across this tree line; and, therefore,
3. Laying errors associated with the "slower crews" are uniformly distributed around the center of the target.

Using the above assumptions, Stollmack estimated (using a graphical procedure, see reference [3], pp. 257-265) that 77.5% of the data points represented "true pinpoints," and the remaining 22.5% represented "false pinpoints." The most significant result from Stollmack's analysis was that he was able to estimate the standard deviation of pinpoint lay errors from the total data and to thus establish some logic for determining the upper limit of lay errors associated with his definition of the term true pinpoint.

Although Project PINPOINT involved several different types of AT weapon systems, no effort was made to relate detection and pinpoint probabilities to the durations and intensities of the various components of the weapons' firing signatures. Also, there was no determination made of which components of the firing signature each observing crew detected prior to laying their sights on the suspected target position. A review of the signature detection literature revealed that little consideration has been given to the problem of relating the detection and pinpoint probabilities to the durations and intensities of the components of the firing signatures for concealed or camouflaged AT weapon systems.

In the section which follows, a pinpoint model which is sensitive to the durations and intensities of the components of the firing signatures is presented.

### Pinpoint Model

As noted previously, the ability of the observer to acquire a target by pinpointing depends upon the intensities and durations of the visual and auditory clues provided by the target's firing signature. The intensities and durations of these characteristics depend upon the propellant and charge composition (as well as numerous other factors such as muzzle velocity, dust, etc.), and they can be reduced at some cost.

The model presented in this chapter may be used in determining the relationships between the intensities and durations of a weapon's firing signature components and its susceptibility to enemy fire.

The process of acquiring a target (laying the sights of a weapon system upon a target) is sequential; i.e., first the observing element must detect some component of the target's firing signature and then once it has detected some component, it attempts to lay its sights on the target such that pinpointing takes place. Thus, an observing element's acquisition state can be described in terms of what will be referred to as a "detection-pinpoint" state composed of two substates. The detection substate is defined by which components of the target's firing signature the observing element has detected, and the pinpoint substate is defined as "pinpoint" or "no pinpoint."

In order to formulate a general model to predict the detection-pinpoint performance of observing elements searching for concealed or camouflaged firing crew-served weapon systems, it is necessary to make certain assumptions regarding the process. The following assumptions are made in the model:<sup>1</sup>

1. The components of the target's firing signature (i.e., flash, smoke, dust, vapor trail, audible report, etc.) occur in an ordered, fixed sequence in time which is independent of the positions of the observer and the crew.
2. In order to lay its sights after the firing of a given round by the target, the observing element must have detected at least one component of the firing signature of that round.
3. Once a component of a given round is detected by an observing element, the remaining components in the sequence (for the given round) are detected with certainty. Thus, the observing element's detection state can be described in terms of the first component in the sequence detected after a given round has been fired.
4. The probability of detecting the  $k^{\text{th}}$  component of the signature of a given round first in the sequence depends only upon which component was first detected on the previous round fired by the target element. Thus, this probability does not depend upon the observing element's detection state prior to the immediately preceding round. In the first round case, this probability is computed using no prior information of component detection.
5. The probability that an observing element lays its sights such that it pinpoints a given firing target after a given round depends only upon which components of that round were detected. (The components detected on a given round can be defined in terms of the first component detected in the sequence of components.)

---

<sup>1</sup>Admittedly, each of the following assumptions may be only approximately true; however, they appear to be reasonable. The relaxation of these assumptions to achieve a greater degree of model realism and the resultant increase in model complexity is not thought to be merited by the increase in accuracy of predictions.



Each of the above assumptions must be tested using experimental data. In particular, if assumption 4 is found to not be true, then it might be found through experimental observation that the probability of the observing element being in a particular detection state after a given round depends only upon his detection states after the previous two, or possibly three, rounds fired. If the probability of an observing element being in a particular state after a given round has been fired depends upon his detection states after the previous  $k$  rounds, then the observing element's detection behavior is what is known as a  $k^{\text{th}}$ -order Markov process. Since it has been assumed that the probability of an observing element being in a particular detection state after a given round depends only upon his detection state after the immediately preceding round, a 1st-order Markov process has been assumed.

A Markov process is described by specifying the initial state and a set of transition probabilities; namely, the set of conditional probabilities of transitioning to any state after the firing of each round, given the observing element's state after the immediately preceding round. Thus, if there are  $m$  components of the firing signature, then there are  $2m + 1$  possible states which describe the observing element's detection-pinpoint state.<sup>1</sup>

The following notation is used to describe the Markov process model. Let  $n_i(t)$  be the number of observing crews for the  $i^{\text{th}}$  detection-pinpoint state at time <sup>2</sup>,  $t$ , after the firing of a given round; and let  $n$  be the total number of observing elements searching for the given target, where  $n = \sum_i n_i(t)$ . The model gives a probability distribution for  $n_1(t), \dots, n_{2m+1}(t)$ . If the number of observing elements,  $n$ , is large, then the proportion  $r_i(t) = n_i(t)/n$  is roughly the population mean,<sup>3,4</sup>  $\rho_i(t) = E[r_i(t)]$ ; where  $R_i(t)$  represents

---

<sup>1</sup>Since it is possible that the observer did not detect any of the target's signature components, there are  $m+1$  possible detection states. For each possible detection state, except for no detection, there are two possible pinpoint states. Thus, there are  $2m+1$  possible detection-pinpoint states to consider.

<sup>2</sup>The discrete independent variable  $t$  is taken to denote the number of the round just previously fired. Thus,  $t=0$  denotes that no rounds have been fired and  $t=N$  denotes the time immediately after the firing of the  $N^{\text{th}}$  round.

<sup>3</sup>The symbol  $E[\cdot]$  is taken to be the expected value of  $[\cdot]$ .

<sup>4</sup>Here it should be emphasized that  $r_i(t)$  is an arithmetic average, while  $R_i(t)$  is a population mean. As the sample size,  $n$ , approaches infinity, the arithmetic average,  $r_i(t)$ , approaches the population mean  $R_i(t)$  with probability one.



the probability of an observing element being in state  $i$  at time  $t$ . Let  $p_{ij}(t)$  denote the conditional probability of an observing element being in acquisition (or detection-pinpoint) state  $j$  at time  $t$  (after the firing of a given round) given that the observing element was in acquisition state  $i$  after the firing of the previous round, then  $R_j(t)$  can be computed as follows:

$$R_j(t) = \sum_{i=1}^{2m+1} p_{ij}(t) R_i(t-1); \quad (9.1)$$

$$j = 1, \dots, 2m+1; t = 1, 2, \dots$$

It seems reasonable to assume that  $p_{ij}(t)$  is constant for all  $t$ , thus, equation 9.1 shall be simplified to the following:

$$\rho_j(t) = \sum_{i=1}^{2m+1} p_{ij} \rho_i(t-1) \quad (9.2)$$

$$j = 1, \dots, 2m+1.$$

Since the number  $p_{ij}$  is a probability, it must be nonnegative, and since one of the  $2m+1$  states must be held at time  $t+1$ , the sum of these probabilities over all  $j$  must be 1.0; that is

$$\sum_{j=1}^{2m+1} p_{ij} = 1.0, \quad i = 1, \dots, 2m+1.$$

By knowing the state of the observing element at  $t = 0$  (i.e., prior to the firing of any rounds), we can predict, in a probability sense, how its states will change after successive rounds have been fired.

It should be observed that the detection-pinpoint state associated with a given observing element at time  $t+1$  depends only upon its state at time  $t$ . The only other factors taken into account explicitly are the environmental properties (ambient light level, meteorological visibility, and ambient noise level), the range between the observing element and the target, the location of the target within the observing element's field of view, and the type of target (including the descriptors which describe the characteristics of its signature components). Other factors are considered or taken into account implicitly. It is assumed that the effects of other influences on the observing element's state of knowledge are of such a nature that their total effect can be considered to be random.

A frequency interpretation to the probabilities defined here can be given even though the probability model is specified for just an individual observing crew. The numbers  $p_{ij}$  depend upon the durations and intensities of the target's firing signature, the sensitivity of the observers comprising the observing element, as well as their skill in laying their sights upon the position from which the observed signature component(s) emanated. One could imagine this individual observing crew or one similar to it as being placed in a large number of similar situations. Suppose in each of these circumstances the observing element is in detection-pinpoint state  $i$ . A count of the number of situations in which it changes to detection-pinpoint state  $j$  yields the relative frequency of this change--which will be approximately  $p_{ij}$ .

The transition probabilities  $p_{ij}$  form a matrix

$$P = \begin{pmatrix} p_{11} & p_{12} & \cdots & p_{1,2m+1} \\ p_{21} & p_{22} & \cdots & p_{2,2m+1} \\ \cdot & \cdot & \cdot & \cdot \\ \cdot & \cdot & \cdot & \cdot \\ p_{2m+1,1} & p_{2m+1,2} & \cdots & p_{2m+1,2m+1} \end{pmatrix}$$

Knowing  $P$  and the individual observing element's detection-pinpoint state at time  $t = 1$  (after the firing of the first round) a probability can be assigned to every sequence of changes of states; that is, probability statements concerning any particular outcome of the observing element's detection-pinpoint state can be made. If the initial state is  $i$ , then the probability of the observer being in state  $j$  at time  $t = 2$  is  $p_{ij}$ .

In order to express the matrix of transition probabilities in terms of more basic concepts, some additional notation must be established. Let

$E_{\infty,0}$  = the state in which the observing element has detected none of the components of the previously fired round and has not pinpointed.

$E_{k,1}$  = the state in which observing element has detected component  $k$  first in the sequence of firing signature components and has pinpoints ( $l = 1$ ) or has not pinpointed ( $l = 0$ ) the target for  $k = 1, 2, \dots, m$ .

$d_{k,u}$  = the conditional probability of the observing element being in detection state  $u$  at time  $t$  given that it was in detection state  $k$  at time  $t-1$ .

$f_{l,u}$  = the conditional probability of the observing element being in the state of pinpointing at time  $t$  given that it was in pinpoint state  $l$  at time  $t-1$  and that it detected component  $u$  first in the sequence of components at time  $t$ .

Using the above notation, the general form of the transition probability matrix is presented in Figure 9.1.

Figure 9.1 clearly depicts the nature of the compound detection-pinpoint process as being composed of, first, detection of the components of the target's firing sequence and, then, the laying of the sights of the observing element's weapon system upon the suspected target position. In the section which follows, the problems involved in estimation of the  $d$  and  $f$  parameters of the detection-pinpoint model are discussed.

### Parameter Estimation

In this section, discussion of a procedure which can be employed to estimate the  $d$  and  $f$  parameters of the detection-pinpoint model is presented. The estimation of the  $d$  parameter is discussed first.

Assume that in conducting the field experiment, the experimenter records the occurrences of transitions from one detection state to another by means of a transition matrix similar to that shown in Figure 9.2. Let  $n_{ab}$  be the number of observing elements who were in detection state  $b$  after time  $t$  and who were previously in detection state  $a$  at time  $t-1$ .

As defined previously, let  $d_{k,u}(t)$  ( $k, u=1, \dots, \infty$ ;  $t=1, 2, \dots, N$ ) be the probability of an observing element being in detection state  $u$  at time  $t$ , given that it was in detection state  $k$  at time  $t-1$ . Here it is assumed that the detection state transition probabilities are stationary from round to round; i.e.,  $d_{k,u}(t)=d_{k,u}$  for  $t=1, 2, \dots, N$ . It is assumed that all observing elements are in state  $\infty$  (that is, they have detected no components of the firing signature) for  $t=0$  (that is, prior to the firing of the first round). An observation on a given individual observing element consists of a sequence of states the element is in at  $t=0, 1, 2, \dots$ , namely,  $k(0), k(1), k(2), \dots$ , (where,  $k(0)=\infty$  for all observing elements). Given the initial state  $k(0)=\infty$ , there are  $(m+1)^N$  possible sequences--where  $N$  equals the total number of rounds fired in the given sequence by a particular crew-served weapon target. These

	$E_{10}$	$E_{11}$	$E_{20}$	$E_{m1}$	$E_{\infty 0}$
$E_{10}$	$d_{11}(1-f_{01})$	$d_{11}f_{01}$	$(1-d_{11})d_{12} \cdot (1-f_{02})$	$\prod_{u=1}^{m-1} (1-d_{1u}) \cdot d_{1m}f_{0m}$	$\prod_{u=1}^m (1-d_{1u})$
$E_{11}$	$d_{11}(1-f_{11})$	$d_{11}f_{11}$	$(1-d_{11})d_{12} \cdot (1-f_{12})$	$\prod_{u=1}^{m-1} (1-d_{1u}) \cdot d_{1m}f_{1m}$	$\prod_{u=1}^m (1-d_{1u})$
$E_{m0}$	$d_{m1}(1-f_{01})$	$d_{m1}f_{01}$	$(1-d_{m1}) \cdot d_{m2}(1-f_{02})$	$\prod_{u=1}^{m-1} (1-d_{mu}) \cdot d_{mm}f_{0m}$	$\prod_{u=1}^m (1-d_{mu})$
$E_{m1}$	$d_{m1}(1-f_{11})$	$d_{m1}f_{11}$	$(1-d_{m1}) \cdot d_{m2}(1-f_{12})$	$\prod_{u=1}^{m-1} (1-d_{mu}) \cdot d_{mm}f_{1m}$	$\prod_{u=1}^m (1-d_{mu})$
$E_{\infty 0}$	$d_{\infty 1}(1-f_{01})$	$d_{\infty 1}f_{01}$	$(1-d_{\infty 1}) \cdot d_{\infty 2}(1-f_{02})$	$\prod_{u=1}^{m-1} (1-d_{\infty u}) \cdot d_{\infty m}f_{01}$	$\prod_{u=1}^m (1-d_{\infty u})$

Figure 9. 1. --Matrix of Transition Probabilities  
for Markov Chain.

Detection State at Time  $t$

		1	2		m	$\infty$
Detection State at Time $t-1$	1	$n_{11}$	$n_{12}$		$n_{1m}$	$n_{1\infty}$
	2	$n_{21}$	$n_{22}$		$n_{2m}$	$n_{2\infty}$
	m	$n_{m1}$	$n_{m2}$		$n_{mm}$	$n_{m\infty}$
	$\infty$	$n_{\infty 1}$	$n_{\infty 2}$		$n_{\infty m}$	$n_{\infty \infty}$

Figure 9. 2. --Matrix of Observed Transitions of Detection States.

represent mutually exclusive events with probabilities

$$d_{k(0) k(1)} \cdot d_{k(1) k(2)} \cdot \dots \cdot d_{k(N-1) k(N)}$$

when the transition probabilities are stationary (i.e., not changing with time).

Let  $n_{k,u}(t)$  denote the number of observing elements in state  $k$  at time  $t-1$  and in state  $u$  after round  $t$ . Then the stationary transition probabilities  $d_{k,u}$  can be estimated using the maximum likelihood estimates (reference [1]) as follows:

$$\hat{d}_{ku} = \frac{\sum_{t=1}^N n_{ku}(t)}{\sum_{t=1}^N \sum_{u=1}^{m+1} n_{ku}(t)}$$

The estimation of  $d_{ku}$  can be verbally described in the following way. Let the entries  $n_{ku}(t)$  for all  $t$  be entered into a two-way  $(m+1)$  by  $(m+1)$  table. The estimate of  $d_{ku}$  is the  $ku^{\text{th}}$  entry in the table divided by the sum of the entries in the  $k^{\text{th}}$  row.

The estimation of the  $f$  parameter of the detection-pinpoint model is somewhat more involved than the procedure for the  $d$  parameter. Recall that  $f_{lu}(t)$  denotes the probability of pinpointing at time  $t$ , given the following occurrences:

1. the observing element was in pinpoint state  $l$  at time  $t-1$ , and
2. the observing element detected component  $u$  first at time  $t$ .

Here it is also assumed that the pinpoint state transition probabilities are stationary from round to round; i.e.,  $f_{lu}(t) = f_{lu}$  for  $t = 1, 2, \dots, N$ . We assume for  $t=1$  that  $l=0$  always.

Let  $m_{lu}(t)$  denote the number of observing elements who had pinpointed at time  $t$  and who were in pinpoint state  $l$  at time  $t-1$  and who also had detected component  $u$  first at time  $t$ . Then the stationary transition probabilities  $f_{lu}$  can be estimated using the maximum likelihood estimates as follows:

$$\hat{f}_{lu} = \frac{\sum_{t=1}^N m_{lu}(t)}{\sum_{t=1}^N m_{lu}(t) + \sum_{t=1}^N \bar{m}_{lu}(t)}$$

where  $\bar{m}_{lu}(t)$  equals the number of observers who were in pinpoint state 1 at time  $t-1$  and who detected component  $u$  first at time  $t$  and who also had not pinpointed at time  $t$ .

The estimation of  $f_{lu}$  can be verbally described most expediently with reference to an information sheet such as Figure 9.3. Figure 9.3 represents a set of hypothetical data. The maximum likelihood estimate of  $f_{lu}$  is the ratio of the number of times that observing elements pinpointed given that they were in pinpoint state 1 after the previous round and given that they had detected component  $u$  first on the current round divided by the number of times that the observing elements were in pinpoint state 1 on the previous round and who had detected component  $u$  first on the current round. For example, for the set of hypothetical data of Figure 9.3, the estimate of  $f_{11}$  would be  $2/3$  since the observing element detected component 1 first a total of three times when his pinpoint state after the previous round was  $l=1$  and remained in the pinpoint state,  $l=1$ , a total of two times.

Time $t$	1	u
	Pinpoint State for Round $n$	Detection State for Round $n$
0	0	6
1	0	5
2	1	3
.	1	2
.	1	1
.	0	1
N-1	1	1
N	1	1

Figure 9.3. --A Set of Hypothetical Data for One Observer When  $m = 5$ .

## Conclusions

Although the model discussed in this paper is capable of representing much more detail than those presented in the reports discussed previously, it is simple in several respects. For a given set of environmental conditions (ambient light level, noise level, visibility range) and a given observing element-target pair at a given range from each other, the model explains changes in the observing element's detection-pinpoint state (after a given round has been fired) in terms of the observing element's detection-pinpoint state at the end of the previous round only, other factors are considered to be random and are not considered explicitly.

In addition, the model, by virtue of its sequential character allows the military analyst to synthesize the results of experimentation with previous target systems in order to predict detection-pinpoint performance of observers searching for a new generation target whose individual target signature components may have characteristics similar to those of weapons previously studied.

## References

1. Anderson, T. W., and Goodman, L. A., "Statistical Inference About Markov Chains," Annals of Mathematical Statistics, Vol. 28 (1957), pp. 89-110.
2. Eckles, A. J., "Draft Operations Plan for Signature 1--A Field Study of the Effects of Signature Variations on Target Disclosure," Aberdeen Proving Ground, Maryland. (Mimeographed)-a.
3. Stollmack, S., "Acquisition of Firing Targets," Chapter 4 (in) Howland, D., and Bonder, S. (eds.) The Tank Weapon System (U), RF 573AR 65-1(S), Systems Research Group, The Ohio State University, Columbus, Ohio, June, 1965.
4. Young, J. P., Eckles, A. J., Parsons, N. W., and Koehler, L. F., Project Pinpoint: Disclosure of Antitank Weapons to Overwatching Tanks (U), Technical Memorandum ORO-T-362, The Johns Hopkins University, Operations Research Office, Bethesda, Maryland, January, 1958.



APPENDIXES

[illegible]

**Figure 109. Type radio net diagram, armored cavalry troop, armored cavalry squadron, armored, armored, mechanized, and infantry divisions.**

## APPENDIX B

### A SAMPLE TRANSCRIPTION OF NET TRAFFIC

Location: Fort Carson, Colorado  
Date: 18 SEP 1968  
Net: Platoon I, Bravo Troop  
Reel: 42-1  
Action: Zone Reconnaissance

Duration is indicated at the end of each message. The beginning of each conversation is indicated by an asterisk (\*).

- 
- 14 this is 10. Move to the banks to your right flank. Hold up and then I'll move on into the wood line. Over. (7.1)
  - This is 14. Roger. Out. (2.5)
  - \* 35 this is 10. Over. (1.5)
  - This is 35. Over. (1.6)
  - This is 10. Spot rep (Spot report). Over. (2.0)
  - 35. Send it. (1.0)
  - (Formatted spot report. See Appendix ) (24.7)
  - \* 35. 77. Your push (frequency). (2.0)
  - This is 35. (1.2)
  - This is 77. Reference your spot report. Were you able to take that vehicle under fire with your own organic weapons? Over. (8.4)
  - This is 35. Negative. He went behind that hill to our direct south before we could get up and get him. Over. (6.1)
  - This is 77. Roger. Keep the reports coming. (3.5)
  - \* 35 this is 15. Over. (1.5)
  - This is 35. (1.3)
  - 15. Do we have the 19 covering the move to the big boy (tank) in my victor? Over. (8.0)
  - This is 35. Say again. (3.5)
  - Can we have 19er covering the move of the big boy in my victor? Over. (3.9)
  - This is 35. That's affirmative. 19er is in battery with other nine elements. Over. (8.5)
  - 15. Rog. Then it won't be necessary for 37 and 15 to move by leaps and bounds. Is that Rog? Over. (8.8)
  - That's affirmative. You will move in bounds. (3.0)

- This is 15. Roger. Out. (5.5)
- \* 35. 10. Over. (1.4)
- 35. (1.1)
- This is 10. Spot rep. Over. (2.0)
- Send it. (1.1)
- Disregard. Out. (2.1)

The above communications illustrate the variation of numbers of messages per conversation, requests for repeats, several formats for establishing and verifying contact and communications with no information content.

## APPENDIX C

### FORMATTED MILITARY COMMUNICATIONS

The following five pages are sample copies of formats characteristically used when transmitting reports of various battlefield activities and situations. These formats are used primarily when sending information to higher levels of command. The conversation durations associated with such reports are generally high with a small variance about the average duration.

SHELLREP, MORTREP, BOMBREP

ALPHA \_\_\_\_\_  
(CALL SIGN)

BRAVO \_\_\_\_\_  
(COORDINATES OF OBSERVER)

CHARLIE \_\_\_\_\_  
(AZIMUTH TO ENEMY CANNON OR ESTIMATED DIRECTION OF  
EVERY GUN BY FURROW, FLASH, SMOKE OR SOUND)

DELTA \_\_\_\_\_  
(ESTIMATED DISTANCE OR LOC OF GUNS OR ANGLE OF FALL)

ECHO \_\_\_\_\_  
(COORDINATES OF AREA SHELLED)

FOXTROT \_\_\_\_\_  
(TIME SHELLING STARTED)

GOLF \_\_\_\_\_  
(TIME SHELLING ENDED)

HOTEL \_\_\_\_\_  
(NUMBER, TYPE AND CALIBER OF GUNS FIRING)

INDIA \_\_\_\_\_  
(NUMBER AND TYPE OF SHELLS)

JULIET \_\_\_\_\_  
(NATURE OF SHELLING (REGISTRATION, HARASSING, EFFECT))

KILO \_\_\_\_\_  
(TIME OF FLASH TO BANG)

LIMA \_\_\_\_\_  
(DAMAGE, USUALLY IN CODE)

Note: SHELLREP - In case of artillery fire.  
MORTREP - In case of mortar fire.  
BOMBREP - In case of enemy aircraft attack.

Note: This report is submitted by individuals and  
units observing or receiving enemy fire by  
most expeditious means available.

SPOT REPORT

ALPHA - What is identification of person sending info.  
BRAVO - What enemy was observed and in what strength.  
CHARLIE - Where and when was the enemy observed.  
DELTA - What was the enemy doing.  
ECHO - What are you doing about it.

SPOT REPORT

ALPHA \_\_\_\_\_  
BRAVO \_\_\_\_\_  
CHARLIE \_\_\_\_\_  
DELTA \_\_\_\_\_  
ECHO \_\_\_\_\_

### TRACE REPORT

(Submit every even hour)

ALPHA: 1. \_\_\_\_\_  
(Center of mass, 1st Platoon)

2. \_\_\_\_\_  
(Enemy contact - Affirm/Negative)

BRAVO: 1. \_\_\_\_\_  
(Center of mass, 2nd Platoon)

2. \_\_\_\_\_  
(Enemy contact - Affirm/Negative)

CHARLIE: 1. \_\_\_\_\_  
(Center of mass, 3rd Platoon)

2. \_\_\_\_\_  
(Enemy contact - Affirm/Negative)

DELTA: 1. \_\_\_\_\_  
(Center of mass - Troop Command Post)

Note: S3 submits similar report for troops and Squadron to Division G3 every even hour plus 10 minutes.

### ROAD RECONNAISSANCE REPORT

ALPHA: From (coord)\_\_\_\_\_ to (coord)\_\_\_\_\_

BRAVO: Type\_\_\_\_\_ (Concrete, black top, dirt, etc.)

CHARLIE: Trafficability (Armor, wheel veh's, etc.)\_\_\_\_\_

DELTA: Gradient\_\_\_\_\_ (Coord and degree of slope)

ECHO: Sharp Curves\_\_\_\_\_ (Coord and radius in feet)

FOXTROT: Cut or Fill (Coord, width, bypass)\_\_\_\_\_

Note: When transmitting by radio, use only letter prefixes to expedite transmission. Code coordinates when sending by radio.



### BRIDGE REPORT

ALPHA: Location: (Coord) \_\_\_\_\_  
BRAVO: Number of spans (or length): \_\_\_\_\_  
CHARLIE: Type (concrete, slab, wood, etc.): \_\_\_\_\_  
DELTA: Width (feet): \_\_\_\_\_  
ECHO: Load Limit (in tons): \_\_\_\_\_  
FOXTROT: By-pass, ford (up and down stream dist.): \_\_\_\_\_

Note: When transmitting by radio, use only letter prefixes to expedite transmission. Code coordinates when sending by radio.

### UNDERPASS REPORT

ALPHA: Location (Coord): \_\_\_\_\_  
BRAVO: Width: \_\_\_\_\_ feet  
CHARLIE: Height: \_\_\_\_\_ feet  
DELTA: By-pass (over or around) coord: \_\_\_\_\_  
ECHO: Type (Rail pad, highway, etc.): \_\_\_\_\_

Note: When transmitting by radio use only lettered prefixes to expedite transmission.

## APPENDIX D

### SUMMARY OF FORT ORD DATA

Location: Fort Ord, California  
 Net: MOMAR Medium Command

The notation (n) on the posture entry indicates a nuclear situation as opposed to a situation in which nuclear weapons were not simulated. The values of Space duration indicate the times between the end of one conversation and the beginning of the next.

<u>Sit'n</u>	<u>Posture</u>	<u>Conversation Durations</u>			<u>Spaces</u>	
		<u>Mean</u>	<u>Std Dev</u>	<u>Number</u>	<u>Mean</u>	<u>Std Dev</u>
2	Attack (n)	39.4	35.4	69	32.9	49.4
6	Attack (n)	31.8	30.2	167	33.8	55.0
7	Defense	46.3	43.5	97	46.9	111.2
8	Attack	38.3	24.3	25	42.0	52.3
11	Attack (n)	31.9	24.4	97	41.2	64.1

The data of the situations summarized above were processed by the statistical analysis computer programs and graphical outputs can be seen in Appendix J.

The data summarized above were edited to attain a greater degree of reality. Their graphical outputs are in Appendix J to allow comparison of the consequent distributions.

APPENDIX E  
COVERAGE OF TAPE RECORDINGS

	18 September 1968      Fort Carson										
	07:00	08:00	09:00	10:00	11:00	12:00	13:00	14:00	15:00	16:00	17:00 18:00
Bravo Troop	_____	_____	_____	_____	_____	_____	_____	_____	_____	_____	_____
Bravo #1	_____	_____	_____	_____	_____	_____	_____	_____	_____	_____	_____
Bravo #2	_____	_____	_____	_____	_____	_____	_____	_____	_____	_____	_____
Charlie Troop	_____	_____	_____	_____	_____	_____	_____	_____	_____	_____	_____
Charlie #1	_____	_____	_____	_____	_____	_____	_____	_____	_____	_____	_____
Charlie #2	_____	_____	_____	_____	_____	_____	_____	_____	_____	_____	_____
Charlie #3	_____	_____	_____	_____	_____	_____	_____	_____	_____	_____	_____
S2 Intelligence	_____	_____	_____	_____	_____	_____	_____	_____	_____	_____	_____
S3 Command and Control	_____	_____	_____	_____	_____	_____	_____	_____	_____	_____	_____

18 September 1968 (night)

20:00 21:00 22:00

Bravo Troop

Bravo #1

Squadron

19 September 1968

07:00 08:00 09:00 10:00 11:00 12:00 13:00

Bravo Troop

Bravo #1

Bravo #2

Charlie Troop

Charlie #1

Charlie #2

Charlie #3

S2 Intelligence

S3 Command and Control

## APPENDIX F

### HISTOGRAMS OF COMMUNICATION DATA

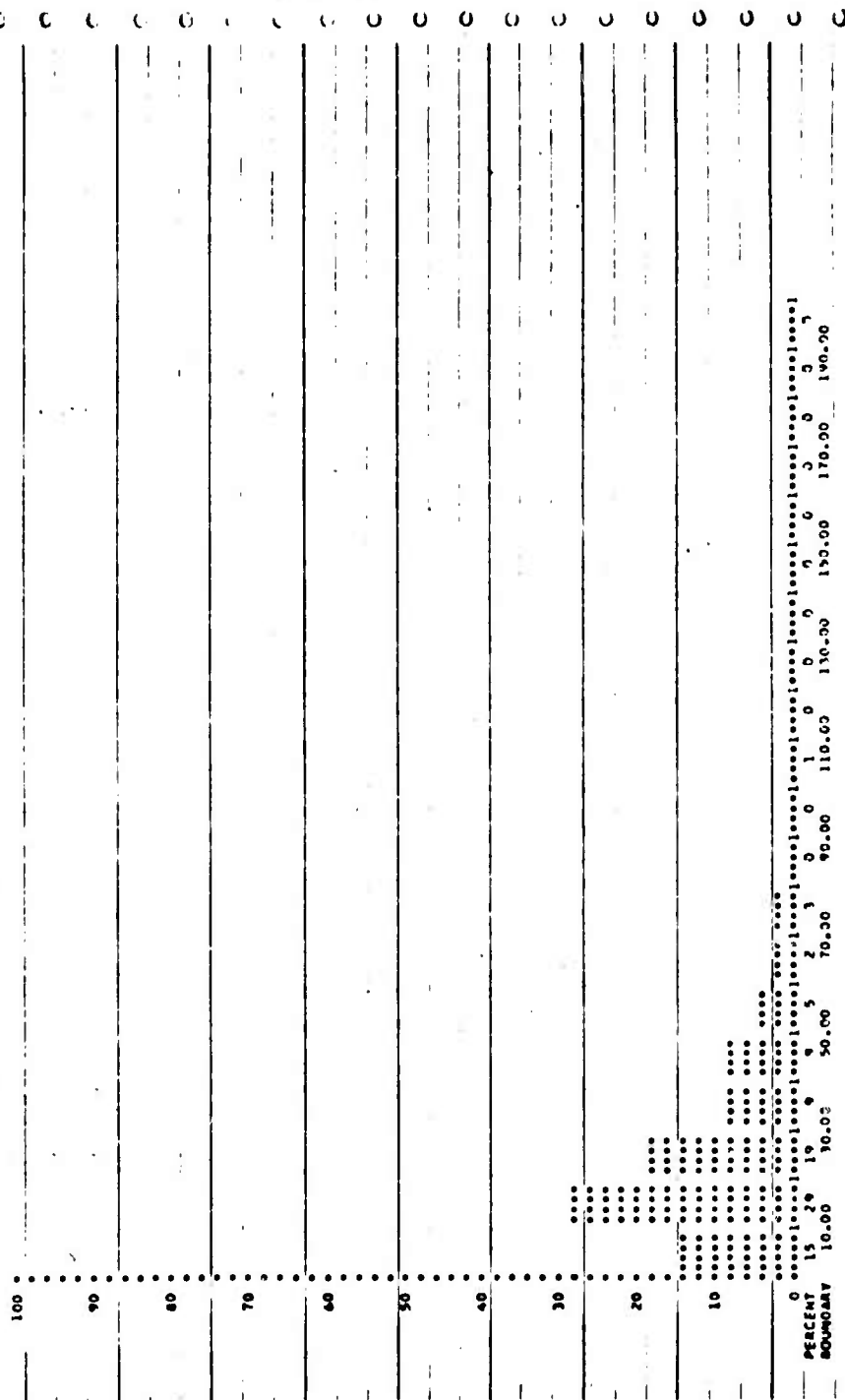
The following sample histograms were prepared from the Fort Carson and Fort Ord data of conversation durations. Because of the large number of data sets, only samples and composites are included. Identification of the data source for each histogram is at the bottom of each page.

Note that the first two histograms illustrate the effect of scaling on the appearance of the grouped data distribution.

MEAN 0.31365202E 02  
 VAR 0.66798205E 03  
 STDEV 0.25984317E 02  
 TMRD 0.36546339E 05  
 SEEM 0.19920529E 01  
 FORD 0.33224377E 07  
 KURT 0.48671740E 01

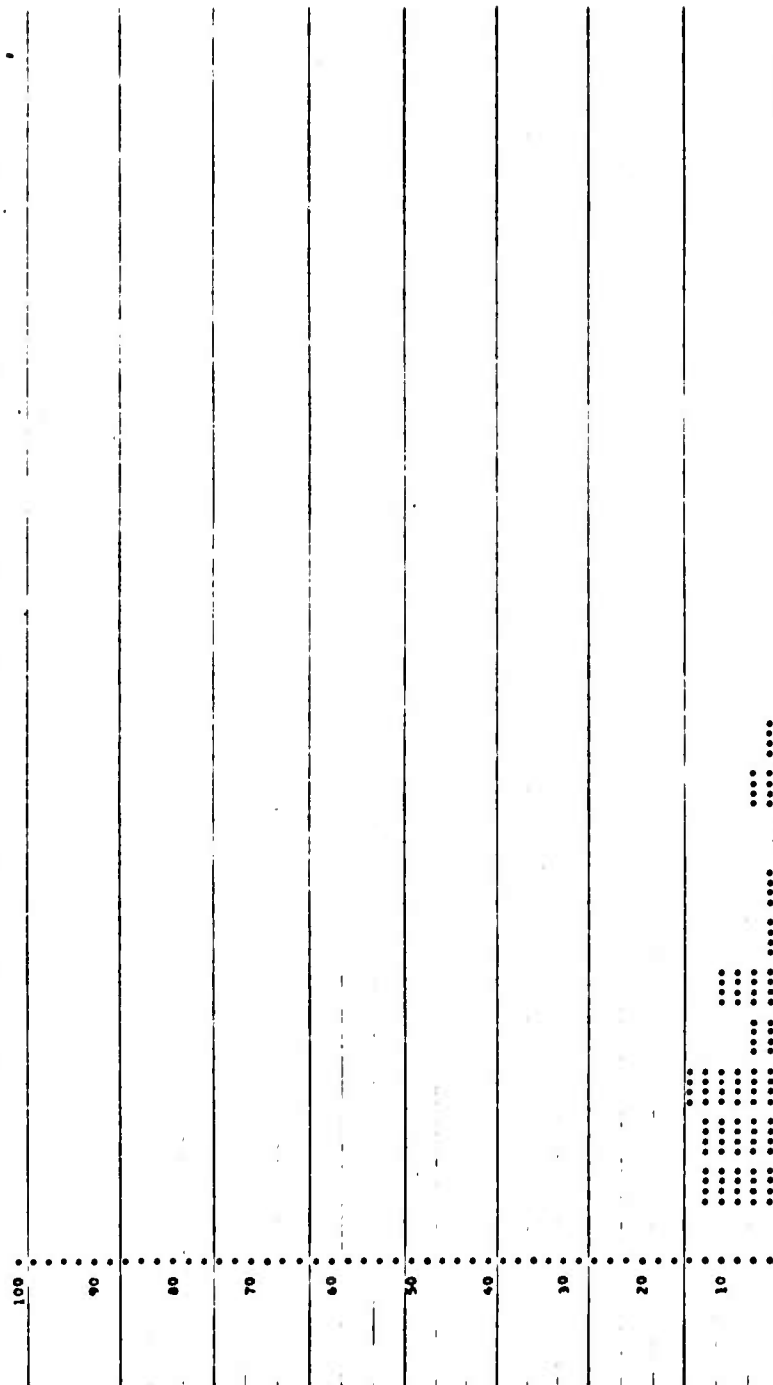
FORM 31

23 3 44 1 29 0 15 0 15 1 1 0 1 0 1 0



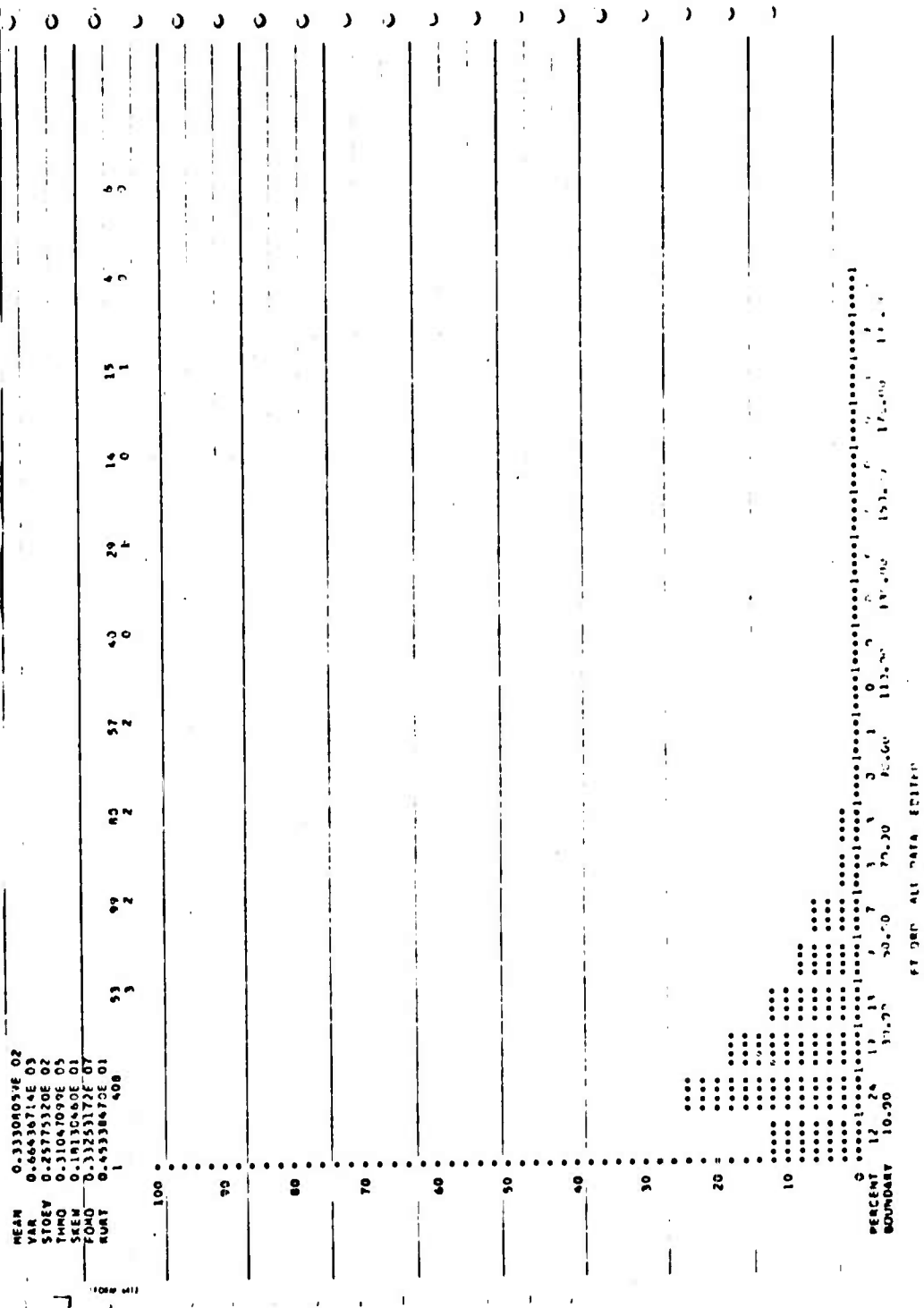
MEAN 0.3136207E 02  
 VAR 0.0699202E 03  
 STDEV 0.2586401E 02  
 TMO 0.3456339E 05  
 SKEW 0.1992083E 01  
 FOMO 0.3522497E 07  
 KURT 0.9847174E 01

2 7 21 1 20 1 24 3 12 3 17 2 1 2 6 1 11 3

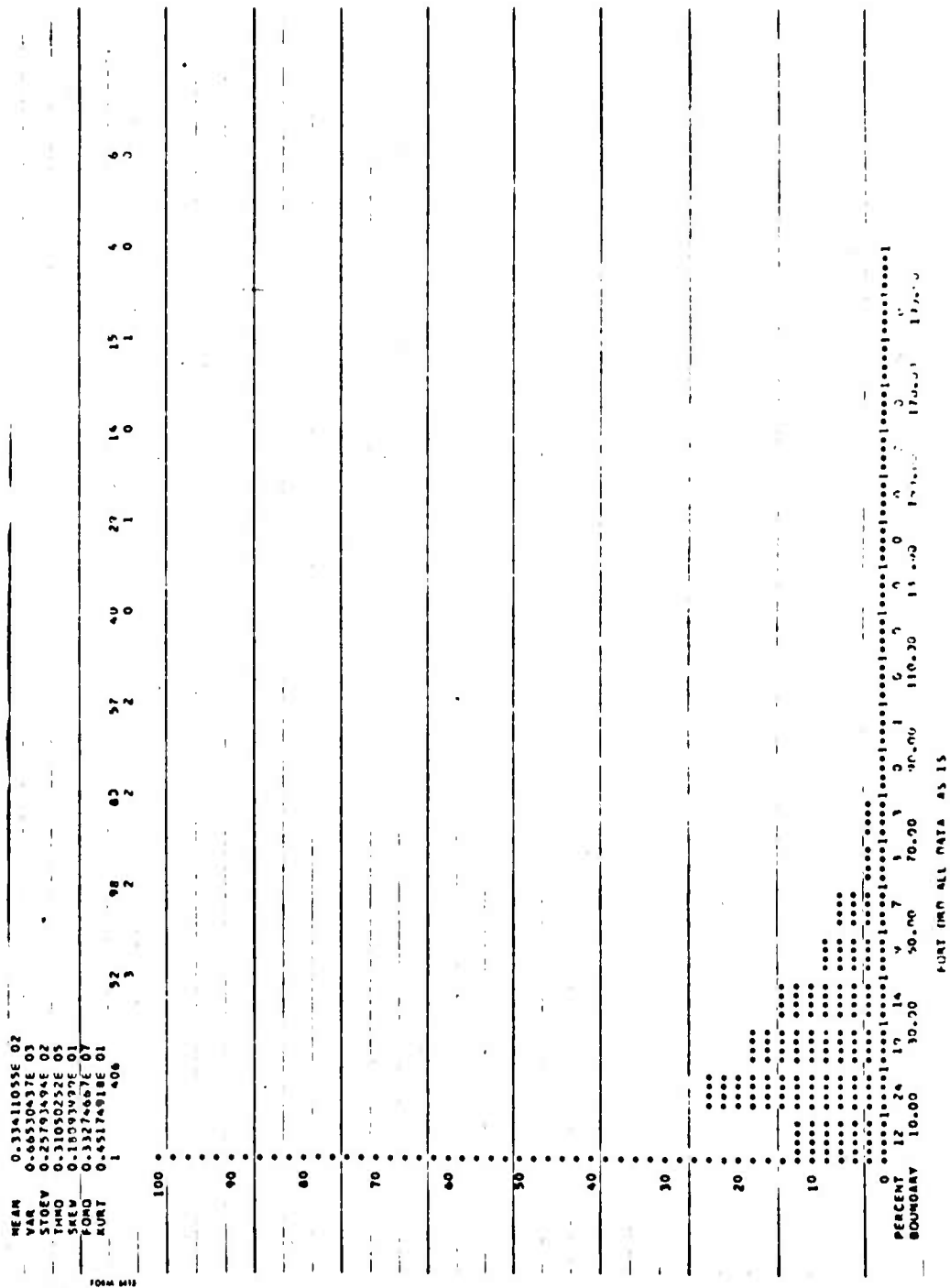


PERCENT	1	13	13	15	7	11	5	4	2	7	4	0	1	1	0	0	3
BOUNDARY	5.00	15.00	25.00	35.00	45.00	55.00	65.00	75.00	85.00	95.00	100.00	100.00	100.00	100.00	100.00	100.00	100.00

FT ORG SITUATION 0







	67	47	38	20	9	5	3	2	1
FOBO	0.6681343E-06								
SUAR	0.3691736E-01								
	1	199							
PERCENT	33	23	19	10	4	2	1	1	0
BOUNDARY	10.00	30.00	50.00	70.00	90.00	110.00	130.00	150.00	170.00

# APPENDIX G

## CHARACTERISTICS OF THE TWO-PARAMETER GAMMA DISTRIBUTION

The gamma probability distribution used in the analyses of the Communication Model is defined by the function:

$$f(x; a, b) = \frac{1}{G(a)b^a} (x^{a-1}) e^{-x/b}$$

where  $G ( )$  is the gamma function as defined and tabulated in many statistics texts, such as the text by Hogg and Craig.<sup>1</sup> The mean of the distribution is equal to the product,  $ab$ , and the variance is equal to the product,  $ab^2$ . The moment generating function of the gamma distribution is:

$$M(t) = \frac{1}{(1-bt)^a} .$$

The parameters of the gamma distribution,  $a$  and  $b$ , are referred to as the shape and scale parameters, respectively. When two gamma distributed random variables are added, the resulting distribution is also gamma if the scale parameters of the addends are equal, regardless of the shape parameters. If, for example, the sum  $Z = X + Y$  defines the random variable  $Z$ , where  $X$  is gamma distributed with parameters  $a_x$  and  $b_x$ , and  $Y$  is gamma distributed with parameters  $a_y$  and  $b_y$ , the moment generating function of  $Z$  is then the product of the moment generating functions of  $X$  and  $Y$ :

$$M(t) = \frac{1}{(1-b_x t)^{a_x}} \cdot \frac{1}{(1-b_y t)^{a_y}} .$$

This product is simply the moment generating function of another gamma distribution if  $b_x$  and  $b_y$  are equal. The parameters of the gamma distribution of  $Z$ , in this special case, would be  $(a_x + a_y)$  and  $(b_x = b_y)$ , respectively, for the shape and scale parameters. When the scale parameters,  $b_x$  and  $b_y$ , are unequal, the resulting moment generating function is not recognizable as belonging to any standard probability distribution.

---

<sup>1</sup>Hogg, R. B and Craig, A. T., Introduction to Mathematical Statistics, (2nd Edition), The Macmillan Company, New York, 1966.

## APPENDIX II

### MAXIMUM LIKELIHOOD ESTIMATORS FOR THE GAMMA DISTRIBUTION PARAMETERS

Greenwood and Durand<sup>1</sup> provide maximum likelihood estimators for the general Type-III density function, of which the gamma distribution is a special case. The notation of Greenwood and Durand will be altered to match that of this paper, especially that in Appendix G. The general Type-III density function may be written as:

$$f(x; a, b, m) = \frac{1}{bG(a)} \left[ \frac{x-m}{b} \right]^{a-1} \exp(-(x-m)/b) \quad (\text{II. 1})$$

where  $G(a)$  is the gamma function.

Then, for a sample of  $n$  observations, where  $x_i$  is the  $i^{\text{th}}$  observed value, the logarithm of the likelihood function is:

$$L = -n a \ln(b) - n \ln(G(a)) + (a-1) \sum_{i=1}^n \ln(x_i - m) - \sum_{i=1}^n (x_i - m)/b \quad (\text{H. 2})$$

Taking partial derivatives of  $L$  with respect to  $a$ ,  $b$ , and  $m$ , and setting them to zero, yields the following three equations which must be simultaneously satisfied to maximize the likelihood function.

$$\frac{\partial L}{\partial a} = -n \ln(b) - n \frac{d}{da} \ln(G(a)) + \sum_{i=1}^n \ln(x_i - m) = 0 \quad (\text{II. 3})$$

$$\frac{\partial L}{\partial b} = \frac{-na}{b} + \sum_{i=1}^n \frac{(x_i - m)}{b^2} = 0 \quad (\text{II. 4})$$

$$\frac{\partial L}{\partial m} = (a-1) \sum_{i=1}^n \frac{1}{(x_i - m)} (-1) - \frac{1}{b} \sum_{i=1}^n (-1) = 0 \quad (\text{II. 5})$$

The maximum-likelihood estimators are then the solutions to the three following simultaneous equations:

---

<sup>1</sup>Greenwood, J. A. and Durand, D., "Aids for Fitting the Gamma Distribution by Maximum Likelihood," Technometrics, Vol. 2, No. 1, February 1960, pp. 55-65.

$$nba = \sum_{i=1}^n (x_i - m) \quad (\text{H. 6})$$

$$-n \frac{d}{da} \ln(G(a)) + \sum_{i=1}^n \ln(x_i - m) = n \ln(b) \quad (\text{H. 7})$$

$$b(a-1) \sum_{i=1}^n \frac{1}{(x_i - m)} = n \quad (\text{H. 8})$$

For the special case of interest in this paper,  $m$  is known and equal to zero. Thus, H.8, which is based on  $\partial L / \partial m$ , becomes meaningless. The simultaneous solution of H.6 and H.7 for  $a$  and  $b$  is then possible. Greenwood and Durand provide approximations to the solutions for  $a$  and  $b$  in the form of polynomials represent regression approximations to maximum-likelihood solutions of several data sets. The statistic is  $y = \ln(A) - \ln(G)$ , where  $A$  is the arithmetic mean of the data and  $G$  is the geometric mean of the data. For the parameter values of interest in this paper, the estimation is:

$$\hat{a} = 1/y (0.5000876 + 0.1648852 y - 0.0544272 y^2).$$

The estimate for  $b$  is then:  $\hat{b} = A/\hat{a}$ . Greenwood and Durand also provide polynomial estimators for the variances and the covariances of the estimates. These estimators follow:

$$\text{var}(\hat{a}) = \hat{a}^2 (1.99629 - 1.21163 y + 0.77255 y^2)$$

$$\text{cov}(\hat{a}, \hat{b}) = \hat{a}\hat{b} (1.99629 - 1.21163 y + 0.77255 y^2)$$

$$\text{var}(\hat{b}) = \hat{b}^2 (1.99780 + 0.73462 y + 0.39306 y^2)$$

The maximum error of the estimate of  $a$  is 0.0088% in the area of interest for this paper. This error limit is valid when the sample population is truly gamma distributed. These estimators are employed in Appendix J and provide gamma distributions which fit the data of interest extremely well.

## APPENDIX I

### GOODNESS-OF-FIT TESTS

We wish to test the hypothesis that  $F(x)$  is the cumulative distribution function of the process which produced a given sample of the random variable  $X$ . By applying certain tests, we can either reject or fail to reject the hypothesis. Two tests which are frequently used are the chi-square test and the Kolmogorov-Smirnov test.

The chi-square test requires that the real  $x$ -axis to be divided into  $k$  intervals, the first and last extending to  $-\infty$  and  $+\infty$ , respectively. The intervals are bounded on the left by  $a_{i-1}$  and on the right by  $a_i$ , where the  $a_i$  are chosen so that  $F(x)$  is continuous at the  $a_i$ . Now, the probability that  $X$  will fall into the  $i$ th interval is  $p_i = \Pr(a_{i-1} < X < a_i) = F(a_i) - F(a_{i-1})$ , where  $F(x)$  is defined for a continuous probability density function to be:

$$F(x) = \int_{-\infty}^x f(t) dt.$$

Then, if we have  $n$  observations, the expected number of these observations falling into the  $i$ th interval will be  $e_i = n(p_i)$ . If the number of observations falling into the  $i$ th interval is  $o_i$ , then we compute the quantity  $W$  by:

$$W = \sum_{i=1}^k \frac{(o_i - e_i)^2}{e_i}.$$

When  $W$  is small, then the sample frequencies agree with the expected frequencies well. On the other hand, when  $W$  is large, a large discrepancy between the expected and sample frequencies has occurred. When  $n$  is large and  $k$  satisfies a specific general condition, the quantity  $W$  can be approximated by the chi-square distribution. The general condition requires that the data be grouped such that  $e_i > 5$  for all  $i$ . When we wish to test the hypothesis that  $F(x)$  is the true distribution function of  $X$ , with significance level  $\alpha$ , we divide the real  $x$ -axis into intervals, compute  $W$ , and compare  $W$  with the tabled chi-square value with  $k-1$  degrees of freedom, where  $k$  is the number of intervals. If  $W$  is greater than the tabled chi-square value, the hypothesis is rejected. If  $W$  is less than the tabled chi-square value, the hypothesis is not rejected at the significance level used.

The difficulty in using the chi-square test lies in the selection of a value of  $n$  and in the selection of interval boundaries. In this study, the continuity requirement is not a problem since time, a continuous quantity, is being measured. An alternative to the chi-square test is the Kolmogorov-Smirnov test. This test has the same objective; i.e., testing the hypothesis that a random variable,  $X$ , comes from a process with cumulative distribution function  $F(x)$ . The Kolmogorov-Smirnov test does not require any grouping of data or other arbitrary decisions. The only requirement is that  $F(x)$  is a continuous function of  $x$ . If we define  $F_n(x)$  to be the sample cumulative distribution function, based on a sample of size  $n$ , then the value  $D_n = \max |F_n(x) - F(x)|$  is a random variable.  $D_n$  is the maximum deviation between the hypothesized and observed cumulative distribution functions over all  $x$ . The random variable  $D_n$  has been shown by Kolmogorov and Smirnov to have the distribution function  $L_n(z)$ , and, when  $n$  is large,  $L_n(z)$  approaches the distribution function:

$$L(z) = 1 - 2 \sum_{r=1}^{\infty} (-1)^{r-1} e^{-2r^2 z^2}.$$

Based on the sample size, a maximum acceptable value of  $D_n$  is tabulated for various significance levels. When the computed  $D_n$  is greater than the tabulated value, the hypothesis is rejected. Otherwise, the hypothesis is not rejected.

Further discussion of the two goodness-of-fit tests and tables of the associated distributions are presented by Whitney<sup>1</sup>. When the sample size is greater than 100 and the significance level is .01, the critical value for  $D_n$  can be approximated by  $1.62/\sqrt{n}$ .

---

<sup>1</sup>Whitney, D. R., Elements of Mathematical Statistics, Henry Holt and Company, New York, 1959.

## APPENDIX J

### THEORETICAL DISTRIBUTIONS WITH PARAMETERS AND GRAPHS

Sample outputs of the estimation procedure and goodness-of-fit program are presented on the following pages along with the gamma distribution parameters that have been found to best describe conversation durations as observed in the Fort Carson and Fort Ord data. Because of the large number of cases, only sample results and composites are included.

The results provided by the program include the arithmetic and geometric means of the data set, with values in seconds. The statistic used for computation of the gamma distribution parameters, as described in Appendix I is printed with the title "Hastings Statistic", since the method of Hastings was used for the regression analysis. The two parameters and their associated variances (computed by the polynomials of Appendix II) are printed. The parameter  $a$  is noted as "ALPHA", and the parameter  $b$  is noted as "BETA".

Numerical values related to the Kolmogorov-Smirnov test are also printed. This test is described in Appendix I. The Kolmogorov-Smirnov statistic is the maximum deviation between the theoretical and data-generated cumulative density functions. The  $x$  value at which this maximum occurred is also printed. The critical value of the test is approximated as discussed in Appendix I. The decision for the test is based on a comparison of the critical value and the Kolmogorov-Smirnov statistic.

The graph accompanying each output presents both the theoretical and data-generated cumulative density function. The theoretical cumulative distribution function is plotted using the character (T); and the data-generated cumulative distribution function is plotted using the character (D). These graphs represent the cumulative distribution function on the vertical scale and time in seconds on the horizontal scale.



---

---

FT ORD SITUATION 6

---

---

NUMBER OF DATA POINTS 151  
ARITHMETIC MEAN 31.367920  
GEOMETRIC MEAN 23.720123

---

---

HASTINGS STATISTIC 0.279462  
COMPUTED PARAMETERS  
ALPHA = 1.939140 VARIANCE = 6.460  
BETA = 16.176193 VARIANCE = 584.515

---

---

KOLMOGOROV-SMIRNOV STATISTIC = 0.094  
OCCURRING AT X = 26.6  
CRITICAL VALUE FOR TEST AT .01 SIGNIFICANCE = 0.13  
DECISION FOR THIS DATA SET---ACPT

---

---

---

---

---

---

---

---

---

---



---

---

FT ORD ALL DATA EDITED

---

---

NUMBER OF DATA POINTS 408  
ARITHMETIC MEAN 33.307037  
GEOMETRIC MEAN 25.301147

---

---

HASTINGS STATISTIC 0.274920  
COMPUTED PARAMETERS  
ALPHA = 1.968953 VARIANCE = 6.674  
BETA = 16.916107 VARIANCE = 637.972

---

---

KOLMOGOROV-SMIRNOV STATISTIC = 0.056  
OCCURRING AT X = 26.7  
CRITICAL VALUE FOR TEST AT .01 SIGNIFICANCE = 0.08  
DECISION FOR THIS DATA SET---ACPT

---

---

---

---

---

---

---

---

---

---

[illegible]

---

---

FORT ORD ALL DATA AS IS

---

NUMBER OF DATA POINTS 406

ARITHMETIC MEAN 33.410049

GEOMETRIC MEAN 25.406082

---

HASTINGS STATISTIC 0.273869

COMPUTED PARAMETERS

ALPHA = 1.975991 VARIANCE = 6.725

BETA = 16.907990 VARIANCE = 637.074

---

KOLMOGOROV-SMIRNOV STATISTIC = 0.056

OCCURRING AT X = 26.7

CRITICAL VALUE FOR TEST AT .01 SIGNIFICANCE = 0.08

DECISION FOR THIS DATA SET---ACPT

---

---

---

---

---

---

---

---

---

---

WAVE	Q	C/F	5.000E-04	7.000E-01	6.000E-01	8.000E-01	1.000E-02
1	1.000E-01						
2	1.000E-01						
3	1.000E-01						
4	1.000E-01						
5	1.000E-01						
6	1.000E-01						
7	1.000E-01						
8	1.000E-01						
9	1.000E-01						
10	1.000E-01						
11	1.000E-01						
12	1.000E-01						
13	1.000E-01						
14	1.000E-01						
15	1.000E-01						
16	1.000E-01						
17	1.000E-01						
18	1.000E-01						
19	1.000E-01						
20	1.000E-01						
21	1.000E-01						
22	1.000E-01						
23	1.000E-01						
24	1.000E-01						
25	1.000E-01						
26	1.000E-01						
27	1.000E-01						
28	1.000E-01						
29	1.000E-01						
30	1.000E-01						
31	1.000E-01						
32	1.000E-01						
33	1.000E-01						
34	1.000E-01						
35	1.000E-01						
36	1.000E-01						
37	1.000E-01						
38	1.000E-01						
39	1.000E-01						
40	1.000E-01						
41	1.000E-01						
42	1.000E-01						
43	1.000E-01						
44	1.000E-01						
45	1.000E-01						
46	1.000E-01						
47	1.000E-01						
48	1.000E-01						
49	1.000E-01						
50	1.000E-01						
51	1.000E-01						
52	1.000E-01						
53	1.000E-01						
54	1.000E-01						
55	1.000E-01						
56	1.000E-01						
57	1.000E-01						
58	1.000E-01						
59	1.000E-01						
60	1.000E-01						
61	1.000E-01						
62	1.000E-01						
63	1.000E-01						
64	1.000E-01						
65	1.000E-01						
66	1.000E-01						
67	1.000E-01						

---

---

CARSON PLATCCN COMPOSITE

---

NUMBER OF DATA POINTS 190

ARITHMETIC MEAN 21.187836

GEOMETRIC MEAN 14.295054

---

HASTINGS STATISTIC 0.393514

COMPUTED PARAMETERS

ALPHA = 1.414292 VARIANCE = 3.279

BETA = 14.981227 VARIANCE = 526.922

---

KOLMOGOROV-SMIRNOV STATISTIC = 0.060

OCCURRING AT X = 11.5

CRITICAL VALUE FOR TEST AT .01 SIGNIFICANCE = 0.11

DECISION FOR THIS DATA SET---ACPT

---

---

---

---

---

---

---

---

---

---

NAME	O	C	2-PLACE 01	4-PLACE 01	6-PLACE 01	8-PLACE 01	1-NOOF 07
1.000F 90							
2.000F 01							
3.000F 01							
4.000F 01							
5.000F 01							
6.000F 01							
7.000F 01							
8.000F 01							
9.000F 01							
10.000F 01							
11.000F 01							
12.000F 01							
13.000F 01							
14.000F 01							
15.000F 01							
16.000F 01							
17.000F 01							
18.000F 01							
19.000F 01							
20.000F 01							
21.000F 01							
22.000F 01							
23.000F 01							
24.000F 01							
25.000F 01							
26.000F 01							
27.000F 01							
28.000F 01							
29.000F 01							
30.000F 01							
31.000F 01							
32.000F 01							
33.000F 01							
34.000F 01							
35.000F 01							
36.000F 01							
37.000F 01							
38.000F 01							
39.000F 01							
40.000F 01							
41.000F 01							
42.000F 01							
43.000F 01							
44.000F 01							
45.000F 01							
46.000F 01							
47.000F 01							
48.000F 01							
49.000F 01							
50.000F 01							
51.000F 01							
52.000F 01							
53.000F 01							
54.000F 01							
55.000F 01							
56.000F 01							
57.000F 01							
58.000F 01							
59.000F 01							
60.000F 01							
61.000F 01							
62.000F 01							
63.000F 01							
64.000F 01							
65.000F 01							
66.000F 01							
67.000F 01							
68.000F 01							
69.000F 01							



---

---

TYPICAL PLATCON AND CC NET MIXTURE

---

NUMBER OF DATA POINTS 415

ARITHMETIC MEAN 27.474823

GEOMETRIC MEAN 19.040325

---

HASTINGS STATISTIC 0.366711

COMPUTED PARAMETERS

ALPHA = 1.508636 VARIANCE = 3.769

BETA = 18.211685 VARIANCE = 769.480

---

KOLMOGOROV-SMIRNOV STATISTIC = 0.050

OCCURRING AT X = 26.6

CRITICAL VALUE FOR TEST AT .01 SIGNIFICANCE = 0.08

DECISION FOR THIS DATA SET---ACPT

---

---

---

---

---

---

---

---

---

---



### Summary of Parameters

Table J. 1

#### Gamma Distribution Parameters

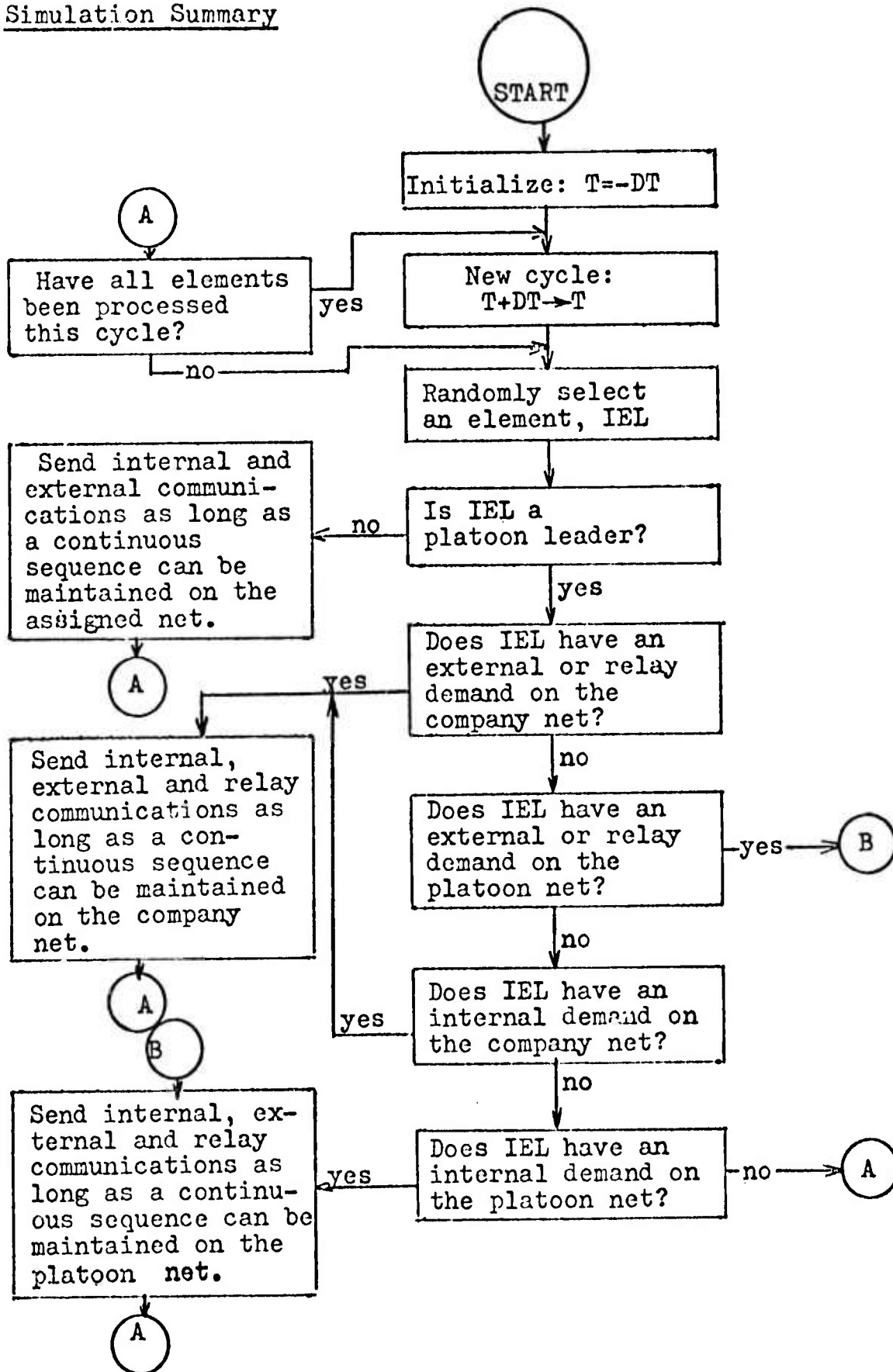
Communication	a	b	Mean	Variance
Internal	1. 70	19. 45 sec.	. 55 min.	. 18 min. <sup>2</sup>
External	1. 83	20. 84 sec.	. 64 min.	. 22 min. <sup>2</sup>
All Company	1. 97	16. 92 sec.	. 55 min.	. 16 min. <sup>2</sup>
All Platoon	1. 41	14. 98 sec.	. 42 min.	. 13 min. <sup>2</sup>

## APPENDIX K

### SIMULATION FLOWCHARTS

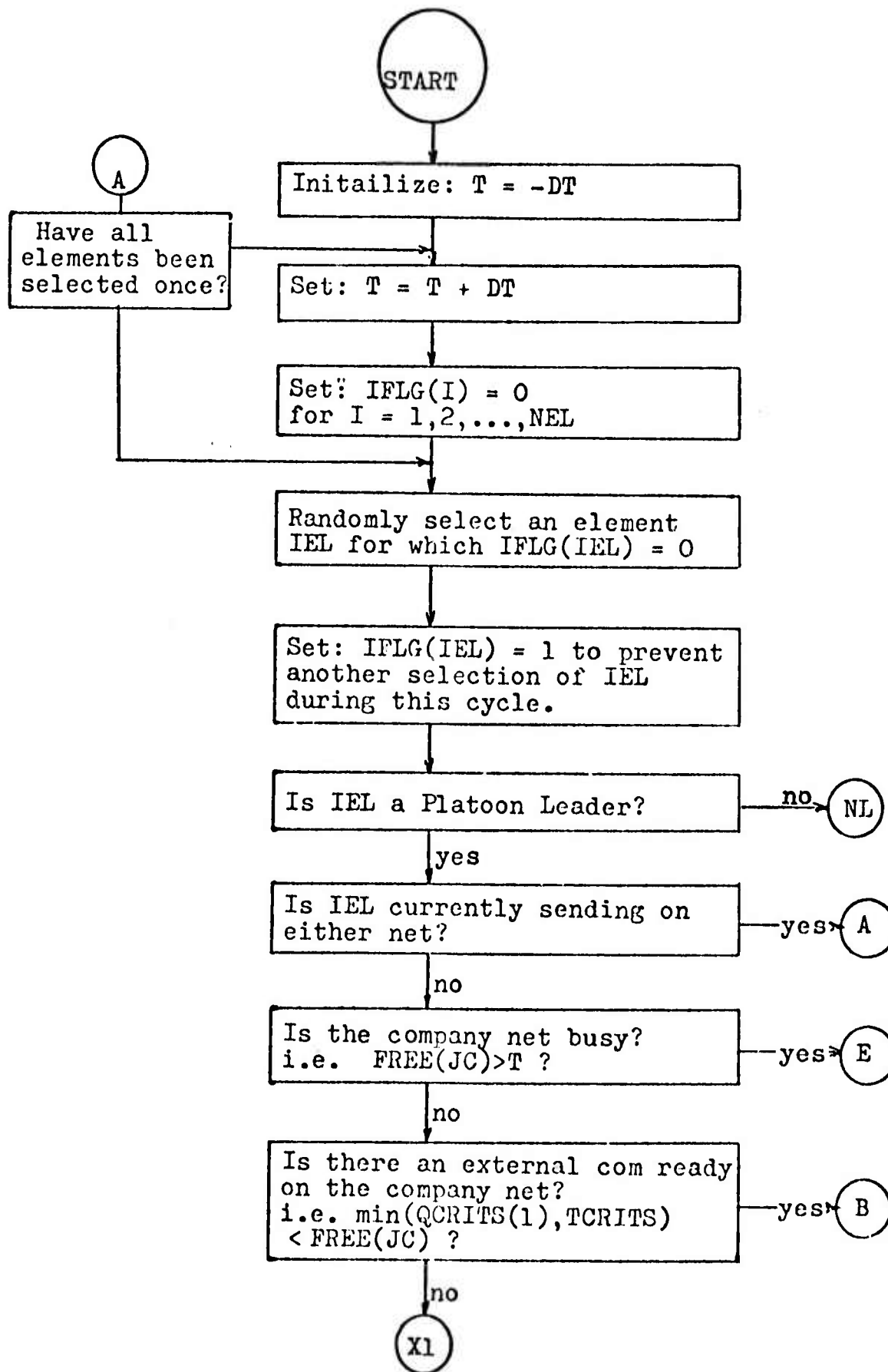
The flowcharts in this appendix are divided into two parts. First, a flowchart of the entire simulation is presented on a single page. This provides a map for the detailed flowchart which follow. The flowchart of the following pages are completely detailed and the variable names used match those used in the computer program. A listing of these variable names and their significance precedes the detailed flowcharts.

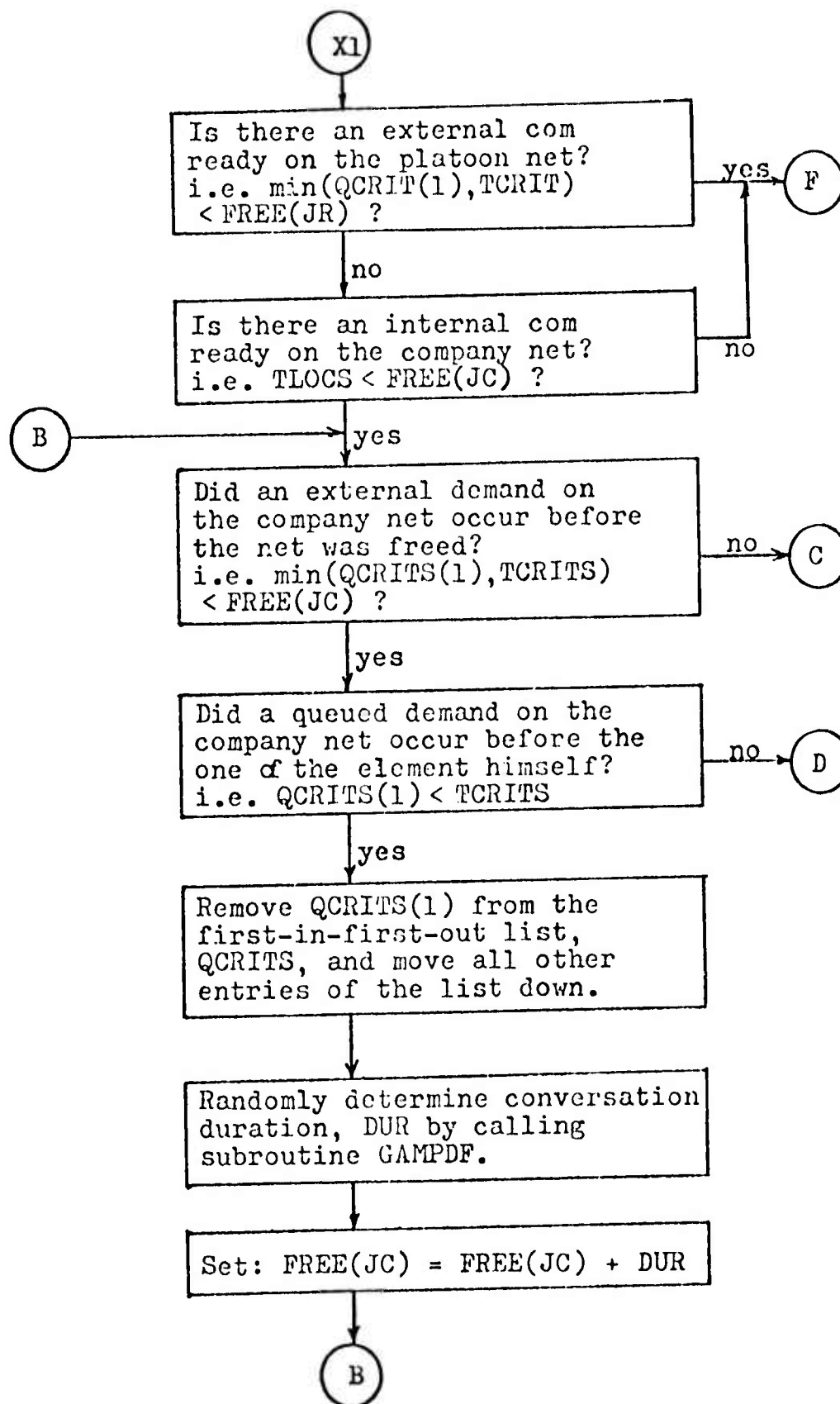
# Simulation Summary



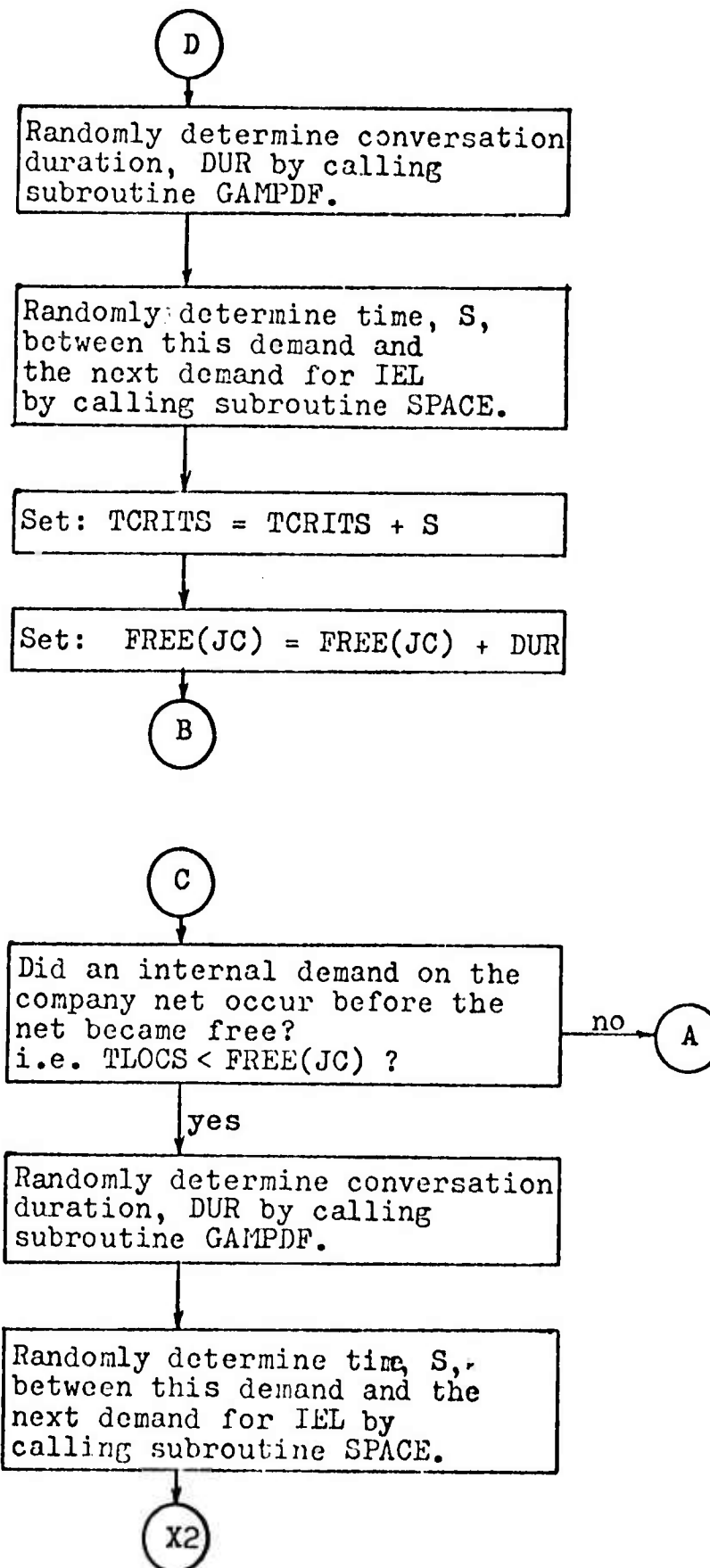
### Simulation Variables

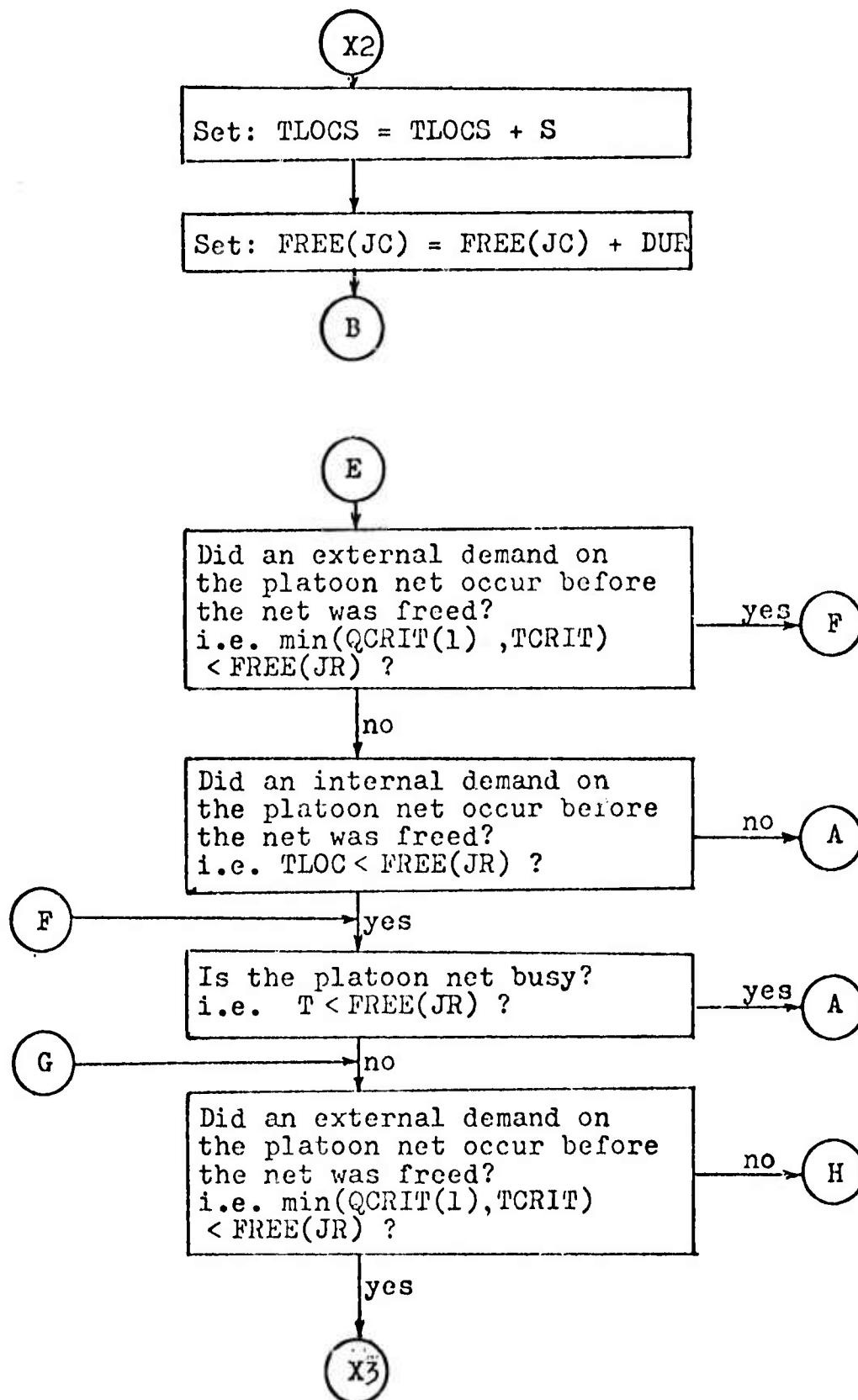
TLOC (i)	Array containing times of first unsatisfied internal demand (platoon net demand for the platoon leaders)
TLOCS (i)	Array containing times of first unsatisfied internal demand on company net for platoon leaders
TCRIT (i)	Array containing times of first unsatisfied external demand (platoon net demand for the platoon leaders)
TCRITS (i)	Array containing times of first unsatisfied external demand on company net for platoon leaders
JR	Net number of element under consideration (platoon net of platoon leaders)
JC	Company net number when platoon leader is element under consideration
T	Time beyond which nets are considered busy for a given cycle
DT	Time between cycles of updating nets
IFLG	Flag to indicate which elements have been selected for net access during a given cycle
IEL	Element number of element under consideration
FREE	Array of times indicating when each net will next be free
QCRIT	Variable length array of communications waiting to be relayed from company to platoon net
QCRITS	Variable length array of communications waiting to be relayed from platoon to company net

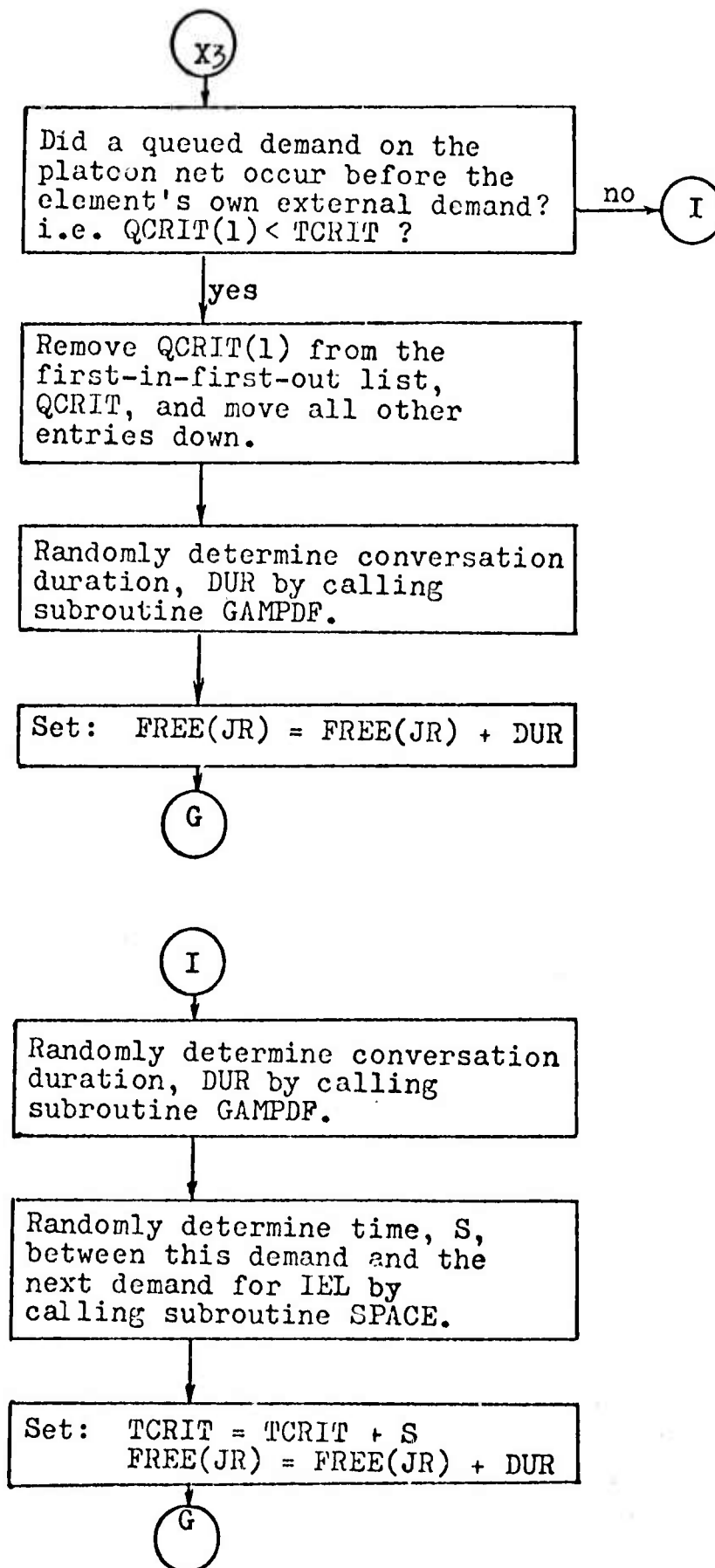


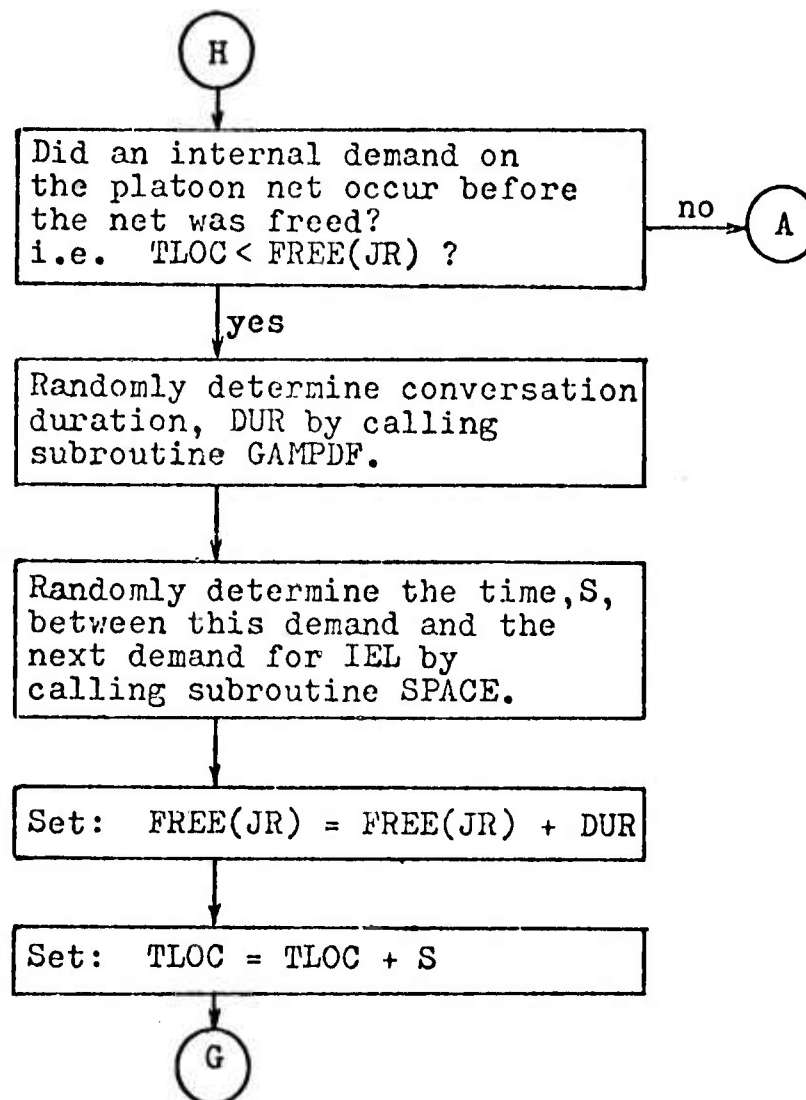


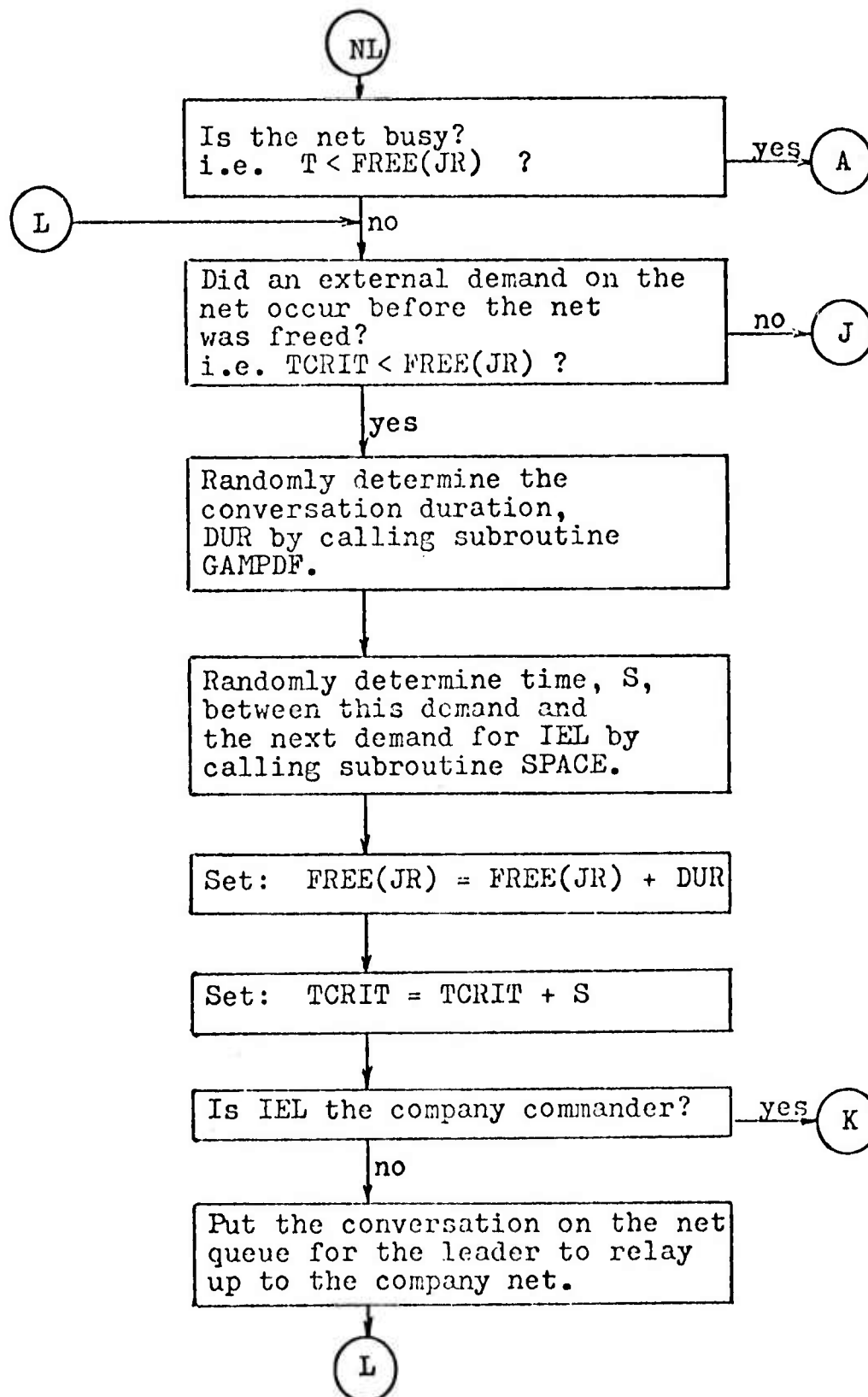


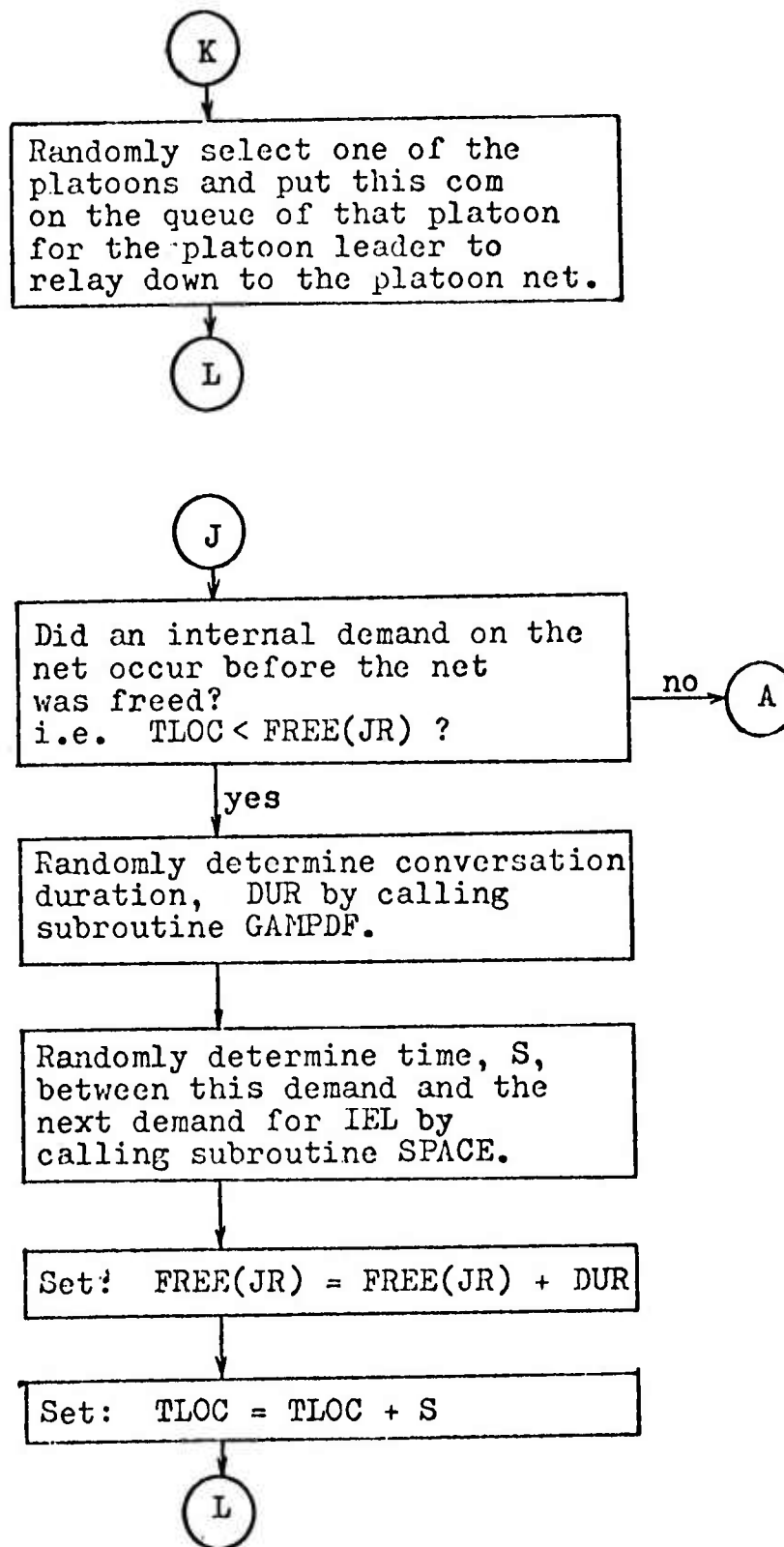












## APPENDIX L

### SOLUTION FOR MISSILE DISPLACEMENT IN THE CONTINUOUS FLIGHT TRACE MODEL

In the continuous flight trace version of the Beam-Rider Missile Model, equation 6.3 specifies the basic assumption characterizing the model. That is,

$$h''(t) = -K( h(t) - C - l(t) ) - \beta( h'(t) - l'(t) ) + \epsilon \quad (6.3)$$

where

$h(t)$  = missile displacement (elevation) at time  $t$

$l(t)$  = tracker line of sight or desired elevation at time  $t$

$$l(t) = Z_0 + Z_1 t$$

$K$  and  $\beta$  are proportionality constants

$C$  = missile constant flight bias

$Z_0$  and  $Z_1$  are constants

$\epsilon$  = a stochastic effect that varies between time intervals of length TMINC but is constant within each time interval.

A solution to equation 6.3 is derived in this appendix for the functions  $h(t)$  and  $h'(t)$ . This solution regards the time parameter,  $t$ , as being zero at the beginning of a computational interval and  $t$  would equal TMINC at the end of the interval; thus,  $\epsilon$  can be regarded as a constant in this derivation. In addition, the initial conditions  $h(0)$ ,  $l(0) = Z_0$ , and  $h'(0)$  are really inputs from the previous time interval once the missile has commenced flying.

The solution for  $h(t)$  and  $h'(t)$  will be derived by taking Laplace transforms of equation 6.3, and the Laplace transforms of  $h(t)$  and  $l(t)$  are represented by:

$$\begin{aligned} h(t) &\longleftrightarrow H(s) \\ l(t) &\longleftrightarrow \frac{Z_0 s + Z_1}{s^2} = L(s) \end{aligned} \quad (L.1)$$

Taking the Laplace transform of equation 6.3,

$$s^2 H(s) - s h(0) - h'(0) = -K(H(s) - C/s - L(s))$$

$$-\beta(s H(s) - h(0) - s L(s) + l(0)) + \epsilon/s$$

(L. 2)

where  $h(0)$ ,  $h'(0)$ , and  $l(0) = Z_0$  are initial conditions of missile elevation, rate of change of elevation, and desired elevation, respectively. Substituting L. 1 into L. 2 and solving for  $H(s)$ ,

$$H(s) = \frac{(Z_0 s + Z_1)(\beta s + K)}{s^2(s^2 + \beta s + K)} + \frac{s h(0) + h'(0) + \beta h(0) - \beta l(0)}{s^2 + \beta s + K}$$

$$+ \frac{KC + \epsilon}{s(s^2 + \beta s + K)}$$

Noting that  $s^2 + \beta s + K = (s + (\beta + \sqrt{\beta^2 - 4K})/2) \cdot (s + (\beta - \sqrt{\beta^2 - 4K})/2)$ , then

$$H(s) = \frac{(Z_0 s + Z_1)(\beta s + K)}{s^2 (s + (\beta + \sqrt{\beta^2 - 4K})/2) \cdot (s + (\beta - \sqrt{\beta^2 - 4K})/2)}$$

$$+ \frac{s h(0) + h'(0) + \beta h(0) - \beta Z_0}{(s + (\beta + \sqrt{\beta^2 - 4K})/2)(s + (\beta - \sqrt{\beta^2 - 4K})/2)}$$

$$+ \frac{KC + \epsilon}{s(s + (\beta + \sqrt{\beta^2 - 4K})/2)(s + (\beta - \sqrt{\beta^2 - 4K})/2)} \quad (L. 3)$$



Taking the inverse transform of L. 3, the displacement (elevation) at time  $t$ ,  $h(t)$ , is determined as:

$$\begin{aligned}
 h(t) = & Z_0 + C + 4\epsilon / (\beta^2 + \omega^2) + Z_1 t \\
 & + \exp(-\beta t/2) \cdot \left[ (h(0) - Z_0 - C - 4\epsilon / (\beta^2 + \omega^2)) \cdot \cos(\omega t/2) \right. \\
 & \left. + (\beta (h(0) - Z_0 - C - 4\epsilon / (\beta^2 + \omega^2)) + 2(h'(0) - Z_1)) \cdot \sin(\omega t/2) / \omega \right],
 \end{aligned}
 \tag{L. 4}$$

where  $\omega = \sqrt{4K - \beta^2}$ ; thus,  $K = (\beta^2 + \omega^2)/4$ .

Recall that  $4K - \beta^2 > 0$  since the missile is assumed to be an underdamped system.

Since equation L. 4 is applied recursively by the Beam-Rider Missile Model,  $h(t)$  at the end of a time interval of length  $TMINC$  becomes the input value  $h(0)$  for the succeeding time interval. In addition,  $h'(t)$  at the end of the time interval must be calculated in order to determine  $h'(0)$  for the next time interval. The expression for  $h'(t)$  is

$$\begin{aligned}
 h'(t) = & Z_1 - (\beta/2) \cdot \exp(-\beta t/2) \cdot \left[ (h(0) - Z_0 - C - 4\epsilon / (\beta^2 + \omega^2)) \cdot \cos(\omega t/2) \right. \\
 & \left. + (\beta (h(0) - Z_0 - C - 4\epsilon / (\beta^2 + \omega^2)) + 2(h'(0) - Z_1)) \cdot \sin(\omega t/2) / \omega \right] \\
 & + \exp(-\beta t/2) \cdot \left[ (Z_0 + C + 4\epsilon / (\beta^2 + \omega^2) - h(0)) \cdot \sin(\omega t/2) \cdot \omega/2 \right. \\
 & \left. + (\beta (h(0) - Z_0 - C - 4\epsilon / (\beta^2 + \omega^2)) + 2(h'(0) - Z_1)) \cdot \cos(\omega t/2) / 2 \right].
 \end{aligned}
 \tag{L. 5}$$

## APPENDIX M

### ESTIMATORS FOR PARAMETERS IN THE CONTINUOUS FLIGHT-TRACE MODEL

#### Introduction

Estimators for the  $\beta$ ,  $\omega$ , and  $C$  parameters in the continuous flight-trace model are derived in this appendix, and these estimators are to be determined from either pitch or yaw flight data for a single missile flight. These data consist of a sequence of points that are uniformly spaced over time with intervals of  $\Delta t$  seconds. The following quantities are required for each point:

1. missile deviation in both pitch and yaw from the tracker's line of sight in meters,
2. tracker's line-of-sight deviation in both pitch and yaw from the true gunner-target line in meters.

Using the above data, estimates of  $\beta$ ,  $\omega$ , and  $C$  are computed for both pitch and yaw inputs in equation L. 4. Note that  $\Delta t$  should be equivalent to TMINC used in subroutine SHILLY.

The approach to determining the requisite estimators used in this appendix is listed below:

1. Specify the distribution of missile displacements for each data point.
2. Show that the maximum likelihood estimates of  $\beta$ ,  $\omega$ , and  $C$  are equivalent to the least-squares estimates and specify the sum of squares that is to be minimized in determining values of  $\beta$ ,  $\omega$ , and  $C$ .
3. Show that the result of step 2 above is equivalent to the maximum likelihood estimates for the discontinuous flight-trace model determined by program MBWEST.

The above steps are accomplished in the following sections of this appendix.

### Distribution of Missile Displacement

Equation L. 4 gives the missile displacement at time  $t$  and is used to determine the probability distribution of missile displacements. Certain inputs are required to evaluate equation L. 4, viz., the status at the beginning of the time interval,  $(h(0), h'(0), Z_0)$ , the tracker's line of sight during the time interval  $(Z_1)$ , and a stochastic effect  $(\epsilon_i)$  on the missile acceleration during the  $i^{\text{th}}$  time interval of length  $\Delta t$ .  $\epsilon_i$  is assumed to vary between time intervals of length  $\Delta t$ , and the values of  $\epsilon_i$  are assumed to be mutually independent and have a normal distribution with mean zero and variance,  $\sigma_c^2$ . The conditional distribution of missile displacement given the inputs  $h(0)$ ,  $h'(0)$ ,  $Z_0$ , and  $Z_1$  is determined in this section.

The function  $h(t)$  given by L. 4 can be regarded as a function of  $\beta$ ,  $\omega$ ,  $C$ ,  $t$ , and  $\epsilon_i$  during the  $i^{\text{th}}$  time interval starting at time  $\Delta t(i-1)$  after the beginning of the missile flight. Letting  $h_i^C(\beta, \omega, C, t, \epsilon_i)$  be that function, then

$$\begin{aligned} h_i^C(\beta, \omega, C, t, \epsilon_i) = & Z_0 + C + Z_1 t + \exp(-\beta t/2) \cdot \left[ (h(0) - Z_0 - C) \cdot \cos(\omega t/2) \right. \\ & + (\beta(h(0) - Z_0 - C) + 2(h'(0) - Z_1)) \cdot \sin(\omega t/2)/\omega \Big] \\ & + \epsilon_i \cdot 4/(\beta^2 + \omega^2) \cdot \left[ 1 - \exp(-\beta t/2) (\cos(\omega t/2) + \beta \sin(\omega t/2)/\omega) \right] \end{aligned}$$

(M. 1)

where

$$h_i^C(\beta, \omega, C, t, \epsilon_i) = \text{missile displacement from the true gunner-target line of sight calculated by the continuous flight-trace model at time } t \text{ since the start of } i^{\text{th}} \text{ time interval given parameter values } \beta, \omega, C \text{ and stochastic acceleration effect } \epsilon_i.$$

Note that  $t = 0$  at the beginning of the time interval and the values for  $h(0)$ ,  $h'(0)$ , and  $Z_0$  are determined from conditions existing at the beginning of the time interval.

Actually the expression for  $h_i^C(\beta, \omega, C, t, \epsilon_i)$  given by equation M. 1 can be rewritten and related to the discontinuous flight trace model. That is,

$$h_i^C(\beta, \omega, C, t, \epsilon_i) = h_i(\beta, \omega, C, t) + \epsilon_i \cdot 4/(\beta^2 + \omega^2) \cdot (1 - \exp(-\beta t/2)(\cos(\omega t/2) + \beta \cdot \sin(\omega t/2)/\omega)) \quad (M.2)$$

where  $h_i(\beta, \omega, C, t)$  = predicted mean missile position given by the discontinuous flight trace model at time  $t$  since the start of the  $i^{\text{th}}$  time interval given parameter values  $\beta, \omega, C$ .

$h_i(\beta, \omega, C, t)$  is given by equation 6.2. In the discontinuous flight trace model actual observations at the end of each time interval are given by

$$x_i = h_i(\beta, \omega, C, \Delta t) + e_i,$$

where  $x_i$  = actual missile displacement at the end of the  $i^{\text{th}}$  time interval ( $\Delta t$  since its beginning),

$e_i$  = a normally distributed stochastic effect with mean zero and variance  $\sigma^2$ .

The above expression for  $x_i$  is equivalent to the expression given on page 8-29 of Volume 1.

Returning to the continuous flight trace model, the conditional distribution of the missile displacement during the  $i^{\text{th}}$  time interval given inputs from the  $i-1^{\text{st}}$  interval are readily determined from equation M.2. Noting the  $\epsilon_i$  is the only stochastic variable in M.2, then  $h_i^C(\beta, \omega, C, t, \epsilon_i)$  is normal with mean  $h_i(\beta, \omega, C, t)$  and variance  $\sigma_C^2 16/(\beta^2 + \omega^2)^2 [1 - \exp(-\beta t/2)(\cos(\omega t/2) + \beta \sin(\omega t/2)/\omega)]^2$ .

#### Maximum Likelihood Estimators for $\beta, \omega$ , and $C$

In this section, an expression is derived which when solved gives the maximum likelihood estimators for  $\beta, \omega$ , and  $C$ , in the continuous flight trace model. Analysis of this expression reveals that the least squares estimates for  $\beta, \omega$ , and  $C$  are equivalent to the maximum likelihood estimates.

The likelihood function for a single missile flight is equivalent to the product of the probability density functions for the conditional distributions of missile displacements at the end of each time interval. That is,

$$L(X, \beta, \omega, C, \sigma_c^2) = \prod_{i=1}^n [\sqrt{2\pi} S_C \exp(-(x_i - h_i(\beta, \omega, C, \Delta t))^2 / (2 S_C^2))] , \quad (M.3)$$

where

$L(X, \beta, \omega, C, \sigma_c^2)$  = likelihood function for a missile flight given parameters  $\beta, \omega, C$ , and  $\sigma_c^2$  and the vector  $X$  of actual missile displacements.

$x_i$  = actual missile displacement at the end of the  $i$ th time interval.

$X$  = vector made up of elements  $x_i, i = 1, 2, \dots, n$

$n$  = total number of time intervals in the missile flight.

$S_C$  = standard deviation of the distribution of conditional missile displacements at the end of each time interval, i.e., standard deviation of the distribution of  $h_i^C(\beta, \omega, C, \Delta t, \epsilon_i)$  values.

$$S_C = \sigma_c \sqrt{4/(\beta^2 + \omega^2)[1 - \exp(-\beta t/2)(\cos(\omega t/2) + \beta \sin(\omega t/2)/\omega)]}$$

The logarithm of the likelihood function is

$$\ln L(X, \beta, \omega, C, \sigma_c^2) = -(\ln(2\pi)/2 + \ln S_C)n - \sum_{i=1}^n (x_i - h_i(\beta, \omega, C, \Delta t))^2 / (2 S_C^2) \quad (M.4)$$

Since the logarithm is a strictly monotonic and continuous function, then a set of values for  $\beta, \omega, C$ , and  $\sigma_c^2$  maximizing the log of the likelihood function gives a maximum value for the likelihood function. Note that  $S_C$  is a function of  $\sigma_c, \beta, \omega$ , and  $C$  so it is not obvious at this point that a least squares solution for  $\beta, \omega$ , and  $C$  also maximizes equation M.4.

To show that the least squares solution is also a maximum likelihood solution, equation M.4 will be differentiated with respect to  $\sigma_c$  and set to zero to uncover relationships at the stationary point(s). That is,

$$\frac{\partial \ln L(X, \beta, \omega, C, \sigma_c^2)}{\partial \sigma_c} = -n/S_C \left( \frac{\partial S_C}{\partial \sigma_c} \right) + \sum_{i=1}^n (x_i - h_i(\beta, \omega, C, \Delta t))^2 \frac{\partial S_C}{\partial \sigma_c} / S_C^3 = 0$$

Multiplying the above equation by  $S_C^3$  and then dividing it by  $\frac{\partial S_C}{\partial \sigma_c}$  under the assumption that  $\frac{\partial S_C}{\partial \sigma_c} \neq 0$  at the stationary point, the following relationship holds at all stationary points of M. 4.

$$-nS_C^2 + \sum_{i=1}^n (x_i - h_i(\beta, \omega, C, \Delta t))^2 = 0$$

The above equation implies that each stationary point of M. 4 has the property

$$S_C^2 = \sum_{i=1}^n (x_i - h_i(\beta, \omega, C, \Delta t))^2 / n \quad (M. 5)$$

Since stationary points incorporate the above relationship, it can be substituted into M. 4, giving

$$\ln L(X, \beta, \omega, C, \sigma_c^2) = -(\ln(2\pi)/2 + \ln S_C)n - n/2 \quad (M. 6)$$

Equation M. 6 is true when the likelihood function assumes a maximum value.

In equation M. 6, only one term is not a constant and is a function of one or more of the parameters  $\beta$ ,  $\omega$ ,  $C$ , or  $\sigma_c^2$ . That is,  $-n \ln S_C$ . Thus, the maximum likelihood estimates of  $\beta$ ,  $\omega$ ,  $C$ , and  $\sigma_c^2$  are obtained when  $S_C$  is a minimum. By equation M. 5, this occurs when the sum of squares  $SS$ , shown below, is a minimum. That is, the maximum likelihood estimates of  $\beta$ ,  $\omega$ ,  $C$ , and  $\sigma_c^2$  for the continuous flight trace model are obtained by minimizing:

$$SS = \sum_{i=1}^n (x_i - h_i(\beta, \omega, C, \Delta t))^2 \quad (M. 7)$$

Equation M. 7 supplies the results sought in this appendix. First, maximum likelihood estimates of  $\beta$ ,  $\omega$ , and  $C$  for the continuous flight trace model are equivalent to least squares estimates. Moreover, these maximum likelihood estimates are equivalent to the maximum likelihood estimates for  $\beta$ ,  $\omega$ , and  $C$  in the discontinuous flight trace model. That is, minimizing M. 7 to obtain least squares estimates of  $\beta$ ,  $\omega$ , and  $C$  is identical to the procedure described for the discontinuous flight trace model on page 8-29 of Volume 1 and computed by program MBWEST.

## APPENDIX N

### COMPUTATION OF STOCHASTIC ACCELERATION ERROR VARIANCES

A procedure for computing the variance of the stochastic acceleration errors;  $\epsilon_i$ ,  $i = 1, 2, \dots, N$ ; employed in the continuous flight-track Beam-Rider Missile Model is derived in this appendix. That is, the values of  $\sigma_{ei}^2$  are determined so that the variance of the missile displacement as a function of time with a fixed tracker line of sight and no constant flight bias is equivalent to an input function determined from missile design analysis. That is,

$z(t)$  = missile displacement at time  $t$  since the beginning of the flight given a fixed tracker line of sight and no constant flight bias, i. e.,  $C = 0$ ,

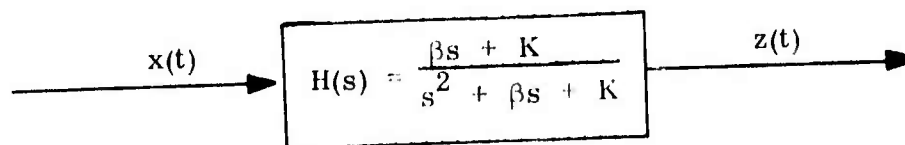
$\sigma_{ei}^2$  = variance of the acceleration error during time interval  $i$ ,

$\text{VAR}(z(t))$  = variance of  $z(t)$  specified by a design analysis, and

values of  $\sigma_{ei}^2$  must be determined so that  $\text{VAR}(z(t))$  is equal to a predetermined functional value. Note that  $z(t)$  is actually composed of a sequence of functions noted as  $h(t)$  in Appendix L.

The solution procedure for values of  $\sigma_{ei}^2$  is derived by finding an expression for  $z(t)$  as a function of values for  $\epsilon_i$ . Then, the variance of  $z(t)$  or  $\text{VAR}(z(t))$  is determined as a function of values of  $\sigma_{ei}^2$ . This functional relationship between  $\text{VAR}(z(t))$  and its input predetermined value is solved recursively to determine values for  $\sigma_{ei}^2$ .

The beam-rider control model can be represented by the block diagram shown below.



The first step in the derivation of a procedure for specifying  $\sigma_{ei}^2$ ;  $i = 1, 2, \dots, N$ ; is to determine the input function  $x(t)$  which generates  $z(t)$  equivalent to a continuous



flight-trace produced by a sequence of stochastic acceleration errors,  $\epsilon_i$ ,  
 $i = 1, 2, \dots, n$ ;

where  $n = [(t - t_1)/\Delta t] + 1$ ,

$t_1$  = beginning of the first time interval,

$[x]$  = greatest integer less than or equal to  $x$ , and

$n \leq N$

let  $Z(s)$  = Laplace transform of  $z(t)$ , and

$X(s)$  = Laplace transform of  $x(t)$ .

Assume for a moment that the flight is sufficiently short that only one time interval of length  $\Delta t$  is involved; thus, only one value of  $\epsilon_i$  is required, viz.,  $\epsilon_1$ . In addition, the assumption is made that the first acceleration error is applied at time zero, i. e.,  $t_1 = 0$ . From equation L. 3, the expression for  $Z(s)$  is

$$Z(s) = \frac{\epsilon_1}{s(s^2 + \beta s + K)} .$$

By definition of a transfer function

$$H(s) = \frac{Z(s)}{X(s)} ,$$

or

$$X(s) = \frac{Z(s)}{H(s)} = \frac{\epsilon_1}{s(\beta s + K)} \quad (N.1)$$

The inverse transform of  $X(s)$  given by N. 1 is \*

$$x(t) = (\epsilon_1/K) (1 - \exp(-Kt/\beta)) \quad (N.2)$$

Rather than one time interval of length  $\Delta t$  with a single value of  $\epsilon_i$  as assumed above, the flight has a sequence of these stochastic acceleration errors.

\* Aseltine, John A., Transform Method in Linear System Analysis, New York: McGraw-Hill Book Company, Inc., 1958, p. 287.

Each error is imposed over a fixed length of time and produces a component of the input function  $x(t)$  shown in the above block diagram. The unit step function  $U(t)$  can be used to represent one of these inputs over a time interval of length  $\Delta t$ . That is,

$$(\epsilon_i/K)(1 - \exp(-K(t - (i-1)\Delta t - t_1)/\beta))(U(t - (i-1)\Delta t - t_1) - U(t - i\Delta t - t_1))$$

is the input during the time interval starting at

$$(i-1)\Delta t + t_1 \text{ and ending at } i\Delta t - t_1,$$

$$\text{where } U(t) = \begin{cases} 1 & \text{if } t \geq 0 \\ 0 & \text{if } t < 0, \text{ and} \end{cases}$$

$$t_1 = \text{time that first time interval commences.}$$

The entire function  $x(t)$  is formed by summing these input components over each time interval up to and including  $t$ . That is,

$$x(t) = \sum_{i=1}^n (\epsilon_i/K) (1 - \exp(-K(t - (i-1)\Delta t - t_1)/\beta)) \cdot (U(t - (i-1)\Delta t - t_1) - U(t - i\Delta t - t_1)) \quad (N.3)$$

A typical input function is illustrated in Figure N.1.

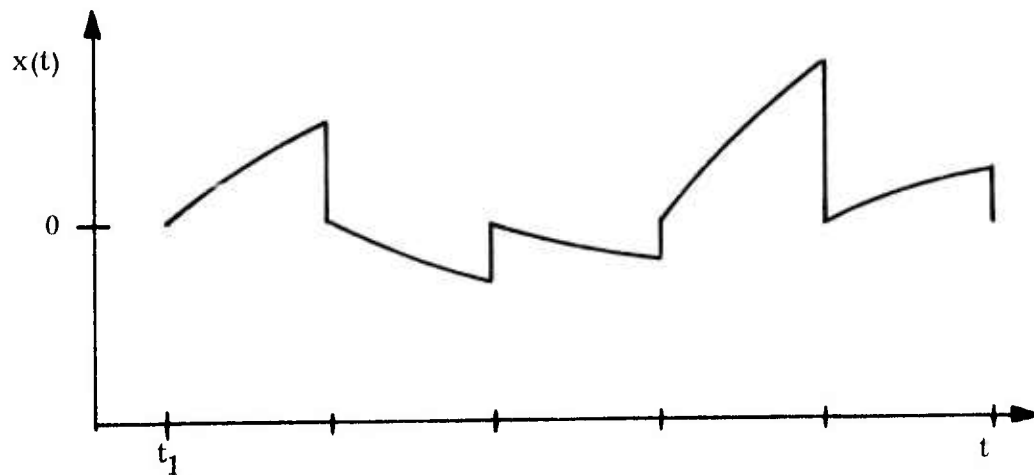


Figure N.1. --Stochastic Input Function  $x(t)$

To calculate the output function  $z(t)$ , the Laplace transform of  $x(t)$  is used. Letting,

$$f(t) \longleftrightarrow F(s)$$

denote Laplace transform pairs in the time and Laplace transform domains, then

$$(\epsilon_i/K) (1 - \exp(-K(t - (i-1)\Delta t - t_1)/\beta)) U(t - (i-1)\Delta t - t_1)$$

$$\longleftrightarrow \frac{\exp(-(i-1)\Delta t + t_1)s\epsilon_i}{s(\beta s + K)}$$

$$U(t - i\Delta t - t_1) \longleftrightarrow \exp(-(i\Delta t + t_1)s)/s$$

$$\exp(-K(t - (i-1)\Delta t - t_1)/\beta) \cdot U(t - i\Delta t - t_1)$$

$$\longleftrightarrow \exp(-(K\Delta t/\beta + (i\Delta t + t_1)s))/(s + K/\beta)$$

Thus,

$$X(s) = \sum_{i=1}^N \left[ \frac{\epsilon_i \cdot \exp(-(i-1)\Delta t + t_1)s}{s(\beta s + K)} - \frac{\epsilon_i \cdot \exp(-(i\Delta t + t_1)s)}{Ks} + \frac{\epsilon_i \cdot \exp(-(K\Delta t/\beta + (i\Delta t + t_1)s))}{K(s + K/\beta)} \right],$$

where

$N$  = the maximum number of time intervals of length  $\Delta t$  in the flight.

Simplifying the above expression,

$$X(s) = \sum_{i=1}^N \frac{\epsilon_i \exp(- (i \Delta t + t_1)s)}{\beta s + K} [(\exp(\Delta t s) - 1)/s + \beta(\exp(- K \Delta t/\beta) - 1)/K] \quad (N.4)$$

Since  $Z(s) = X(s) H(s)$ ,

then

$$Z(s) = \sum_{i=1}^N \frac{\epsilon_i \exp(- (i \Delta t + t_1)s)}{s^2 + \beta s + K} [(\exp(\Delta t s) - 1)/s + \beta(\exp(- K \Delta t/\beta) - 1)/K] \quad (N.5)$$

Also, since  $K = (\beta^2 + \omega^2)/4$ ,

$$Z(s) = \sum_{i=1}^N \frac{\epsilon_i \exp(- (i \Delta t + t_1)s)}{(s + \beta/2)^2 + \omega^2/4} [(\exp(\Delta t s) - 1)/s + 4\beta(\exp(- (\beta^2 + \omega^2) \Delta t/(4\beta)) - 1)/(\beta^2 + \omega^2)] \quad (N.6)$$

In order to invert  $Z(s)$  to find  $z(t)$ , several transform pairs, listed below, are used.

$$\frac{1}{(s + \beta/2)^2 + \omega^2/4} \longleftrightarrow 2 \exp(- \beta t/2) \sin(\omega t/2)/\omega \quad (N.7)$$

$$\frac{\exp(- (i\Delta t + t_1)s)}{(s + \beta/2)^2 + \omega^2/4} \longleftrightarrow 2 \exp(-\beta x/2) \sin(\omega x/2) U(x)/\omega \bigg|_{x = t - i\Delta t - t_1} \quad (\text{N.8})$$

$$\begin{aligned} \frac{1}{s((s + \beta/2)^2 + \omega^2/4)} &\longleftrightarrow \int_0^t \left(\frac{2}{\omega}\right) \exp(-\beta x/2) \sin(\omega x/2) dx \\ &= \frac{4(\exp(-\beta t/2) (\beta \sin(\omega t/2) - \omega \cos(\omega t/2)) + \omega)}{\omega(\beta^2 + \omega^2)} \end{aligned}$$

(N.9)

$$\frac{\exp(- (i\Delta t + t_1)s)}{s((s + \beta/2)^2 + \omega^2/4)} \longleftrightarrow$$

$$\frac{4(\exp(-\beta x/2) (\beta \sin(\omega x/2) - \omega \cos(\omega x/2)) + \omega)}{\omega(\beta^2 + \omega^2)} \cdot U(x) \bigg|_{x = t - i\Delta t - t_1} \quad (\text{N.10})$$

Substituting the above transform pairs into equation N. 6,

$$\begin{aligned}
 z(t) = & \sum_{i=1}^n \frac{4 \epsilon_i (\exp(-\beta x/2) (\beta \sin(\omega x/2) - \omega \cos(\omega x/2)) + \omega) \cdot U(x)}{\omega(\beta^2 + \omega^2)} \Big|_{x = t - (i-1)\Delta t - t_1} \\
 & - \sum_{i=1}^n \frac{4 \epsilon_i (\exp(-\beta x/2) (\beta \sin(\omega x/2) - \omega \cos(\omega x/2)) + \omega) \cdot U(x)}{\omega(\beta^2 + \omega^2)} \Big|_{x = t - i\Delta t - t_1} \\
 & + \sum_{i=1}^n \frac{8 \epsilon_i \beta (\exp(-\beta x/2) \sin(\omega x/2) (\exp(-(\beta^2 + \omega^2)\Delta t/(4\beta)) - 1)) \cdot U(x)}{\omega(\beta^2 + \omega^2)} \Big|_{x = t - i\Delta t - t_1} \\
 & = \sum_{i=1}^n \frac{4 \epsilon_i (\exp(-\beta x/2) (\beta \sin(\omega x/2) - \omega \cos(\omega x/2)) + \omega) U(x)}{\omega(\beta^2 + \omega^2)} \Big|_{x = t - (i-1)\Delta t - t_1} \\
 & + \sum_{i=1}^n \frac{4 \epsilon_i \beta \exp(-\beta x/2) \sin(\omega x/2) (2 \exp(-(\beta^2 + \omega^2)\Delta t/(4\beta)) - 3) \cdot U(x)}{\omega(\beta^2 + \omega^2)} \Big|_{x = t - i\Delta t - t_1} \\
 & + \sum_{i=1}^n \frac{4 \epsilon_i (\exp(-\beta x/2) \cos(\omega x/2) - 1) U(x)}{(\beta^2 + \omega^2)} \Big|_{x = t - i\Delta t - t_1} \quad (N. 11)
 \end{aligned}$$

Note that the above expression for  $z(t)$  contains one source of random variables. Namely, the sequence of values  $\epsilon_i$ ,  $i = 1, 2, \dots, N$ . Thus, the

variance of the output flight trace is given by

$$\begin{aligned}
 \text{VAR}(z(t)) = & \sum_{i=1}^n \left( 16 \sigma_{ci}^2 \left( \frac{(\exp(-\beta x/2) (\beta \sin(\omega x/2) - \omega \cos(\omega x/2)) + \omega) U(x)}{\omega(\beta^2 + \omega^2)} \right) \right. \\
 & \left. + \frac{\beta \exp(-\beta x/2) \sin(\omega x/2) (2 \exp(-(\beta^2 + \omega^2)\Delta t/(4\beta)) - 3) U(x)}{\omega(\beta^2 + \omega^2)} \right. \\
 & \left. + \frac{(\exp(-\beta x/2) \cos(\omega x/2) - 1) U(x)}{(\beta^2 + \omega^2)} \right)^2 \Bigg|_{x = t - (i-1)\Delta t - t_1}^{x = t - i\Delta t - t_1} \quad (N.12)
 \end{aligned}$$

The above equation is the desired relationship between the input function  $\text{VAR}(z(t))$  and the sequence of values  $\sigma_{ci}^2$ .

To compute values for  $\sigma_{ci}^2$ , a recursive solution is used. First, the value for  $\sigma_{c1}^2$  is determined by solving equation N.12 for  $\text{VAR}(z(t - \Delta t - t_1))$ . Using this value of  $\sigma_{c1}^2$ , then the value of  $\sigma_{c2}^2$  is determined by solving equation N.12 for  $\text{VAR}(z(t - 2\Delta t - t_1))$ . This process is repeated until  $\sigma_{cN}^2$  is determined.

## APPENDIX O

### DETERMINATION OF DEMAND RATES

The times of occurrence of demands on the nets monitored during the Fort Carson experiment could not be determined precisely. The only indication that a demand had occurred was the transmission of a communication. When a demand on a net occurred while that net was busy, the sender was forced to wait until the net was freed. Since no precise demand data could be collected from the tape recordings, an approximation was necessary.

An average rate of generation of demands can be determined by observing net usage over a long period of time and taking a time average. This rate, applied to the standard Poisson demand distribution, approximates the observed long-run demand distribution. The Poisson assumption has been frequently applied to queueing problems and is generally satisfactory to describe randomly occurring demands. The assumption underlying the Poisson distribution is that the probability of the occurrence of a demand during a short time period is independent of the length of time since the occurrence of the preceding demand. The random activity on the battlefield tends to provide events randomly which elicit communications, independent of the time of occurrence of the last communications.

The rates of generation of demands found to describe the communication activity during the Fort Carson experiment are 0.950 conversations per minute on the platoon nets and 0.837 conversations per minute on the company net. The sources of these conversations are listed in Table O.1.

Table O.1

#### Origins of Conversations

Element	Platoon Net	Company Net
All relay elements (Platoon leader and sergeant combined)	87%	70%
Non-relay elements	13%	--
Company Commander	--	30%



The phenomenon of communications being forgotten or outdated during waiting times has been ignored in this analysis. The communication activity observed during the Fort Carson experiment led this author to believe that these effects are not significant in the type of system being modeled. The waiting times observed were not sufficiently long that forgetting would occur or that communications would become untimely.

The platoon leaders and platoon sergeants are considered as common sources of demands on the communication system. While it is seldom the case that they divide the load evenly, the relative amount of activity of these two types of elements varies widely from platoon to platoon and from situation to situation. For this study, they will be considered to each contribute half of their accumulated total demand rate on the system.

With the observed rate of conversation transmission on the platoon nets being 0.95 conversations per minute, and with platoon elements (nonleaders) contributing 13% of that, a demand rate of 0.02 conversations per minute for each of the seven nonleaders per platoon approximates the situation closely. Approximately half of the conversations initiated by the nonleaders prove to be worthy of relay to the company net. The resulting rates for the nonleaders is then 0.01 conversations per minute for internal communications and 0.01 conversation per minute for external communications.

The remainder of the platoon net activity consists of relays from the company commander and the relay elements (platoon leaders and sergeants). The observed rates of relays from the company commander is approximately 0.05 conversations per minute. The remaining 0.76 conversations per minute of platoon net activity is divided equally between the platoon leader and the platoon sergeant. Of the communications of these two elements, approximately one-third have been classified to be external-type communications (critical) within the context of this study. The resulting rates for each of the relayers are then 0.25 conversations per minute for internal communications and 0.13 conversations per minute for external communications.

With a demand rate of 0.837 conversations per minute on the company net, and with 30% of that being attributed to the company commander, his rate of demand is 0.25 conversations per minute. Approximately 60% of the communications of the company commander are eventually relayed to the platoon nets, resulting in an external demand rate of 0.15 conversations per minute and an internal demand rate of 0.10 conversations per minute for the company commander.

Of the remaining net activity on the company net, 0.21 conversations per minute are attributed to relays from the platoon nets. The six relayers on the company net contribute the remainder of the net traffic. The observed net traffic indicates that their rate of demand for external-type communications is much lower than their rate of demand for internal-type communications. The rates have been approximated as 0.025 conversations per minute for internal-type communications and 0.04 conversations per minute for external-type communications for each of the platoon leaders and platoon sergeants.

## APPENDIX P

### GENERATION OF GAMMA DISTRIBUTED RANDOM TIMES

When one wishes to generate random variables which have a particular distribution, two things are useful: a generator of uniformly-distributed random numbers, and the inverse of the cumulative distribution function of the desired distribution. If  $f(x)$  is a probability density function and

$$F(x) = \int_0^x f(t) dt,$$

then  $F(x)$  is the cumulative distribution function of  $f(x)$ . A typical cumulative distribution function is illustrated in Figure P.1.

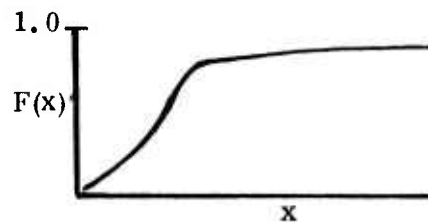


Figure P.1.--Cumulative Distribution Function

Given the cumulative distribution function,  $F(x)$ , a sample value having this distribution function can be generated by simply drawing a uniformly distributed random number from the interval  $(0, 1)$  and solving for the value of  $x$ , making  $F(x)$  equal to the random number. When a simple closed form of the inverse of  $F(x)$  exists, this procedure provides an ideal tool for simulation. When the inverse of  $F(x)$  is cumbersome to evaluate, the problem is more difficult.

The gamma distribution used to approximate conversation durations in this paper has no convenient mathematical inverse. Since only a small family of gamma distributions were needed to describe the processes of interest herein, a regression procedure was used to provide a functional approximation to the inverse of the cumulative distribution function. To do this, by numerical integration 1540 points from the cumulative distribution functions of seventy gamma distributions (with shape parameters ranging from 1.1 through 2.1 and scale parameters ranging from 15 through 27) were generated. These points were subjected to multiple regression to yield  $x$  as a function of a random number  $r$  and  $a$  and  $b$ , the distribution parameters. The approximation is used in subroutine GAMPDF of the simulation and in DYNCOM to generate times for the various gamma distributions.

## DISTRIBUTION LIST

Organization	Number of Copies
Chief, Office of Naval Research (Code 491) Methodology Division, Naval Analysis Group Department of the Navy ATTN: Mr. J. R. Marvin (Code 405D) Washington, D. C. 20360	1
Deputy Under Secretary of the Army (Operations Research) Washington, D. C. 20312	1
Commander U. S. Army Materiel Command ATTN: AMCPA 5001 Eisenhower Avenue Alexandria, VA 22333	1
Commander U. S. Army Materiel Command 5001 Eisenhower Avenue Alexandria, VA 22333	1
Commander U. S. Army Watervliet Arsenal ATTN: FWEWV-RDR Watervliet, NY 12189	1
Director Army Materiel Systems Analysis Agency ATTN: AMXSY-D Aberdeen Proving Ground, MD 21005	1
Commander U. S. Army Armament Command ATTN: AMSAR-SA Rock Island, IL 61201	1
Commander U. S. Army Armament Command ATTN: SARRI-LR Rock Island Arsenal, IL 61201	1

# DISTRIBUTION LIST (CONTINUED)

Organization	Number of Copies
Commander U. S. Army Combined Arms Developments Activity ATTN: ATCACA Fort Leavenworth, KS 66207	1
Commander U. S. Army Infantry School ATTN: Chief, Combat Materiel Division Fort Benning, GA 31905	1
Commander U. S. Army Armor Agency ATTN: CAGAR-OR Fort Knox, KY 40121	1
Commander U. S. Army Training and Doctrine Command Fort Monroe, VA 23651	1
Professor of Ordnance U. S. Military Academy ATTN: MADN-F West Point, NY 10996	1
Commander U. S. Army Missile Command ATTN: AMSMI-W Redstone Arsenal, AL 35809	1
Commander U. S. Army Missile Command ATTN: AMSMI-RD Redstone Arsenal, AL 35809	1
Commander U. S. Army Missile Command ATTN: AMSMI-CS Redstone Arsenal, AL 35809	5

DISTRIBUTION LIST (CONTINUED)

Organization	Number of Copies
Defense Documentation Center Cameron Station Alexandria, VA 22314	12
Battelle Memorial Institute ATTN: RACIC 505 King Avenue Columbus, OH 43201	1